# Natural ventilation strategies to enhance human comfort in high-rise residential buildings in Thailand

Thesis submitted in accordance with the requirements of the University of Liverpool for the degree of Doctor in Philosophy

By

**Pimolsiri Prajongsan**

School of Architecture, University of Liverpool

August 2014

# Natural ventilation strategies to enhance human comfort in high-rise residential buildings in Thailand

Pimolsiri Prajongsan

## Abstract

In this study a thermal comfort ventilation strategy called '*ventilation shaft*', which is a vertical shaft located at the rear of a single-sided unit and with an exhaust at the building's flat roof, is proposed for a single-sided residential unit in high-rise buildings in Bangkok. The main aim is to investigate its potential to maximize the unit's indoor air velocity and to extend the occupants' thermal comfort, which, therefore, reduces high electricity consumption due to cooling systems.

By using the validated CFD code in DesignBuilder simulation software, the ventilation shaft's effectiveness was examined and its design was optimized. It was found that the proposed strategy can effectively increase the unit's air velocity from 0.05ms$^{-1}$ to 1.44ms$^{-1}$ (approximately 36% of the external wind speed of 4ms$^{-1}$under wind incident angle of 0°). The external wind speed and direction relating to the unit's main window were found as the most influential external parameters, while the vertical shaft's size as well as the inlet and outlet's size and location with respect to the occupied area were the most influential design factors to determine its performance. A shaft height of at least 1m above the building flat roof, as well as an opening width of at least 50%-75% of the wall's width, is recommended for ensuring the best results. Openings' length, particularly the inlet's, only to cover the occupied level is also suggested to avoid excessive solar heat gain from the environment.

Regarding thermal comfort, the ventilation shaft with its optimal design was attached to the rooms from floor 6th to floor 25th of the hypothetical building and found able to produce the required air speed for creating physiological cooling effect in most units. This could extend the occupants' thermal comfort time for up to 33% and 64% per day for a south- and a north-facing unit in the hypothetical building, respectively based on ASHRAE's adaptive comfort model, and could lead to significant energy savings of up to 68.8MW per annum and 5,291MW per annum for a typical residential building in Bangkok based on a typical electric ceiling fan and a split type air conditioner respectively. In conclusion, the proposed ventilation shaft is an effective wind-induced strategy to increase the air velocity and create cross ventilation in a single-sided residential unit, which can enhance the natural ventilation potential to provide thermal comfort and reduce the a/c systems dependency in typical high-rise residential buildings in Bangkok and other hot-humid climates.

# Acknowledgement

First of all, I wish to express my deepest appreciation to my supervisor ***Professor Steve Sharples***, who always reminded me that '*doing a PhD is like making your own trip – you decide on where to go and how to get there*'. I am so glad that he decided to hop on board with me since the very beginning - he has been the best navigator and the greatest companion anyone could ever wish for! Now I have arrived at my first destination, and with becoming a researcher, about to reach the next.

Next, I would like to acknowledge my gratitude to the following organizations and special people: firstly, the ***Energy Policy and Planning Office (EPPO)***, Ministry of Energy and the Royal Thai Government for their financial support granted for my PhD study; the academic staff, both at ***The University of Sheffield*** and ***The University of Liverpool***, for their support throughout my student life; ***Dr.Acharawan Chutarat*** for kindly lending me an anemometer for the on-site measurements, and ***Assistant Professor Panita Wongmahadlek***, ***Dr.Nuanwan Tuaycharoen*** and ***Dr.Sureepan Supansomboon*** for their support and continual friendship.

Furthermore, I wish to thank my friends at 100 and 102 Gell Street, S3 7QW, Sheffield – ***Dr.Orawan and Dr.Phisut Apichayakul***, ***Assistant Professor Tharinee and Dr.Satta Panyakaew***, ***Dr.Wisaruda Suppharangsan***, and ***Dr.Narumon Chunlahawanit***, who welcomed me and my family and made us feel at home since our first day in the UK! I would also like to thank my academic friends at the School of Architecture, The University of Sheffield – ***Dr.Sushardjanti Felasari*** and her family, ***Dr.Hong-Seok Yang***, ***Dr.Michael Barclay***, ***Dr.Sahar Zahiri*** and ***Dr.Ali Kashkooli***, who have been my cheerful companions along this journey; ***John Brownhill*** – the best landlord in Sheffield; our family's dear friends at the Sheffield University's Nursery- ***Lesley***, ***Stacey***, ***Nat*** and ***Clare*** for their generosity and friendship. Every single day in the UK would not be so enjoyable and pleasant without them!

And finally, I would like to express my deepest thankfulness to my family, especially to my beloved husband and son - ***Mr.Apichai*** and ***Master Paraan Prajongsan***. Without their love I would never even dare to make this journey. You two are the most precious gift in my life and the smiles on your face every morning are my greatest source of energy – I love you always :)

***Pimolsiri Prajongsan***

# Table of Contents

# List of Figures

## Chapter One:

## Chapter Two:

## Chapter Three:

## Chapter Four:

## Chapter Five:

## Chapter Six:

# List of Tables

### Chapter One:

### Chapter Two:

### Chapter Four:

## Chapter Five:

## Appendix A:

## Appendix B:

## Appendix C:

# Chapter One

## Introduction

## 1.1 Background to the study

### *1.1.1 Introduction*

In Thailand the residential sector is responsible for 21% to 23% of overall electricity consumption. It has continually increased by approximately 5% per year (see Figure 1-1) and about 30% to 35% of this usage is consumed in Bangkok alone (DEDE, 2014).

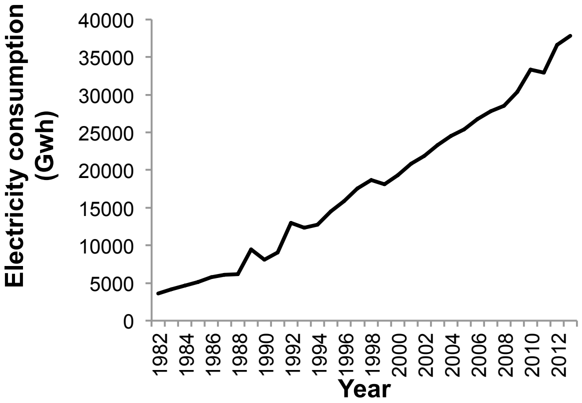

**Figure 1-1** Electricity consumption in residential sector in Thailand from 1982 to 2013 (DEDE, 2014).

One key building type that is responsible for this problem is high-rise residential buildings, which have become popular in the Bangkok urban area during the last ten years. Such buildings mostly have a double-loaded corridor with single-sided residential units on either side of their internal corridor. Without suitable strategies, almost all units are air-conditioned (a/c). However, a/c systems are energy expensive and previous works relating to passive cooling strategies for this building type in Thailand are still scarce.

In this thesis a comfort ventilation strategy called '*ventilation shaft*' is proposed and its performance to increase indoor air velocity and thus provide cooling effect and enhance the occupants' comfort is investigated in detail. The main intention for proposing such a strategy is to reduce the high electricity demand due to cooling systems in residential units in typical high-rise buildings in Bangkok.

### *1.1.2 Climatic conditions of Bangkok*

Thailand is classified as a hot-humid country with high air temperature, high relative humidity and low wind speed for most of the time. Its climate is relatively uniform throughout the year with a small seasonal change. Hot summer months (February to May) are characterised by a high sun angle and high air temperature (Tantasavasdi et al., 2001). The rainy season (June to September) has a lower temperature, but greater relative humidity (RH) and the winter season (October to January) has the lowest sun angle with a moderate air temperature and low wind condition.

Bangkok is situated at about the centre of the country at latitude 13.44°N and longitude 100.3°E. An average mean air temperature of Bangkok ranges between 28°C during winter months to 29°C during rainy months and 30°C during summer months with an average daily diurnal variation between 5°C and 6°C (see also Table A-1 in Appendix A). Daily maximum air temperature can be normally expected during the afternoon, while the minimum temperature can be generally experienced during early morning (see Figure 1-2). In short, Bangkok air temperature ranges from 24°C to 32°C and relative humidity varies from 68% to 75% (MET, 2010).

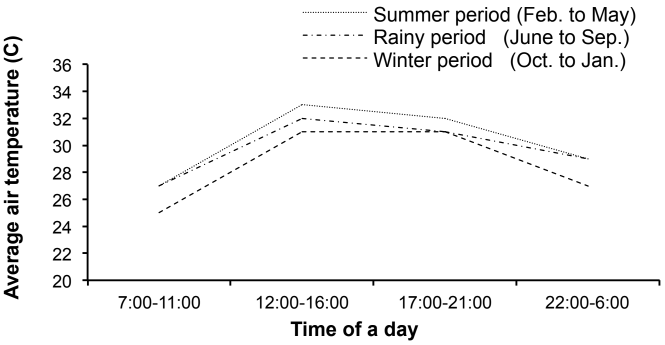

**Figure 1-2** Average hourly air temperatures in different times of a day in three seasons according to Bangkok's weather data between 1999-2008 (Thailand Meteorological Department 2009).

Bangkok's prevailing wind conditions are mainly dominated by southwest and northeast monsoons. During summer and rainy seasons southern and southwestern winds are the predominant wind directions with 30% and 33% calm period, respectively (Figure 1-3). Eastern wind is dominated during winter season with greater percentage of calm period. The first and second highest wind speed frequencies are found at 1-2m/s and 2-3m/s and can rise up to an average maximum of 6m/s. However, this high wind speed is much less frequent (MET, 2010, Waewsak et al., 2002). During a day, a stronger wind speed is found to occur commonly during the daytime while much weaker wind speed occurs at night and early morning (Figure 1-4).

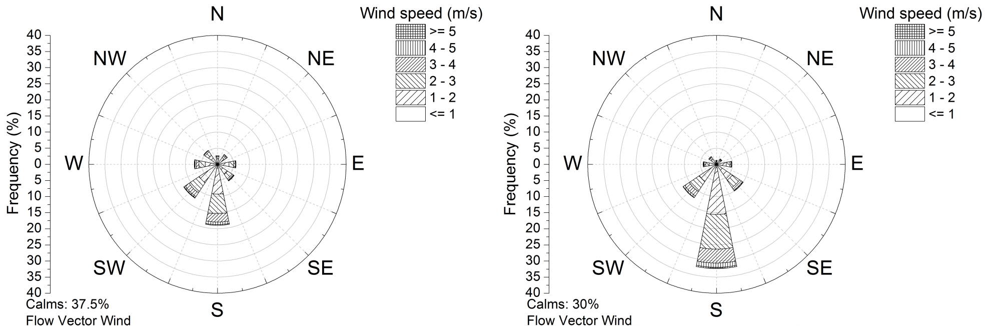

Annual

Summer months

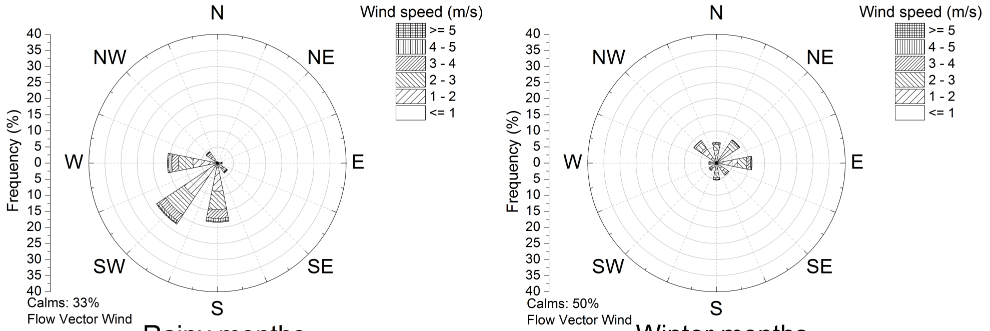

Rainy months

Winter months

**Figure 1-3** Bangkok annual and seasonal wind speed frequency (%) and directions (degree from the north) according to Bangkok's weather data between 1999-2008 (MET, 2009).

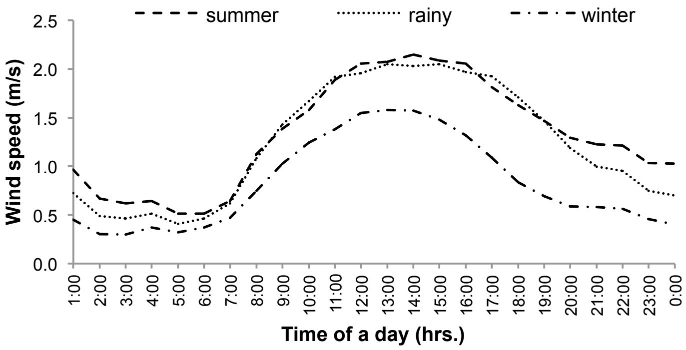

**Figure 1-4** Bangkok's average hourly wind speed of a day in different seasons (MET, 2010).

With these climatic conditions Bangkok's microclimate is considered to lie outside the thermal comfort range for most time of the year according to ASHRAE's Psychrometric chart (Khedari et al., 2000c, Tantasavasdi et al., 2001, ASHRAE, 2009). Its average monthly mean dry-bulb temperature and relative humidity for fifteen years recorded at 7:00hrs. and 13:00hrs. were plotted against ASHRAE's Psychrometric chart in a study (Khedari et al., 2000c) and all the monthly lines were found to lie outside the ASHRAE comfort zone. This indicates a large amount of discomfort time during a year.

This is further confirmed by the analysis of Bangkok's mean hourly temperature regarding to monthly thermal comfort range based on ASHRAE's adaptive comfort model (ASHRAE, 2009) in Table1-1 (see also Table A-2 in Appendix A). Approximately 51% of the time in a year was found to be outside the thermal comfort range. This is especially during 10:00hrs. and 19:00hrs. when high air temperature can be commonly experienced.

**Table 1-1** Mean hourly dry-bulb temperature (MET, 2010) compared to monthly thermal comfort range according to ASHRAE's adaptive comfort model (ASHRAE, 2009).

| Month/ Time of a day (hrs.) | 0100 | 0200 | 0300 | 0400 | 0500 | 0600 | 0700 | 0800 | 0900 | 1000 | 1100 | 1200 | 1300 | 1400 | 1500 | 1600 | 1700 | 1800 | 1900 | 2000 | 2100 | 2200 | 2300 | 2400 |
|---|---|---|---|---|---|---|---|---|---|---|---|---|---|---|---|---|---|---|---|---|---|---|---|---|
| Jan | 25.9 | 25.5 | 25.1 | 24.8 | 24.5 | 24.2 | 24.2 | 25.0 | 26.8 | 28.4 | 29.9 | 30.9 | 31.6 | 32.0 | 32.2 | 31.9 | 31.1 | 29.8 | 28.7 | 27.8 | 27.3 | 26.9 | 26.6 | 26.2 |
| Feb | 26.7 | 26.5 | 26.2 | 26.0 | 25.7 | 25.5 | 25.5 | 26.3 | 27.9 | 29.3 | 30.6 | 31.5 | 32.2 | 32.6 | 32.8 | 32.6 | 31.7 | 30.4 | 29.2 | 28.3 | 27.9 | 27.6 | 27.3 | 27.0 |
| Mar | 27.9 | 27.7 | 27.5 | 27.4 | 27.1 | 26.9 | 27.1 | 28.1 | 29.5 | 30.9 | 32.0 | 32.8 | 33.3 | 33.6 | 33.7 | 33.4 | 32.5 | 31.2 | 30.0 | 29.2 | 28.8 | 28.6 | 28.4 | 28.2 |
| Apr | 28.9 | 28.6 | 28.5 | 28.4 | 28.2 | 28.0 | 28.3 | 29.4 | 30.9 | 32.1 | 33.1 | 33.8 | 34.3 | 34.4 | 34.4 | 34.1 | 33.3 | 31.9 | 30.8 | 30.2 | 29.8 | 29.6 | 29.3 | 29.1 |
| May | 28.3 | 28.1 | 27.8 | 27.6 | 27.4 | 27.2 | 27.8 | 29.0 | 30.4 | 31.4 | 32.1 | 32.5 | 32.6 | 32.7 | 32.7 | 32.5 | 31.7 | 30.6 | 29.6 | 29.2 | 28.9 | 28.8 | 28.6 | 28.4 |
| Jun | 28.1 | 27.9 | 27.7 | 27.6 | 27.4 | 27.2 | 27.7 | 29.0 | 30.0 | 31.0 | 31.6 | 32.2 | 32.5 | 32.5 | 32.4 | 32.1 | 31.3 | 30.3 | 29.4 | 29.0 | 28.8 | 28.7 | 28.5 | 28.3 |
| Jul | 28.0 | 27.8 | 27.6 | 27.5 | 27.2 | 27.1 | 27.5 | 28.6 | 29.7 | 30.6 | 31.4 | 31.9 | 32.1 | 32.2 | 32.1 | 31.7 | 31.1 | 30.1 | 29.3 | 28.9 | 28.7 | 28.5 | 28.4 | 28.2 |
| Aug | 27.7 | 27.5 | 27.3 | 27.2 | 26.9 | 26.7 | 27.1 | 28.1 | 29.2 | 30.3 | 31.0 | 31.6 | 31.9 | 31.9 | 31.9 | 31.5 | 30.8 | 29.9 | 29.1 | 28.6 | 28.4 | 28.2 | 28.1 | 27.9 |
| Sep | 27.2 | 26.9 | 26.8 | 26.6 | 26.4 | 26.2 | 26.5 | 27.5 | 28.9 | 30.0 | 30.9 | 31.4 | 31.8 | 31.8 | 31.7 | 31.3 | 30.5 | 29.6 | 28.8 | 28.3 | 28.0 | 27.8 | 27.5 | 27.3 |
| Oct | 27.1 | 26.8 | 26.6 | 26.4 | 26.2 | 25.9 | 26.2 | 27.4 | 29.0 | 30.3 | 31.1 | 31.7 | 31.8 | 31.9 | 31.7 | 31.2 | 30.3 | 29.5 | 28.9 | 28.4 | 28.1 | 27.9 | 27.6 | 27.3 |
| Nov | 26.7 | 26.4 | 26.1 | 25.8 | 25.5 | 25.1 | 25.3 | 26.7 | 28.4 | 29.8 | 30.8 | 31.5 | 31.9 | 32.0 | 31.9 | 31.5 | 30.7 | 29.6 | 28.9 | 28.4 | 28.0 | 27.7 | 27.3 | 27.0 |
| Dec | 25.5 | 25.1 | 24.7 | 24.4 | 24.0 | 23.6 | 23.7 | 24.7 | 26.5 | 28.2 | 29.6 | 30.4 | 31.1 | 31.4 | 31.4 | 31.1 | 30.3 | 29.1 | 28.2 | 27.6 | 27.1 | 26.7 | 26.2 | 25.9 |

▨ **Air temperature within thermal comfort range indicating comfort hours**

☐ **Air temperature beyond thermal comfort range indicating discomfort hours**

### *1.1.3 Previous studies on passive cooling for residences in Thailand*

According to the Bangkok weather data analysis a suitable passive cooling design strategy is required for improving human thermal comfort during discomfort hours. Without passive strategies, mechanical systems are frequently employed in a residence to provide occupants' thermal comfort. However, a/c systems are energy expensive. Approximately 22% of total electricity in Thailand is consumed by the residential sector (DEDE, 2010) and cooling systems accounts for 60% of the total electricity use in this sector (Chirarattananon and Chaiwiwatworakul, 2006).

With the concern of high energy intensive a/c systems, various passive cooling strategies have been proposed for residences in Thailand. However, almost all studies focus on detached houses or low-rise residences and there is no work concerning natural ventilation strategies for high-rise residential buildings which have become popular in Bangkok's urban areas recently due to the high demand of residences close to works. Moreover, these strategies attempt mainly to reduce external heat gain to get into the indoor environment, especially through the building roofs, and to induce indoor ventilation rate by using stack effect from air temperature differences. However, due to the fact that there is a low and inadequate indoor-outdoor temperature difference for creating effective stack ventilation in Thailand, such proposed stack-driven ventilation strategies may either hardly improve indoor thermal environment or increase the occupants' thermal comfort. For such situations comfort ventilation strategies to provide direct cooling effect to the occupants are preferred.

### *1.1.4 High-rise residential buildings in Bangkok*

In Thailand a high-rise building is defined as a building with a height of at least 23m. It is approximately eight storeys depending on a building's floor-to-floor height. In recent years, extensive high-rise residential buildings have been built in Bangkok urban area (Figure 1-5 left). The number of condominium units has been continually increasing, especially those with one-bedroom (Figure 1-5 right), while the number of detached and semi-detached houses in the outskirts of Bangkok have become attenuated. This is due to a high demand for residences that are adjacent to work.

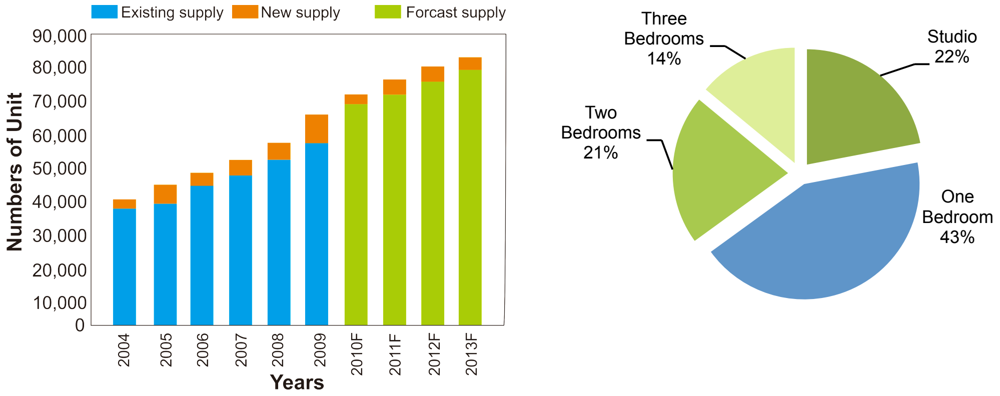

**Figure 1-5** Supply of condominium in Bangkok from 2004 to 2013Forecast (left), and Existing supply in Bangkok by residential type (right) (Branage-thaicoon, 2010).

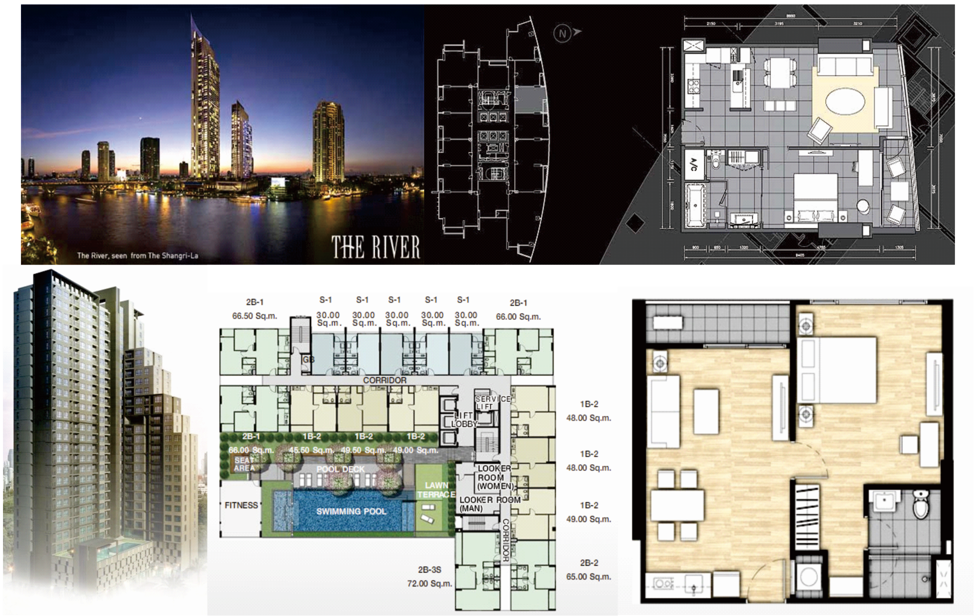

**Figure 1-6** External view, typical floor plan and unit floor plan of existing condominiums in Bangkok urban area; (above) The River (www.theriverbangkok.com), and (below) The Hive Taksin (www.sansiri.com).

However, there are some drawbacks to typical condominiums in Bangkok regarding natural ventilation and indoor thermal comfort. A unit in a condominium can have less external perimeters and external openings comparing to a detached and semi-detached house. Moreover, these condominiums are typically double-loaded corridor buildings with residential units located on either side of an internal corridor (see typical floor plans in Figure 1-6). Without any space between the units due to the limitation of space, all residential units become single-sided ventilated with external openings only on one wall of the unit. These features have a great disadvantage in terms of building energy efficiency and they are technically unsuitable for buildings in hot-humid climates as they limit the opportunity to apply effective cross natural ventilation in a building (Givoni, 1998). Without any passive cooing strategies, most units in a condominium are dependent on a/c systems, which are high energy consumption.

### *1.1.5 Summary*

Thailand is a hot-humid country with high air temperatures and humidities and low wind speeds throughout the year. Bangkok is its capital and it is situated at about the centre of the country. Bangkok's weather data shows that its climatic conditions lay outside the thermal comfort range for much of the year. For this situation passive cooing strategies, particularly comfort ventilation which is recommended by extensive studies, are significant to improve indoor thermal comfort conditions, to extend comfort hours and to reduce the use of mechanical cooling systems.

However, previous works associated with comfort ventilation in Thailand are scarce. This is especially true for high-rise residential buildings, which have become popular in Bangkok's urban area for the last ten years. Most of the previous works were concentrating on low-rise residences and they all focused on using stack ventilation to induce indoor air ventilation rate. Yet the air movement attaining from stack forces is much lower than what is required for providing cooling effect to enhance human thermal comfort.

In this study a comfort ventilation strategy called '*ventilation shaft*' is proposed particularly for high-rise residential buildings. It is a wind-induced natural ventilation strategy which has been suggested to be more effective to stack force for improving cooling effect under hot-humid climate. Its performance to increase indoor air velocity and to extend comfort hours inside a typical residential unit in high-rise buildings in Bangkok is investigated in detail.

## 1.2 Aims and objectives of the study

A strategy called '*ventilation shaft*' is proposed for a residential unit in high-rise buildings. The aim of the study is to investigate its potential to maximise the unit's indoor air velocity and to extend thermal comfort hours, thereby reducing the high electricity consumption due to cooling loads from air-conditioning systems.

The main objectives of the study are as follows:

1) To assess the potential of the proposed strategy to increase indoor air velocity and to extend thermal comfort period based on the concept of percentages comfort hour per day
2) To discover the influence of different variables on the performance of the ventilation shaft strategy, including external parameters i.e. climatic conditions, and internal parameters i.e. the strategy's designs and configurations
3) To develop the strategy's optimal geometry and position that provide the best result of indoor air velocity and airflow distribution
4) To assess and validate the suitability of the available predicting tools and research methods for evaluating natural ventilation strategies

## 1.3 Research Questions

According to the aims and objectives stated above the main research questions of the study are as follows:

1) How feasible is the proposed ventilation shaft strategy to increase average indoor air velocity and to improve thermal comfort conditions in a residential room with single-sided ventilation in Bangkok?
2) What are the most effective design configurations of the strategy for achieving best results of high indoor air velocity?
3) How effective is the strategy to extend comfort hours in the building when the strategy is incorporated into a building?

## 1.4 Scope of the study

The study will focus on a wind-induced natural ventilation strategy to improve thermal comfort for a single-sided unit in typical high-rise residential buildings in hot-humid countries. In order to avoid excessive study time, the scope of the study have been set as follows:

1) **Hypothetical building**: As the proposed strategy focuses on a single-sided room in a high-rise residential building in Bangkok, a hypothetical building was formulated in the study to represent typical characteristics of such a building type in Bangkok (Further details can be found in Chapter Five: Research Design).
2) **Studied room and main occupied area for the study**: As most parts of the study are focusing on the effects of various variables that influence the strategy's performance to increase room's indoor air velocity, the ventilation shaft will be

assumed to connect to only one residential room on the 23rd floor of the building called '*studied room*'. Also the main occupied area, which is the room's main activity area, will be set up as the main area for investigating the strategy's performance (Further details can be found in Chapter Five: Research Design).

3) **Weather data**: Bangkok's weather data will be employed throughout the study (Further details can be found in Appendix A: Bangkok's weather data).

## 1.5 Structure of the thesis

The thesis is divided into seven main chapters. The introduction and the background to the study are given in Chapter One to provide the necessary context for this study. The study's major aims and objectives, the research questions and the scope of the study are also listed in this chapter. In Chapter Two the basic knowledge of natural ventilation and thermal comfort as well as the cooling effect due to elevated air movement, which are the most significant topic relating to this study, are reviewed and discussed. Then the proposed ventilation shaft strategy and its principle is explained in Chapter Three.

In Chapter Four the available research methods for investigating natural ventilation in buildings are reviewed. Advantages and weaknesses of each method are also discussed based on relevant literatures and the most suitable method for this study is then established. Later the procedures to achieve the study's aim and objectives are explained in detail in Chapter Five. The formulated building for this study is also demonstrated in this Chapter. In Chapter Six the results of this study are reported according to the procedures established and finally the obtained results are discussed in Chapter Seven. The main conclusion of this study is also included in this final chapter.

Additional information is provided in the appendices: Appendix A includes Bangkok's weather data and the wind pressure coefficient for the formulated hypothetical building employed in this study; Appendix B includes the measured and simulated data used for validating the chosen simulation software; Appendix C includes the main results of the study and Appendix D includes the list of the published paper according to the results of this study.

# Chapter Two

## Natural ventilation in buildings and thermal comfort

### 2.1 Introduction

Natural ventilation is recommended as one of the most effective passive cooling tools to extend comfort conditions while reducing the use of mechanical cooling systems for buildings in hot-humid countries (Haase and Amato, 2006, Aynsley, 2007, Nguyen and Reiter, 2014). In this chapter the principles of natural ventilation in buildings are reviewed. Its mechanism and principles are described in order to develop the understanding of natural ventilation's behavior, which is, in turn, significant for designing the proposed strategy. Next, natural ventilation induced strategies previously employed are reviewed together with their performances to increase indoor air movement. In the last part the principle of thermal comfort and the physiological cooling effect due to elevated air movement, which is the basic principle of the proposed strategy, are explained.

### 2.2 Natural ventilation in buildings

#### *2.2.1 Introduction*

'*Natural ventilation*' is the term used for describing the airflow to or from a building through designed openings in the building envelope that is caused by naturally produced pressures due to wind or/and stack effects (Awbi, 2003).This is different from the term '*infiltration'*, which refers to the leakage of air in to or from a building due to the imperfect construction or the porosity of building materials. During the last three decades natural ventilation in buildings has become a focus of researchers' attention. This is because it provides high indoor environmental quality, user satisfaction, while consuming considerably lower energy and produces much lower environmental impact comparing to mechanical ventilation systems (Awbi, 2008, Ghiaus and Allard, 2005).

‘*Building ventilation*’ includes all thermal procedures when the air in an internal area of closed space is replaced by external air masses that enter through building openings (Visagavel and Srinivasan, 2009). Building ventilation systems have three significant functions (Givoni, 1976, Szokolay, 2004, Ghiaus and Allard, 2005): (i) to maintain healthy indoor air quality by decreasing the concentration of indoor pollutants - called ‘*health ventilation’*; (ii) to provide direct comfort and prevent discomfort due to wetted skin - called ‘*thermal comfort ventilation*’; and (iii) to cool building structures when indoor air temperature is higher than ambient temperature - called ‘*structural cooling ventilation’* (such as that in (Yik and Lun, 2010, Jamaludin et al., 2014, Leite and Frota, 2013). These systems can be mechanical or natural. While the former systems use mechanical devices as the main tools to drive air into and out of a building, the latter systems depend greatly on natural forces.

### 2.2.2 Natural ventilation mechanism

The mechanism or the energy that drives natural ventilation in and around buildings is the pressure difference (*Δp)* between the indoor and outdoor environment due to wind or/and stack forces (Awbi, 2008).

#### 1) Wind force

Natural ventilation in a building due to wind force is developed by the differences in the wind pressure distributions ($p_w$) around the building, which is influenced by the building geometry itself and its orientation relative to the prevailing wind direction (Awbi, 2008). The windward side of a building, called ‘*pressure zone’*, is subjected to positive wind pressure coefficients, while the leeward side and low pitch building roofs are subjected to negative wind pressure coefficients and called ‘*suction zone’*. For the building side-facades the pressure coefficient can be either positive or negative depending on their inclination with respect to the prevailing wind direction (see Figure 2-1).

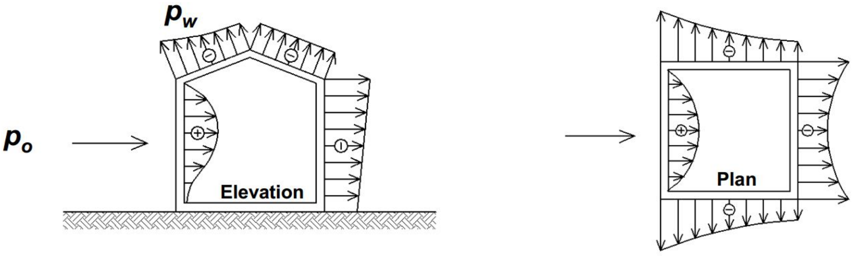

**Figure 2-1** Wind pressure distribution on a pitched roof building (Awbi, 2003) [$Pw$ is wind pressure and $\rho_o$ is the air density].

External air is driven through building openings from the pressure zone on a building windward side where the pressure is higher and leaves the building through the openings at the suction zone on the leeward side where the pressure is relatively lower (see Figure 2-1). The pressure difference between building openings is, therefore, the main factor to determine the airflow rate in the building. The greater the pressure difference between the openings on the windward side (the inlets) and on the leeward side (the outlets), the higher the indoor airflow rate will be. In order to examine the building indoor airflow rate due to wind force, it is necessary to firstly obtain wind pressure distribution of each building opening.

The wind pressure distribution over the surfaces of a building is not uniform. It diminishes outwards from the center of the pressure zone (see Figure 2-1). This pressure distribution at different points of a building can be estimated using Eq. 2-1 (Awbi, 2003).

$$\boldsymbol{p_w = 0.5C_p\rho_o\overline{V}^2} \qquad \textbf{Eq. 2-1}$$

where $Pw$ is wind pressure; $\rho_o$ is the air density; $\overline{V}$ is wind speed at datum level, usually at the height of the opening or a reference point on the building e.g. roof (ms-$^{1}$); and $C_p$ is a dimensionless pressure coefficient.

The value of the wind pressure coefficient ($C_p$) is dependent on building configuration regarding to external wind velocity and direction, and its location with respects to its neighboring topography and vegetation (Klevien, 2003). Different points on a building envelope have different $C_p$ values. As it is influenced by various factors it is, therefore, hard to give an exact $C_p$ value for a particular point on a building surface. In the past $C_p$ values could be predicted from the pressure measurement in a wind tunnel or could be estimated using Eq. 2-2.

$$\boldsymbol{C_p = (p - p_o)/0.5\rho_o\overline{V}^2} \qquad \textbf{Eq. 2-2}$$

where $p$ is static pressure at some point on a building (*Pa*); $p_o$ is static pressure of the free stream corresponding to $\overline{V_r}$ (*Pa*); $\rho_o$ is density of free stream (*kgm*$^{-3}$); $\overline{V}$ is free stream velocity normally calculated at building height or other reference height (*ms*$^{-1}$). Wind speed at a specific height can be predicted as a function of the wind velocity that is measured at 10m above the ground, which is commonly measured and recorded by a local Meteorological Office, using a '*Power law*' wind profile (Eq.2-3) (Awbi, 2003, Awbi, 1994).

$$\boldsymbol{\frac{V_1}{V_{10}} = K{z_1}^a} \qquad \textbf{Eq. 2-3}$$

where $V_1$ and $V_{10}$ are the wind speed (in ms$^{-1}$) at a particular height ($z_1$) (in metres) and at 10m above the ground level; *K* is the coefficient and *a* is the exponent which is depending on terrain roughness i.e. *K* and *a* are constant at 0.35 and 0.25, respectively for urban areas (Santamouris and Asimakopoulos, 1996).

Alternatively, wind pressure coefficients can be approximated by using Computational Fluid Dynamics (CFD) simulation, which has been developed since the 1970s, or a number of software packages developed recently. While some software packages can only estimate an average $C_p$ value for different building facades, others are able to predict the $C_p$ value of a specific point in the particular façade under specific situations. *CPBANK*, for instance, is developed from the results of extensive tests performed in a wind tunnel laboratory and can estimate an average $C_p$ value on a façade of a building with specific geometries and locations (Ghiaus and Allard, 2005). In contrast *CpCalc+*, which was proposed by the *PASCOOL* project (Allard, 1998); and *CpGenerator*, which was developed by TNO Building Research (http://cpgen.bouw.tno.nl/cp/), are able to predict the $C_p$ value at a specific point of a building facade under particular building geometry, orientation and surroundings. Both *CpCalc+* and *CpGenerator* have similar approaches and capacities, and have been developed from the data obtained from either a literature review or experimental studies.

### *2) Stack or buoyancy force*

Stack or buoyancy pressure at a building opening is created from the variation in air density which is the result of temperature difference between the indoor and outdoor environment (Szokolay, 2008), and across the openings (Awbi, 2003). Stack pressure can be found within a room of significant height either with one large opening or with more than one opening at different levels (see Figure 2-2a and Figure 2-2b). Also, stack pressure can occur in a room with a vertical stack (Figure 2-2c). In the case with one large opening, air is driven due to the pressure difference between the upper and lower zone of the opening, while it is driven due to the pressure difference between the two openings with different positions in the case with more than one opening and with a chimney.

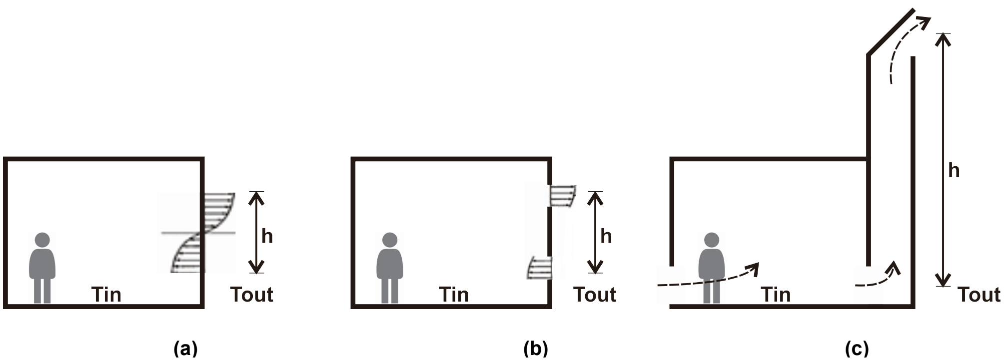

**Figure 2-2** Stack driven natural ventilation: (a) in a room with one large opening; (b) a room with two openings at different height; and (c) a room with a vertical stack [adapted from (Allocca et al., 2003, Szokolay, 2008)].

When the indoor air temperature is higher than the ambient temperature, an over-pressure is created at the upper part of a building and the under-pressure is formed at the lower part. The warmer air, which is lighter, rises to the upper part of the room or the stack and flows out of the room at the warm zone, while this air is replaced by cooler and heavier outdoor air, which is driven into the room at the bottom part. However, the opposite flow direction may be found when a building indoor air temperature is lower than the ambient temperature (Givoni, 1976). Stack pressure can be calculated using Eq.2-4 (Awbi, 2003).

$$\boldsymbol{p_s = -\rho_o g h (1 - \frac{T_o}{T_i})} \qquad \textbf{Eq. 2-4}$$

where $T_o$ is reference or outdoor air temperature (*K*); $T_i$ is the internal air temperature (*K*); $\rho_o$ is air density at the reference temperature or $T_o$ ($kgm^{-3}$); *g* is acceleration due to gravity (9.81 $ms^{-2}$); *h* is the difference in height between two openings (*m*) (see Figure 2-2).

Alternatively, natural ventilation due to stack effect can be determined by the vertical distance to the neutral pressure plane or level (*NPL*) (Ghiaus and Allard, 2005). *NPL* is created at a certain height where the upper and under pressures are equal. This level sets itself so that the airflow entering and leaving a room are balanced. The air above this level will be driven out through the building outlets, while the air below this level will be pulled into the building inlets. The *NPL* location depends greatly on size and location of openings, indoor-outdoor air temperature difference, and external wind conditions (Ghiaus and Allard, 2005). It usually places itself close to the largest openings. *NPL* can be approximated using equation (Eq.2-5) (Klevien, 2003).

$$\boldsymbol{h_o = \frac{{A_1}^2 h_1 + {A_2}^2 h_2}{{A_1}^2 + {A_2}^2}} \qquad \textbf{Eq. 2-5}$$

where $h_o$ is the neutral pressure plane level above floor level (*m*); $A_1$ and $A_2$ are the area of the lower and upper openings, respectively ($m^2$); $h_1$ and $h_2$ are the vertical distances between the floor and the lower and upper openings, respectively (*m*).

Under a room with only stack ventilation, external air will enter into a building only through the openings that are lower than the *NPL* location. Therefore, the top opening is suggested to be as large and as high as possible so that the *NPL* would be at the highest possible position and so that the external air can enter to the largest possible part of the building (comparing different *NPL* in Figure 2-3a, b, c and d). This top opening is also suggested to be on the leeward façade, so that wind and stack effect can drive air in the same direction.

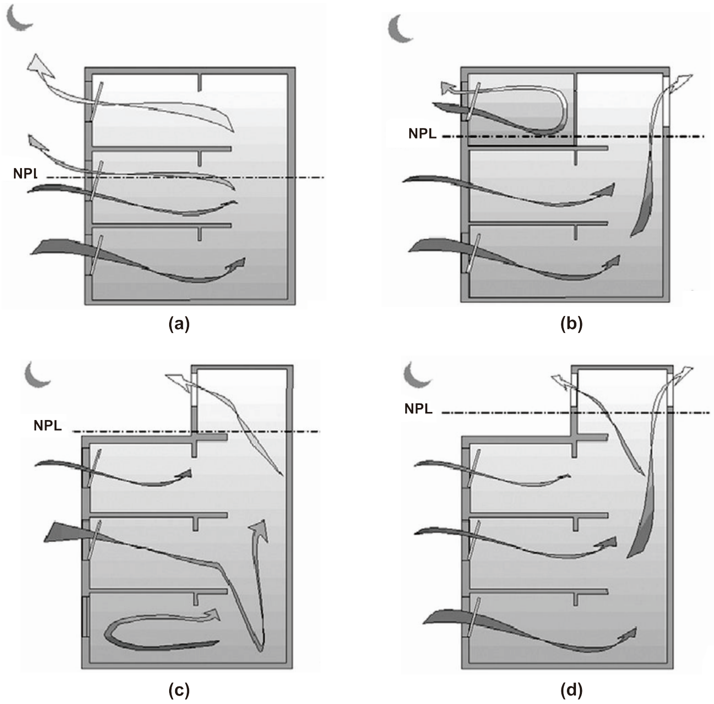

**Figure 2-3** Different locations of *NPL* in a room with different opening designs (Ghiaus and Allard, 2005).

According to both equations (Eq.2-4 and Eq.2-5), it can be seen that stack pressure is depending greatly on the temperature difference and the distance between the inlet and the outlet openings i.e. the higher the temperature difference and the distance between these two, the higher the stack pressure and so the indoor airflow rate.

However, air movement due to stack force is commonly much weaker than that due to wind force. It is also proportional to the height difference between inlet and outlet openings and to the temperature difference between indoor and outdoor air. Airflow due to stack effect is, therefore, relatively small in low-rise buildings, particularly for buildings in warm climates where indoor-outdoor air temperature differences are low.

***3) Combined wind and stack forces***

Wind and stack forces usually act simultaneously on a building under a real situation and the airflow through a building is determined by their combined effects (Awbi, 2003). Wind and stack may operate to either reinforce or to oppose each other. The two pressures will increase the airflow if both pressures have the same sign, while negative results will occur if both pressures have opposite sign (Figure 2-4a and b). These combined effects depend on: i) the position of building inlet and outlet openings with respect to external wind direction (Givoni, 1976, Klevien, 2003, Awbi, 2003, Larsen and Heiselberg, 2008); ii) air temperature difference between indoor and outdoor environment; and iii) the effective opening area (Givoni, 1976, Santamouris and Asimakopoulos, 1996). Upward airflow can be found in a building when both wind and stack effects assist each other, while either upward or downward airflow may be found when both effect obstruct each other depending on the combination of wind and stack pressures (Awbi, 2003).

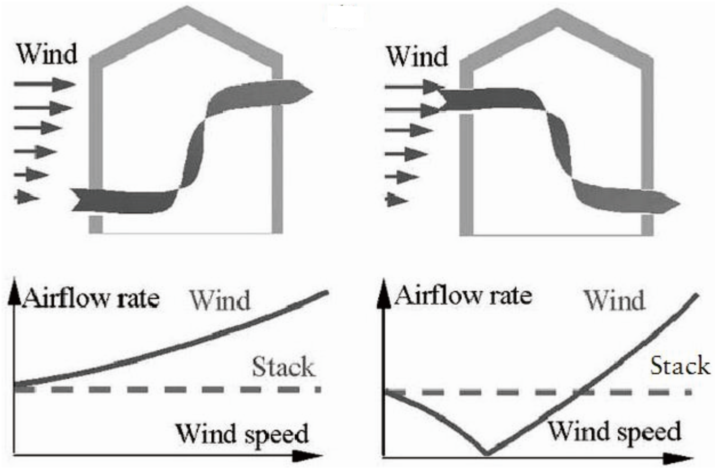

(a) (b)

**Figure 2-4** Combined effects of wind and stack forces: (a) adding effects of wind and stack forces; and (b) obstructed effects of wind and stack forces (Ghiaus and Allard, 2005).

Wind and stack effects create different indoor airflow patterns due to their inertia (Awbi, 2003). When wind force is dominant or when it is the only force, air speed has high velocity for the same air mass quantity (Givoni, 1976), and the airflow distribution is relatively easier to control by opening design, especially an inlet (Awbi, 2003). When wind effect is either absent, insufficient (external wind speed is below 2ms$^{-1}$ (Allocca et al., 2003)), or impractical (e.g. in single-sided ventilated buildings), stack effect will be the dominant force. However, the internal air speed due to stack force is usually much weaker, especially at the inlet, which is insufficient to produce any cooling effect for the occupants in hot-humid climates. Moreover, stack dominated airflow pattern is hard to control by building design as its inertia force is relatively small and not significant to direct the flow.

In this study the major aim is to develop a natural ventilation strategy that can produce a physiological cooling effect and improve the occupants' comfort. In order to do so, air movement with high velocity (*ms*$^{-1}$) rather than high mass flow rate (*kgs*$^{-1}$), or volume flow rate (*ls*$^{-1}$ or *m*$^{3}$*s*$^{-1}$), is the most significant criterion. Natural ventilation that is driven mainly by wind force is therefore, preferable.

### *2.2.3 Natural ventilation principles*

Natural ventilation principles indicate the characteristics of the relationship between indoor ventilation and its outdoor environment. It shows how the natural mechanisms are applied to ventilate a building and how air is introduced into and exhausted from the building (Klevien, 2003). Principles of natural ventilation can be classified into three main groups i.e. single-sided, cross and stack ventilation (Figure 2-5).

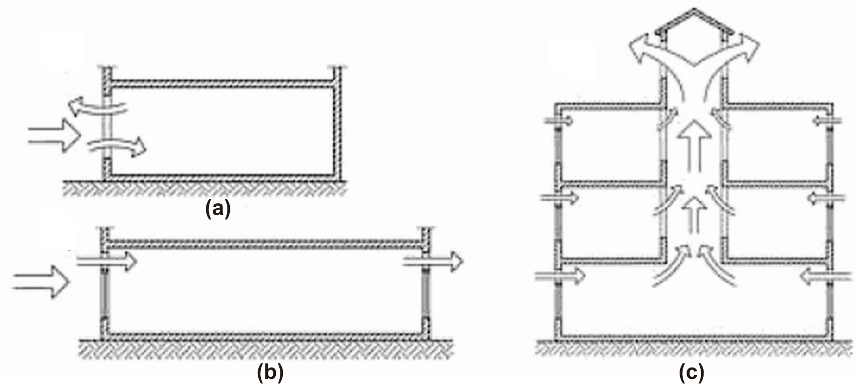

**Figure 2-5** Natural ventilation principles: (a) single-sided ventilation; (b) cross ventilation and (c) stack ventilation (Awbi, 2008).

***1) Single-sided ventilation***

Single-sided ventilation is the principle when natural ventilation enters and leaves a building either from the same opening, or from another opening(s) that is situated on only one side of the ventilated space (Awbi, 2003, Awbi, 2008) (see Figure 2-5a). Typically, airflow in a single-sided ventilated building is driven by the combined wind and stack forces, which are influenced by external wind speed and indoor-outdoor air temperature difference (Larsen and Heiselberg, 2008). When external wind speed is low and stack effect is dominant, outdoor air is driven into a building through the lower opening and driven out of a building from the upper one. On the other hand, airflow with relatively high velocity and reversed direction may occur when the wind effect is dominant and the stack effect is diminished. However, this is also a dependence on the vertical location of the room in the building block. For example, in the study by Allocca et al. (2003) the studied room was located in the middle level of the 3-storey building and a reversed flow was found when the external air speed became greater than 3 ms$^{-1}$ and up to 8 ms$^{-1}$ (Allocca et al., 2003). This wind-dominated airflow commonly occurs during the summer period in hot-humid countries when external wind speed is relatively strong, while indoor-outdoor air temperature difference is relatively low.

Another contributing factor for determining the single-sided ventilation's performance is opening design (numbers and locations of openings). In a room with a single opening, particularly a small one, wind force is dominant and the performance is, therefore, mainly dependent on external wind conditions (speed and directions). In order to add the effectiveness of the principle to increase indoor air velocity, a single-sided room is recommended to have more than one opening located at different heights in the room so as to obtain an additional effect from stack force (Allocca et al., 2003). In such case high velocity can be found at the lower openings and the air would flow upwards before it leaves a building through the upper opening with a relatively weaker velocity (Eftekhari et al., 2003).

Although single-sided ventilation is simple and widely employed, it has some drawbacks. It has uncontrollable flows, usually only low air velocities, and is found to be effective only over a short distance from the opening. The UK Building Research Establishment or BRE (2005), CIBSE (1997) and numerous studies (Awbi, 2003, Awbi, 1998, Klevien, 2003, Ghiaus and Allard, 2005) have suggested a maximum room depth of 2 or 2.5 times the floor-to-ceiling height or a distance of less than 6m for a single-sided ventilated room to ensure healthy indoor air quality. However, such an airflow would be very weak and single-sided ventilation is, therefore, suitable only for providing healthy indoor environment, but cannot provide the required velocity for producing a cooling effect or comfort in buildings in hot-humid climates.

### ***2) Cross ventilation***

Cross ventilation or two-sided ventilation is a principle whereby air enters into a room (or a building) from an opening(s) on one side, sweeps through the indoor space and leaves the room through an opening(s) on another side (which is located either on the opposite wall or the adjacent wall) (see Figure 2-5b) (Awbi, 2003). In a cross-ventilated room, external air is typically driven in the room through windward openings and driven out through leeward openings mainly due to wind force. In this case stack force may help in driving indoor air only when there is a significant vertical distance (height) between the openings in the room.

According to CIBSE (1997) cross ventilation is suggested to be effective even for a room with a deep-plan up to 12m (Awbi, 1994), or the depth of 2.5 times to 5 times the room ceiling height (Klevien, 2003, Awbi, 2003). Cross ventilation is also recommended as a simple and most effective natural ventilation principle for buildings in hot-humid countries to remove internal heat and to improve human thermal comfort by increasing the physiological cooling effect (Givoni, 1976, Awbi, 2003, Ghiaus and Allard, 2005). Compared to a single-sided ventilated room, a room with cross ventilation has airflow with a much greater velocity. Givoni (1976) found that the average velocity in a single-sided room could be 10%-15% of the external wind speed, while in a cross ventilated room it could be 30% to 50% depending on size and position of the openings regarding to the prevailing wind speed and direction, and the axis between the inlet and the outlet openings (see Table 2-1).

**Table 2-1** Average indoor air velocity in a room with single-sided and cross ventilation as a percentage of external wind speed (Givoni, 1976).

| Natural ventilation principle | Location of openings | Wind direction (Incident to opening(s)) | Total width of openings/ Indoor air velocity as percentage to external wind speed (%) | | | |
|---|---|---|---|---|---|---|
| | | | 2/3 of the wall | | 3/3 of the wall | |
| | | | Average | Maximum | Average | Maximum |
| Single-sided ventilation | Single opening in pressure zone | Perpendicular | 13 | 18 | 16 | 20 |
| | | Oblique | 15 | 33 | 23 | 36 |
| | Single opening in suction zone | Oblique | 17 | 44 | 17 | 39 |
| | Two opening in suction zone | Oblique | 22 | 56 | 23 | 50 |
| Cross ventilation | One opening in pressure zone and another in adjacent wall | Perpendicular | 45 | 68 | 51 | 103 |
| | | Oblique | 37 | 118 | 40 | 110 |
| | One opening in pressure zone and another in suction zone | Perpendicular | 35 | 65 | 37 | 102 |
| | | Oblique | 42 | 83 | 42 | 94 |

According to Table 2-1 air velocity in a single-sided room is very small and much lower than that in a cross-ventilated room for both wind directions. The best result for a single-sided ventilation room occurs when there are two openings in suction zone under oblique wind incident angle. However, these are still smaller than the worst result of the cross ventilated room (comparing the average velocity of 23% in single-sided ventilated room and 35% in cross ventilated room).

The performance of cross ventilation is subjected to many factors includings: i) external wind speed; ii) building orientation ragarding to the prevailing wind direction; iii) building geometries; and iv) the size and position of inlet and outlet openings. Melaragno (1982) has proposed a guideline for estimating the average indoor air velocity in a cross ventilated room without internal partitions under different wind directions as a function of opening sizes (Table 2-2) (Allard, 1998)

**Table 2-2** Average indoor air velocity in a cross ventilated room with different opening sizes under two wind directions (Melaragno (1982) cited in (Allard, 1998).

| **Wind direction** | **Opening sizes according to the wall's width** | | **Average indoor air velocity as percentage to external wind speed (%)** |
|---|---|---|---|
| | **Inlet width** | **Outlet width** | |
| Perpendicular | 1/3 | 1/3 | 35 |
| | 1/3 | 2/3 | 39 |
| | 1/3 | 1 | 44 |
| | 2/3 | 1/3 | 34 |
| | 2/3 | 2/3 | 37 |
| | 2/3 | 1 | 35 |
| | 1 | 1/3 | 32 |
| | 1 | 2/3 | 36 |
| | 1 | 1 | 47 |
| Oblique (45˚) | 1/3 | 1/3 | 42 |
| | 1/3 | 2/3 | 40 |
| | 1/3 | 1 | 44 |
| | 2/3 | 1/3 | 43 |
| | 2/3 | 2/3 | 51 |
| | 2/3 | 1 | 59 |
| | 1 | 1/3 | 41 |
| | 1 | 2/3 | 62 |
| | 1 | 1 | 65 |

According to the study, average air velocity was found to increase with the openings' width and the best result occurred in the case with the maximum inlet's and outlet's width i.e . inlet and outlet widths were equal to the room wall's width. It was also, found that a room under an oblique wind direction had a relatively better result for average air velocity than that under a perpendicular wind for almost every opening size. This finding has comfirmed the proposal stated by Givoni (1976), where a building was suggested to be orientated obliquely to the prevailing wind direction. Givoni (1976) also suggested to position the openings at adjacent walls, instead of on opposite walls. This was because when two openings were at opposite walls, external air would be driven straight from the inlet to the outlet and, therefore, would ventilate only a limited section of the room between the two openings (Figure 2-6a). On the other hand, the intake air would be driven with wider recirculation and higher average velocity when the airflow changes its direction within the room when the two openings are located on adjacent walls (Figure 2-6b).

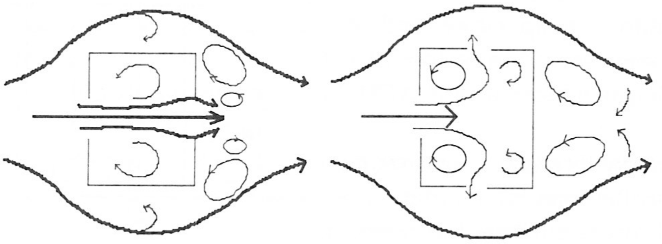

(a) (b)

**Figure 2-6** Airflow pattern in and around a building (a) with two openings on opposite walls; and (b) with two openings on adjacent walls (Santamouris and Asimakopoulos, 1996).

Also, Tantasavasdi et al (2006) investigated air velocity in a room with different principles in a typical two-storey house in Bangkok using CFD code (*PHOENICS*), and found that cross (two openings on opposite walls) and two-sided ventilation (two openings on adjacent walls) produced much higher average air velocities than single-sided ventilation. However, relatively higher average indoor air velocities with an even distribution were found in a cross ventilated room, rather than in two-sided ventilated room with the same effective opening areas, as that was suggested in Givoni (1976) (Figure 2-6). This different result might be because of the different tools employed for these two studies. While air velocities were measured only for a few locations by Givoni, due to the limitation of the small-scale experiment in a wind tunnel, the velocities throughout the room were calculated using CFD. In Tantasavasdi et al's study openings on opposite walls could make the airflow evenly distributed which, therefore, produced higher average velocities across the room. Also, according to this study, the average air velocity in a room with openings on adjacent walls decreased when the effective opening area increased beyond 20% of the room floor area due to the short circuit when the incoming air moves directly out of the room from the inlet through the outlet (Tantasavasdi et al., 2006).

According to the literature reviewed here cross ventilation, particularly that in a room with two openings on opposite walls, one in the windward side and the other is in the leeward side, is favourable for producing evenly distributed airflow with high velocity that is sufficient to improve thermal comfort conditions in buildings in hot-humid climates.

### ***3) Stack ventilation***

Stack ventilation is a useful principle when the required indoor air movement cannot be achieved solely by wind effect. In such situations stack effect can be used as an additional driving force. However, stack pressure is rather small and either large openings or more than one opening at different heights are required to ensure a good result. Stack ventilation is therefore useful for a building with great height space such as that with atria or a stack (see

Figure 2-5c). Employing a stack or vertical shaft with opening(s) that extends above a building may be, therefore, useful for a high-rise building with deep-plan layout (comparing Figure 2-5b and Figure 2-5c). This is due to the high pressure-difference increased by the induced negative pressure at the stack opening(s). As a result, internal air is driven upwards due to the high pressure-difference between the inlet (building window) and the outlet (exhaust at the stack-top). This principle is also useful regardless of building orientation related to prevailing wind direction, as its performance was found to be relatively independent of wind direction (Santamouris 2005).

However, stack ventilation can produce uncontrollable indoor air movement with only small velocity. This principle is, therefore, useful only to maintain healthy indoor air quality, and provide occupants' favourable breeze when indoor air temperature and the ambient air temperature are within an acceptable range, but cannot improve human comfort in hot-humid regions.

### *2.2.4 Summary*

Building ventilation systems have three significant functions in building design i.e. to provide healthy air, to produce thermal comfort to indoor living spaces, and to cool the building's structures. These systems may be naturally or mechanically driven. However, natural ventilation systems have become favored as they can provide high indoor environmental quality and are the occupants' preference, while consuming much lower energy. Natural ventilation systems employ naturally produced pressure differences due to wind and/or stack forces to drive air though a building. While the former mechanism drives the air from the building pressure zone to the building suction zone, the latter mechanism draws the hotter air to rise up and draws the colder external air into the bottom part of a building. These two driving forces may reinforce or oppose each other in a real situation depending on their combination. When wind force is dominant, airflow with much greater velocity can be expected. Conversely, airflow driven by stack force is hard to control, due to its relatively small inertia, and has much weaker velocity. For buildings in hot-humid countries cross ventilation is thus recommended as the most useful principle for improving indoor comfort conditions. As its dominating driving force is wind effect, cross ventilation can provide high indoor velocity that is required for producing cooling effect for the occupants under such climatic conditions. However, when cross ventilation is not possible additional natural ventilation induced strategies may be required.

## 2.3 Natural ventilation induced strategies

### *2.3.1 Introduction*

The main characteristics of hot-humid climates include high ambient air temperatures, high relative humidities (RH), small diurnal air temperature ranges throughout the year, low average wind speeds, and a small range of average monthly air temperatures (which do not exceed 1°C to 3°C (Givoni, 1976), or 5°C (Szokolay, 2004)). For these particular conditions there are two principal strategies that are crucial for improving indoor thermal conditions including: i) preventing indoor air temperatures rising during the hot day; and ii) providing continuous air movement at a high velocity to produce a cooling effect (Givoni, 1976, Lei, 2009), which is the main objective of this study.

In a situation when basic natural ventilation principles involving single-sided, cross and stack ventilations explained above are impossible or ineffective to provide the required continuous and high velocity airflow, additional strategies may be introduced to improve natural ventilation potential for providing comfortable indoor environments.

In this section natural ventilation induced strategies including wing-walls, wind-towers and solar ventilation strategies, are reviewed and discussed in order to attain the crucial knowledge for developing the ventilation strategy for improving indoor thermal environment in a residential building in hot-humid climates, which is the study's aim.

### *2.3.2 Wing-walls*

The wing-wall, a strategy proposed by Givoni in 1962 (Givoni, 1994), is suggested for enhancing natural ventilation in a building where cross ventilation is impossible – for example, a room with only one external wall. Such a room could have very poor indoor airflow due to its small stack pressure difference. However, an effective air movement as that found in a cross ventilated room is still possible, even when the prevailing wind direction is at a very small angle (nearly parallel) to the main façade, by employing wing-walls (Givoni, 1976, Givoni, 1991, Givoni, 1998).

Givoni (1976, 1991, 1998) has proposed the strategy called '*wing-walls'* or external vertical projections to be installed at two openings, which are positioned at the upwind and downwind side of a single-sided room (see Figure 2-7b). This creates high positive pressure (+ in the Figure) in front of the first opening, which acts as an inlet, and negative pressure or suction (- in the Figure) in front of the other opening, which acts as an outlet. As a result of high artificial pressure difference between the two openings, external air is driven into the room through the first opening and extracted through the second opening, creating cross ventilation (Givoni, 1976, Givoni, 1991, Givoni, 1998). This principle may be also useful for inducing indoor air movement in a room with more than one external facades as can be seen in Figure 2-7a and c.

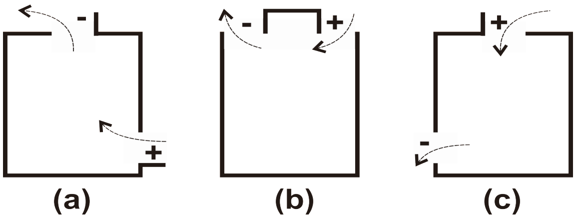

**Figure 2-7** Different principles of the wing-wall [adapted from (Allard, 1998)].

There are studies that have investigated the performance of wing-walls using small-scale models and wind tunnel (Givoni, 1976, Givoni, 1991), and Computational Fluid Dynamics (CFD) modeling software (Mak et al., 2007, Liu, 2006). It was found that wing-walls could significantly increase indoor air movement in a building with single-sided ventilation, particularly when the prevailing wind direction is oblique to the building main façade. In the study of Givoni (1976) average indoor air velocity in a room with wing-walls was found as 36% of the reference external wind speed (wind incident angle - $\theta$ of 45˚), while that in a room with two openings but without wing-wall, and a room with only one central opening with the same operable area were found as only 15.7% and 3.3%, respectively (comparing the middle picture in the first, the second and the third row in Figure 2-8). A similar trend was also found in the study of Mak et al (2007). Based on the CFD simulation (FLUENT), the average indoor air velocity in the room with wing-wall was found in the study to be as high as 40% of the ambient wind speed (under wind incident angle of 45˚). Conversely, an average air velocity only 15% of the ambient wind speed was found in the room without a wing-wall (Mak et al., 2007).

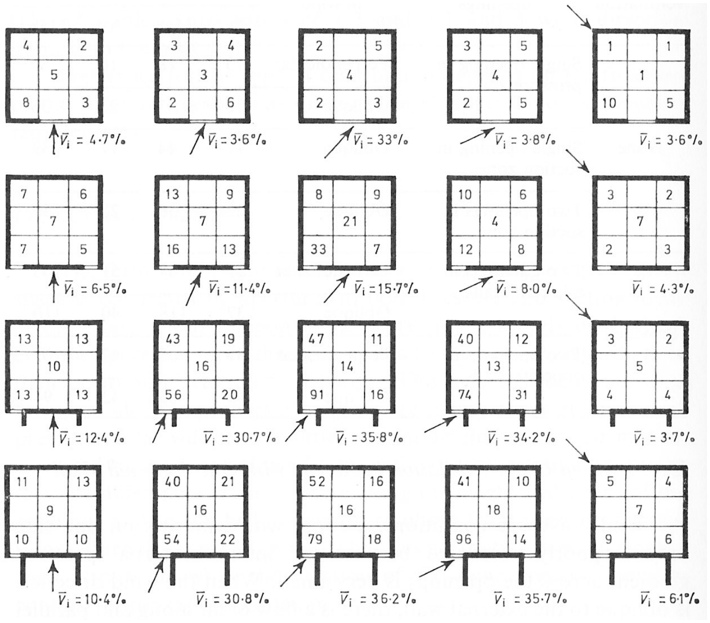

**Figure 2-8** Average air velocity in a room with different opening designs as a percentage of the external wind speed: (first row) a room with one opening; (second row) two openings; (third row) two openings with normal wing-walls and (fourth row) two openings with extended depth wing-walls (Givoni, 1976).

The effectiveness of wing-walls depends greatly on external wind conditions i.e. wind speed and wind direction according to the openings (Givoni, 1976, Liu, 2006, Mak et al., 2007). High external wind speed and oblique wind incident angle are suggested to produce the best results of indoor air movement i.e. high average velocity and air change rate. Incident wind angles ranging between 20˚ and 70˚ to the main facade (Givoni, 1976), particularly at 45˚ (Liu, 2006, Mak et al., 2007), was found to provide the highest average air velocity (see Figure 2-9 and 2-10). As found in Mak et al (2007), average velocity increased when incident angle moved away from 0˚ and reached its maximum at 45˚ before gradually reducing when incident angles were 67.5˚ and 135˚ (Figure 2-10) (Mak et al., 2007). At the same time it was found in the same studies (Givoni, 1976, Mak et al., 2007) that opening size and wing-wall depth had no significant influence on the strategy's performance i.e. similar average velocities were found across different opening widths and wing-wall depths for various wind incident angles.

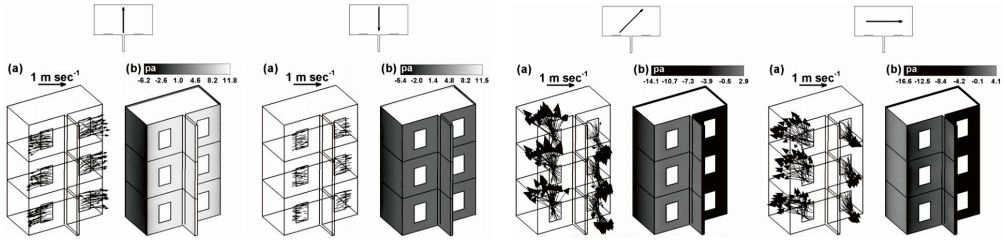

(a) (b) (c) (d)

**Figure 2-9** Airflow vectors and static pressure on a building main façade with wing-wall under external wind speed of 1ms$^{-1}$ and various incident wind angles: (a) 0° incident angle or external wind direction perpendicular to the building main façade; (b) 180°; (c) 45° and (d) 90° (Liu, 2006).

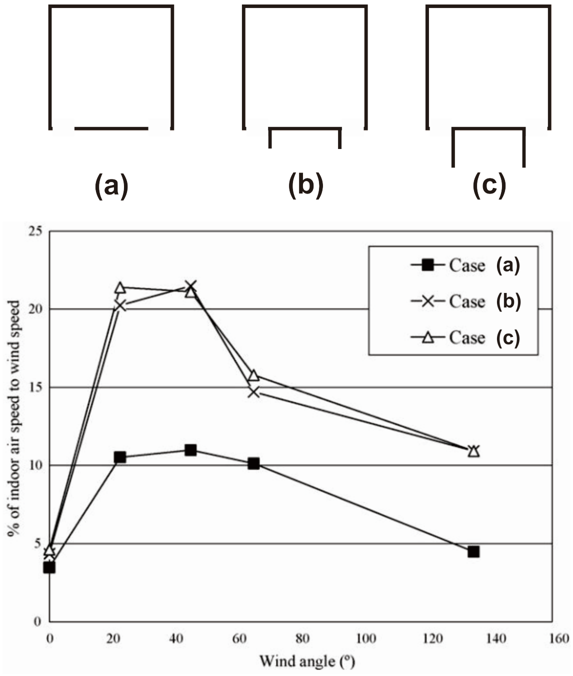

**Figure 2-10** Average air velocity in a room with and without wing-walls for different wind incident angles as a percentage of external wind speed: case (a) a room without a wing-wall; case (b) a room with two openings and a wing-wall depth of 1/3 width of the wall; and case (c) a room with a wing-wall of depth double the opening width (adapted from Mak et al., 2007).

According to the above studies the wing-wall is an effective wind-induced strategy to induce indoor air velocity. This is especially true for a single-sided ventilated room as it successfully increases the average velocity in the room to as high as 36% of the ambient wind speed, which is in the same range of that produced in a cross ventilated room i.e. 30%-50% (Givoni, 1976). Creating high wind pressure differences across inlet and outlet openings is, therefore, a crucial technique to successfully induce indoor air movement to meet the required velocity.

### *2.3.3 Wind-towers*

Traditional passive cooling wind-tower systems have been used in the hot climates of the Middle East and Eastern Asia for centuries (Ghiaus and Allard, 2005). It is sometime called '*wind catcher*' in the literature as it catches cool outdoor wind from the higher elevation and directs the air downwards into a living space based on wind force. This strategy employs a vertical shaft as low as 2m to as high as 20m above a building roof level with opening(s) located close to its top and at the building level (Bahadori, 1994). The shaft is, therefore, a connection between an internal space and the external environment.

The traditional wind-tower employs both wind and stack effect to capture stronger and cleaner air (less dust) above the ground and drives it into a building. It is suggested as a suitable strategy for hot-arid climates where daily variations in temperature are high i.e. high air temperature during daytime and low during nighttime (Bansal et al., 1994a). The strategy is also useful for buildings that are located in a dense area where buildings are situated very close to each other and having more than one opening in a room is limited.

During the early time of a day, when the tower's walls are still cool as they store the coolness from the night, a downdraught is created. Cool external air is driven into the building through the opening on top of the shaft (inlet), sinks to the building level and is then exhausted through the building opening(s) (outlet), which may be in the tower itself or in the building to encourage cross flow through the main activity area (Khan et al., 2008, Bansal et al., 1994a) (see Figure 2-11a). During the night, the reverse flow direction occurs as the internal air is heated up by the warm surface of the rooms and the tower. It is then driven upwards through the tower due to buoyancy, creating an up-draught (Allard, 1998) before it is exhausted from the building through the tower openings, which now become outlets (Bansal et al., 1994a) (see Figure 2-11b). For the latter case (an up-draught) the wind tower works as a wind extractor to exhaust the comparative hotter air to the ambient, which can be advantageous for warm-humid climates (Gonzalez-Trevizo et al., 2013). However, it is important to ensure that the ambient temperature does not exceed 37°C.

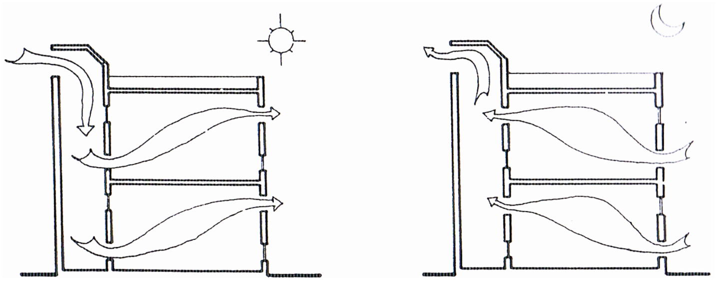

**Figure 2-11** Operating principles of wind-tower system: (a) a downdraught during daytime; and (b) the reverse updraught during nighttime (Bansal et al., 1994a).

The effectiveness of wind-towers is determined by various factors including: i) the incidence angle at the inlet and the outlet openings (Khan et al., 2008); ii) the openings size and locations (Ghiaus and Allard, 2005); and iii) the tower geometries i.e. height, cross sectional area and shape of the tower (Bouchahm et al., 2011, M.H. et al., 2014). To ensure a good result, inlet and outlet openings are suggested to be located at the windward and the leeward sides of a building, respectively, to take advantage of additional wind effects due to high wind pressure differences across the openings (Allard, 1998). The high location of the tower openings is also suggested for ensuring high inlet wind pressure and the insensitivity to external wind direction (Ghiaus and Allard, 2005, Bansal et al., 1994a).

However, the traditional wind-tower is expensive to build and maintain. Also, intake air quality and quantity are difficult to control as a short circuit may occur when the intake air flows out of the tower through another tower opening. Conventional wind-towers, thus, are not suggested for an area with very low wind speed i.e. average wind speed less than 4ms$^{-1}$ (Bahadori, 1994, Bahadori et al., 2008). Moreover, wind and stack forces may oppose each other, which results in even lower indoor airflow rates. As a result, improved designs of wind-tower were proposed. By integrating with other advanced technologies and other systems, modern wind-towers are more effective in producing indoor comfort conditions (Khan et al., 2008). Automatic control dampers, for example, are employed for preventing any short circuits when there is more than one opening in the tower. Modern wind-tower may be also incorporated with:

i) evaporative cooling systems e.g. wetted column and wetted surfaces inside the tower, evaporative cooling pads at the top of the tower (Bahadori, 1994, Bahadori et al., 2008), and a pool at its bottom (Bouchahm et al., 2011) to reduce indoor air temperature and to increase indoor relative humidity, particularly in hot-arid climates;

ii) solar collectors or solar chimney (Hughes et al., 2012), which helps promoting stack effect ventilation during the low-wind period;

iii) other air intakes or/and air extractor devices to induce indoor air velocity e.g. PV powered fan (Hughes et al., 2012).

Furthermore, wind-tower systems can be re-designed based on their original form. A wind-tower with a Venturi-shaped roof and a disc-shaped roof (*VENTEC*), for instance, employ a typical wind-tower with a shaped-roof on the tower-top (Figure 2-12) (Haw et al., 2012, Blocken et al., 2011). These roofs create the Bernoulli Effect with positive pressure above and negative pressure below the roof which sucks the air out of a building through any openings at the top of the tower (see Figure 2-12a). As a result higher indoor airflow can be expected regardless to high pressure-difference between the inlet and the outlet openings. Empirical studies investigated the performance of wind-induced wind-tower with designed-roofs and found that they effectively induce indoor airflow rate (Blocken et al., 2011, Hooff et al., 2011, Haw et al., 2012). Haw et al (2012) examined the effectiveness of a wind-tower with a Venturi-shaped roof and the system was revealed to successfully induce an extraction flow rate and air changes per hour (ACH) in the experimental house under the hot-humid climate of Malaysia (Figure 2-12b). The extraction flow rate and air changes per hour were measured as 10,000$m^3h^{-1}$ and 57ACH under the reference wind speed of 0.1$ms^{-1}$, which was much higher compared to the 20ACH under the reference wind speed of 1$ms^{-1}$ that was obtained in the case with the wind-tower only (Bansal et al., 1994a, Bahadori, 1994).

**(a)** **(b)** **(c)**

**Figure 2-12** Wind-tower with Venturi-shaped and disc-shaped roof: (a) the Bernoulli Effect of the designed roofs (inverted airplane wind profile); (b) a house with venturi-shaped roof (Haw et al., 2012); and (c) a reduced-scale building with a VENTEC roof (Blocken et al., 2011).

Although traditional wind-towers employ both wind and stack forces, it is suggested that they are suitable for hot-arid climates where the diurnal temperature range is high and not suitable for an area where average ambient wind speeds are less than 4$ms^{-1}$. For hot-humid climates, where there is low diurnal temperature range and low prevailing wind speeds, this strategy seems not to be favourable. However, the idea of increasing negative pressure, and so the pressure difference between the inlet (buildings' openings) and the outlet (openings below the Venturi-shaped roof or disc-shaped roof) is a very interesting idea, which seems to have high potential to induce indoor air velocity for a building in hot-humid regions.

### *2.3.4 Solar ventilation strategies*

Solar ventilation or solar-induced ventilation strategies refer to the strategies that employ stack force due to solar radiation heating to enhance indoor natural ventilation. The concept of solar ventilation has been applied to buildings for several centuries in different climates, including hot-humid. During a hot and windless day, when wind and stack forces are weak and insufficient to create the required air movement, specially designed building elements e.g. solar walls, solar chimney, and ventilated (or double-skin) façade may be operated for maximizing indoor-outdoor temperature differences, and thus the stack effect (Bansal et al., 1994a, Khanal and Lei, 2011). Solar ventilation strategies basically employ a chimney or a channel (vertical or inclined) with an air gap in between the two panels involving: i) a solar collector (solar wall or storage wall) to maximize the absorptance and minimize the emittance of solar radiation that reaches the surface; and ii) a transparent cover with high solar transmissivity to maximize solar heat gain (Zhai et al., 2011). The principal driving mechanism of airflow is stack force (Gan, 2006). The air in between the channel is heated up and rises due to the heat that is obtained from solar radiation and stored within the solar wall. This hot air is then exhausted through the outlet at the chimney's top. However, it should be noted that this stack induced ventilation is different from that due to normal internal heat gain in a building. This is because typically it is recommended to keep a building's air temperature as relatively low as possible so as to avoid indoor thermal discomfort due to overheating. Conversely, these solar ventilation systems are specially designed to be hot but to be isolated from the building's occupied area to maximize indoor ventilation without creating discomfort due to internal heat (Bansal et al., 1994a).

Solar ventilation strategies can be employed for different purposes i.e. heating, ventilating and insulation, depending on the details of the systems (Zalewski et al., 2002, Zhai et al., 2011, Chan et al., 2010) (Figure 2-13). However, the heating and insulting modes are beyond the scope of this study and, therefore, only the natural ventilation mode to induce indoor air movement will be discussed.

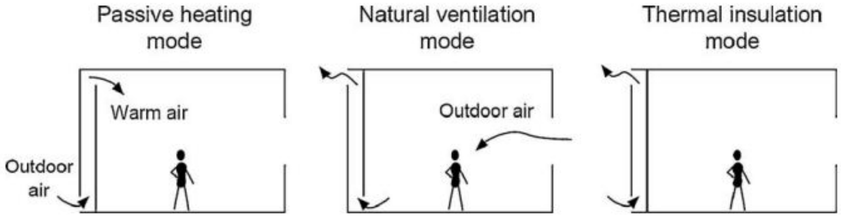

**Figure 2-13** Different modes of solar ventilation strategies (Chan et al., 2010).

***1) Solar walls***

Solar walls employ a glazing pane as an outer layer covering a building façade. It is typically used as a passive heating technique in cold climates as it can trap and transmit heat from solar radiation efficiently into a specified room (Sadineni et al., 2011). However, it can be also be employed as a passive cooling strategy by protecting a building from direct solar radiation (insulation mode) and enhancing indoor air movement, which is the main focus of the study.

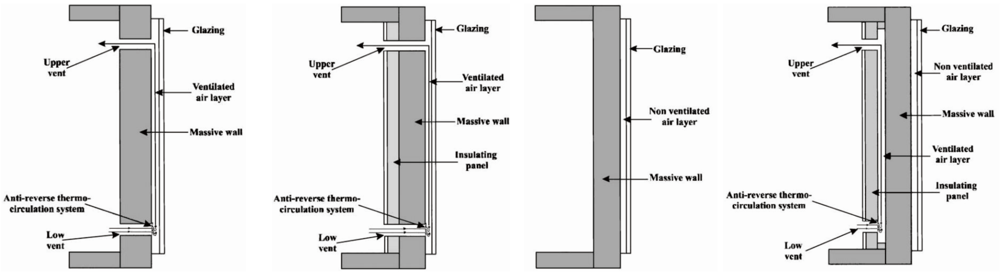

(a) (b) (c) (d)

**Figure 2-14** Different types of solar walls: (a) Standard Trombe-wall; (b) Insulated Trombe-wall; (c) Non-ventilated solar wall and (d) Composite solar wall (Zalewski et al., 2002).

There are four main types of solar wall: i) standard Trombe-wall; ii) insulated Trombe-wall; iii) non-ventilated solar wall; and iv) composite solar wall (see Figure 2-14). The standard Trombe-wall (Figure 2-14a) was introduced by Trombe in the 1960s (Zalewski et al., 2002). It principally consists of three main elements: i) a heavy masonry wall, which is painted black on the external surface and acts as a solar collector; ii) a glass cover to trap infrared radiation; and iii) an air channel in between the two panels, which can be connected to the room using two vents – one at the bottom and the other at the top of the wall (Arumi and Hourmanesh, 1977). The original Trombe-wall was found to successfully save about 70% of annual building energy used due to heating and cooling systems in temperate regions (Arumi and Hourmanesh, 1977).

After the standard Trombe-wall was introduced various modifications have been made in order to improve the system's performance. First, the insulation layer is installed on the inner surface of the massive wall (Figure 2-14b) to improve the thermal resistance of the Trombe-wall and to avoid excessive overheating due to south-facing glazing (Chan et al., 2010, Zalewski et al., 2002). Later, the composite solar wall (or Trombe-Michel wall) was introduced (Figure 2-14d). This system is similar to the Insulated Trombe-wall except it has a ventilated air layer between the insulation layer and the massive wall to improve the system's performance to reduce solar heat gain and overheating through the building façade during hot summer days by using both insulation layer and air layer as the thermal resistance. The performance of solar walls is found to depend on: i) the design and configuration of a building especially the building orientation according to the sun path; and ii) the detail and the operation of the system, particularly the material properties and thickness of the massive wall (Arumi and Hourmanesh, 1977, Zalewski et al., 2002). Different types of solar wall are also found to be suitable for different purposes under particular climatic conditions. A comparative study among different types of solar wall is, thus, recommended before applying the system to ensure its suitability for each specific case (Zalewski et al., 2002).

For hot-humid climates solar walls may be used as insulation (Figure 2-15c) and to maximize indoor air movement when the upper vent is closed while the adjustable damper installed at the upper part of glazing is opened (Figure 2-15a and b). For such a case the stack force generated by the solar heated air due to convection and radiation from the massive solar wall draws hot internal air from the lower vent out to the ambient through the outlet (with damper) (Chan et al., 2010). However, it should be noted that these systems are based on stack force, which may be useful to provide acceptable indoor air quality but may not be able to create the required air velocity for producing a cooling effect and comfort for hot-humid countries.

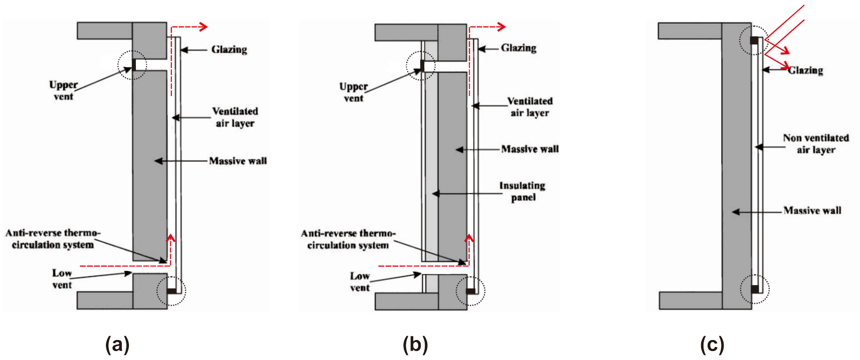

**Figure 2-15** Diagram of airflow in solar walls with different modes: (a) and (b) indoor ventilation enhancing mode in a Standard Trombe-wall and in Insulated Trombe-wall and; and (c) solar radiation protection mode (adapted from Zalewski et al., 2002).

### *2) Solar chimneys*

A solar chimney works on a similar mechanism to solar walls. It employs glazing to be installed in the south wall (vertical) or in a building roof (inclined) to enable solar energy to be collected in the absorber wall and enhance pressure difference between the inlet (a building opening) and the outlet (at the chimney top). External air enters the building through the inlet and it is driven through the chimney due to stack force before being exhausted through the chimney outlet (Chungloo and Limmeechokchai, 2007, Nugroho, 2009, Chan et al., 2010, Zhai et al., 2011) (Figure 2-16). A solar chimney can be vertical or inclined (Figure 2-16) at some suitable angle to capture maximum solar radiation (Mathur et al., 2006). While the vertical absorber can be integrated on a building façade at any building level, inclined absorbers are commonly mounted on a building rooftop, so that it is also called ‘*roof solar chimney’* (RSC).

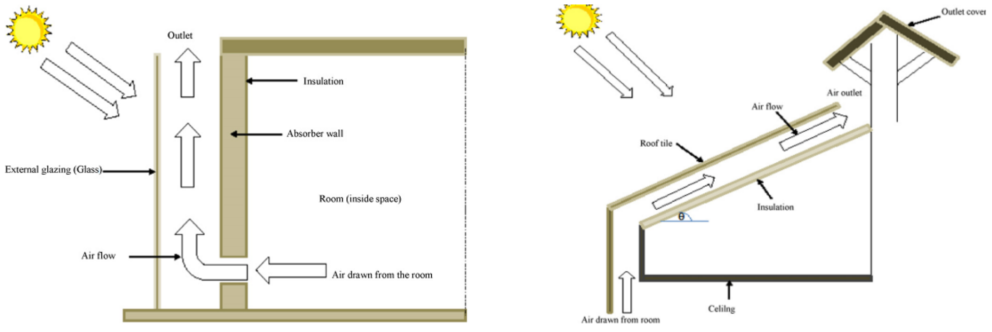

**(a)** **(b)**

**Figure 2-16** Solar chimney principle and main elements: (left) wall solar chimney and (right) inclined roof solar chimney (Khanal and Lei, 2011).

Extensive studies have investigated the performance of solar chimneys under different climates, including hot-humid climates, and have identified the system’s optimal geometries and construction characteristics for minimizing indoor air temperature and maximizing indoor airflow rate (Khedari et al., 1997, Khedari et al., 2000a, Khedari et al., 2000b, Hirunlabh et al., 2001, Pavlou et al., 2009, Nugroho, 2009, Punyasompun et al., 2009). Solar radiation is found to be the most influential external factor for determining the chimney performance (Mathur et al., 2006, Wong and Heryanto, 2004); while the orientation (vertical solar chimney) and the inclination (inclined or roof solar chimney) of the system absorber according to the building’s latitude are the most significant internal factors (Mathur et al., 2006, Harris and Helwig, 2007, Chungloo and Limmeechokchai, 2007, Pavlou et al., 2009, Khanal and Lei, 2011). According to these findings the inclined solar chimney is, therefore, suggested to be preferable to the vertical chimney for hot-humid climates. This is because the inclined solar chimney is able to receive higher solar radiation levels due to the higher altitude of the sun during summer time (Mathur et al., 2006). The effectiveness of a solar chimney is also influenced by other factors including:

i) the temperature differences between the inlet and the outlet openings (Hamdy and Firkry, 1998);

ii) the system's geometries and configurations i.e. the chimney aspect ratio (stack height/air gap width) (Bansal et al., 1993, Bansal et al., 1994b, Bansal et al., 2005, Gan, 1998, Allocca et al., 2003, Ong, 2003, Nugroho, 2009, Mathur et al., 2006, Afonso and Oliveira, 2000, Wei et al., 2011), the distance between inlet and outlet, aperture areas (ratio between the inlet and outlet area) (Mathur et al., 2006), aperture locations (Punyasompun et al., 2009), and the inclination angle (Khanal and Lei, 2011);

iii) the properties and the thickness of the system components i.e. the solar absorbance of the absorber wall and the solar transmittance of the glazing (Lee and Strand, 2009, Harris and Helwig, 2007).

The basic concept of the solar chimney can also be adapted so as to suit particular situations. For instance, recently a solar chimney with aluminum vertical ducts was introduced for a retrofitted three-storey building in Singapore (Figure 2-17) (Tan and Wong, 2012). This specially designed system was found to effectively increase indoor air velocity by up to 0.4ms$^{-1}$ and 0.6ms$^{-1}$, depending on the position of the duct inlet according to the occupied level above the room floor (Tan and Wong, 2012). Furthermore, a solar chimney can be incorporated with different evaporative cooling systems to create a passive solar cooling effect e.g. a water spraying system (*wetted roof*) (Chungloo and Limmeechokchai, 2007, Chungloo and Limmeechokchai, 2009), a roof pond (*Skytherm*), and an evaporative cooler ceiling (Miyazaki et al., 2011). For such integrated systems, the roof surface temperature is decreased as the water evaporates and, therefore, the room temperature is reduced (Chan et al., 2010).

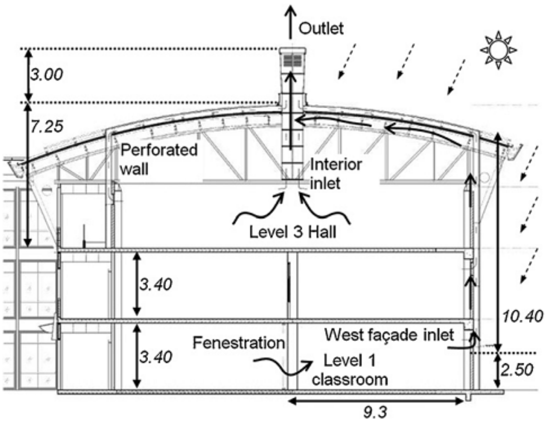

**Figure 2-17** Principle of an aluminum ducts solar chimney to enhance indoor air movement (Tan and Wong, 2012).

Although the solar chimney is found to reduce indoor air temperature and increase indoor airflow rate even when there is no wind, the airflow generated by a normal solar chimney without additional devices was generally found to be very low i.e. less than $0.05ms^{-1}$ (Khedari et al., 2000a) – this is because its main driving force is stack. This velocity is insufficient to produce any cooling effect and thermal comfort under hot-humid climatic conditions of Thailand. Therefore, alternative designs and strategies may be expected to improve this situation (Barozzo et al., 1992).

### *3) Double-skin facades*

The double-skin façade (DSF) is one of the most popular advanced façade systems that have been employed for high-rise buildings, especially in temperate regions. This is due to its aesthetic and its performance for protecting the internal environment from undesirable external conditions e.g. noise, extreme climatic conditions and wind (Oesterle et al., 2001, Gratia and Herde, 2007). Working similarly to other solar ventilation strategies, its key elements involve: i) exterior glazing, which is usually a hardened single glazing; ii) interior glazing, which is mostly an insulating double glazing unit; and iii) air cavity, which may be air tight to act as thermal and acoustic insulation (Oesterle et al., 2001, Gratia and Herde, 2007, Chan et al., 2009) (Poirazis, 2006, Wong et al., 2008), or ventilated to acts as passive ventilation strategy (Oesterle et al., 2001, Wong et al., 2008). In some cases adjustable sun shading devices are also installed in the intermediate space for thermal control (Wong et al., 2008). However, this technique does not employ a massive wall or absorber. On the other hand it uses layers of glazing that allow a visual contact with the surroundings and which admit a large amount of daylight.

A double-skin façade can be grouped according to: i) its form of the divided intermediate space (Figure 2-18); ii) its ventilation types (natural and mechanical); and iii) its airflow concept to suit different applications and seasonal requirements (exhaust air, supply air, static air buffer, external air curtain and internal air curtain) (Figure 2-19) (Oesterle et al., 2001, Haase et al., 2009, Poirazis, 2006). Based on the intermediate space form a double-skin façade can be divided into four main types (Figure 2-18) (Oesterle et al., 2001) involving: i) Box-type window, which consists of a frame with operable external openings that allow intake air to ventilate both the intermediate space and internal rooms; ii) Shaft-box façade, which consists of box-type windows with continuous vertical shafts extending over a building height to ensure an increased stack effect and preferable in terms of insulation against external noise; iii) Corridor façade, of which the intermediate space closed at the level of each building floor and the openings are laid out in staggered form from bay to bay to avoid the short circuit airflow; and iv) Multistory façade with the adjoined intermediate space and large intake and exhausted openings near the ground floor and the roof that requires the mechanical ventilation system behind the façade.

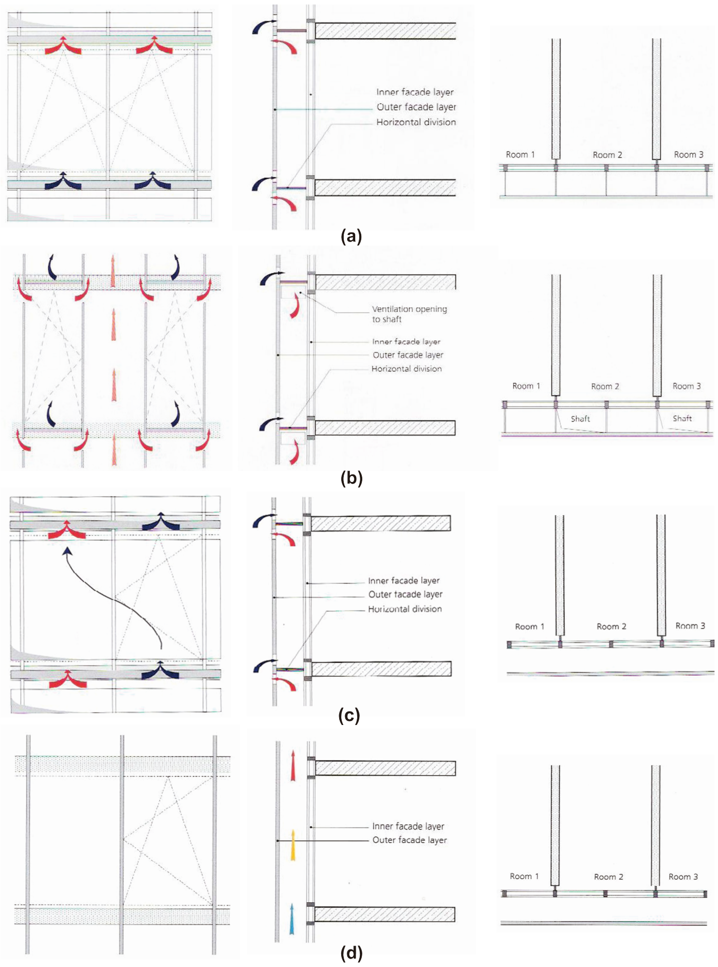

**Figure 2-18** Types of Double-skin façade according to the intermediate space form: Elevation (left), section (middle) and plan (right) of (a) Box-type window; (b) Shaft-box façade; (c) Corridor façade and (d) Multi-storey façade (Oesterle et al., 2001).

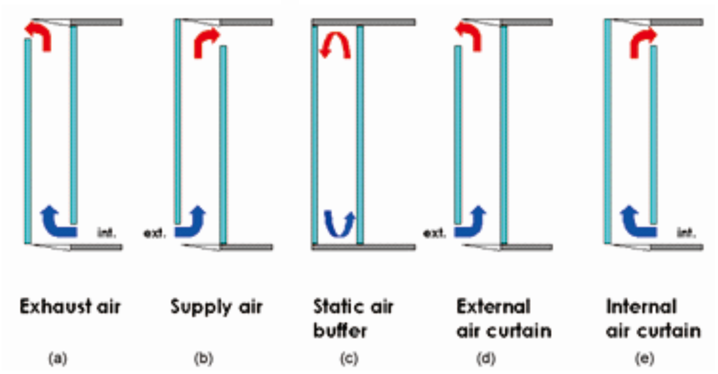

**Figure 2-19** Airflow concepts of double-skin façade: (a) Exhaust air; (b) Supply air; (c) Static air buffer; (d) External air curtain and (e) Internal air curtain (Haase and Amato, 2009).

Different types of double-skin façade are suitable for different purposes under different climates and seasons. Therefore, it is crucial to conduct a comparative study among different forms of intermediate space, airflow concepts and opening modes before employing a double-skin façade to the specific cases. For instance, the double-skin façade type, which performs as insulation, may be useful for buildings in cool climates as it leads to heating load reduction. On the other hand the ventilated double-skin facade that acts as a passive stack-induced ventilation strategy is favourable for buildings in hot-humid regions. This is because it increases the airflow rate within the intermediate space which, in turn, increases the room heat exhausting rate and, therefore, reducing building cooling load. However, it is crucial to ensure that there is a suitable shading device to avoid excessive heat gain due to solar radiation for such cases.

The internal openings between the room and the air cavity in the ventilated system may also be used as the additional outlet openings for inducing room air movement and improving the occupants' thermal sensation. This can be seen from previous studies (Haase and Amato, 2009, Haase et al., 2009, Baldinelli, 2009, Wong et al., 2008). Haase et al. (2009) studied the performance of a ventilated double-skin façade with different glazing types, window sizes and orientations under the hot-humid climate of Hong Kong and found the reduction in annual cooling load to be 11%-12% and in the peak load during summer by 19%-20%. Similarly, Baldinelli (2009) proposed a double-skin façade coupled with a movable shading system at the outer skin to avoid overheating and discomfort in warm climates. The system was found to give better results on energy savings by up to 60kWh per year per façade square meter compared to common glazed and opaque walls. Wong et al. (2008) also examined the thermal performance of a building with a ventilated-shaft design under the Singapore climate. The system was reported not only to reduce the internal operative temperature, which thus extends thermal comfort acceptability and reduces energy consumption due to cooling, but to also improve the stack effect of natural ventilation and induce indoor airflow rates within the intermediate space. Xu & Ojima (2007) examined the performance of a double-skin façade with six different opening modes during different seasons in a two-storey house in Japan (Xu and Ojima, 2007). Working together with wind force, this double-skin façade in summer mode i.e. all ventilation openings in the system open and all the interior openings completely closed, was found to increase the airflow rate inside the intermediate space by up to $750m^3h^{-1}$ (air velocity $0.34ms^{-1}$). The heat gain due to the solar radiation from the system was also found to be exhausted by natural ventilation for 6%-10% which leads to cooling load saving.

The elements and configurations of a double-skin façade also have a great influence on its effectiveness to reduce indoor air temperature, increase indoor airflow rate and reduce the risk of overheating during summer. These involve orientation; the width of the intermediate space (air gap) (Sadineni et al., 2011, Gratia and Herde, 2004a, Gratia and Herde, 2004b, Chan et al., 2009); insulation levels (Gratia and Herde, 2007); the properties of the glazing panes (Sadineni et al., 2011, Haase et al., 2009); types and locations of shading devices (Gratia and Herde, 2004b, Baldinelli, 2009); and the size and position of openings (Haase et al., 2009, Chou et al., 2009). As a double-skin façade's main driving force is stack, due to absorbed solar radiation, its performance is influenced mainly by building orientation according to the sun path (Wong et al., 2008). For the northern hemisphere, a double-skin façade is thus suggested to be south facing due to high solar radiation (Wong et al., 2008). For the width of the intermediate space the thermal resistance of tall air cavity in a double-skin façade is found to increase with the air gap’s width as the air gap acts as a thermal resistance due to the low conductivity of air (Gan, 2001).

In summary, a double-skin façade is widely employed in high-rise office buildings due to its aesthetic and its performance to protect the inner space from its undesirable environmental conditions, to reduce high room temperature and to provide indoor environment with healthy ventilation. However, double-skin façade, similarly to other solar ventilation strategies, is based on stack force. As the result it can produce indoor airflow with only small velocity, which is insufficient to produce any physiological cooling effect or thermal comfort, even when coupled with wind force.

### *2.3.5 Summary*

Employing natural ventilation strategies for enhancing thermal comfort in a building in hot-humid climates is challenging. This is due to their high ambient temperature and humidity with low wind speed and small diurnal air temperature range. Natural ventilation is also inconsistent. However, natural ventilation has become a focus of researchers' attentions as it is favored by occupants over mechanical ventilation systems and it can provide high indoor environmental quality while consuming much less energy.

Various natural ventilation induced strategies that have been employed for improving thermal comfort conditions in buildings in hot-humid climates have been reviewed in this section, including wing-walls, wind towers and solar ventilation strategies (solar walls, solar chimneys and double-skin facades). This is to identify significant existing knowledge for developing a proposed natural ventilation strategy for a single-sided ventilated room in Bangkok. According to the literature the strategies that are based on wind force e.g. wing-walls or modern wind-towers with designed shaped roofs, can effectively produce indoor airflow with the high velocity that is required for producing physiological cooling effect and thermal comfort under tropical climates. With its optimal design the wing-wall is found to produce indoor airflow for up to 40% of the reference wind speed. This average air velocity can be as high as 0.4ms$^{-1}$ to 1.6ms$^{-1}$ according to Bangkok’s typical wind speeds of 1ms$^{-1}$ to 4ms$^{-1}$, respectively. On the other hand, strategies that are based mainly on stack force can produce only a low room air velocity i.e. commonly less than 0.05ms$^{-1}$. Stack driven strategies e.g. solar ventilation are therefore suitable for providing only healthy ventilation to ensure acceptable indoor air quality, but not thermal comfort ventilation under tropical climates.

In summary, natural ventilation strategies that are based on wind forces are favourable for buildings in hot-humid countries, including Thailand, compared to stack-driven strategies. This is mainly because they can provide controllable distributed airflow with the high velocity that is required to create direct cooling effect and thus improve occupants' comfort sensation. In the next sections the thermal comfort and the cooling effect due to the elevated air movement are explained in detail.

## 2.4 Thermal comfort

Thermal comfort is the pleasant environmental conditions that are able to provide a human's thermal preference. In this study, thermal comfort is the major criterion for assessing the performances of natural ventilation enhancement strategies in tall single-sided residential buildings.

According to the American Society of Heating, Refrigerating and Air-Conditioning Engineers (ASHRAE, 2013) thermal comfort is defined as that condition of mind which express satisfaction with the thermal environment. In most cases, the term '*thermal comfort*' has a similar meaning to '*thermal neutrality'*, which means the condition in which the occupants would prefer to be neither warmer nor cooler (Fanger, 1970). To understand and to be able to assess the thermal comfort for a particular environment the knowledge of heat balance between the human body and its environment is crucial.

### *2.4.1 Heat balance equations*

In order to enable the vital organs to function properly and to achieve thermal comfort the human thermoregulatory system tries to maintain the body core temperature constant within a particular range of temperatures despite changes in ambient temperature (Fanger, 1970, Awbi, 2003). By permitting physiological adjustments to thermal stress caused by internal and external thermal disturbances the body temperature control centre, called "*hypothalamus",* tries to keep an average core temperature ($Tc$) of about 37°C. This leads to different reactions within the body. For example, the regulatory system would increase heat loss by means of vasodilation in the skin and sweating when the core temperature becomes elevated as the ambient temperature increases in a warm environment (Sandberg et al., 2008).

According to this concept it can be concluded that the human thermoregulation tries to keep the whole body heat balance within equilibrium i.e. the heat storage within a body is equal to heat produced within the body and heat exchange between the body and its environment due to radiation, convection, conduction and evaporation (Sandberg et al., 2008, Yau and Chew, 2014). This can be expressed as:

$$\boldsymbol{S = M + W + R + C + K - E - RES} \qquad \textbf{Eq. 2-6}$$

where $\boldsymbol{S}$ is the heat storage on body, W; $\boldsymbol{M}$ is metabolic rate or the body heat production rate resulting from the oxidation of food and depending on their diet and level of activity, W; $\boldsymbol{W}$ is mechanical work, W; $\boldsymbol{R}$ is heat exchange by radiation occurring between the surface of the body (clothing and skin) and the surrounding surfaces (internal room surfaces), W; $\boldsymbol{C}$ is heat exchange by convection mainly occurring between a body and the surrounding air caused by a relative movement between the body and air, W; $\boldsymbol{K}$ is heat exchange by conduction through clothing W; $\boldsymbol{E}$ is evaporative heat loss due to diffusion of water vapor through the skin tissues and due to evaporation of sweat from the skin surface, W; $\boldsymbol{RES}$ is heat loss by respiration, W (Awbi, 2003).

A condition of equilibrium occurs when the heat storage in the body ($\boldsymbol{S}$) according to Eq. 2-6 or the sum of heat production and heat loss processes is equal to zero. In contrast, a negative or a positive value of $\boldsymbol{S}$ indicates a falling or rising body temperature, respectively (Awbi, 2003).

To achieve the heat balance equilibrium and thermal comfort there are six primary factors including air temperature $(ta)$, mean radiant temperature $\overline{(tr)}$, air velocity $(v)$, relative humidity (RH), physical activity $(M)$ and thermal resistance of clothing $(Icl)$ (Sandberg et al., 2008). These factors are interconnected and their effects in comfort cannot be considered independently. Moreover there are found to be other factors that may affect a person's perception of climatic comfort such as age, sex, state of health and acclimatization.

### *2.4.2 Thermal comfort models*

As thermal comfort is a significant criterion for determining human preference and performance numerous studies have attempted to define environmental indices as well as thermal comfort models for assessing thermal comfort in particular internal environment. Below are two major ways of looking at thermal comfort.

### 1) Fanger's PMV

Fanger has developed a thermal comfort model based on the physical assessment of the body heat exchange with the environment and supported by extensive studies on human with different age, race and adaptation under well-controlled environments in environmental chambers. He proposed that a person senses his/her own temperature and not those of the environment, and he specified three requirements for a person to achieve thermal comfort including (Awbi, 2003):

- The body must be in thermal equilibrium with the environments i.e. the rate of heat loss to the environment balances the rate of heat production.
- Thermal sensation is related to skin temperature and therefore the mean skin temperature $(\boldsymbol{Ts})$ should be at an appropriate level.
- There should be a preferred rate of sweating as the rate increases with metabolic rate.

To evaluate and analyze different environments from a climatic comfort points of view, Fanger proposed the indices of predicted mean vote (PMV) to estimate the mean thermal sensation vote for big groups of people based on a standard score by taking into account the primary six factors indicated above. It is represented by a seven-point thermal sensation scale from +3 indicating '*hot*' to 0 indicating '*neutral'* and -3 indicating '*cold*'. He proposed an equation based on the imbalance between the actual heat flow from the body in a given environment and the heat flow required for optimum comfort at specific activities as:

$$\boldsymbol{PMV = [0.303^{-0.036M} + 0.028]L} \qquad \textbf{Eq. 2-7}$$

where $M$ is metabolic rate and $L$ is thermal load, defined as the difference between the internal heat production and the heat loss to the actual environment for a person hypothetically kept at comfort values of skin temperature and evaporative heat loss by sweating at the actual activity level (Yau and Chew, 2014).

Based on the experimental data, Fanger also correlated the percentage ratio of people who were dissatisfied with their thermal environment and produced the predicted percentage of dissatisfied (PPD) to be plotted against PMV (see Figure 2-20).

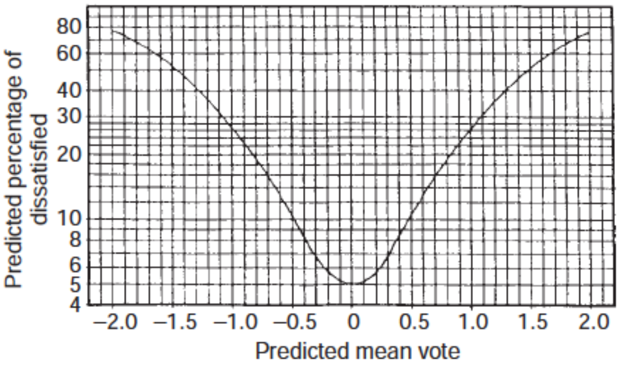

**Figure 2-20** Predicted percentage of dissatisfied as a function of predicted mean vote (Awbi, 2003)

Figure 2-20 represents a symmetrical curve with a minimum value of 5% corresponding to the lowest PPD and the ISO Standard 7730 recommends a PPD limit of 10%, which corresponds to $-0.5 \leq PMV \leq +0.5$. The expression of PPD as a function PMV can also be used (Eq.2-8).

$$\boldsymbol{PPD = 100 - 95exp - \{0.03353(PMV)^4 + 0.2179(PMV)^2\}} \qquad \textbf{Eq. 2-8}$$

However, there are numerous studies arguing that Fanger's PMV is not suitable for assessing thermal comfort for particular condition including naturally ventilated environments. This is because Fanger's model was developed based on the experimental data obtained from well-controlled environment in environmental chambers and thus it is more suitable for '*steady-state'* thermal environment. On the contrary people in naturally ventilated environments tend to adapt to their environment by making adjustments to themselves and their surrounding in order to reduce discomfort (Nicol et al., 1995, Nicol and Humphreys, 2002, Nicol, 2004, Rupp and Ghisi, 2014, Nguyen and Reiter, 2014). According to these studies the occupants in naturally ventilated buildings, especially those who live in hot-humid countries, were found to accept a higher temperature range than that suggested by ISO 7730 and ASHRAE standards 55-2013 (Yau and Chew, 2014, Kwong et al., 2014).

### *2) Adaptive thermal comfort models*

Adaptive thermal comfort models were initiated in the 1970s with the purpose of improving human comfort and reducing energy consumption (Brager and De Dear, 1998, Nicol et al., 1995). Unlike Fanger's PMV, the basis of adaptive model is that people have a natural tendency to adapt to changing conditions in their environments and their thermal perception is highly influenced by contextual factors such as climatic setting, social conditioning and economic considerations (De Dear and Brager, 1998, De Dear and Brager, 2001).

According to extensive field experimental studies of adaptive thermal comfort, it was found that there are other factors that may have influences on a person's perception of thermal comfort which were ignored in Fanger's models. These factors can be categorized into three main groups (Brager and De Dear, 1998, Brager and Dear, 2000),

i) Behavioral adaptations (behavioral feedback or adjustment) which are all modifications, both consciously and unconsciously, that people make to alter their body's thermal balance such as personal adjustment (clothing, activity, posture, eating and drinking hot or cold food or beverage, moving to a different locations); technological or environmental adjustment (modifying their environmental conditions when it is possible such as opening windows or tuning on fans or operating air conditioners); and cultural adjustment (scheduling activity or adapting dress code). These adaptations offer the best opportunity for people to control their thermal environment, which is a significant issue for designing naturally ventilated buildings.

ii) Physiological adaptations (acclimatization): These adaptations refer to all the changes in the physiological responses, which result from a prolonged exposure to particular thermal conditions. Numerous studies show that comfort preference is subjective, depending on acclimatization to a particular climate i.e. people from a hot and humid climate can tolerate higher air temperatures due to long-term several generation experience of this climatic condition (Khedari et al., 2000c, Tantasavasdi et al., 2001). Likewise Cowan (1991) found that the upper limit of comfort can be 1.0K higher for every 12 degree change in latitude and the upper limit of comfort for Bangkok can be as high as approximately 28˚C, while Busch (1995) indicated that the upper limit of comfort for Thai workers can be up to 28˚C in air-conditioned buildings and 31˚C in naturally ventilated buildings (Nicol et al., 1995).

iii) Psychological adaptation (expectation - perceptual adaptation): These adaptations refer to all the effects of the past experiences and expectations, which are mainly dependent on outdoor temperature, that can alter people's perceptions and reactions to their physical conditions (Brager and Dear, 2000).

Contrary to Fanger's model, the adaptive comfort models do not predict comfort responses of people but rather the thermal conditions under which people are expected to be comfortable in buildings (Awbi, 2003). Based on experimental data obtained from on-site studies it has been found that an acceptable degree of comfort in residential and office buildings could be achieved over a comparatively wider range of temperatures (Nicol and Humphreys, 2002) and a higher upper limits of comfort temperatures (Djamila et al., 2013) compared to those suggested by Fanger's model (see Figure 2-21 for example).

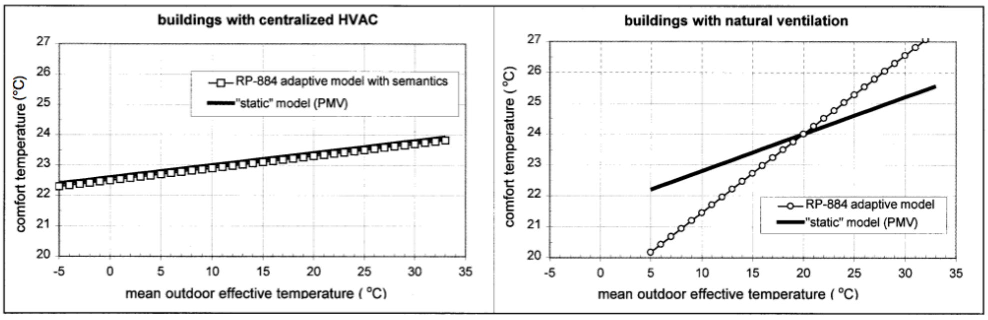

**Figure 2-21** The comparison of comfort temperatures suggested by Fanger's PMV and an adaptive model: (left) for the buildings with centralized HVAC; and (right) for the buildings with natural ventilation (Brager and Dear, 2000).

In Auliciem's research there is a statistical relationship that states that indoor air comfort temperature is influenced by outdoor temperature. It is also found that external weather condition is a significant parameter that has an indirect impact upon the human heat balance comparatively to the six main factors. In the perception of adaptive models, thermal comfort temperature is therefore a function of outdoor temperature (Yau and Chew, 2014). Table 2-3 shows a list of adaptive comfort models which are regression equations proposed by many researchers (Table 2-3). It can be seen that these comfort temperatures in adaptive models are not constant as that in Fanger's model. They are, rather, developed based on their correlations of the average indoor comfort and outdoor air temperatures which vary from month to month (Brager and De Dear, 1998).

**Table 2-3** List of adaptive thermal comfort models.

| Researcher(s) | Research Findings |
|---|---|
| Humphreys (1975) in (Givoni et al., 2006) | $Tn = 2.56 + 0.83Toi$<br>where $Tn$ is neutral thermal sensation (˚C), $Toi$ is indooroutdoor monthly mean air temperature (°C) |
| Humphreys (1978) in (Nicol et al., 1995) | $Tc = 12.1 + 0.543To$<br>where $Tc$ is comfort temperature in free-running buildings (˚C) and $To$ is mean outdoor temperature (˚C). |
| Humphreys (1978) in (Szokolay, 2008). | $Tn = 11.9 + 0.534To.avp$<br>where $Tn$ is thermal neutrality for free-running buildings (˚C) and $To.avp$ is the month's mean outdoor operative temperature (˚C). |
| Auliciems (1981) in (Brager and De Dear, 1998) | $Tn = 0.48Ti + 0.14Tm + 9.22(r = 0.95)$<br>where $Tn$ is temperature neutrality for all buildings (˚C), $Ti$ is indoor temperature (˚C), $Tm$ = mean outdoor temperature (˚C),.<br>* However,, this equation is suggested by Brager and deDear (1998) as unstable due to the inter-correlation between the two independent variables i.e. $Ti$ and $Tm$. |
| Auliciems and De Dear (1986) in (Nicol et al., 1995, Szokolay, 2008) | $Tc = 17.6 + 0.31To.av$<br>where $Tc$ is comfort temperature (˚C) and $To.av$ is mean outdoor temperature. |
| Humphreys (1976, 1978 and 1981) in (Nicol et al., 1995) | For climate-controlled buildings: $Tc = 0.16Tm + 18.6$<br>For free-running buildings: $Tc = 0.53Tm + 11.9$<br>where $Tc$ is comfort temperature and $Tm$ is mean monthly outdoor temperature. |
| Griffiths (1990) in (Szokolay, 2008) | $Tn = 12.1 + 0.534To$<br>where $Tn$ is thermal neutrality (˚C) and $To$ is average outdoor air temperature (˚C). |
| Ahmed (1995) in (Nicol et al., 1995) | Neutral temperature for Dhaka's conditions: $Tn = 2.56 + 0.831Tm$<br>where $Tn$ is neutral thermal sensation (˚C) and $Tm$ is mean temperature (˚C) with tolerance band of +/-2˚C. |
| Nicol & Roaf (1996) in (Szokolay, 2008) | $Tn = 17 + 0.38To.av$<br>where $Tn$ is thermal neutrality (˚C) and $To.av$ is average outdoor air temperature of the month (˚C). |
| De Dear (1997) in (Szokolay, 2008) | $Tn = 17.8 + 0.31To.av$<br>where $Tn$ is thermal neutrality (˚C) and $To.av$ is average outdoor air temperature of the month (˚C). |
| Humphreys & Nicol (2000) in<br>(Nicol and Humphreys, 2002) | $Tc = 13.5 + 0.54To$<br>where $Tc$ is comfort temperature in free-running buildings (˚C) and $To$ is mean outdoor temperature.<br>* The comfort zone is within +/-2˚C where there is no possibility of changing clothing or activities as well as without air movement. |
| (Brager and Dear, 2000) | For centralized HVAC buildings: $Ts = 0.51Top - 11.96$<br>For naturally ventilated buildings: $Ts = 0.27Top - 6.65$<br>where $Ts$ is thermal sensation (˚C) and $Top$ is mean indoor operative temperature (˚C). |
| Khedari (2003) in<br>(Givoni et al., 2006) | $Ts = (0.4441 - 0.0777 * AS^{0.5})Ta - 11$<br>where $Ts$ is thermal sensation (˚C), $Ta$ is indoor air temperature and $AS$ is air speed. |
| (De Dear and Brager, 2001) | $Tc = 0.31To + 17.8$<br>Upper 80% acceptable limit: $= 0.31To + 21.3$<br>Upper 90% acceptable limit: $= 0.31To + 20.3$<br>Lower 80% acceptable limit: $= 0.31To + 14.3$<br>Lower 90% acceptable limit: $= 0.31To + 15.3$<br>where $Tc$ comfort temperature (˚C), $To$ is mean outdoor temperature (˚C). |
| ASHRAE (2013) | $Toc = 18.9 + 0.255Tout$<br>Where $Toc$ is operative temperature (˚C) and $Tout$ is outdoor air temperature (˚C).<br>*The upper and the lower limit of comfort temperature are $Toc + 2.5$˚C and $Toc - 2.2$˚C, respectively, which is acceptable for 80% of the occupants. |

### *2.4.2 Summary*

It is obvious that the Fanger and adaptive models are different in many aspects. The former is found to be suitable for assessing thermal comfort for steady-state conditions, such as those that are commonly found in a/c buildings, while the latter is more suitable for a building with greater variation in internal thermal condition i.e. naturally ventilated building. As this study focuses on naturally ventilated building in hot-humid climates then adaptive models are, therefore, preferable.

## 2.5 Cooling effect of elevated air movement

### *2.5.1 Introduction*

The cooling effects of air movements inside a building are governed by three mechanisms: i) under proper conditions, wind-driven airflows can offset internal and solar heat gains by replacing warm air with cooler external air and thus lowering indoor air temperature when ambient temperature ($T_{out}$) is lower than indoor air temperature ($T_{in}$); ii) natural airflow through a building can cool down the building structure by carrying away the sensible heat restored in its thermal mass; and iii) induced air movement can cool building occupants directly by promoting heat dissipation from the occupants' skin, thus increasing physiological cooling and comfort (Ernest et al., 1991, Szokolay, 2008). Whilst the first two mechanisms require only small air exchange rates (volume flow rates in $m^3s^{-1}$ or $Ls^{-1}$), such as that can be found in the studies (Jamaludin et al., 2014, Yik and Lun, 2010), the last one needs a high air velocity at the occupants' skin surface ($ms^{-1}$) to achieve thermal comfort.

In this section the principles of the physiological cooling effect of indoor air motion on human thermal comfort, together with the findings from previous studies regarding to preferred air speeds to offset high indoor temperatures and the upper limit of acceptable velocity, are reviewed.

### *2.5.2 Cooling effect of elevated air movement*

There are six main variables that have an effect on human thermal comfort. These involve four physical variables (air temperature, mean radiant temperature, air velocity and relative humidity) and two behaviorally regulated variables (metabolic rate and clothing insulation) (Fountain and Arens, 1993). Among these variables, air velocity is suggested as crucial for hot-humid climates as it has a great effect on human thermal comfort.

An increase in air velocity has been recommended as a significant strategy for improving the occupant's thermal comfort for buildings in hot-humid countries, including Thailand (Byrne et al., 1985, Chow et al., 2010, Prianto et al., 2000, Toftum, 2004, Khedari et al., 2000c, Hyde, 2000, Aynsley, 2007, Indraganti et al., 2014, Toe and Kubota, 2013). Increasing air movement in such conditions has two direct effects on human thermal comfort (Givoni, 1981). Firstly, increasing local air motion across the skin surface increases convective heat transfer, which has a strong influence on improving thermal sensation (Fountain and Arens, 1993). Secondly, it increases the efficiency of sweat evaporation from the skin, thus minimizing discomfort due to skin wetness under high humidity situations (Givoni, 1981, Allard, 1998, Szokolay, 2008, Givoni, 1994). Together these two mechanisms produce a physiological cooling effect and enhance human thermal comfort. It is, therefore, advisable in hot-humid climates to maintain a high-enough air speed over the human body so that the required evaporation can be obtained (Givoni, 1998). This is especially true when the ambient temperature is below the skin temperature i.e. below 35° as both convective and evaporative cooling can operate in the same direction. However, it should be noted that an increase in air motion still might be acceptable and beneficial even when the indoor air temperature is raised due to the warm incoming air when the ambient temperature is higher than the indoor air temperature, especially for buildings in hot-humid regions (Givoni, 1994). This is because the upper limit of comfort temperature is shifted upwards with a higher air speed.

The preference and positive effect of air velocity on occupants' thermal sensation was found in the 1950s as Macfarlane (1958) suggested that the thermal comfort zone temperatures are likely to be raised by 0.55K for every 0.15ms$^{-1}$ of elevated air movement at the occupants' skin when the indoor air temperatures do not exceed 33°C (Aynsley, 2007). Since then air velocity has been included as one main variable for determining thermal comfort in various international guidelines. These are, for example, ASHRAE's comfort zone and Olgyay's Bioclimatic chart. In the late 1950s, ASHRAE conducted an experimental study to examine the cooling effect of elevated air movement on comfort under various air temperatures (22.5°C to 29.5°C) and air velocities (0.2ms$^{-1}$ to 0.8ms$^{-1}$) and found a strong relationship among these two parameters and comfort. Later Olgyay (1963) undertook a thorough study to define the comfort zone i.e. the range of environmental conditions within which the average person would feel comfortable for different climates and established a guideline for indicating comfort zone for warm climates (Auliciems and Szokolay, 2007) (Figure 2-22). In the chart the comfort zone range is illustrated with the lines to show the extended upper boundary when air movement is at different velocities (from 0.1ms$^{-1}$ up to 1ms$^{-1}$). Increasing air speed by 0.1ms$^{-1}$ and 1ms$^{-1}$, for example, could extend the upper limit of comfort zone from 30°C to approximately 32°C and 35°C respectively, depending on relative humidity (RH) ranging between 10% and 85%. Similarly, Toe and Kubota (2013) examined the ASHRAE RP-884 database for hot-humid climates and found the positive effect of indoor air velocity on elevating the upper limit of comfort temperatures when indoor operative temperatures exceed 25°C, especially for high air speed i.e. 0.65ms$^{-1}$ and beyond (Toe and Kubota, 2013).

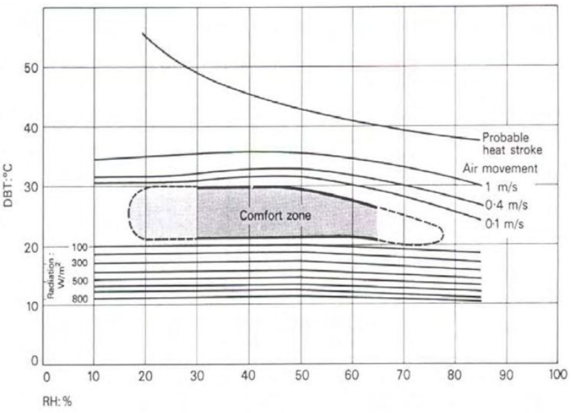

**Figure 2-22** Bioclimatic chart for warm climates adapted from Olgyay (1963) (Auliciems and Szokolay, 2007).

Byrne et al (1985) has also found a strong relationship between discomfort and air velocity, air temperature and humidity and had introduced a graphical tool called '*Discomfort Index*' for determining the potential energy saving of increased indoor air movement to maximize the occupants' comfort under relative humidity between 20% and 80% (Figure 2-23). Discomfort rate was found to increase with temperature and humidity, and the combination of these two was discovered to affect comfort more than either parameter alone. It was concluded in the study that increases in air speed such as that was obtained from wind-induced ventilation was able to effectively produce human comfort in hot-humid climates (Byrne et al., 1985).

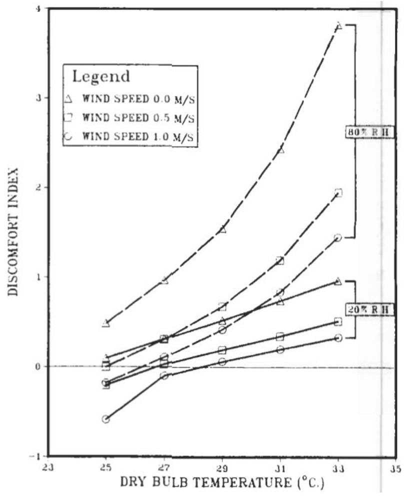

**Figure 2-23** Discomfort as a function of dry-bulb temperature, relative humidity (RH) (20% and 80%) and air velocity (0ms$^{-1}$, 0.5ms$^{-1}$ and 1ms$^{-1}$) (Byrne et al., 1985).

ASHRAE (2013) also provides a chart for determining the required air speeds to offset high operative temperatures above warm-temperature boundaries of about 28°C based on theoretical calculations (Figure 2-24). The chart shows the preferred air speed for up to 1.6ms$^{-1}$ to improve the occupants' comfort for different levels of temperature difference ($\bar{T}r - ta$, where $\bar{T}r$ is the mean radiant temperature and $Ta$ is an air temperature). It can be seen that elevated air speed is less effective when $\bar{T}r$ is low and $Ta$ is high, comparing to that when $\bar{T}r$ is high and $Ta$ is low i.e. lower air speed is required for the latter case. These charts are suggested to be applied to the occupants with light clothing (clothing insulation between 0.5clo and 0.7clo), who perform near sedentary activity and have a full control of the local air speed under typical ventilation i.e. turbulence intensity ($Tu$) of 30% to 60% and the elevated air speed chart may be used to offset an increase in air temperature by up to 3K above the warm temperature boundary of the comfort zone chart (about 30°C to 31°C) (ASHRAE, 2009). It should be also noted that the beginning point of the curve in Figure 2-24 starts when air speed is 0.2ms$^{-1}$. This is because there is no cooling effect produced by an air speed lower than this value.

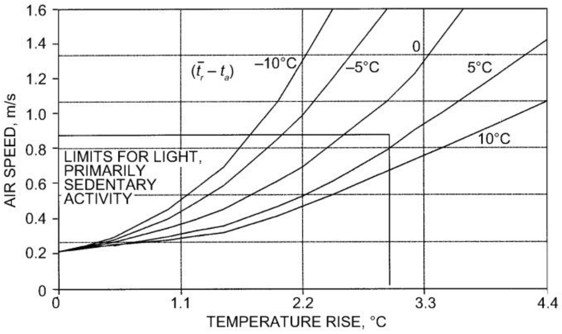

**Figure 2-24** ASHRAE's suggested air speeds to offset for high temperature above warm temperature boundary (Stephen and Turner, 2011, ASHRAE, 2009, Olesen and Parsons, 2002, Olesen, 2004).

Another guideline for approximating the preferred air speeds for different operative temperatures and clothing insulation levels (*clo*) when the occupants do or do not have control on their local air speed was suggested by Arens et al (2009), and Stephen & Turner (2011) (Figure 2-25). Air speed ranges between 0.1ms$^{-1}$ and 1.2ms$^{-1}$ were suggested as the required velocity under operative temperatures between 20°C and 31°C. It can be seen from Figure 2-25 that low air speed i.e. less than 0.2ms$^{-1}$ (called still air in the chart) can provide comfort for the temperature up to only 27.5°C, while air speed of 1.2ms$^{-1}$ could raise the upper limit of comfort temperatures to 31°C. According to the chart the occupants control on local air movement is also recommended when air speed is beyond 0.8ms$^{-1}$, the upper limit of acceptable air speed suggested by ASHRAE so as to avoid discomfort due to draught.

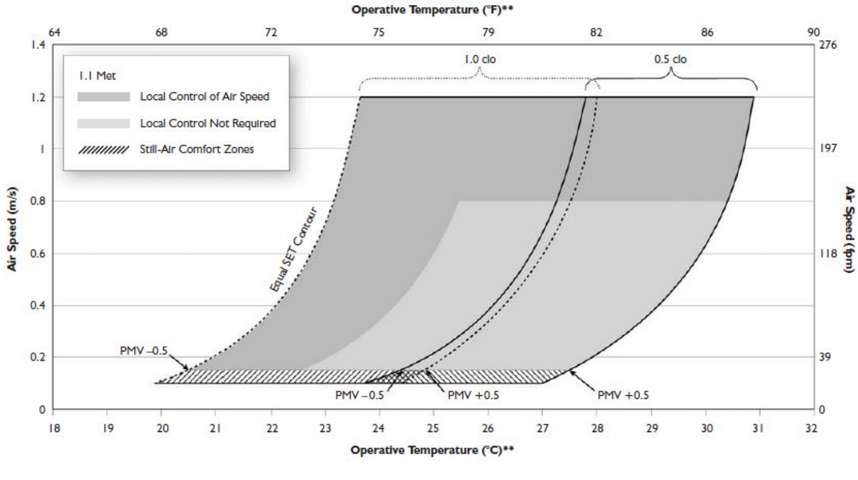

**Figure 2-25** Elevated air movement to improve occupants' comfort with and without occupants' local control in warm climates (Arens et al., 2009, Stephen and Turner, 2011).

In addition to the above guidelines, there have been numerous studies since the 1950s that examine and confirm the effect of increased air speed for compensating for high temperatures i.e. higher velocity is required for enhancing comfort sensation when room air temperature increases. These studies have also suggested the preferred air speeds for compensating for particular temperatures. In the physiological research conducted by Givoni (1963) the effect of air speeds up to 4ms$^{-1}$ on human comfort and general feeling of pleasantness was monitored. The subjects were found comfortable at the room temperature of 30°C with the air speed of 2ms$^{-1}$ without noticing excessive wind (Givoni, 1992). In another study by Givoni increased air speed was discovered to reduce heat sensation and improve human thermal comfort as it increased the convective heat loss and reduced the skin temperature from the human body. This is especially true at room air temperatures below approximately 33°C (Givoni, 1998). An increase in air velocity might be desirable even when the temperature rose to above 37°C, which was advisable to increase heat sensation and produce discomfort. This was because it could reduce the skin wetness which may be found as favorable (Givoni, 1998). Additionally, Givoni has suggested an indoor air velocity of 1.5ms$^{-1}$ and 2.0ms$^{-1}$ to be applicable for improving the occupants' comfort at maximum ambient temperature of 28°C and 32°C, respectively under the diurnal temperature range less than 10°C (see Figure 2-26) (Givoni, 1991, Givoni, 1992, Givoni, 1998).

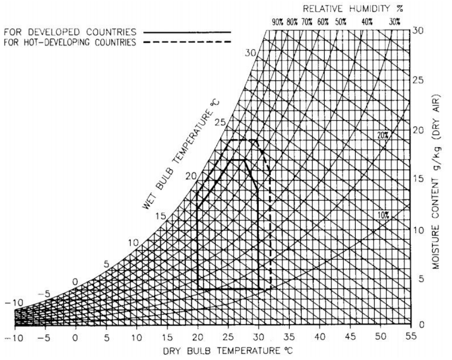

**Figure 2-26** Extended comfort boundaries by air speed of 2ms$^{-1}$ (Givoni, 1992).

In Fountain et al (1994) various recommendations of preferred air velocities to offset high air temperatures obtained from various laboratory studies were summarized in a chart (see Figure 2-27a). According to the chart air speeds for up to 1.2ms$^{-1}$ were suggested for providing comfort under an operative temperature range between 22°C and 31°C. Similar result can be also found in Tanabe (1988). In this study comfort reactions of Japanese subjects at various air speeds (up to 1.6ms$^{-1}$) and air temperatures during summer (27°C to 31°C) with relative humidity at 50% and 80% were examined. The preferred air speeds were found to increase with air temperatures (Figure 2-27b) i.e. air speeds at 1ms$^{-1}$ and 1.6ms$^{-1}$ were preferred at the temperatures of 28°C and 31°C, respectively (under 50%RH) (Givoni, 1998). It is to be noted that an air speed range above the upper limit suggested by ASHRAE of 0.8ms$^{-1}$ is employed in these studies and is still preferred by the subjects.

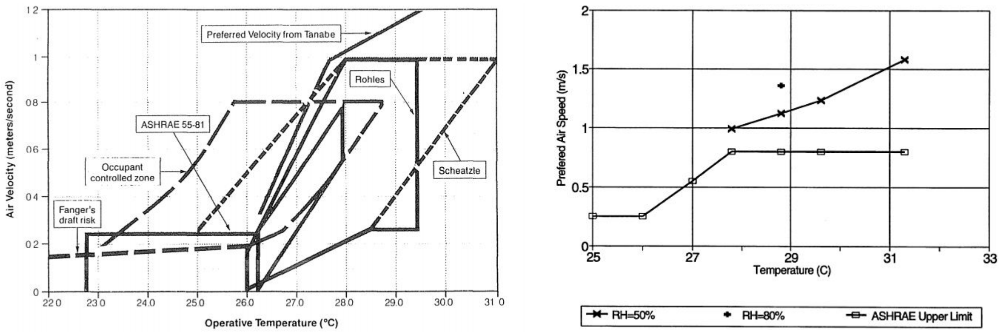

**(a)** **(b)**

**Figure 2-27** Recommended air speeds for compensating high air temperatures: (a) After Fountain et al (1994); and (b) after Tanabe (1988) (Givoni, 1998).

There are also many studies conducted in hot-humid climates that confirm the cooling effect of elevated air movement to compensate for high temperatures and extend the upper limit of the comfort range (see Table 2-4).

**Table 2-4** Studies relating to the cooling effect of elevated air movement to compensate for high temperature

| Year | Climate | Findings | Reference(s) |
|---|---|---|---|
| 2001 | Tropics (Thailand) | The upper limit of comfort in Thailand extended to 29.1°C, 29.9°C and 31.3°C with air speed of 0.2ms$^{-1}$, 0.4ms$^{-1}$ and 1.0ms$^{-1}$, respectively. | (Tantasavasdi et al., 2001) |
| 2003 | Tropics (France) | Air speeds of 0.1ms$^{-1}$ to 2.0ms$^{-1}$ provided occupants' thermal comfort in a house under room temperature of 28°C with 70% RH. | (Prianto and Depecker, 2003) |
| 2006 | Tropics (Singapore) | People in the Tropics preferred elevated local air velocity to offset high room temperature. The air velocities from 0.3ms$^{-1}$ to 0.45ms$^{-1}$ were required for air temperature of 23°C, while higher velocities from 0.3ms$^{-1}$ to 0.9ms$^{-1}$ were required at ambient temperature of 26°C. | (Gong et al., 2006) |
| 2009 | Tropics (South China) | The upper limit of comfort extended from 26°C to 29°C when air velocity was increased from 0.25ms$^{-1}$ to 1.5ms$^{-1}$. This limit could further extend to 29.5°C when the Predicted Percentage of Dissatisfied (PPD) increased from 10% to 20%. | (Lei, 2009) |
| 2011 | Tropics (North-east Brazil) | Minimum air velocity to achieve 90% of thermal comfort when air temperatures were between 24°C and 27°C, 27°C and 29°C, and 29°C and 31°C were found as 0.4ms$^{-1}$, 0.41-0.8 ms$^{-1}$, and more than 0.81 ms$^{-1}$, respectively. | (Candido et al., 2011) |
| 2014 | Tropics (South India) | The upper limit of comfort temperatures of the occupants in office buildings in India was increased by 2.7K to up to 30.1°C in natural ventilation and 28.6°C in a/c modes, when the air speed was increased for 1ms-$^{1}$ due to the ceiling fans. | (Indraganti et al., 2014) |

The perception of thermal comfort in hot-humid climates is also found to increase with elevated air velocity due to electric fans. In McIntyre (1978), for example, the subjects' comfort in a room with locally controlled ceiling fans were investigated and the comfort was found to increase for the room air temperature of 30°C with air velocity up to 2ms$^{-1}$ (Givoni, 1998). Spain (1987) also found that air movement with still air (less than 0.25ms$^{-1}$), moderate air (0.25ms$^{-1}$ to 1.5ms$^{-1}$) and high air (more than 1.5ms$^{-1}$) produced by ceiling fans were able to produce occupants' comfort under room temperatures up to 27.8°C, 29.4°C and above 29.4°C, respectively (Spain, 1987). Likewise, Fountain et al (1994) conducted an experimental study to examine the effect of locally controlled air movement (between 0ms$^{-1}$ and 1ms$^{-1}$) under the air temperature range between 25.5°C to 28.5°C. In this study the subjects in an open-plan office were given control of air flow velocity from a desk fan. It was concluded that the percentage of satisfied people was found to increase with air velocity (Fountain et al., 1994). The chart for predicting the percent of satisfied people (*PS*) as a function of air temperature and air velocity was also provided in the study (Figure 2-28).

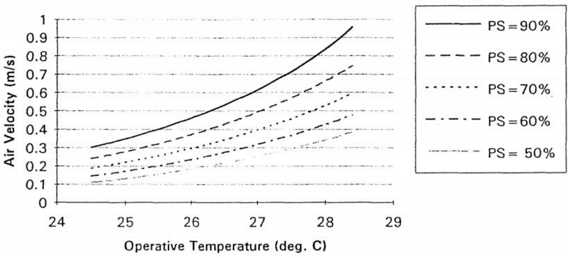

**Figure 2-28** The predicted percent satisfied (*PS*) of different air velocities as a function of operative temperature (Fountain et al., 1994).

Similarly, Mallick (1996) investigated the effect of elevated air speeds (0.15ms$^{-1}$ to 0.45ms$^{-1}$) produced by ceiling fans on the occupants' comfort under different air temperatures (ranging between 24°C and 32°C) and relative humidities (between 50% and 90%) in a hot-humid climate of Bangladesh, and found that the comfort temperatures increased with air speed. However, this is effective only for certain values (see Table 2-5) i.e. there was no appreciable change in the comfort temperature range found when air speed was less than 0.3ms$^{-1}$. Therefore, it was concluded in the study that air movement with a low velocity i.e. less than 0.3ms$^{-1}$, can only contribute to health ventilation and cannot provide any cooling effect or thermal comfort (Mallick, 1996).

**Table 2-5** Comfort temperatures for different air speeds generated by ceiling fans under hot-humid climate of Bangladesh (Mallick, 1996).

| Fan speed setting | Air speed ($ms^{-1}$) | Comfort temperature range (°C) | Mean comfort temperature (°C) |
|---|---|---|---|
| None | 0 | 24-33 | 28.9 |
| Slow | 0.15 | 24-33 | 29.5 |
| Medium | 0.30 | 26.4-35.2 | 30.9 |
| Fast | 0.45 | 27-35.8 | 31.6 |

Findings from Khedari et al (2000) also confirm the positive effect of employing ceiling fans on extending occupants' thermal comfort in hot-humid countries. Based on questionnaire results, a ventilation comfort chart for identifying the required air speed to compensate for high air temperature in offices and classrooms under a relative humidity range of 50% and 80% of Thailand was developed (Figure 2-29). Electric fans that generated air speeds of $0.2ms^{-1}$ to $3.0ms^{-1}$ were found to provide thermal comfort under room temperatures of 26°C to 36°C with relative humidities between 50% and 80%. Increased air speed for $1.0ms^{-1}$ was able to offset room temperatures by 2K to 6K, depending on the rate of relative humidity. It was also discovered that humidity rates has a great influence on the strategy's performance i.e. the higher the relative humidity rate, the lower the effectiveness of elevated air movement to provide comfort. The study also suggested that low air speed i.e. $0.2ms^{-1}$ is sufficient only to produce acceptable comfort at air temperature of 28°C and much higher air speeds i.e. $3.0ms^{-1}$ are required at air temperatures above 34°C (Khedari et al., 2000c). Similarly, the comprehensive survey study by Indraganti et al (2014) has found a positive effect of ceiling fans on thermal comfort as an increase in air speed of about $1ms^{-1}$ was found to increase the mean comfort temperature in office buildings in India's hot-humid cities by 2.7°C to 30.1°C in natural ventilation mode and 28.6°C in a/c mode (Indraganti et al., 2014).

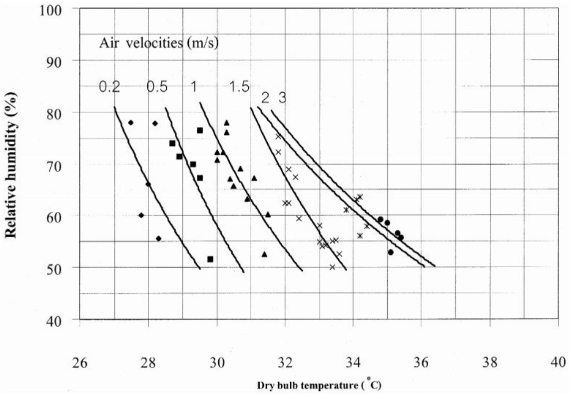

**Figure 2-29** Thailand ventilation comfort chart for offices and classrooms (Khedari et al., 2000c).

Moreover, elevated air movement is found preferable even for air-conditioned (a/c) spaces. In the experimental study, Chow et al (2010) investigated thermal sensation of the occupants in a/c office environments under hot-humid climate of Hong-Kong with an air temperature range of 25°C to 30°C and relative humidity of 50% to 85%. Thermal comfort limits in such environments were extended by the cooling effect of elevated air speed (see Table 2-6). By increasing the air speed from below 0.2ms$^{-1}$ to 1.0ms$^{-1}$ the upper limit of thermal comfort was extended from 24.9°C to 26.4°C, and from 26.8°C to 28.3°C. This is approximately 1.5°C of maximum comfort temperatures is increased. An air velocity up to 0.2ms$^{-1}$ was found preferable under indoor air temperature at 25°C, while higher velocities of 1.2ms$^{-1}$ to 3.1ms$^{-1}$ were required when air temperatures rose to between 27°C and 30°C. According to the study an increase in air speed of 1.0ms$^{-1}$ is suggested to compensate for high temperatures for up to 2°C. The study found that the upper limit of thermal comfort for a/c buildings in the tropics was higher than that was suggested by ASHRAE and concluded that elevated air movement is an effective and cheap strategy to improve thermal comfort for buildings in hot-humid climates comparing to the strategy for reducing either air temperature or humidity.

**Table 2-6** Comfort air speeds at different room temperatures for sedentary working environment with a/c systems under the climates of Hong Kong (Chow et al., 2010).

| Air temperature (°C) | Comfort air speed (ms$^{-1}$) | Range of air speed for 90% comfort (ms$^{-1}$) | |
|---|---|---|---|
| | | Lower bound | Upper bound |
| 25 | <0.2 | 0 | 0.99 |
| 26 | 0.59 | 0 | 1.63 |
| 27 | 1.22 | 0.18 | 2.26 |
| 28 | 1.85 | 0.81 | 2.90 |
| 29 | 2.49 | 1.45 | 3.53 |
| 30 | 3.12 | 2.08 | 4.17 |

In Figure 2-30 the suggested air speeds for different air temperatures that are found in the literatures are illustrated. The chart shows a range of preferred air speeds ranging from 0.1ms$^{-1}$ to 3.1ms$^{-1}$ which are recommended for improving human comfort under particular air temperatures ranging from 25°C to 35°C. It can be seen from the chart that the higher the air temperatures, the greater the air speeds are preferred for producing comfort.

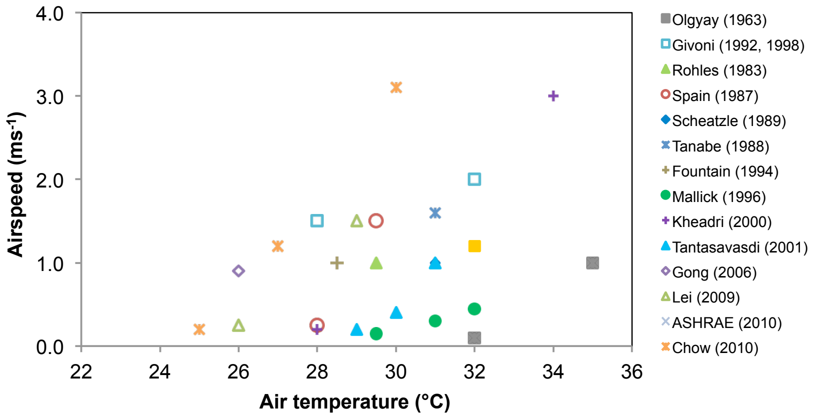

**Figure 2-30** Suggested air speeds to compensate for high air temperatures according to various literatures.

Furthermore, a number of equations have been proposed for estimating the preferred air speeds to compensate for high air temperatures (Table 2-7).

**Table 2-7** Equations for estimating preferred air speeds for compensating for high air temperatures according to various literatures.

| **References** | **Findings** |
|---|---|
| Drysdale (1952)<br>(Szokolay, 2000) | Suggested air speed of 0.15ms$^{-1}$ to compensate for 1K, for air speed up to 1ms$^{-1}$ and air temperature up to 37°C and proposed a function as:<br>$\boldsymbol{dT = 6.7v}$<br>Where $dT$ is the cooling effect compensated by elevated air velocity (K), $v$ is air velocity (ms$^{-1}$) at the body surface. |
| Rohles et al (1974)<br>(Szokolay, 2000) | Suggested air speed of 0.48 ms$^{-1}$ to compensate for every 1K, and proposed a function form as:<br>$\boldsymbol{dT = 2.08v}$ |
| Aren & Watanabe (1986)<br>(Szokolay, 2000) | Suggested the extensions to the comfort zone of Psychrometric chart using air velocity of 0.5 ms$^{-1}$ for 3.1K. This gives a function as:<br>$\boldsymbol{dT = 8.26(v - 0.25)}$ |
| Olgyay (1953) | Proposed Psychrometric chart and indicated the required air velocity of 0.5ms$^{-1}$, 1.0ms$^{-1}$ and 1.5ms$^{-1}$ to compensate for high air temperature of 2.5K, 5K and 7.5K, respectively. |
| Humphrey & Nicol (1995)<br>(Szokolay, 2000); | Proposed the cooling effect (K) as a function of an elevated air velocity (ms$^{-1}$) as:<br>$\boldsymbol{dT = 7 - \left[\frac{50}{4+10\sqrt{v}}\right]}$ |
| Szokolay (2000, 2014) | Proposed the preferred air velocity (ms$^{-1}$) to offset for high air temperature (K) as a function below:<br>$\boldsymbol{dT = 6Ve - (1.6Ve)}$<br>Where $Ve$ is an effective velocity, which is equal to $v - 0.2$ ms$^{-1}$ and it should be noted that this expression is valid up to 2ms$^{-1}$. |

In Figure 2-31 the elevated air speeds that are suggested to compensate for high temperature according to the equations from the literatures listed in Table 2-7 are plotted against each other.

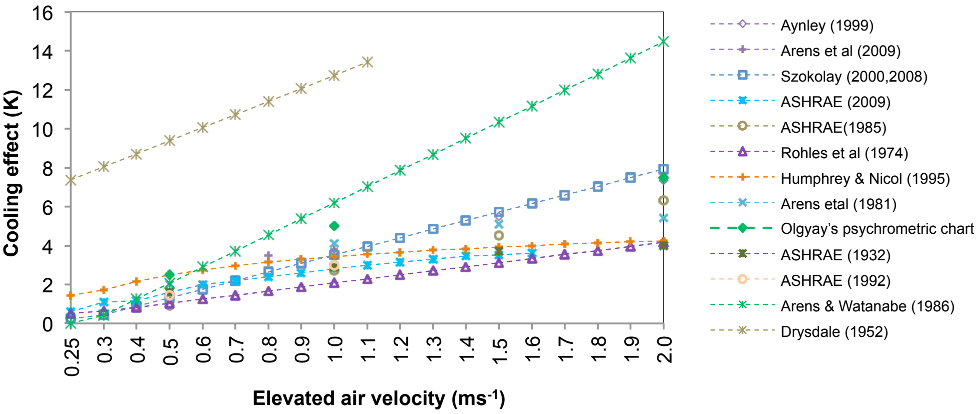

**Figure 2-31** Suggestions on the cooling effect as a function to elevated air velocity according to various literatures.

According to literatures there is obviously a wide range of suggested air speeds to compensate for high temperatures and there is no exact recommendation on specific air speed for a particular air temperature. This may be because the perception of comfort is dependent varying from person to person. However, all the findings lead to the same principle i.e. the physiological cooling due to elevated air movement is an effective strategy to offset for high air temperature and to enhance human comfort, particularly in hot-humid climates. In this study the model developed by Szokolay (Szokolay, 2000, Szokolay, 2008), which can provide an average result of the cooling effect produced by elevated air velocities among extensive studies indicated in Table 2-7, will be adopted to estimate the required air velocity for particular temperatures. For the next section, another significant issue on thermal comfort and air movement, which is the upper limit of acceptable air speeds, is discussed.

### *2.5.3 Upper limit of acceptable air velocity for tropical climates*

Although elevated air movement is preferable and sometimes required for producing cooling effect and thermal comfort, high air velocity may cause discomfort or disturbance in some situations. There are international standards and recommendations regarding to this concern. ASHRAE Fundamental (2013), for example, recommended the highest indoor air speed allowed as 0.8ms$^{-1}$. Air movement beyond this rate was suggested may produce disturbance by causing the paper to fly, particularly in office environment, and occupant's discomfort due to cool draught which is an undesired local cooling of the human body caused by air movement (Givoni, 1994). Olgyay (1992) and Hyde (2000) suggested the upper limit of acceptable air speeds without discomfort draught is about 1.0ms$^{-1}$ (Olgyay, 1992, Hyde, 2000). Olgyay (1992) also defined the desirable breeze as air movement occurring when air temperatures were above 23.9°C (over-heated period) and the undesirable air movement as that occurring during a cold (under-heated period) i.e.

temperature is below 23.9°C. Also, he has indicated the probable effect of different air speeds on human as in the Table 2-8.

**Table 2-8** Probable effect of air speeds on human perception (Olgyay, 1992).

| Air speeds ($ms^{-1}$) | Probable effect on human |
|---|---|
| Up to $0.25ms^{-1}$ | Unnoticed |
| $0.25\text{-}0.51ms^{-1}$ | Pleasant |
| $0.51\text{-}1.02ms^{-1}$ | Generally pleasant with a constant awareness of air movement |
| $1.02\text{-}1.52ms^{-1}$ | Slight draught to annoying draught |
| Above $1.52ms^{-1}$ | Requires corrective measures if work and health are to be kept in high efficiency |

Szokolay (2008) produced similar conclusion regarding to subjective reactions to different air speeds (Table 2-9). According to these studies the air movement with the velocity less than $0.25ms^{-1}$ seems not to produce any effect on human perception (unnoticed), while that between $0.5ms^{-1}$ to $1ms^{-1}$ could create pleasant, and beyond this range may create annoying and discomfort. For such environments with high air speed, the occupants' full control over their local air movement is therefore recommended.

**Table 2-9** Subjective reactions to different air speed (Szokolay, 2008).

| Air speeds ($ms^{-1}$) | Subjective reactions |
|---|---|
| Up to $0.1ms^{-1}$ | Stuffy |
| Up to $0.2ms^{-1}$ | Unnoticed |
| Up to $0.5ms^{-1}$ | Pleasant |
| Up to $1.0ms^{-1}$ | Awareness |
| Up to $1.5ms^{-1}$ | Draughty |
| Above $1.5ms^{-1}$ | Annoying |

However, these suggested upper limits of air velocity were suggested to be far restrictive for occupants in hot climates as people who live in naturally ventilated buildings usually accept and, in some situations, prefer a wider range of temperatures and air speeds as normal (Givoni, 1994). This is because the acceptable rate of air movement has a strong link with climatic conditions i.e. a risk of unacceptable air movement was found to occur in moderate and cool environments i.e. temperature up to 22°C and 23°C, while draught was generally not found at typical indoor air speed i.e. up to $0.4ms^{-1}$ at higher temperature i.e. above 23°C, or at raised activity levels (Toftum, 2004).

In a physiological research by Givoni (1963) the effect of air speeds on comfort was examined. The subjects were found to be comfortable without noticing excessive wind under the air speed of up to $2ms^{-1}$, and the general feeling of pleasantness was monitored even under the air speed of up to $4ms^{-1}$ (Givoni, 1994). Givoni (1991) also defined the indoor air speed of $1.5ms^{-1}$ to $2.0ms^{-1}$ as "*very light breeze*" for restoring comfort in hot-humid climates.

These fovourable air speeds, which was indicated as "*annoying*" in the other studies (Olgyay, 1992, Szokolay, 2008), are obviously much higher than the upper limit recommended by ASHRAE.

Recommendations on employing high air velocity beyond the ASHRAE's suggested boundary to improve human comfort under hot-humid countries are also found in many studies (see Table 2-10).

**Table 2-10** The acceptable air speeds under hot climates.

| References | Findings |
|---|---|
| Roles et al (1983), Tanabe & Kimura (1987,1989) in (Fountain and Arens, 1993) and Tantasavasdi et al in (Tantasavasdi et al., 2001) | Suggested air speeds as high as 1ms$^{-1}$ for restoring comfort in hot climates. |
| Lei in (Lei, 2009) | Suggested air speed as high as 1.5ms$^{-1}$ for offsetting high temperature in the warm-humid climate of Southern China. |
| Bansal et al in (Bansal et al., 1994a) | Suggested the range of wind speed between 0.53ms$^{-1}$ and 3.04ms$^{-1}$ with the minimum of 0.29ms$^{-1}$for warm and humid climates. |
| Khedari et al in (Khedari et al., 2000c) | Suggested air speed of up to 3ms$^{-1}$ offset for high room temperature (above 34°C) during summer of Thailand. |
| Candido et al in (Cândido et al., 2010) | Concluded that the people in the tropics prefer higher local air speed range than the maximum velocity permissible by ASHRAE Standard even in the situations where the subjects have no control over local air movement. |
| Chow in (Chow et al., 2010) | Found that occupants in a/c environments preferred air speeds above 0.2ms$^{-1}$ under indoor air temperature at 25°C and that of 1.2ms$^{-1}$ to 3.1ms$^{-1}$ at 27°C and 30°C. |

In Table 2-11, air speed ranges that have been found as acceptable or preferable in the studies conducted in hot-humid climates are compared to the upper limit of acceptable air velocity allowed in ASHRAE's.

**Table 2-11** Acceptable air velocity found in the reviewed literatures.

| Reference | Climate |
|---|---|
| ASHRAE (2013) | n/a |
| Olgyay (1992) | n/a |
| Szokolay (2014) | n/a |
| Roles et al(1983) | n/a |
| Tanabe & Kimura (1987, 1989) | n/a |
| Tantasavasdi et al (2000) | n/a |
| Hyde (2000) | Tropics |
| Givoni (1963) | Tropics |
| Toftum (2004) | Tropics |
| Lei (2009) | Tropics |
| Bansal et al (1994) | Tropics |
| Khedari et al (2000) | Tropics |
| Chow et al (2010) | Tropics |

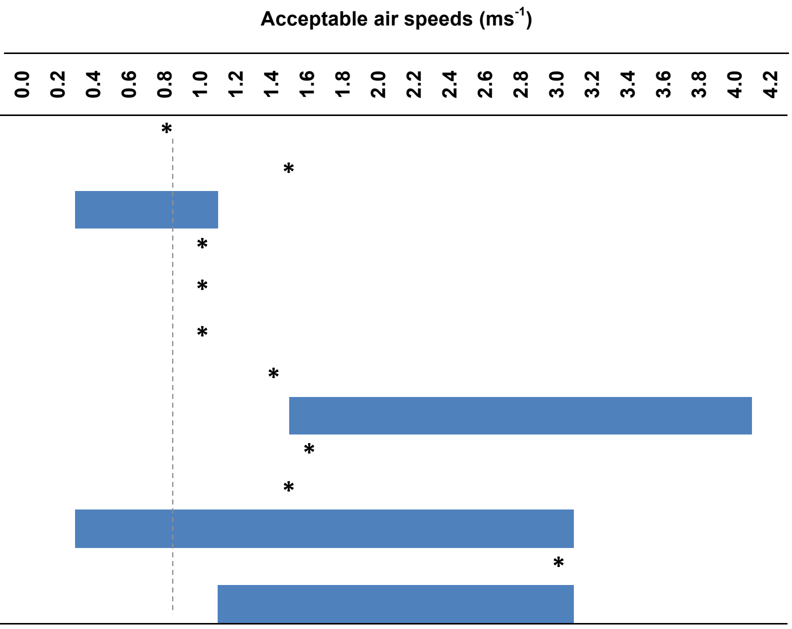

According to Table 2-11 there is a wide range of suggested air speeds varying from 0.2ms$^{-1}$ to 4.0ms$^{-1}$. The star (*) in the Table refers to the upper limits of air speed suggested in the particular studies, while the dark blue lines show the acceptable or preferable ranges of air speed that are found in the literatures. It can be seen that all upper limit suggested are beyond the permissible air speed recommended by ASHRAE (dash line). It is also found that the maximum rates of all acceptable air speed range, particularly that obtained from research under tropic climates, are much greater than ASHRAE's. This may be because the upper limit of acceptable air speed suggested in ASHRAE is developed based on a concern of office environment under cold climates. This limit is, therefore, much lower than that would be acceptable by people in naturally ventilated buildings under tropic climates, especially for residential buildings. In such situations the air speed limit is based on its effect on comfort, which depends on the temperature and humidity rate. For people in tropical countries, who becomes passively acclimatized to high temperature and get used to employing high air velocity e.g. from electric fans to improve their comfort, air movement with higher velocity than suggested in ASHRAE is still acceptable and pleasant.

### *2.5.4 Summary*

Indoor air movement has three main functions i.e. to replace warm indoor air with cooler outdoor air; to cool down a building structure; and to induce the building occupants' thermal sensation. While only a small air exchange rate is required for achieving the former two functions, air movement with high velocity across the occupants' skin surfaces, called '*thermal comfort ventilation'*, is crucial for producing physiological cooling effect for maintaining and improving human thermal comfort in hot-humid climates.

In hot-humid climates an increase in air movement produces two direct positive effects on human thermal comfort including: i) improving thermal sensation by inducing convective heat transfer and; ii) reducing discomfort due to wetted skin by inducing sweat evaporation from skin surface. This physiological cooling effect is suggested by extensive research as a significant strategy for increasing occupants' comfort and reducing building energy consumption due to cooling systems for buildings in hot-humid countries, particularly when ambient temperature is below indoor temperature. However, there are studies that indicate the positive effect of elevated air movement even for high ambient temperature as the upper limit of comfort would be shifted upwards with a higher air velocity.

The physiological cooling effect of elevated air movement has been investigated since 1950s. The strong relationship between comfort and air speed has been found and thermal comfort ventilation has been suggested as a passive design strategy for the tropics since then. Various standards and recommendations include air velocity as one of the main parameters for defining comfort and the wide range of preferred air speed for restoring and improving comfort under different conditions i.e. temperatures and humidity have been proposed. Also, a number of equations have been introduced for predicting the cooling effect of elevated air speed for compensating for high temperature.

The last major topic discussed here is the upper limit of acceptable air speed for residential buildings in hot-humid climates. While international standards e.g. ASHRAE has suggested a maximum acceptable air speed of 0.8ms$^{-1}$ and indicated that air velocities above this level may produce disturbance and may create discomfort due to cool draught. However, there are a number of studies that mention that these recommendations may be far too restrictive for the tropics, particularly for residential buildings. In these studies air velocities even as high as 3ms$^{-1}$to 4ms$^{-1}$ at the occupants' skin surface are indicated as preferable or, in some situations, required for restoring or producing comfort conditions for un-conditioned buildings in hot-humid countries.

## 2.6 Summary and conclusions for the study

In this chapter the background theory of natural ventilation in buildings is reviewed. Natural ventilation in buildings is driven by the pressure difference between the indoor and outdoor environment due to the combined effect of stack and wind forces. While airflow distribution due to stack force is hard to control due to its weak inertia, airflow due to wind force can be controlled by openings design. Wind force is also favourable over stack force as it can provide air movement with high velocity, which can produce physiological cooling effect and improve the occupants' comfort directly. For buildings in hot-humid countries, wind-driven principles such as cross ventilation are therefore preferable.

However, there are situations where such principles are impossible e.g. in a single-sided ventilated building, or impractical e.g. when external wind speed is very low. For these cases, additional devices or natural ventilation induced strategies are required for improving occupants' comfort. In this chapter three chosen strategies are reviewed with an intention to identify their significant characteristics for inducing indoor air velocity and thus comfort for buildings in hot-humid climates.

It is found that the strategies based mainly on wind driven e.g. wing-walls or wind-towers with Venturi-shaped roof can effectively produce high indoor air velocity, while those are based on stack driven e.g. solar ventilation strategies can produce only small airflow rate, which is insufficient to produce any cooling effect or comfort. These wind-driven strategies are basically developed by creating the high wind pressure-differences between the inlet and outlet openings i.e. by increasing positive pressure at the inlet and negative pressure at the outlet. This effective principle will be, therefore, employed as the main idea for developing the proposed strategy for single-sided ventilated residential buildings in Bangkok in the next chapter.

# Chapter Three

## Ventilation shaft: the proposed strategy

### 3.1 Introduction

Thailand is a tropical country with high ambient air temperatures, high humidities and low prevailing wind speeds for most of the year. These climatic conditions lead to a large amount of thermal discomfort time i.e. there is approximately 51% of the time during a year when conditions are outside the thermal comfort range according to ASHRAE's adaptive comfort model (2013) (see Table 1-1 in Chapter One). For a building in such hot-humid climates, thermal comfort ventilation is recommended as the most effective passive design strategy to provide thermal comfort conditions with no or low energy consumption. This can be especially effective for cross ventilation, where external air is driven into the room from one opening and exhausted through the other opening(s) with a high average velocity due to great wind pressure difference between these openings.

However, there are some situations where such strategies are impossible or inefficient e.g. when a building or a room has only single-sided ventilation. In these rooms the air velocity is very weak, and is insufficient to produce any cooling effect. As a result, mechanical cooling systems are frequently employed to provide the occupants' comfort. Over recent years a large number of high-rise residential buildings have been built in Bangkok. Unfortunately, almost all of these buildings are double-loaded corridor with one internal corridor on each floor and the residential units located on their either side. As a result almost all units are single-sided ventilated and all of them employ air-conditioning (a/c) systems to provide the occupants' thermal comfort.

In this chapter the findings from a survey on high-rise residential buildings in Bangkok, which is this study's main focus of interest, are first described to illustrate the typical characteristics of this building type. Then, the results of a pilot study conducted by the author to investigate the indoor air velocities in a chosen single-sided residential unit in Bangkok are summarized. Finally, a wind-induced ventilation strategy, which has high potential to increase the effectiveness of natural ventilation to improve thermal comfort conditions in typical residential units under hot-humid climates, is proposed.

## 3.2 High-rise residential buildings in Bangkok

Residential buildings in Bangkok can be categorized into three main groups relating to their typical floor layouts. These involve i) tower type, where there is a central core (staircase and escalators) with small numbers of residential units per floor located around the core; ii) unit type, where there are more than one cores (mostly staircase only) and each core connects to up to three to six residential units; and iii) corridor type, where there is a central core connected to an internal corridor and residential units are located on the either side of the corridor (Figure 3-1a, b and c, respectively).

(a)

(b)

(c)

**Figure 3-1** Different layouts of residential buildings in Bangkok: (a) tower-type; (b) unit type; and (c) corridor type [adapted from (Imano et al., 2008)].

High-rise residential buildings in Bangkok, which have been completed in the last five years were surveyed by the author. It was found that none of them has a unit type layout as this layout may suit only buildings of no more than four storeys (Figure 3-1b). Only a few of them are tower-type (Figure 3-1a), such as *The PANO*, which is an award-winning six-star riverfront condominium; *The MET*, which is a luxury, awards-winning condominium; and *KEYNE*, which is a high-class condominium in the business center of Bangkok (Figure 3-2a, b and c). These properties either have one main vertical circulation core with wings consisting of a small number of residential units per floor e.g. *the PANO* (Figure 3-2a) and *KEYNE* (Figure 3-2c); or have more than one tower, each of which has a vertical core with small numbers of residential units located around the core e.g. *the MET* (Figure 3-2b). It can be seen that, for a tower-type buildings, there is a possibility for each unit to have two external walls and to be able to employ cross ventilation.

(a) (b) (c)

**Figure 3-2** High-rise residential buildings in Bangkok with tower-type layout; (a) typical floor plan and one-bedroom unit layout of *The PANO* (www.thepano.com); (b) *The MET* (www.met-bangkok.com); and (c) *KEYNE* (www.sansiri.com).

On the other hand all other high-rise residential buildings in Bangkok are corridor-type. In these properties the ratio between a salable (unit area) and unsalable area (e.g. corridor and service area) is high. As a result these buildings mostly employ only one main circulation core with a central corridor on each floor. Residential units are situated on the either side of the corridor and therefore most of them have single-sided ventilation. Examples are *The River*, which is a luxury riverfront condominium (Figure 3-3a); and other middle-class condominiums e.g. *Lumpini Park* and *Apple Condo* (Figure 3-3b and c). It can be seen that there is only a small chance for each unit in these buildings either to have more than one external wall or to employ cross ventilation.

(a) (b) (c)

**Figure 3-3** High-rise residential buildings in Bangkok with corridor-type layout; (a) *The River* (www.theriverbangkok.com); (b) *Lumpini Park* (www.lpn.co.th); and (c) *Apple Condo* (www.applecondo.com).

However, a single-sided ventilated room is found to have poor ventilation as the airflow is driven mainly due to stack force based on a small temperature difference between the upper and the lower part of the same window. Also single-side ventilation is suggested to be effective only for a short distance from the opening due to its weak inertia.

Moreover, a single-sided room's poor ventilation is confirmed by the findings from a pilot study conducted by the author. Indoor air velocities in a chosen one-bedroom apartment unit (35m$^2$ floor area) on the 13th floor of an existing 26-storey condominium (*Lumpini Place Pinkloa 2*) in Bangkok were measured at periods for 24hours in February, 2010 using a calibrated Airflow Anemosonic UA30 anemometer. The chosen building is a corridor-type building with only one core (Figure 3-4a). In this building almost all units are single-sided with two top-hung windows in a bedroom's wall (each with 0.8m$^2$ operable area) on the same external wall (Figure 3-4c and 3-4d). In the study the author had set twelve measuring points in the room (Figure 3-4b) and the air velocity was measured from one point to another every 2 hours. During the measurements the external windows were both fully opened, while all the doors were closed and so the room had single-sided ventilation. Average air velocities of the twelve points were found to be very low i.e. between 0ms$^{-1}$ and 0.05ms$^{-1}$, for an external wind speed range of 0.2ms$^{-1}$ to 2.0ms$^{-1}$. These average velocities are insufficient to produce any cooling effect and thermal comfort, according to the literatures reviewed in the last chapter.

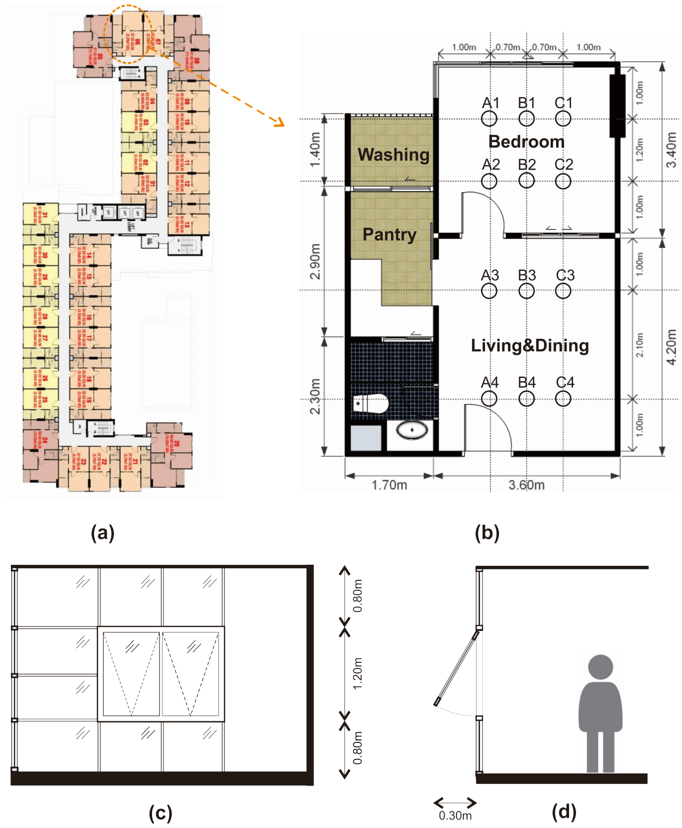

(a) (b)

(c) (d)

**Figure 3-4** Building’s floor layout and a room with grids for indoor air velocity measurement: (a) Building’s typical floor layout; (b) Unit floor layout; (c) Room’s external façade with top-hung windows; and (d) Detail of the room’s main window.

According to the survey and the pilot study explained above, the residential units in typical high-rise buildings in Bangkok are mostly single-sided and their indoor airflow is very low, which is suggested to be effective only to maintain reasonable indoor air quality. Such air movement is, however, insufficient either to compensate for high air temperatures or to produce any direct cooling effect for the occupants under the hot-humid climate of Thailand. As a result, all of these residential units employ air conditioning systems to achieve thermal comfort. However, air conditioners have a high energy demand. In order to enhance the potential of natural ventilation to provide comfort in such units, passive natural ventilation strategies, especially wind-induced approaches, are required.

In this study a natural ventilation strategy driven mainly due to wind effect is proposed for a single-sided ventilated residential unit in typical high-rise buildings in Bangkok. This particular strategy is developed with an intention to increase indoor air velocity, to improve thermal comfort conditions, and thus reduce air-conditioners dependent and energy consumption due to cooling load in such units.

## 3.3 Ventilation shaft: the proposed strategy

For buildings in hot-humid regions thermal comfort ventilation driven by wind force is recommended as the most effective passive design strategy to provide occupant thermal comfort. This passive strategy requires air movement with high speed at the occupants' body level to increase convective heat transfer and to encourage the sweat evaporation from the occupant's skin, which directly enhances human thermal comfort. Also, high air movement is an effective tool for removing hot internal air and the high temperature stored in the rooms' surfaces when ambient temperature is less than indoor air temperature. This process creates an indirect cooling effect and improves the room's thermal comfort conditions. As it employs high air movement to achieve its functions, thermal comfort ventilation is therefore normally specified in terms of air velocity rather than air change rate or airflow rate.

However, achieving the required indoor air velocity range for improving thermal comfort conditions in a room with single-sided ventilation under hot-humid climates, especially that with only one window, can be challenging. This is because the ventilation in such rooms is based mainly on a weak stack effect, which is unable to create high airflow (Figure 3-5a). In such situations wind-induced natural ventilation strategies are needed.

In this study a wind-induced strategy called '*ventilation shaft*' is proposed (Figure 3-5b). Similar to the wing-walls and wind-towers with a Venturi-shaped roof reviewed in Chapter Two, the proposed strategy is based on an idea to create an artificial negative pressure so that the pressure difference between the inlet and outlet openings is high enough to drive the external air into and across the room's occupied area - thereby producing a cooling effect for the occupants. The proposed strategy employs a vertical shaft with an exhaust opening at its top to attach to a residential unit at its rear wall, opposite the room's main facade (Figure 3-5b). The room is connected to the shaft by a set of grilles (vent) and its window will act, mostly, as an inlet.

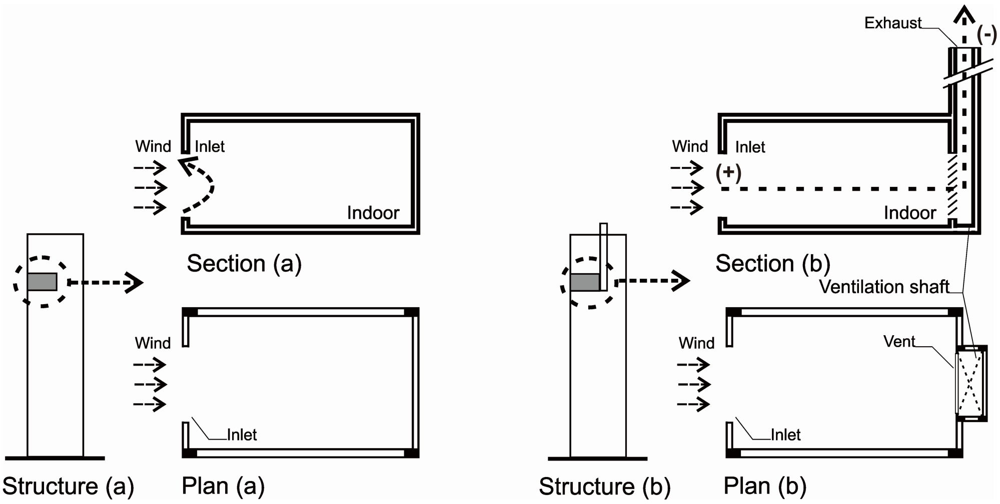

(a) (b)

**Figure 3-5** Principle of ventilation shaft: (a) air movement in a single-sided room without a ventilation shaft; and (b) the room with ventilation shaft (Prajongsan and Sharples, 2012b, Prajongsan and Sharples, 2012a).

When the room's window is on the windward side with respect to the prevailing wind direction, it will be subject to high positive pressure (+ in the Figure 3-5b) while the exhaust opening at the shaft's top is subject to negative wind pressure or suction (- in the Figure 3-5b). In this case the pressure-difference between the room's window, which acts as the inlet, and the shaft's opening, which acts as the outlet, will be maximized. The external air will be driven through the inlet and pushed across the room through the rear vent before it will be driven upwards and exhausted from the building through the shaft's opening due to strong suction force. On the contrary, when the room's window is on the leeward side of the building, it will become subject to high negative pressure. This window will, therefore, act as an outlet, while the shaft's exhaust will be subject to a comparatively smaller negative pressure and will act as the inlet. As a result the opposite direction of the room airflow will be reversed i.e. external air will be driven into a building through the roof's opening and exhausted through the room's window instead.

In this study the proposed ventilation shaft strategy is hypothesized to be able to increase the potential of natural ventilation to induce thermal comfort of the occupants in a single-sided ventilation unit of the typical high-rise residential building in Bangkok by increasing air velocity in the room's main occupied area.

## 3.4 Summary

In this chapter the typical characteristics of high-rise residential buildings in Bangkok and their drawbacks in terms of building ventilation and thermal comfort are analyzed and concluded. Almost all of this building type is found to be double-loaded corridor with the residential units located on the either side of an internal corridor on each floor. This leads almost all the units to be single-sided. In order to improve the thermal comfort conditions in such residential units, the proposed wind-induced strategy called '*ventilation shaft'*, is introduced. Based on the similar concept of wing-walls and wind-tower with venturi shaped-roof, the ventilation shaft strategy employs a vertical shaft with an opening at its top which is subject to negative pressure to increase high pressure difference between the inlet (room's window) and the outlet (shaft's opening). The proposed strategy is hypothesized to be able to effectively increase a single-sided ventilated room's average indoor airflow to achieve the required velocity for producing cooling effect, to create a cross ventilation, and to enhance thermal comfort for the residences, which is the main objective of the study.

# Chapter Four

## Natural ventilation research methodology

### 4.1 Introduction

In order to investigate the performance of wind-induced natural ventilation strategies including the proposed strategy, there are several available methods can be adopted. In this chapter some of these methods together with their applicability and limitations are reviewed regarding to the study's main objective i.e. investigating the performance of the proposed wind-induced natural ventilation strategy in terms of detailed airflow field within a single-sided ventilated room. In the last part of the chapter the most suitable method for this present study is established.

### 4.2 Methods for investigating natural ventilation in buildings: The review

In order to study the complex behaviors of natural ventilation in buildings and to investigate the performance of natural ventilation strategies for improving indoor thermal comfort conditions, there are a number of available methods that can be employed. In this section, two main categories of methods for natural ventilation studies found in literatures are reviewed and discussed in order to establish the most relevant method for this present study. These categories involve: i) modeling methods and ii) full scale methods.

#### *4.2.1 Modeling methods*

Modeling techniques are very useful methods for studying natural ventilation in and around buildings as they allow the effect of different scenarios and parameters on natural ventilation to be investigated with small cost and time consumption comparing to full-scale methods. These techniques also allow ventilation strategies or devices that do not existed to be assessed. Modeling methods can be grouped further into three sub-categories including: i) analogue models; ii) numerical models and iii) physical model. Each of these methods is explained and their applicability to investigating natural ventilation strategies is discussed below.

### *1) Analogue models*

Analogue models use other physical variables that are more readily manipulated by the experimenters such as electric circuit constant or water (or sometimes treated water such as salted water) to represent the characteristics of ventilation (Hitchin and Wilson, 1967). These techniques therefore depend mainly on the construction of an analogue between the characteristics of two variables. Such analogies may be established via an explicit mathematical model for the ventilation processes, or by a direct correspondence between the two sets of variables. However, the correspondence between analogue and actual phenomena is usually imperfect. The methods' accuracy would depend on the accuracy of the simulation and the knowledge of the various heat flow paths (Hitchin and Wilson, 1967).

Also, analogue models are not popularly employed in wind-dominated natural ventilation studies. Almost all of the literatures that employed analogue models in the last ten years focus on stack-driven ventilation. This may be because it is suitable for re-producing the characteristics of stack-driven ventilation that is difficult to be obtained from other methods. Some of these studies use salted-water as the working fluid (salt-bath technique) (Hunt and Kaye, 2006, Lin and Lin, 2014, Lin and Tsai, 2013), or other fluids such as ethanol (Stavridou and Prinos, 2013) to represent particular characteristics of ventilation in each study.

Here are three examples of natural ventilation studies by Livermore, Woods, and Chenvidayakarn which employed analogue models using water as the working fluid to investigate stack-driven natural ventilation (Livermore and Woods, 2006, Chenvidyakarn and Woods, 2007, Livermore and Woods, 2007). Although these studies are slightly different in their aims they all focused on investigating the behavior of stack-driven natural ventilation under particular situations. The predicted results obtained from the analogue models are also used to compare and validate the developed theoretical models. In these experimental studies an acrylic tank (with hole(s) to represent opening(s)) was used as a scale model to represent the concerned building. Then the model was placed in a large reservoir, which represented the ambient condition. A set of controlled heating wire was placed at the specific locations within the model as to represent the heat load produced by the building occupants and appliances in the real situation. Then heat distribution within the model under particular conditions (depending upon the aims in each of the studies) could be obtained by using thermocouples to measure the temperatures at different locations within the models and within the reservoir (ambient condition). Airflow distribution within the model under concerned situations can also be obtained by using shadowgraph technique. According to these studies the analogue models are useful techniques for gaining more understanding in natural ventilation behavior and for validating the theoretical models. This is especially true when stack-driven ventilation is the main focus of a study as this type of ventilation is very difficult to be accurately predicted by using other modeling techniques i.e. numerical and physical models as it is hard to meet the similarities between the model and the real situation required.

### *2) Numerical methods*

Numerical methods use numerical approximation for obtaining the solutions for particular problems. In these methods mathematical problems are formulated so that they can be solved with arithmetic operations. These methods are employed in extensive fields of study including natural ventilation in buildings. They range from a simple algorithm such as analytical and empirical models to very complex computer simulation models such as multi-zone network models, zonal models and computational fluid dynamics (CFD).

i) **Analytical and numerical models**: Analytical and empirical models offer simple and quick approaches that can provide an approximation of indoor ventilation performances. They are very similar as both of them are simple algorithms developed from the conservation equations of mass, energy and chemical species and both are based on some approximations (Chen, 2009, Chen et al., 2010).

Analytical models use simple mathematical models that are derived from the fundamental equations of fluid dynamics and heat transfer e.g. mass, momentum energy and chemical-species conservation equations (Chen, 2009). They are probably the oldest methods in natural ventilation studies that are still widely employed, especially at the early design stage, because of their simplicity for implementation as well as their richness in physical meaning and low requirements in computing resources. However, they have to be used within the limits of their applicability.

According to the literatures found most analytical models were developed and employed for predicting the overall airflow rate in a room or a building under particular situations. For example, Yang et al (2005) adopted a simple analytical model to evaluate the potential of natural ventilation in terms of airflow rate due to the combined effects of wind and stack force for low-rise residential buildings in four cities of China. The model was found to be helpful for the designer to determine the ventilation rate that is required for ensuring the acceptable indoor air quality during the design stage (Yang et al., 2005). Similarly, Li, and Delsante (2001) also developed analytical models for sizing ventilation openings to ensure the required airflow rates and temperatures for the particular situation i.e. a single-zone building with two openings and internal thermal mass (Li and Delsante, 2001). The other studies by the same authors also employed analytical models for predicting natural ventilation due to the combined effect of wind and stack forces for particular opening designs (Li et al., 2000, Li et al., 2005, Yang et al., 2013).

Analytical methods are also employed for investigating and optimizing the performance of different natural ventilation strategies in terms of airflow rate such as the one-sided wind catcher (Dehghan et al., 2013); the '*ventilated and screened wall systems'* (VSWS) (Davidovic et al., 2012); the solar chimney with solid adsorption cooling cavity (Dai et al., 2003); and the solar chimney (Bassiouny and Korah, 2009). Furthermore, analytical models are widely adopted for validating the applicability of other methods, particularly computer simulations, to predict ventilation flow rate (Schulze and Eicker, 2013, Allocca et al., 2003); and sometime even for developing a new building performance simulation software or introducing new features to existing software. There is, for instance, an integrated model incorporating passive airflow components e.g. solar chimney, wind-tunnel and earth-air tunnel into a coupled multi-zone ventilation and building thermal model e.g. *COMIS-TRNSYS* (Alemu et al., 2012).

It can be seen that analytical approaches are simple and quick for estimating natural ventilation performance for the pre-design stage. Nevertheless, they use simplifications both for geometry and thermo-fluid boundary conditions to obtain solutions. They are also case dependent i.e. the equations obtaining for one case may not be suitable for another without any modifications, which is a major drawback with respect to parametric studies.

Slightly different empirical methods are the simplified approaches for approximating airflow rate or mean air velocity within a building zone during the earliest design phase. They are developed based on the general correlations between variables that are found from experimental studies. These expressions combine the airflow with a number of associated parameters e.g. temperature difference, external wind speed and basic building configurations, as well as fluctuating terms to estimate a bulk airflow rate or air velocity in a building (Allard, 1998).

There are empirical models that are developed based on the data obtained either from experimental studies or building simulation software for estimating natural ventilation inside a building under particular conditions. These empirical models include, for example, the models developed in many studies to estimate ventilation rate in a single-sided room for a specific condition under some particular assumptions (Caciolo et al., 2013, Wang and Chen, 2012, Larsen and Heiselberg, 2008); the CSTB methodology (1992) and the Ernest methodology (1991) for predicting the wind-induced indoor air movement under the effects of various parameters (Allard, 1998); Melaragno's tabulated data (1982) for predicting mean indoor air velocity for cross ventilated rooms with different openings' sizes and wind directions; Givoni's tabulated data (1976) for estimating average and maximum indoor air velocity for single-sided and cross ventilated rooms with different opening widths and wind directions; as well as Givoni's model (1978) for calculating the average indoor air velocity in the rooms with a square floor plan and with identical upwind and downwind openings located on opposite walls (Eq.4-1).

$$\boldsymbol{V_i = 0.45(1 - e^{-3.48x})V_r} \qquad \textbf{Eq. 4-1}$$

where $V_i$ is the average indoor velocity; $x$ is the ratio of the opening's area to wall area where the opening is located; and $V_r$ is the reference external wind speed (Allard, 1998).

Empirical models are useful for predicting natural ventilation performance during the design stage, both in terms of bulk ventilation rates and indoor air velocity in a single-zone building. However, they are not suitable for complex cases and cannot be considered for general use as they are developed based on experimental data under particular circumstances and assumptions as discussed in (Ai and Mak, 2014). Moreover, they are to be applied only within the limit of their applicability with simple geometries. Most of all, they are not practical for parametric studies with numbers of alterations in geometry and variables.

ii) **Multi-zone network models:** Multi-zone models are the simplest computer simulation models among numerical methods. They use a network approach i.e. the tested building is represented by the numbers of zones that are interconnected by flow paths forming a network of nodes and resistances. Volumetric flows at specific points (nodes) across the field are then calculated based on their pressures, which are the function of the wind and temperature difference on either side of the flow path (Eq. 4-2).

$$\boldsymbol{Q = C(\Delta p)^n} \qquad \textbf{Eq. 4-2}$$

where $Q$ is the volumetric flow rate; $\Delta p$ is the pressure difference across the airflow path; $C$ is an empirical discharge coefficient; and $n$ is the empirical exponent which may vary from 0.5 (for large openings) to 0.65 (for crack-like openings) (Bradley and Utzinger, 2007).

Together with this power law (Eq. 4-2) multi-zone models are based on three important assumptions: i) the resistance to airflow of a flow-limitation path between building zones is much greater than that to the airflow of the zones themselves; ii) the pressure varies hydrostatically within a building zone is only true when airflow within the zones and thus, airflow in and out of the paths connecting different zones is zero; and iii) the temperature within a given zone are uniform (Bradley and Utzinger, 2007). According to these assumptions, each zone in the room is typically well mixed or homogeneous as the air within each zone is considered to be at the same state throughout the zone at any given time, including its temperature, pressure and contaminant concentration (Emmerich et al., 2009, Chen, 2009).

Since the 1970s many multi-zone programs have been developed, such as *BREEZE*, *COMIS* (Conjunction of Multizone infiltration Specialist), *AIRNET, ESP* (Environmental System Performance), *Tas-Flows, AIOLOS,* and *CONTAM*. They are mostly used for predicting bulk air exchange rate and airflow distribution in a building with or without mechanical ventilation systems (Feustel and Dieris, 1992). The most significant feature of these programs is their ability to simulate the flows, both under steady state and transient situations, in a building with a large number of zones or rooms for a long period of up to a year. For example, Bojic and Kostic (2006) employed *COMIS* for assessing the air quality of a typical apartment unit due to infiltration (Bojic and Kostic, 2006), and Koinakis (2005) adopted the same simulation package to investigate the effect of various internal openings arrangements on air change rate in an existing two-storey house. In the latter study the predicted results in terms of air change rate per hour (ACH) were also validated based on the measured data obtained from the tracer gas decay experiments in the house before the simulation model was used further for parametrical investigations (Koinakis, 2005).

Multi-zone models are also incorporated with other building performance simulation models e.g. zonal or CFD models, to produce more accurate predictions on detailed airflow in each building zone (Chen, 2009). In the studies by Dorer and Weber (1999) and Haase et al (2009) the multi-zone model, *COMIS*, was coupled with a thermal building simulation program (*TRNSYS*) to investigate different passive design strategies and the effect of double-skin facades' designs and configurations on building energy efficiency, respectively (Dorer and Weber, 1999, Haase et al., 2009). Similarly, Bradley and Utzinger (2007) used the coupled *CONTAM* and *TRNSYS* to study the performance of different natural ventilation control strategies i.e. purely mechanical, purely occupant control and occupant control with humidity lockout control in order to develop the control recommendations for a particular building regarding to its energy efficiency (Bradley and Utzinger, 2007).

In conclusion, multi-zone models are very powerful tools for estimating bulk airflow in a large building and for assessing the performance of building ventilation, but with a relatively small computing demand. However, they may not be suitable for the cases concerning natural ventilation with large (low resistance) orifices, in which the wind can flow at comparatively high velocities, leading to poorly mixed indoor air. In addition, they are incapable of giving detailed information on air temperature and velocity distribution for a particular building zone (Haghighat et al., 2001, Chen, 2009), which are the main output required in this present study.

iii) **Zonal models:** Zonal models are an intermediate approach between the multi-zone and CFD models. They can provide more information on a room's thermal conditions compared to the multi-zone models but with less detail than CFD models. These models are based on the assumption of the non-uniformity of the thermal parameters in each small zone in the room. With these models, a studied room or building is divided into a limited number of macroscopic zones, typically less than 1000 for a three dimensional space, and the indoor air temperature of each cell is then calculated based on measured airflow patterns or mass and energy balance equations (Eq. 4-3 and Eq. 4-4) (Awbi, 2003, Chen, 2009).

$$\sum_j \boldsymbol{m}_{\boldsymbol{j}\to\boldsymbol{i}} = \mathbf{0} \qquad \textbf{Eq. 4-3}$$

where $m_{j\to i}$ is the mass flow rate from neighboring cell, $j$, to current cell, $i$; and the energy balance equation is:

$$\sum_j \emptyset_{j\to i} + \emptyset_{source} = \boldsymbol{\rho}_{\boldsymbol{i}} \boldsymbol{V}_{\boldsymbol{i}} \boldsymbol{c}_{\boldsymbol{p}} \frac{\partial \boldsymbol{T}_{\boldsymbol{i}}}{\partial \boldsymbol{t}} \qquad \textbf{Eq. 4-4}$$

where $\emptyset_{j\to i}$ is the energy flow rate from neighboring cell, $j$, to current cell, $i$; $\emptyset_{source}$ is the heat source from cell $i$; and the term in the right side of the equation is the energy accumulated in cell $i$ (Chen, 2009).

Different to the multi-zone models, where the well-mixed assumption of physical parameters is adopted, zonal models e.g. *POMA* (Pressurized zOnal Model with Air-diffuser) and *ESP* are more suitable for the cases with large indoor space or with displacement ventilation. They are also favorable for those cases in which the effects of radiant and convective heating and cooling systems are being considered. In addition, zonal models are sometime coupled with other methods for estimating indoor thermal parameters and the heating and cooling load of HVAC systems in a building (Chen, 2009).

Recently zonal models have been employed for predicting thermal parameters in many studies, most of which focus on natural ventilation or hybrid ventilation in large enclosures. This is because zonal models are able to give the global information on thermal parameters with less computing demand compared to CFD models, especially for a large building. In the study by Gao et al (2006), for instance, a zonal model was applied to investigating the performance of the combined stratification cooling and natural ventilation in a large enclosure in terms of mean airflows and vertical temperature distributions (Gao et al., 2006). Likewise, Haghighat et al (2001) adopted POMA to obtain the global information on thermal parameters i.e. temperature distributions and airflow patterns in a room with mechanical ventilation in order to investigate the effects of the room's layout, air supply diffuser and partitions' height on indoor thermal comfort conditions (Haghighat et al., 2001). DeBlois et al (2013) also employed the *ESPr* zonal model to quickly investigate the potential of a roof integrated solar chimney of a detached house for inducing the chimney mass flow rate and thus reducing the room's air temperature due to radiation (DeBlois et al., 2013).

In conclusion, zonal models are useful tools for providing the information of thermal parameters in the macroscopic approach. They can provide information with more detail than multi-zone models, but with less computing demand comparing to CFD models. Nevertheless, they are developed based on mass and energy balance equations, while the momentum equation is ignored so as to reduce the computing times. They could therefore suffer from uncertainty when the cases are dealing with a strong momentum force airflow e.g. in the jet region or thermal plume region. For such cases, CFD with a much greater number of cells would be preferred. Moreover, it was found that the zonal models are not superior to a very coarse-grid CFD simulation in terms of computing cost (Chen, 2009).

iv) **Computational Fluid Dynamics (CFD) models:** Computational Fluid Dynamics (CFD) models have been used for airflow studies since the 1970s when Nielsen (1973) employed an early CFD model to predict the flow in a ventilated room (John D. Anderson, 1995, Nielsen, 2007). Since then CFD models have become a popular method for predicting building ventilation both in practice and research communities. Below is the basic information of CFD:

- **Principles**: In order to study fluid flow, including airflow, it should be noted that the physical aspects of any fluid flow are basically governed by three fundamental principles involving i) mass is conserved; ii) Newton's second law $(F = ma)$; and iii) energy is conserved (John D. Anderson, 1995). These principles can be expressed in terms of basic mathematical equations including: the equation of continuity; three momentum equations or Navier-Stokes equations (one for each coordinated direction); the energy equation; and the transport equation for contaminant distribution (Nielsen, 2007). These equations are coupled and non-linear so that they are impossible to be solved directly. CFD models employ numerical methods to solve these equations to provide a very detailed analysis of the air and energy flow throughout a considered space in a microscopic approach (Nielsen, 2007).

- **Turbulence models**: The approaches or the computational procedures to enable numerical calculation of the mathematical equations above can be grouped into two major classes relating to their complexity and computational intensive (Awbi, 2003). The first group e.g. DNS (direct numerical simulations) and LES (large eddy simulation) attempts to resolve the turbulent fluctuations, which are caused by instabilities between inertia and viscous forces. This principle, however, requires very fine grid and time steps. LES, for example, solves three-dimensional, time-dependent airflow fields based on the space filtering of the turbulence structures. The fluid flow is separated into large eddies and small eddies. While the former ones are solved by the governing equations, the latter ones are approximated and described by suitable subgrid-scale models (Evola and Popov, 2006). These turbulence models e.g. LES, are therefore seldom used unless extreme precision is required and are generally used in engineering applications by CFD modelers (Awbi, 2003, Evola and Popov, 2006).

The second group of turbulence models, such as RANS (Reynolds averages Navier-Stokes) equations, are developed based on the time-averaging of the flow file governing equations where all of the unsteadiness is considered as part of turbulence and is averaged out (Evola and Popov, 2006). These models therefore are much less time-consuming compared to DNS and LES, while they are able to give a reasonably accurate prediction of thermal parameters, particularly for small-scale applications such as in a normal room or small building. RANS turbulence modeling, particularly the standard $k-\varepsilon$, is therefore widely used by most of the commercial CFD software (Allocca et al., 2003, Nielsen, 2007). However, it should be noted that there are some difficulties with the standard $k-\varepsilon$ in describing the airflow in some particular cases. For example, the flow field with low-Reynolds number conditions, such as the airflow close to the surfaces, and with strong streamline curvature such as the external flow, especially in the area of airflow separation and large-scale application such as for urban wind studies (Evola and Popov, 2006, Nielsen, 2007, Awbi, 2003).

Many attempts have been made to compare the applicability of these turbulence models for particular airflow problems (Jiang and Chen, 2003, Posner et al., 2003, Evola and Popov, 2006, Hooff et al., 2011, Hussain and Oosthizen, 2012, Caciolo et al., 2012, Shen et al., 2012, Kobayashi et al., 2013). For the cases concerning internal flows with normal streamline, one of the following models is suggested suitable: RANS's standard $k-\varepsilon$; Low $Re$ model; RNG model; ASM model and LES model (Awbi, 2003). Among these models Reynolds averages Navier-Strokes (RANS) and the large-eddy simulation (LES) are the most common in airflow study.

- **Boundary conditions**: Boundary conditions are the physical parameters that must be specified on the boundary of and within the flow field to define a closed system of flow transport equations (Awbi, 2003, Nielsen, 2007, Awbi, 2008). These physical quantities may be calculated based on available analytical equations or other methods e.g. small-scale or full-scale measurements (Wong and Heryanto, 2004, Lo et al., 2013) and thermal simulations (Nielsen, 2007). After the boundary conditions are defined, the distribution of airflow and heat transfer within the room or the domain boundary can be fully described. There are two significant issues for specifying the boundary conditions for a flow i.e. the location of the computational domain, and the accuracy of the defined conditions to represent the realistic situations. In the general cases of room airflow, the domain boundary is placed at the internal surfaces of the considered room e.g. walls and openings. However, a larger computational domain that includes some outdoor environment is sometimes required. This is, for instance, the case when air velocity at the room's openings is not available. In many cases the defined boundary conditions are based on the measured data from small-scale or full-scale experiments to ensure their accuracy and meaningfulness (Wong and Heryanto, 2004), (Lo and Novoselac, 2013).

- **Numerical techniques**: Numerical discretization techniques are introduced to render the problem to a solvable level. In practice, there are two main numerical techniques for solving Navier-Stokes equations i.e. the finite volume method (FVM) and the finite element method (FEM). However, most of the CFD codes for room airflow analysis use the finite volume method because of its ability to realistically reflect the physical phenomenon with robustness and small computational time (Awbi, 2003). In the FVM technique the studied building or room is divided into a number of small cells using computational grid and the dependent variables are evaluated at the grid points (the intersection point of grid lines). Computational fluid dynamics then solve flow problems numerically by replacing the integrals or the partial derivatives in these equations with discretized algebraic forms, which in turn are solved to obtain numbers for the flow field values at discrete points in time and/or space (John D. Anderson, 1995).

- **Computational grid**: In additional to the suitable numerical technique, the prediction of the airflow is based on the suitable computational grid generation. In order to ensure the accuracy of the predictions, the suitable grid systems and the fine grid resolution are suggested to minimize false diffusion and dispersive errors, particularly in the areas with large gradients (Nielsen, 2007, Awbi, 2008). A sufficient grid cell quality is significant as distorted or degenerated cells may introduce numerical errors. Grid independence study is therefore recommended prior to the main study. This is not only to ensure the accurate but also the good convergence and plausible results.

Typically grid distances between about 100mm and 300mm are suggested for a normal room (the size of 5m.) and a larger room (size of 20m.), respectively and the finer grid cells are suggested in the regions of important flow phenomena. A rough guideline of grid numbers for a typical room can be also approximated as a function of the room's volume (Eq. 4-5).

$$\boldsymbol{N = 44.4 \times 10^{3} V^{0.38}} \qquad \textbf{Eq. 4-5}$$

where $N$ is a numbers of cells and $V$ is the room volume ($m^{-3}$). This formula is valid for a standard CFD model with two-equation turbulence modeling with wall functions. It should be also noted that $N$ must be at least 100 times higher when Large eddy simulation (LES) turbulence model is employed (Nielsen, 2007).

Computational fluid dynamics (CFD) models have been adopted in extensive numbers of studies due to their applicability that allows a wide range of flow phenomena to be investigated. CFD models have been widely employed for investigating the performance of ventilation strategies, and sometime architectural elements, in terms of thermal comfort and indoor air quality. For instance, Printo and Depecker adopted a CFD model with the standard $k-\varepsilon$ turbulence to investigate the effect of various architectural elements i.e. balcony and opening designs as well as an internal division, on indoor velocity distribution and thermal comfort conditions in a two-storey house under the hot-humid climate (Prianto et al., 2000, Prianto and Depecker, 2002, Prianto and Depecker, 2003). Li and Mak (2007) also employed a CFD commercial code with the standard $k-\varepsilon$ turbulence for assessing the performance of wind-catcher to induce building's indoor air movement under different wind speeds and directions. The chosen turbulence model was also examined in the study by comparing the predicted results of pressure and air velocity against the measured data obtained from the published literature. It was concluded in the study that the standard $k-\varepsilon$ turbulence model is applicable for investigating natural ventilation strategies' performance (Li and Mak, 2007). Likewise Kobayashi et al (2013) employed the CFD model with the standard $k-\varepsilon$ model and the Reynolds stress (RSM) to analyze the ventilation performance of the wind-induced monitor roof to induce indoor airflow rate in a two-storey house. The predicted airflow rate was found to have a good agreement to the measured data obtained from wind-tunnel experiments (Kobayashi et al., 2013).

CFD models have recently been coupled with other methods to achieve the studies' objectives. Tablada et al (2009), for example, used a coupled CFD commercial code (the standard $k-\varepsilon$ turbulence model) with a building energy simulation (BES) program to examine the positive effect of shading devices for inducing indoor air movement and improving indoor thermal comfort conditions in a residential building during a summer period. Internal air velocity and pressure coefficients obtained from the CFD code were used as inputs for BES calculations and comfort analysis. In order to validate the CFD program, the predicted data were compared against wind-tunnel experiments. It was found that the CFD model could produce accurate velocity profiles close to the upstream and downstream facades and acceptable data for natural ventilation analysis. The numerical model (RANS and the standard $k-\varepsilon$) was then concluded as a suitable tool for indoor airflow analysis (Tablada et al., 2009). Yik & Lun (2010) also employed CFD simulation software using the standard $k-\varepsilon$ to predict $Cp$ values for specific locations of a window and employed *COMIS* to predict airflow rates in a unit of Hong-Kong public residential buildings to examine the potential of natural ventilation to reduce the room's air temperature (Yik and Lun, 2010).

Furthermore, CFD models are also used for producing information on thermal parameters under particular situations, which are very useful for gaining more understanding on natural ventilation behavior in reality and for developing new methods for assessing different natural ventilation strategies' performance. This is because CFD simulations can provide the detailed information on air velocities in three dimensions and in a large space that cannot be produced by other methods. They are also flexible as they allow several changes and opening designs in the concerned room or building to be investigated with small effort. In Bastide et al (2006), for example, the indoor air velocities predicted by CFD simulations were used to develop the new modeling approach called the '*well-ventilated percentage of a living space due to natural ventilation'* for evaluating different natural ventilation strategies to increase thermal comfort and reduce building energy consumption due to a/c systems. The model is developed based on a time analysis so that the potential of different designs to provide required natural ventilation over a specific time period could be estimated roughly which can be helpful for the architects to evaluate their design's performance in terms of comfort and energy efficiency with small cost and time (Bastide et al., 2006).

In conclusion, CFD models are effective tools for building ventilation studies as they offer rich detail about airflows in and around a building due to both wind and stack effects with smaller cost and time compared to other methods. They also provide a high degree of flexibility for different changes in design and condition, which is significant for parametrical studies, as various variables can be easily altered in modeling process. However, there are few important issues that need special care when employing CFD models in order to avoid uncertainties and errors as well as to ensure accurate results without excessive computing time. These include a suitable simulation method (steady-state and unsteady-state approach); a suitable turbulence model; a proper defined computation grid; and accurately defined boundary conditions. CFD models together with all settings are, therefore, recommended to be validated against trustable data such as the measured data from either small-scale or full-scale experiments to ensure their accuracy and reliability.

### *3) Physical models*

Physical models or reduced scale models have been extensively used for investigating natural ventilation in and around buildings in various approaches. They use measuring techniques and scaling laws to investigate the impacts of different variables on natural ventilation performance. In general physical models or scale models are very useful methods to simulate the behavior of full-scale system so that full-scale values of interested quantities can be obtained from values measured on a model by applying known scaling factors. This is especially true when it is impossible or impractical to test in full-scale i.e. when a situation does not exist, when various model alterations are required in a study or when changes in various parameters are concerned.

However, there are two issues of awareness based on the scaling laws that should be concerned when small-scale technique is employed (Etheridge and Sandberg, 1996, Sandberg et al., 2008, Hitchin and Wilson, 1967):

i) **Similarity of boundary conditions**: For two flows to be similar the conditions e.g. free stream condition, a specified external wind profile, a shape of any solid boundaries and a temperature at the defining boundaries should be similar; and

ii) **Equality of dimensionless parameters**: For two flows to be similar the dimensionless numbers relevant to the actual physical process involved should be equal e.g. Reynolds numbers (a ratio between viscosity and inertial forces); Grashof number (a ratio of buoyancy force to viscos force); Prandtl (a ratio of momentum diffusivity to thermal diffusivity); Froude numbers (a the ratio of characteristic velocity to a gravitational wave velocity); or Peclet numbers (the study of transport phenomena in fluid flows).

There are extensive studies on natural ventilation in buildings that employ physical model techniques, all of which using the advantage of scale models in well-controlled environments i.e. a test chamber or a boundary layer wind tunnel to gain more understanding of natural ventilation behavior under particular situations. Most studies found in literatures employ atmospheric boundary layer (ABL) wind tunnel technique as an experimental tool for exploring the effect of the ambient on the pressure on buildings or the flow through openings. Different types of terrain in real situations can be generated in an atmospheric boundary layer wind tunnel by roughness elements and spires. The properties of the boundary layer are quantified in terms of shape of the vertical velocity profile and roughness height and friction velocity (Sandberg et al., 2008, Hitchin and Wilson, 1967). Then the building surface pressure or flow pattern can be observed by many ways depending on the objectives of each study.

There are studies that employ scale model technique as the main tool. There is, for example, a study by Dutt, A.J. et al. (1992) that employs a 1:100 scale model in a boundary layer wind tunnel and on-site full scale measurement to investigate natural ventilation and thermal comfort in a two-storey community center in Singapore (Dutt et al., 1992). In this study the measured data i.e. velocity coefficient, which is a ratio of air velocity at an interested point to the outdoor reference velocity, that was obtained from on-site full scale measurements was compared to that from a wind tunnel test. For the full-scale study the indoor air velocities at various locations were measured using a low velocity flow analyzer and probes while external wind conditions were measured using Cup anemometer and wind vane placed at 10m above the ground level upwind of the experimental building. For the scale model test the internal and external air velocities were measured using thermistor sensors. Both of the measured results of velocity coefficient obtained from on-site full scale measurements and wind tunnel tests were found to agree well and it was therefore concluded that a wind tunnel was a useful tool for natural ventilation and thermal comfort studies. A study by Tecle et al. (2013) also used a wind tunnel experiment as the main method to study a wind-driven natural ventilation for a low-rise building. In the study a model testing scale of 1:20 was used to investigate the effect of various openings' sizes and locations on indoor ventilation rate $(Q)$ under different external wind directions (Tecle et al., 2013).

In other studies scale model technique were employed to produce important information which was then used as the inputs for other techniques. A study by Lo et al (2013), for instance, a boundary layer wind tunnel experiment and CFD numerical model were combined to investigate wind-induced cross ventilation (Lo et al., 2013). In the study a 1:25 scale model was placed in an environmental wind tunnel for attaining the façade pressure which was then used as the input boundary conditions for more investigations of cross ventilation in terns of airflow rate in a CFD simulation model. The predicted data of airflow rates under studied situations obtained from the coupled wind tunnel and CFD model were found to agree well to full-scale measurements obtained from the previous studies by the authors and therefore the coupled method of wind tunnel and CFD model was concluded as an effective tool for cross ventilation studies.

Two studies by Wong et al. also employed a combined method of wind tunnel experiments and CFD simulations to study the potential of proposed active stack (extract fan) to enhance natural ventilation in terms of ventilation rate in residential apartment building in Singapore (Priyadarsini et al., 2004, Wong and Heryanto, 2004). A scale model of 1:5 was connected to a shaft with an electric fan atop to vertically draw the air out of the model. Omni directional velocity and temperature transducers were used to measure air velocities and air temperature at different locations of the test model. Then the measured data was used as input boundary conditions for more investigations to optimize the proposed strategy in CFD simulations. The study concluded that the proposed strategy was useful for inducing indoor air velocity within a typical apartment unit, especially during nighttime when the external wind speed tends to be relatively low.

There are also extensive studies employing small-scale experiments to validate predicted information obtained from other methods, especially for numerical models. A study by Hoof et al. (2011), for example, employed wind tunnel experiment to evaluate the applicability of two CFD turbulence models i.e. RANs and RNG $k-\varepsilon$ for predicting mean wind speed and surface pressures at specific locations inside a venturi-shaped roof (Hooff et al., 2011). A 1:100 scale model with a venturi-shaped roof was placed in an ABL wind tunnel and the surface pressures at different positions of the roof were measured using amplified differential pressure sensors. Wind speeds within the roof were measured using NTC resistor elements while mean external wind speed and turbulence intensity caused by different wind directions were measured using hot-wire anemometers. In the study it was concluded that both CFD turbulence models provide acceptable predictions of both mean wind speed and surface pressures inside the roof comparing to experimental results. Similarly, Jiang et al. (2003) uses wind tunnel experiments to validate LES turbulence model in CFD simulation in terms of detailed airflow fields i.e. mean and fluctuating velocity, and pressure distribution under different opening designs (Jiang et al., 2003). In a wind tunnel a laser Doppler anemometer (LDA) was used to measure detail velocity. It was found in the study that the predicted data of airflow pattern as well as air velocity in and around the building agrees well with the measured data.

A study conducted by Dehghan et al. (2013) used wind tunnel experiments, flow visualization tests as well as analytical modeling to investigate the influence of wind speed and direction on the performance of various designed one-sided wind catcher models in terms of induced airflow rate and pressure coefficients (Dehghan et al., 2013). A 1:40 scale model was used in the study. A low speed smoke tunnel was used to visualize flow pattern in and around the models. Internal pressure taps were installed at various locations for measuring the variation of pressure along the internal surfaces of wind catcher. Velocity distribution was measured using a single constant temperature hot-wire anemometer. The measured data was then compared to the proposed theoretical model and the model was found to give a good prediction on wind catcher performance under interested wind speeds and directions.

In conclusion, physical models are effective and relatively economical for designers to evaluate the performance of their designs in terms of natural ventilation during design stage. They can provide many types of information i.e. wind pressure coefficient, ventilation rate and internal air movement that commonly required in natural ventilation studies. However, there is some caution when employing small-scale technique i.e. these models could represent realistic results only when the flows in the models are similar to those in reality. This requires an understanding of scaling laws i.e. similarity of boundary conditions and equality of dimensionless numbers. As a result, small-scale experiments are more applicable for wind-dominated cases where heat transfer is rarely involved, while they are not suitable for stack-driven ventilation (Chen, 2009). Also, the measured data from small-scale experiments are limited only to a few measuring points and instrumentation used for velocity measurement may disturb airflow patters (Jiang et al., 2003). Accordingly, a small-scale technique is sometimes coupled with other methods, particularly CFD simulation models, to allow natural ventilation to be investigated in more detailed.

### 4.2.2 Full scale methods

Full-scale methods use measuring techniques to investigate natural ventilation. They are widely accepted as the best method to represent realistic situations, particularly for stack-dominated cases, as modeling methods cannot generate some dimensionless numbers required by scaling laws (Jiang and Chen, 2003). Full scale methods can be further categorized into two main groups involving: i) laboratory experiments and ii) on-site measurements. Each of these methods, together with their applicability, are discussed below.

#### *1) Laboratory experiments*

Laboratory experiments employ a full-scale model of building part(s) or devices and place them in a large laboratory or a study chamber (or sometimes wind tunnel) where the characteristics of ambient conditions are generated. Laboratory experiments are therefore suitable methods when the effects of controlled environmental conditions on natural ventilation, in particular building designs, are being considered. Also, these methods are applicable for assessing thermal comfort or for investigating the effects of exposed environmental conditions on human sensation (Sandberg et al., 2008). This is because the model is built to its real scale.

As laboratory experiments offer reliable and trustable results in terms of replicating the real situations they are widely employed for validating a predicted value obtained from other methods, particularly computer simulation methods. A study by Freire et al. (2013) using a full-scale model in a wind tunnel and on-site measurements were both used for validating various empirical models previously used to estimate airflow rate in single-sided and cross natural ventilation (Freire et al., 2013). Similarly, in a study by Stavrakakis et al. (2008), a full scale controlled environmental chamber was employed to validate the applicability of a turbulence model in CFD simulations (RANS) to predict temperature and velocity distribution in a cross ventilation room driven by both wind and stack forces (Stavrakakis et al., 2008). In the full scale test the internal temperatures and velocities at different locations were measured using thermo-anemometer multi probes for every 60 seconds while wall and surface temperatures were measured using thermo-couples. It was concluded in the study that the RANS turbulence model gives a good predictions of thermal conditions for the particular situations. Jiang & Chen (2003) also employed full-scale experiments to validate two CFD turbulence models (RANS and LES) for their applicability to predict detailed airflow characteristics in and around a single-sided room as well as indoor ventilation rate (Jiang and Chen, 2003). A tracer gas method was used to measure ventilation rates by injecting the tracer gas $SF_6$ into a chamber at a constant rate and then measuring the gas concentration. As a result the ventilation rate can be calculated based on a time delay between the tracer gas entering and leaving a chamber. It was found that LES is relatively preferable to RANS for such stack-driven ventilation case.

In conclusion, laboratory experiments use full-scale models and measuring techniques for investigating natural ventilation under controlled ambient conditions. It is therefore useful for considering the effects of parameters, such as building geometry and ambient conditions, on natural ventilation behavior. For these methods, a full-scale model is used and so that the scaling laws, which can be difficult to achieve, especially for stack-driven ventilation, can be ignored. Laboratory experiments are thus accepted as the best approach to represent the many realistic situations. However, the resolution of the data is often very low as it may not be practical to measure ventilation parameters in many locations in a large model. Furthermore, it may not be practical for parametric studies where large numbers of model alterations may be required.

***2) On-site measurements***

Similarly to laboratory tests, on-site measurements employ measuring techniques to investigate natural ventilation. However, on-site measurements are conducted in an existing building or a mock-up model that is built and placed in a real ambient environment. These techniques are valuable when the natural ventilation behavior in real situations is concerned and they are accepted as the best method for producing the most realistic information.

There are a number of study that have employed on-site measurements to provide very good information that leads to a greater understanding of natural ventilation behaviors in real situations. In a study by Lo & Novoselac (2012), for instance, an on-site measurement technique was used to gain more understanding of wind-driven cross ventilation (Lo and Novoselac, 2012). Extensive data of internal thermal conditions within a one-storey house, together with ambient conditions, were measured simultaneously using the following instruments: wind speeds and directions were measured using an ultrasonic anemometer; flow rate through the openings were measured using a Pitot tube grid and pressure-based flow meters; façade pressures due to the wind were measured using pressure transducers and pressure tabs; and $CO_2$ concentrations were measured using $CO_2$ meters. These extensive data are very useful for giving an understanding of wind-driven cross ventilation and can be employed for future validation studies.

In some studies on-site measurement is used for assessing the performance of different natural ventilation strategies on thermal comfort under a real situation. For example, a study by Kubota et al. (2009) employed on-site measurements to investigate the potential of three natural ventilation strategies i.e. full-day, day-time and nighttime ventilation to enhance the occupants' thermal comfort in a terraced house under the climatic conditions of Malaysia (Kubota et al., 2009). Two similar houses were employed in the field measurements. Indoor measuring sensors were placed within the houses with different strategies to measure air temperatures, relative humidity and air velocity. This information was then used for thermal comfort evaluation.

Moreover, on-site measurement techniques are widely employed for generating significant data for other methods or for validating the predicted results obtained from other methods, particularly computer simulation models. For example, Sadafi et al. (2011) used on-site measured data to develop a baseline model of a house with an internal courtyard (Sadafi et al., 2011). In the study air temperatures, globe temperature, relative humidity and air velocities were measured using thermal comfort data loggers every ten minutes for three days. This information was then used as a baseline model for comparing to other cases of a house with alternative designs of internal courtyard. Yang et al. (2014) used field measured data to validate the applicability of CFD simulation model to predict the induced air exchange rate per hour (ACH) in a common public housing when a central ventilation shaft was employed (Yang et al., 2014). The predicted data were found to agree well with the measured data and they were then used for evaluating human thermal comfort.

Caciolo et al. (2011) also used field measurements to gain more understanding of the mechanisms of flow produced by stack and wind driven forces as well as to validate the existing correlations for predicting air exchange rate generated in a single-sided ventilated room (Caciolo et al., 2011). In the study flow visualization was used to test airflow field; thermal anemometer was used to measure average air velocity and turbulence rate as well as air temperature; 2D particle image velocimetry (PIV) was used to observe the quantity and quality of flow field near the opening; and tracer gas decay method ($SF_6$) was used to measure air change rate.

Although on-site measurements are very useful for providing a good understanding of natural ventilation in a real situation, they are not suitable for cases when controlled thermo-fluid boundary conditions are required. In addition the resolution of the data is often very low as it is not practical to measure ventilation parameters in large numbers of locations in a large building.

In conclusion, full-scale methods use measuring techniques and they can provide the most realistic information on natural ventilation compared to modeling methods as they can express the phenomenon in a way that is physically much more similar to the reality. While laboratory experiments allow natural ventilation behavior and the effects of parameters on natural ventilation strategies under particular environmental conditions to be investigated in detail; on-site measurements can provide the best understanding of natural ventilation in realistic situations. In addition they are both useful for validating the validity and the accuracy of other thermal predictive methods. However, they can be cost-expensive and time-consuming, particularly for the cases with large numbers of alterations and considered parameters. Also there may be unexpected disturbances and the errors from the physical experiments and measuring instruments that may affect the accuracy of the measured data.

According to the reviews and discussions on available methods for natural ventilation study above, each of the method has different strengths and weaknesses based on their principles, characteristics and applicability.

i) **Modeling methods:** These methods use representative modeling techniques with some assumptions to replicate the realistic conditions concerned. Some modeling techniques use other physical variable to represent the characteristic of ventilation (analogue models); some use mathematical model to represent the situations (numerical models); while the others uses physical models and scaling laws to replicate the real situation (physical models). Due to their principles of simulating the real situations, they allow building parts, strategies or devices that do not exist in real situation to be assessed in detail. They also allow numbers of model alterations to be investigated under controlled ambient conditions with small cost and time. These methods are therefore very useful for early-design stage as well as for parametric studies. However, modeling methods are developed based on some assumptions. Their accuracy is dependent mainly on the accuracy of the simulation and the knowledge of researcher on fluid flow as well as measuring techniques.

ii) **Full-scale methods**: These methods use measuring techniques to investigating ventilation under controlled environment (laboratory experiments) or within an ambient situation (on-site measurement). They are accepted as the best methods to provide the most realistic situations, particularly for stack-driven ventilation which is hardly re-produced in modeling techniques. However, full-scale methods are cost and time expensive. They are, therefore, not suitable for parametric studies when various model alterations are required. The resolution of measured results are also relatively low comparing to modeling techniques, particularly for computer simulation techniques, as it is not practical to conduct measurements in large numbers of locations within a considered building.

After the methods widely employed in natural ventilation studies are reviewed here, each method together with their applicability regarding on the objectives of this present study will be discussed and the most relevant method for this present study will be established in the next section.

## 4.3 The chosen method for the study

In order to choose the main method for this study, there are vital factors for consideration, consisting of i) the objectives of the study; ii) the cost and time required; and iii) the availability of facilities. In this section the discussion based on the suitable methods for this present study is presented.

To achieve the main objectives of this study i.e. i) to investigate the potential of the proposed wind-induced natural ventilation strategy called '*ventilation shaft*' to increase indoor air velocity and to extend thermal comfort in a single-sided apartment unit under hot-humid climatic conditions of Bangkok, ii) to parametrically investigate the influence of different variables on the strategy's performance, as well as iii) to optimize the designs and configurations of the strategy; a large number of cases with different changes in variables and designs is conducted. This requires a predictive method that is i) applicable for producing detailed information in indoor thermal condition, especially indoor air temperature at specific times of the day and detailed air velocity at different locations inside the apartment unit under different external wind conditions; and ii) flexible enough for parametric study with small cost and time-consuming.

Regarding to these objectives and requirements CFD simulation is desirable due to its high capability that allows different alternative designs and parameters to be analyzed in details with comparatively less cost and time consuming. Also, CFD models have been successfully used for investigating natural ventilation, both driven by stack and wind force, in terms of detailed indoor room temperature and airflow distribution, and for a single-sided and cross-ventilated room as can be seen in the reviewed in the previous section. In this present study the available CFD program, DesignBuilder, is therefore adopted as the main tool. It is described in more detail in the following section.

### *4.3.1 DesignBuilder*

In this study, the CFD code from DesignBuilder software v.2.3.5.034 (DesignBuilder, 2006b) is employed as the main tool.

i) **Principle**: DesignBuilder's CFD uses the numerical method known as a primitive variable method, which involves the solution of a set of equations that describe the conservation of heat, mass and momentum (DesignBuilder, 2006a). The equation set consists of three velocity component momentum equations (Navier-Stokes equations), the temperature equation, and the turbulence model for kinetic energy and dissipation rate of turbulence kinetic energy. The equations contain a set of coupled non-linear second-order partial differential equations with the following general form (Eq. 4-6), in which $\phi$ represents the dependent variables:

$$\frac{\partial}{\partial t}(\rho\phi) + div(\rho u\phi) = div(\Gamma\ grad\ \phi) + S \qquad \textbf{Eq. 4-6}$$

where $\frac{\partial}{\partial t}(\rho\phi)$ represents the rate of change, the $div(\rho u\phi)$ represents convection, the $div(\Gamma\ grad\ \phi)$ represents diffusion and $S$ is a source term (DesignBuilder, 2006a).

ii) **Turbulence model**: DesignBuilder's CFD uses RANS's standard $k - \varepsilon$ turbulence model (Eq. 4-7) which is suggested for natural ventilation studies in a normal room due to its applicability for proving acceptably accurate predictions in thermal parameters with relatively less computational time compared to more sophisticated DNS and LES models.

$$\mu_t = C_\mu \rho \frac{k^2}{\varepsilon} \qquad \textbf{Eq. 4-7}$$

where $k$ is turbulence kinetic energy, and $\varepsilon$ is dissipation rate of turbulence kinetic energy (DesignBuilder, 2006a).

iii) **Numerical technique**: For its numerical technique, DesignBuilder's CFD adopted the popular '*finite volume method'* (PVM) that involves re-casting the differential equations into the form of a set of finite difference equations by sub-dividing the considered space or calculation domain into a set of non-overlapping adjoining rectilinear volumes or cells known as the '*finite volume grid*'. The equation set is then expressed in the form of a set of linear algebraic equations for each cell within the grid and the overall set of equations is solved using an iterative scheme (DesignBuilder, 2006a). The non-linearity of the equation set is accounted for by the use of a nested iterative scheme whereby each dependent variable equation set, such as velocity components and temperature, are solved iteratively within an overall outer iterative loop and at the termination of each outer iteration, the most recent values of dependent variables are fed back into the dependent variable coefficients. Then the outer iterative loop is repeated until the finite difference equations for all cells are satisfied by the current values of the appropriate dependent variables, at which point the scheme is converged. The main mechanism to ensure that the variables change slowly is that of false time steps which can slow the change in dependent variables in order to arrive at a more stable solution (DesignBuilder, 2006a).

iv) **Computational grid**: For computational grid, DesignBuilder' CFD uses a non-uniform rectilinear Cartesian grid i.e. the grid lines are parallel with the major axes i.e. main walls and openings, and the space between the grid lines (a grid region) enables non-uniformity. The grid regions and the merge tolerance setting i.e. how the very narrow grid regions are to be merged together to avoid unstable solutions and excessive calculation run times and memory usage due to the cell with a high respect ratio, can be defined by the user. Prior to the main part of this study, the grid dependency test, as suggested by many studies, was performed to ensure good convergence and accurate prediction.

v) **Boundary conditions**: In terms of boundary conditions for internal CFD analysis, as in this study, DesignBuilder's CFD establishes the boundary conditions based on the values calculated by the thermal modeling software EnergyPlus, which is built within the DesignBuilder environment (DesignBuilder, 2006a). These consist of the building's location and constructional components; opening sizes and operation schedule; internal heat gain (occupants, lighting and appliances); supply diffuser and extract grilles; and weather data. The wind speed at any building height above the ground is calculated based on free stream wind speed at 10m above the ground and its surrounding terrain using an empirical relationship suggested by ASHRAE. Detailed information on the boundary conditions established for this study can be also found in the next chapter.

vi) **Wind pressure coefficient ($Cp$)**: Another significant parameter for investigating the performance of natural ventilation strategies, especially the wind-dominated, is the wind pressure coefficient ($Cp$). The differences among these pressure coefficients at different building openings are the main factor to quantitatively determine the air movement in the building i.e. the higher the pressure the greater the airflow in the building. However, the default $Cp$ values provided in DesignBuilder's CFD, obtained from the *Air Infiltration and Ventilation Centre* (AIVC) database, are recommended only for low-rise buildings no higher than three-storeys (see Table A-3 in Appendix A). For this study, in which the main considered building is a high-rise building, such DesignBuilder's default $Cp$ values cannot be used. Other techniques that are applicable for estimating $Cp$ values for a high-rise building are therefore required.

The $Cp$ values, particularly for specific points on the building surfaces, are difficult to obtain as they are not uniform across the building surfaces but vary, and are influenced by many factors e.g. building geometry, façade detailing, position on the façade, the degree of exposure and sheltering, wind speed and direction (Cóstola et al., 2009). $Cp$ values can be obtained either from primary or secondary sources (Cóstola et al., 2009). The former sources e.g. full-scale measurements, reduced-scale measurements in wind tunnels and CFD simulations, are considered as the most reliable $Cp$ data sources. They provide the data for specific buildings and take into account most of the influential parameters. Full-scale measurements provide the most representative description of $Cp$ without the requirement to reproduce boundary conditions. By using ultrasonic anemometers and pressure transducers, the high quality data about the pressure at the building façade can be directly obtained. Nevertheless, full-scale measurements are complex, expensive and can be uncertain due to many factors; they are therefore mainly used for validation purposes and some expertise may be required (Cóstola et al., 2009). For the design stage, wind tunnel experiments or external CFD simulations are preferred e.g. Yik&Lun (2010) used external CFD to predict $Cp$ values for specific location on a façade of Hong-Kong public residential buildings under particular surrounding building blocks (Yik and Lun, 2010). These data banks from primary sources are also useful for developing the secondary sources for estimating the $Cp$ values.

The secondary sources, such as $Cp$ databases and analytical models, provide low-cost data of $Cp$ values for ventilation studies. These secondary sources are also employed in building energy simulations (BES) and airflow network (AFN) programs. For $Cp$ databases, such as those from AIVC and ASHRAE, $Cp$ data obtained from one or more sources are compiled and classified regarding to some parameters e.g. building shape and orientation to incident wind angle. On the other hand, analytical models for predicting $Cp$ values consist of a set of equations to calculate $Cp$ for a specific building configuration with a comparatively user-friendly way to access a broader range of building configurations and situations. These models, such as Swambi & Chandra (1988), *CPBANK, CpCalc+* and *CpGenerator*, are generally developed using regression techniques to analyze a large amount of $Cp$ data (Cóstola et al., 2009). Each of these models has its applicability and limitations. *CPBANK* contains a set of $Cp$ values files for different building geometries and exposures based on wind tunnel studies and can give approximated $Cp$ values for a building similar to the *CPBANK* type (Allard, 1998). *CpCalc+*, developed by Grosso et al (1995), can be used for predicting the $Cp$ values for any location on the building envelope (Good et al., 2008). However, the application of *CpCalc+* is limited to low-rise buildings with building shapes that are close to rectangular in form. This is because the tool is developed based on a parametric analysis of wind tunnel test results for a rectangular shaped building with either a flat or tilted roof for a given terrain roughness, density of surrounding buildings, shape ratio and wind direction (Allard, 1998, Good et al., 2008). Similarly to *CpCalc+, CpGenerator* is based on experimental data from TNO Building Research (TNO-Webapplications) and can predict $C_p$ value for a specific point on a building façade and roof of a building with or without a pitched roof based on fits of measure data regarding on the terrain roughness, building orientation and geometry.

In conclusion, primary sources e.g. small- and full-scale measurements and CFD simulation, are the most promising technique for obtaining $C_p$ data. However, they are cost-expensive and require some expertise, especially for full-scale measurements. For general ventilation studies secondary sources, both databases and analytical model, are preferred. For this present study *CpGenerator* was adopted to provide $C_p$ data at the specific location on a building façade due to its simplicity as well as low cost and low computing time compared to other methods.

### *4.3.2 CpGenerator*

*CpGenerator* is a user friendly application that is capable for predicting $C_p$ values on a building envelope based on the fits of measured data (TNO-Webapplications). Its algorithms are based on systematically performed wind tunnel tests and on the published results from in-situ measurements obtained from extensive numbers of research. It can provide the $C_p$ value for a defined position on a building envelope for a building with different geometries, orientation, terrain roughness (plain pasture, open agriculture land, cultivated land, open suburb or village, normal suburb or industrial estate, and large town), and obstacles (geometries and locations regarding to the tested building) by comparing the case with its data file (TNO-BuildingResearch). Most importantly, it can give a prediction on $C_p$ values for a specific point on high-rise buildings, which are the main building type considered in this study. Although this application has been validated in many studies by comparing the predicted $C_p$ value against the measured data, including a study within the European research project *HybVent* (TNO-BuildingResearch), the $C_p$ value predicted by *CpGenerator* together with the thermal parameters predicted by DesignBuilder's CFD is validated again before these models will be adopted for the main study.

## 4.4 Validation of DesignBuilder

Before DesignBuilder was adopted for this study, its calculation methods, turbulence models as well as its capability for thermal parameters predictions under particular building configurations and specific weather conditions were investigated. The $C_p$ values obtained from the chosen tool i.e. *CpGenerator*, the software's default weather data and the user's ability to generate a simulated model and to define other related settings were also examined. First, the software's default weather data for Bangkok was compared to the average weather data obtained from Thai Meteorological Department between 1999 and 2008. Then, two validation studies were conducted by comparing the predicted thermal parameters against measured data obtained from the in-situ measurements in two existing buildings: i) a two-storey house; and ii) a single-sided apartment unit in a high-rise residential building.

### *4.4.1 DesignBuilder's default Bangkok weather data*

DesignBuilder uses EnergyPlus format (epw) hourly weather data for defining external conditions for all simulations. These data sets derive from hourly observations at a specific location. For Bangkok, the weather information is obtained from ASHRAE International Weather for Energy Calculation (IWAC), which is the result of ASHRAE research project conducted from up to 18 years (DesignBuilder, 2006a). In order to ensure its ability to represent the real thermal conditions of Bangkok, these weather data are compared to the average values of weather data obtained from the Thai Meteorological Department (MET) between 1999 and 2008.

Table 4-1 presents Bangkok's weather data based on hourly data from the EnergyPlus and the average hourly data recorded between 1999 and 2008 by the Thai Meteorological Department. It can be seen that for average mean dry bulb temperature and relative humidity, both data sets have similar trends among different seasons. The annual average values between the two sets are also very close, although the software's default data seem to slightly under-estimate the annually average mean dry-bulb temperature and relative humidity with a deviation of approximately 2% and 3%, respectively. Both software's hourly dry-bulb temperature and relative humidity can, therefore, be applied for all simulations in this study without alteration.

**Table 4-1** Summary of the weather data obtained from the Thailand Meteorological Department (MET) and DesignBuilder's EnergyPlus.

| **Weather parameters** | **Measured data (Average data from 1999 to 2008) (MET, 2010)** | | | | **DesignBuilder's default data (DesignBuilder, 2006b)** | | | |
|---|---|---|---|---|---|---|---|---|
| | **Annual** | **Summer (Feb-May)** | **Rainy (Jun-Sep)** | **Winter (Oct-Jan)** | **Annual** | **Summer (Feb-May)** | **Rainy (Jun-Sep)** | **Winter (Oct-Jan)** |
| Average mean dry-bulb temperature (°C) | 29.1 | 29.8 | 29.2 | 28.1 | 28.5 | 29.5 | 28.8 | 27.2 |
| Average relative humidity (%) | 72 | 72 | 75 | 68 | 70 | 68 | 75 | 68 |
| Mean wind velocity ($ms^{-1}$) | 1.1 | 1.3 | 1.2 | 0.8 | 2.9 | 3.2 | 3.3 | 2.2 |
| Main wind direction (degree) | 180° | 180° | 225° | 90° | 180° | 180° | 225° | 0° |
| Second main wind direction (degree) | 225° | 225° | 180° | 45° | 225° | 225° | 180° | 45° |
| Most frequency speed ($ms^{-1}$) and (Frequency as %) | 1-2$ms^{-1}$ (31%) | 1-2$ms^{-1}$ (34%) | 1-2$ms^{-1}$ (32%) | 1-2$ms^{-1}$ (28%) | 2-3$ms^{-1}$ (28%) | 2-3$ms^{-1}$ (31%) | 2-3$ms^{-1}$ (27%) | 2-3$ms^{-1}$ (31%) |
| Second most frequency speed ($ms^{-1}$) and (Frequency as %) | 2-3$ms^{-1}$ (18%) | 2-3$ms^{-1}$ (21%) | 2-3$ms^{-1}$ (19%) | 2-3$ms^{-1}$ (13%) | 1-2$ms^{-1}$ (21%) | 1-2$ms^{-1}$ (28%) | 3-4$ms^{-1}$ (22%) | 1-2$ms^{-1}$ (28%) |
| Frequency of calm period (%) | 37% | 30% | 33% | 50% | 4% | 8% | 1% | 8% |

Figure 4-1 shows the comparison of average hourly outdoor dry-bulb air temperatures throughout the day for different seasons obtained from MET and EnergyPlus. This chart emphasizes a good agreement between the two data sets for average hourly dry-bulb air temperatures. The relative errors between the data sets are between -2% and 6%, with an average relative error of only 2.2% and in most cases the absolute differences are less than 1.8°C.

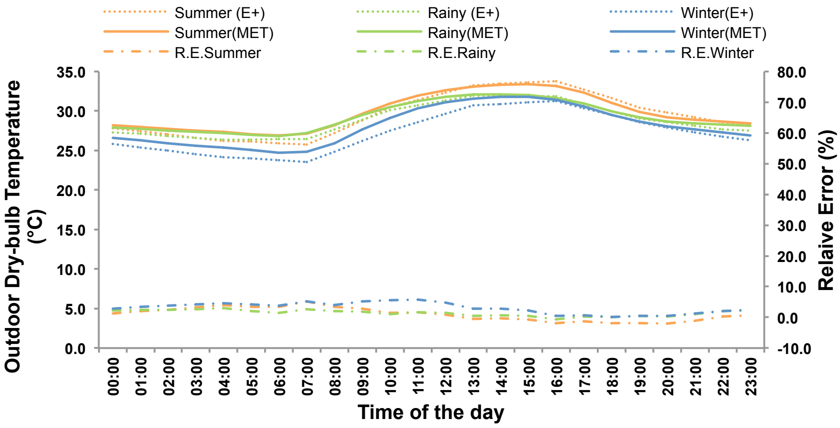

**Figure 4-1** Comparison of hourly outdoor dry-bulb temperature obtained from Thai Meteorological Department (MET) and EnergyPlus (E+) with their relative error (R.E.).

In terms of wind conditions, EnergyPlus provides a similar trend of the annually main and second main wind directions to that from MET, as can be seen in Table 4-1. However, the hourly wind speeds obtained from EnergyPlus are obviously greater than those from MET. Although both data sets have a similar trend during the day (Figure 4-2), the data from EnergyPlus are obviously greater than those from MET at all times i.e. the most frequency wind speed found annually from EnergyPlus is between 2ms$^{-1}$ and 3ms$^{-1}$ while that from MET is only 1ms$^{-1}$ to 2ms$^{-1}$ (Table 4-1). The annually average wind speed from the software and Thai Meteorological Department are 2.9ms$^{-1}$ and 1.1ms$^{-1}$, respectively and their deviations can be as high as 200% with the maximum absolute difference as high as 2.6ms$^{-1}$. This great difference may be because of many factors, one of which is that these data sets are recorded at different locations.

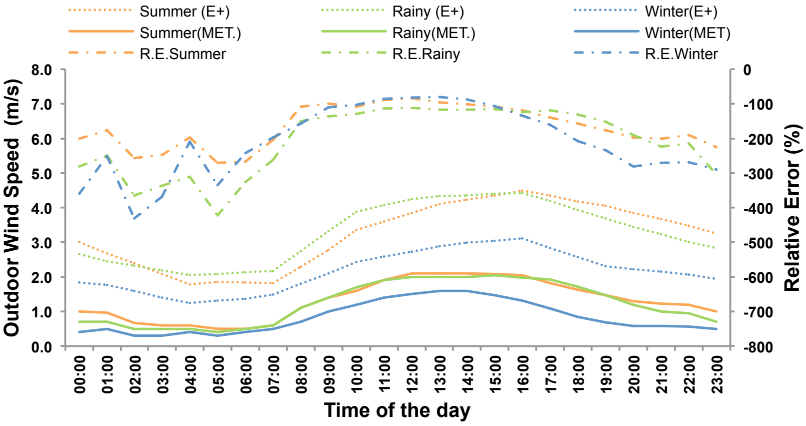

**Figure 4-2** Comparison of hourly outdoor wind speed from Thai Meteorological Department (MET) and EnergyPlus (E+)with their relative error (R.E).

The outdoor wind speeds from MET used in this study have been recorded from the Bangkok metropolis area, which is likely to have a relatively lower wind speed than that in other areas of Bangkok. On the other hand the data from EnergyPlus may be recorded from another area with less wind obstacles, such as Bangkok Port (Klong Toei) or airport (Don Muang). This difference may have an effect on the simulation results of indoor air velocity as the software may give an over-predicted result for the cases located in metropolis area of Bangkok. However, it should be noted that this default wind speed data will be manually adapted in the main study in order to investigate the effectiveness of the proposed strategy for inducing indoor air movement and to examine the effect of various parameters on its performance.

### *4.4.2 An existing two-storey house*

After the software's default weather data were investigated, the performance of DesignBuilder's CFD and other settings to predict indoor thermal parameters, particularly indoor air temperature and air velocity and distribution, were examined. Both predicted average indoor air temperatures and indoor air velocities obtained were compared against the measured data from the in-situ measurement in an existing two-storey house. The main reason for using this building was because of the availability of the full building construction details and measured data.

The building (150m$^2$) is a two-storey house located in Nakorn-Pathom province, which is about 45km west of Bangkok (Figure 4-3). The house is one of the three that have been built for full investigations in the research project called '*Energy Efficiency House*' conducted by the School of Architecture, Silpakorn University and funded by the Energy Policy and Planning Office, Ministry of Energy, Thailand during 2006-2007 (Puthipirot et al., 2007). For the validation a living room (12.25m$^2$ floor area with *W x L x H* of 3.6x4.5x3.0m$^3$) on the ground floor of the house was employed. The room is cross-ventilated with side-hung windows on the north and the south, as well as large grilles and a door on the west (operable area of 5.7m$^2$ for each opening and 1.6m$^2$ for the door) (see Figure 4-4). The main building construction and materials are listed in Table 4-2.

**Figure 4-3** A two-storey house for validation study: the front view with the living room on the ground floor at the right.

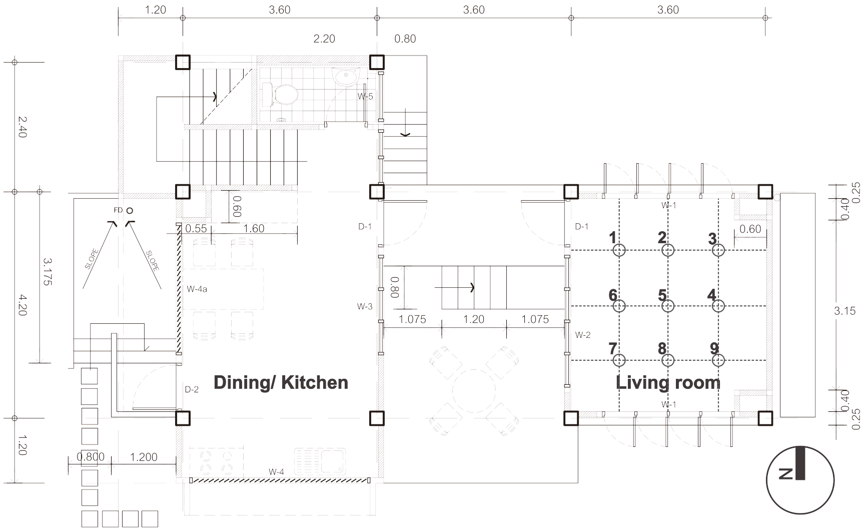

**Figure 4-4** Ground floor layout with the location of the living room (showing the 9 grid points for velocity measurements).

**Table 4-2** List of the house's materials and simulation settings.

| Elements | Details |
|---|---|
| Wall materials | Concrete block (75mm thick) with inner and outer cast concrete (U-Value of $3.623Wm^{-2}K$). |
| Floor materials | Reinforced concrete covered with ceramic tiles. |
| Ceiling materials | Gypsum board (9mm thick) with no insulation materials. |
| Glazing | Single clear glass (6mm thick) (U-Value of $5.801Wm^{-2}K$). |
| Other internal heat gain and furniture | All equipment are set as OFF and there is no furniture to represent the empty room in the real situation. |

The measurements were conducted for three consecutive days during 1st and 3rd September 2006. During these measurements all the openings involving all windows and the door remained fully open. Data loggers (Testo 175-H2) were located at the centre of the rooms at 1m above the room floor for measuring air temperature and humidity at ten minutes interval.

The software called '*Comfort Software Basic'* V3.2 Sp3 was applied for managing all data. For indoor air velocity, a handheld hot-wire anemometer (TESTO V1 Anemometer) was used for measuring the air velocity from one point to another for all nine measuring points across the room (see Figure 4-4) at about 1m above the floor with the interval period between each set of measurements being every two hours for a 24-hour period.

In the simulations, DesignBuilder v.2.3.5.034 was employed. The building model was built based on the configurations and materials used in the real house. The software's default weather data for Bangkok, including hourly dry-bulb temperature and relative humidity, as well as wind directions, were employed in the study; However, the average hourly wind speeds during the rainy season, i.e. between June and September, obtained from the Thai Meteorological Department were used rather than those from the software's default data. This was because the software's default data of outdoor wind speed is over-predicted as found in the previous section.

After the model was built and all the information regarding the design parameters specified, hourly air temperature inside the living room during the particular period (3rd September in this study) was calculated by the software's EnergyPlus function. Then this model, together with its information including outdoor climatic conditions, calculated hourly indoor air temperature and surfaces temperatures were directly imported as the boundary conditions for the CFD calculation.

For the CFD calculation steady-state conditions were assumed. The automatically calculated false time step was employed as the relaxation method in order to slow the change in independent variables for a more stable and converged solution. The RANS's standard $k-\varepsilon$ turbulence model was used as well as the power-law discretization scheme. The non-uniform rectilinear Cartesian grid with the grid space of 0.1m, as recommended for a room with normal size (no larger than 6m) (Nielsen, 2007) and grid line merge tolerance setting of 0.03m (Figure 4-5) were defined. This led to cell numbers of 35 cells, 40 cells and 32 cells for the x-, y-, z- axis, respectively. The maximum grid cell's respect ratio was less than 5.0. The software's default wind pressure coefficient ($Cp$) values, which are derived from the AIVC Application Guide: A guide to energy-efficient ventilation and suggested suitable for use in basic calculation for buildings with no more than three stories were employed in this study (see Table A-3 in Appendix A). All the openings were set as fully open for all time so as to represent the real situation. The CFD calculation results were only taken when the simulations had converged or when the calculations reached beyond 2000 iterations. The isothermal function of the CFD was set as '*OFF*' so as to keep the energy equation for all the calculations. The surface heat transfer coefficients were to be calculated using wall functions rather than defined by the author. The results of air velocities across the room could then be calculated for every hour during the specific day (3rd September). Finally, both the average daily air velocities for each of the nine measuring points and the average velocities across the room for the 24-hours period were compared to the measured data.

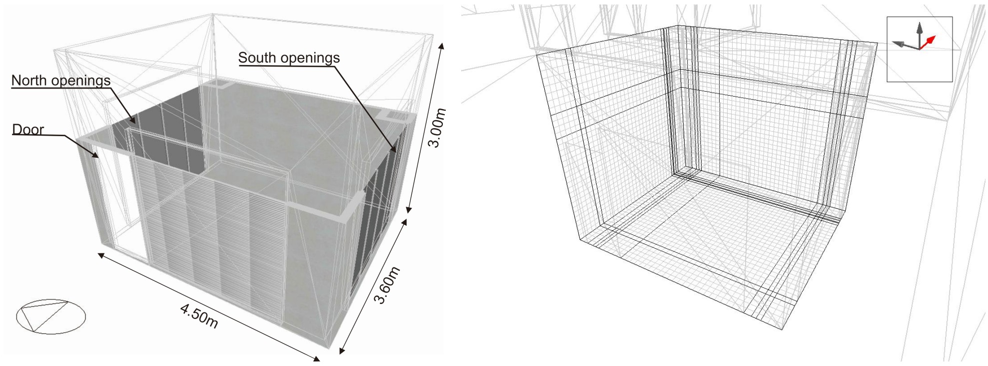

**Figure 4-5** The model of living room: (left) its geometry and orientation; and (right) its computational grid for the simulations.

According to the simulations the room temperatures for this specific day are within the range of 24.5°C and 32.6°C with an average of 28.1°C under the average dry-bulb temperature of 27.9°C. This predicted data shows a similar range to that from the measurements i.e. within the dry-bulb temperature range of 25.1°C and 34.1°C with an average of 29.1°C under the average dry-bulb temperature of 29.0°C (see Table B-1 in Appendix B). The ratios between hourly indoor and outdoor air temperatures, both from the measurements and the simulations, are presented against each other in Figure 4-6 (left). The agreement between the two sets emphasizes the software's ability to estimate accurate indoor air temperature regarding the specific situations. The right chart in Figure 4-6 also illustrates the agreement between the measured and the predicted ratios of indoor to outdoor air temperatures. It can be seen that these ratios are mostly within a range of +/-5% deviation. The ability of the chosen modeling software to provide an accurate prediction of the indoor air temperature under the particular situations is, therefore, apparent.

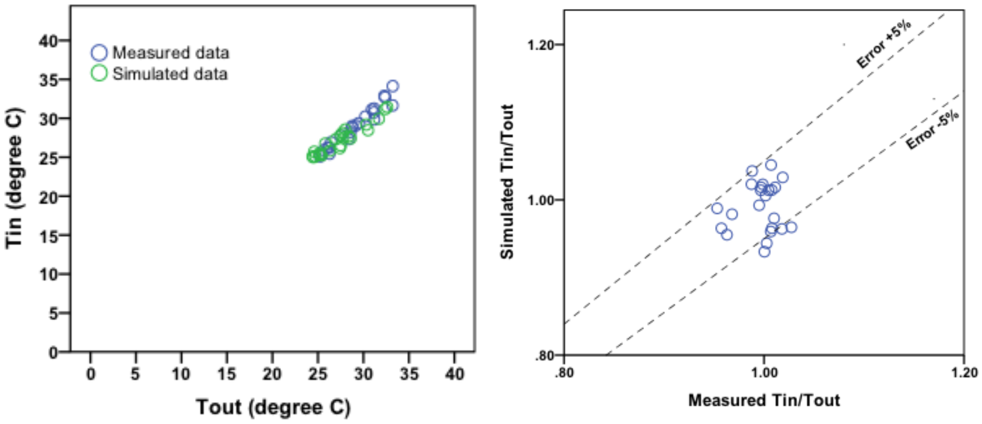

**Figure 4-6** Comparison between the measured and predicted temperatures of the living room in the two-storey house: (left) Measured and predicted indoor air temperatures as the function of the outdoor dry-bulb temperatures; and (right) Measured and predicted ratios with error lines (+/-5%).

The relationship of indoor air velocities ($V_{in}$) and outdoor wind speeds ($V_{out}$) that are obtained both from the simulations and the measurements are also illustrated in the left chart (Figure 4-7), while average hourly indoor air velocities at different measuring points are presented in the right chart (see Table B-2 in Appendix B). In both charts it can be seen that the data sets have similar ranges of indoor and outdoor air velocity i.e. the minimum and maximum of indoor air velocities are between 0.2ms$^{-1}$ and 0.7ms$^{-1}$, while that of outdoor wind speeds are between 0.4 ms$^{-1}$ and 2.0 ms$^{-1}$, respectively.

Although there are some differences between the two data sets i.e. the average indoor air velocities from the measurements are relatively higher than that from the simulations for the same range of outdoor wind speed, the difference between the average indoor velocities between these sets is only 13%. The average absolute difference between the two data sets is also found to be only 0.07ms$^{-1}$ i.e. the average measured and predicted indoor velocities are 0.34ms$^{-1}$ and 0.27ms$^{-1}$, respectively. This difference is found very low and insignificant for the physiological cooling effect point of view. Therefore, the predicted indoor air velocities under the particular external wind conditions are of acceptable accuracy.

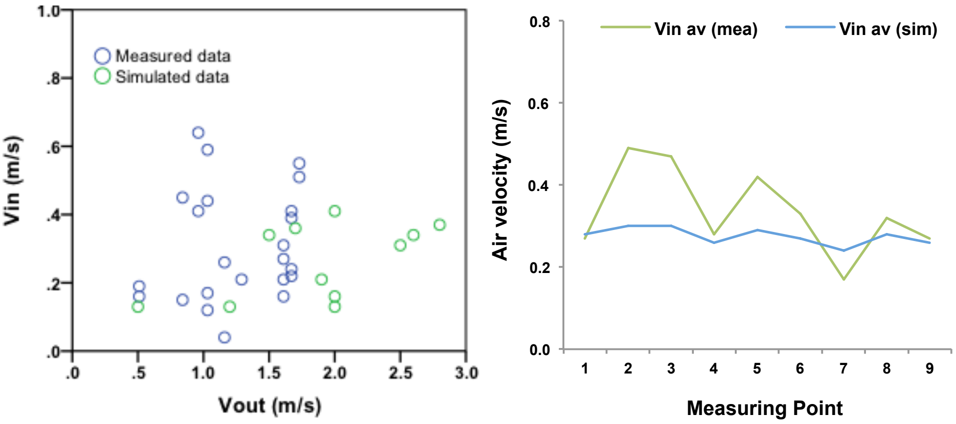

**Figure 4-7** Comparison of the measured and predicted indoor air velocities in the living room: (left) indoor air velocity ($V_{in}$) as the function of the outdoor wind speed ($V_{out}$); and (right) average indoor air velocities ($V_{in.av}$) at different measuring points.

Similarly, the airflow distribution across the living room predicted by DesignBuilder's CFD has the same trend as that from the measurements (Figure 4-7 right). The highest air velocities occurred within the main airflow axis across the room between the north and the south windows i.e. at the measuring point numbers 2, 5 and 8 (Figure 4-4). However, the measured data seems to have a greater fluctuation across the room compared to the simulated data. This may occur because of the errors in the measurements as one hand-held anemometer was used to record air velocity from one location to another. These recorded velocities may be the result of different reference wind speeds, while the simulated velocities across the room are calculated simultaneously.

### *4.4.3 Apartment unit with single-sided ventilation*

In the second validation study the ability of DesignBuilder's CFD to predict the indoor thermal conditions within a high-rise building with single-sided ventilation, and the capability of *CpGenerator* to provide accurate $Cp$ values for the particular building geometries under specific surroundings, were investigated. The simulated indoor air temperature as well as indoor air velocity and distribution across a single-sided ventilated room for the specific times were compared against the measured data obtained from an existing high-rise apartment building in Bangkok.

The measurements were carried out in a typical one-bedroom apartment units (35m$^2$ floor area) of an existing 26-storey apartment building (72.8m height) in Bangkok called '*Lumpini Place Pinklao 2'* (Figure 4-8). The building is located in a suburban area of Bangkok. It is a corridor-type building that accommodates 651 residential units with one main vertical core (elevators) and a central corridor on each floor. The measurements were conducted in the washing room (2.5m$^2$ floor area) of the unit on floor 13$^{rd}$ (Figure 4-9). The room is single-sided ventilated with only one external opening on the north (3m$^2$ effective opening area). The measurements were conducted during the summer period in May 2010. Indoor air temperatures as well as air velocities were measured at 1.2m above the room’s floor using a calibrated ultrasonic anemometer (Airflow Anemosonic UA30 as in Figure 4-10) fixed with a camera tripod. The detailed information of the anemometer used is listed in Table 4-3.

**Figure 4-8** Exterior view and building floor layout of Lumpini Place Pinkloa 2: (left) External view and (right) Ground floor layout.

**Figure 4-9** Floor Layout of the unit on the 13rd floor for the measurements: (above) the location of the studied unit; (middle) the location of the anemometer in the measurements; (below-left) the washing room view from the pantry; and (below-right) the bedroom.

**Figure 4-10** Anemometer used in the measurements - AIRFLOW Anemosonic UA30: A handheld digital ultrasonic anemometer.

**Table 4-3** Detail information of anemometer used in measurements.

| Instruments | Parameters | Range | Accuracy |
|---|---|---|---|
| AIRFLOW Anemosonic UA30 | Air velocity | 0.0ms$^{-1}$ to 30ms$^{-1}$ | Better than +/-0.01 ms$^{-1}$ |
| | Air temperature | 0°C to 60°C | +/-1.0°C |

In the measurements the anemometer was used for recording air temperatures and air velocities at 30-minute intervals for 72-hour periods. However, it should be noted that the instrument has its own limitations e.g. the capacity for storing the measured data and the limited battery lift-time. These limitations led to some missing data during the field measurements. The average data for each hour of the day obtained from 72-hours of measurements were therefore used for comparing with the simulated data. For the outdoor wind speeds, the average wind speed at the same hour of the day during May obtained from the Thai Meteorological Department between 1999 and 2008 was employed rather than installing a weather station in the tested building. This was because of the inadequacy of the instrument in the study. These wind speed data were also used as inputs for all the simulations.

For the simulations the studied building with the chosen apartment unit were built using DesignBuilder v. 2.3.5.034. The list of the model information including materials and other model settings can be found in Table 4-4. The software's default weather data for Bangkok was employed for all the simulations. This is except for the external wind speeds. The steady state was assumed in all simulations. The standard $k-\varepsilon$ turbulence model as well as the power-law discretization scheme was used. The non-uniform rectilinear Cartesian grid with the grid space of 0.1m and grid line merge tolerance of 0.03m was set. This led to the x-,y- and z- cell numbers of 13, 21 and 28, while the maximum gird ratio was 4.34. The door in this room was set as '*Close*', while the external opening was fully open at all times to keep the room as single-sided ventilated as in the real situation. For the wind pressure coefficient ($Cp$), *CpGenerator* was employed to give the $Cp$ values rather than the software's default $Cp$

data (see Table A-4 in Appendix A). This is because DesignBuilder's default $Cp$ values are recommended only for a building no more than three-storey high.

**Table 4-4** List of the apartment's materials and simulation settings.

| Elements | Details |
|---|---|
| External wall materials | Concrete with 2%steel (75mm) with cast concrete on both sides (12.5mm each side) (U-Value of 5.236Wm$^{-2}$K). |
| Internal wall materials | Brick (105mm) with plaster on both sides (U-Value of 1.69Wm$^{-2}$K). |
| Floor materials | Reinforced concrete covered with ceramic tiles. |
| Building roof | Concrete with 2%steel (75mm). |
| Ceiling materials | Gypsum board (9mm thick) with no insulation materials. |
| External glazing | Single clear glass (12mm thick) (U-Value of 6.121Wm$^{-2}$K). |
| Internal glazing | Single clear glass (6mm thick) (U-Value of 6.121Wm$^{-2}$K). |
| Occupancy | 2 peoples in the unit. |
| Lighting | 25Wm$^{-2}$. |
| Other internal heat gain and furniture | No other equipment set, No HVAC system. |

After the model was built the hourly indoor air temperatures of the room were calculated using EnergyPlus. This simulated data were then compared against the measured data and also directly imported as the boundary conditions for the CFD calculations. The predicted room temperatures were found to be within the range of 30.5°C and 36.2°C with an average of 33°C for an outdoor air temperature range between 27.2°C and 32.7°C with an average of 29.8°C (see Table B-3 in Appendix B). These are very similar to the average hourly data obtained from the measurements i.e. within the range of 30.6°C and 37.4°C with an average of 33.4°C for an outdoor air temperature range between 27.8°C and 38.5°C with an average of 31.6°C that are obtained from the Thai Meteorological Department. In the left chart of Figure 4-11 the relationship between the indoor and outdoor air temperatures obtained from the measurements and the simulations are illustrated. This emphasizes the agreement between the two data sets as the predicted data are all within the similar range as the measured data. This agreement can also be seen in the right chart in Figure 4-11 as the deviations between the two data sets are mostly within a range of +/-5%. These comparisons demonstrate the ability of the software as well as the input data for predicting the indoor air temperatures regarding to the specific outdoor thermal environment.

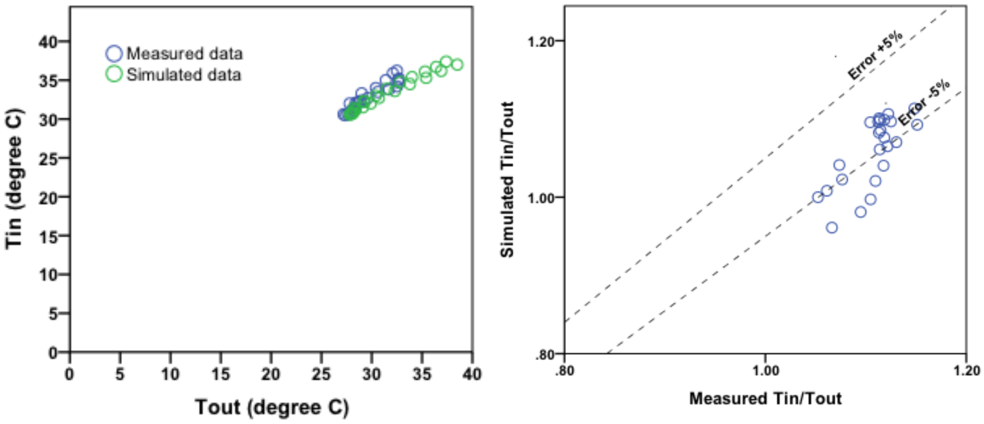

**Figure 4-11** Comparison between the measured and predicted temperature of the washing room in the apartment unit on floor 13rd: (left) Measured and predicted indoor air temperature as a function of the outdoor dry-bulb temperature (Measured and Simulated Tin/Tout); and (right) Measured and predicted ratio with error lines (+/-5%).

The left chart in Figure 4-12 illustrates the measured and predicted indoor air velocities ($V_{in}$) as a function of their reference wind speed ($V_{out}$). Both measured and simulated indoor velocities were found to be very low i.e. within the range of 0.02ms$^{-1}$ and 0.3ms$^{-1}$ with an average of 0.12ms$^{-1}$ under the wind speed range between 0.40ms$^{-1}$ and 2.20 ms$^{-1}$ (see Table B-4 in Appendix B). In the right chart (Figure 4-12) the ratio between the indoor and outdoor air velocities obtained from the measurements and the simulations are presented against each other in order to illustrate how much the two data sets agree. Although the data from both sets exhibit some scatter within both charts, the ratios between the indoor and the outdoor wind speed are very close i.e. the measured and predicted ratios are approximately 11% and 12%, respectively. This illustrates that DesignBuilder's CFD and *CpGenerator* employed together with other relating settings are able to provide an acceptable prediction in indoor air movement under the defined outdoor wind conditions.

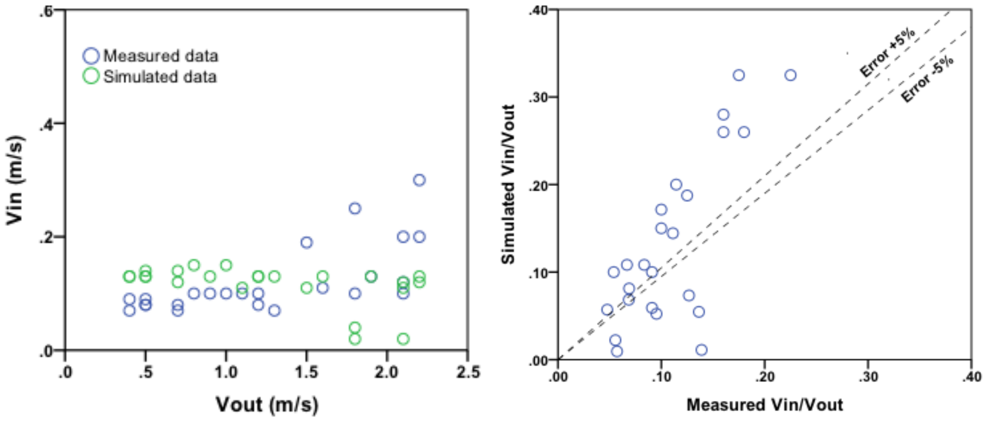

**Figure 4-12** Comparison between the measured and predicted air velocities of the washing room in the apartment unit on floor 13rd: (left) Measured and predicted indoor air velocities as a function of the outdoor wind speed (Measured and Simulated Vin/Vout); and (right) Measured and predicted ratio with error lines.

In this section the ability of the chosen software i.e. *DesignBuilder* and *CpGenerator* to predict the indoor thermal parameters for specific building configurations and weather conditions was investigated. First, DesignBuilder's Bangkok default weather data, obtained from ASHRAE International Weather for Energy Calculation (IWAC), were compared to Bangkok's weather data obtained from the Thai Meteorological Department (MET) between 1999 and 2008 in order to ensure that the default weather data provided by the software can represent the real weather conditions in Bangkok. Hourly air temperatures as well as wind speeds and directions obtained from the software were compared to that from MET. Both software's default dry-bulb temperatures and relative humidity were found to agree well with the measured data. The average relative error between both data sets is only 2.2% and 2.8%, respectively. However, hourly wind speeds obtained from the software were found to be obviously greater than those from MET. While the software's default wind speeds are $2ms^{-1}$ and $3ms^{-1}$ with an annually average of $2.9ms^{-1}$, the wind speeds obtained from MET were between $1ms^{-1}$ and $2ms^{-1}$, with an average of $1.1ms^{-1}$. This difference may lead to the over-prediction in indoor air velocity. DesignBuilder's default weather data for Bangkok, except for hourly wind speeds, will be therefore employed for the study. On the other hand, the average hourly wind speeds for each month that are obtained from MET will be used for the simulations in the main study.

Then two validation studies were conducted in order to examine the applicability of DesignBuilder and CpGenerator to give an accurate prediction on indoor thermal conditions. The simulated hourly air temperatures as well as air velocities and distribution are compared to the measured data obtained from the field measurements in two existing buildings i.e. the two-storey house and the 26-storey residential building.

For the former study the indoor air temperatures and velocities measured in the living room were compared to the simulated data. A good agreement between the two data sets is found. Both indoor and outdoor air temperatures that are obtained from the simulations and the measurements are within the same range and the relative errors between the two indoor to outdoor air temperatures ratios are only within +/-5%. In terms of indoor air velocities the average indoor velocities for 24-hour period obtained from the measurements and the simulations are very close i.e. 0.34ms$^{-1}$ and 0.27ms$^{-1}$, respectively. The ratios between the indoor and outdoor air speed obtained from the measurements and the simulations are found at 35% and 22%, respectively. These differences are acceptable in terms of air velocity as they are inconstant and highly dependent on various factors particularly for external wind conditions. In terms of airflow distribution the average air velocities at different locations in the room from the simulations was compared against the measured data. The simulated air velocities at different locations throughout the room were found to agree well to the measured date. This result demonstrates the software's ability reproduce the same airflow pattern found in the measurements.

In the last validation study the measured data from the field measurements in the washing room of the one-bedroom apartment unit in an existing residential building in Bangkok (Lumpini Place Pinkloa 2) were compared to the simulated data. The room is a single-sided ventilated with only one external opening. Similarly to the previous validation study, the software can provide a good prediction on the indoor air temperatures and velocities. The deviation between the measured and the simulated indoor air temperatures is within +/-5%; and the ratios between the indoor and outdoor air velocities those are obtained from the measurements and the simulations are very close i.e. 11% and 12%, respectively. These agreements emphasis the capability of the chosen software i.e. DesignBuilder and CpGenerator as well as other relating input data and settings to reproduce the real thermal conditions inside the particular buildings.

According to these validation studies, although there are slight differences between the results of the simulations and the field measurements, it can be inferred that the chosen software is appropriate to examine the phenomena occurring in the measurements. The use of DesignBuilder and CpGenerator, together with other relating settings, to investigate the performance of the proposed ventilation strategy to induce indoor air velocity and thermal comfort under different environmental conditions and strategy's configurations is therefore considered as acceptable.

## 4.5 Summary

In this Chapter, two major methods available for investigating the performance of wind-induced natural ventilation strategies in a building were reviewed involving modeling and full scale methods. Developed from different principles, each method has advantages and disadvantages. These methods were compared and discussed regarding the objectives of this study i.e. i) to investigate the potential of the proposed strategy to increase indoor air velocity and to extend thermal comfort in a single-sided apartment unit under hot-humid climatic conditions of Bangkok, ii) to parametrically investigate the influence of different variables on the strategy' performance, as well as iii) to optimize the designs and configurations of the strategy. This is in order to establish the study's main method.

According to these objectives, as well as the study's limitation of cost and time, CFD code from DesignBuilder was chosen as the most appropriate method for the study due to its high capability that allows different alternative designs and parameters to be analyzed in details with comparatively less cost and time consuming. Also, *CpGenrator*, which is a web-application that can provide $C_p$ data at the specific location on a building façade, is employed as the DesignBuilder's default $C_p$ data is recommended only for a building no higher than three-storey. Although DesignBuilder and *CpGenrator* have been previously validated in other studies, their ability to provide acceptably accurate predictions of thermal and flow parameters was also examined in this study.

# Chapter Five

## Research design

### 5.1 Introduction

The proposed ventilation shaft strategy is hypothesized to effectively induce a single-sided room's air movement and increase the occupants' thermal comfort. In order to assess this hypothesis, as well as to accomplish the study's objectives described in Chapter One, the research design is particularly created for this study. In this chapter the research design will be presented in detail by beginning with the formulation of the hypothetical building that will be adopted for the study. Then the study's main criterion for assessing the hypothesis will be described as well as the CFD settings and assumptions made for the simulations in this study. In the last part the study procedure will be explained in detail.

### 5.2 Hypothetical building for the study

The hypothetical building is formulated in the study with the purpose of testing the study's hypothesis and achieving the study's objectives. The building is designed to represent the typical characteristics of high-rise apartments in Bangkok according to the survey on the apartment projects developed in Bangkok between 2007 and 2010 conducted by the author.

According to the more than fifteen projects surveyed, most of the apartment buildings in Bangkok were found to be located either within Bangkok's central business district (CBD), along the Chao-Phraya River, or along the sky-train and underground-train networks (*BTS* or *Bangkok Mass Transit System,* and *MRT* or *Mass Rapid Transit*). These projects were between 22 and 70 storey tall with residential units beginning from floor 4th to floor 10th. The lower floors are mostly used for other purposes, such as parking and shops. Generally, it could be approximated that the lower floors, about one-fifth to one-sixth of the building, were used for other purposes rather than accommodation. Also, it was found that almost all of the projects were corridor-type (Figure 3-1c in Chapter Three). Only a few projects, which were all luxury apartments, were tower-type (Figure 3-1a in Chapter Three). Most of the apartment units were one-bedroom units with a floor area between 33m$^2$ and 58m$^2$ depending on projects, and most importantly all of them were single-sided ventilated with the opening(s) located only on one side of the room.

According to these findings the hypothetical building is formulated as a middle-class, corridor-type apartment building with 25-storeys. The building is 75m tall with the width and length of 72m and 16m, respectively (Figure 5-1left). It is assumed to locate in an urban area of Bangkok. The apartment units begin at the 6$^{th}$ floor, which is about one-six of the building height. Each floor contains 17 one-bedroom apartment units so that there are in total 340 units in the building. The building's constructional span is 6 x 8m$^2$ and the floor-to-floor height is 3m. The building's main circulation core, including elevators and staircase, is located at the center of the northern side of the building. There is a 4m wide corridor on each floor with the apartment units located on its either side (see Figure 5-1right for the typical floor layout).

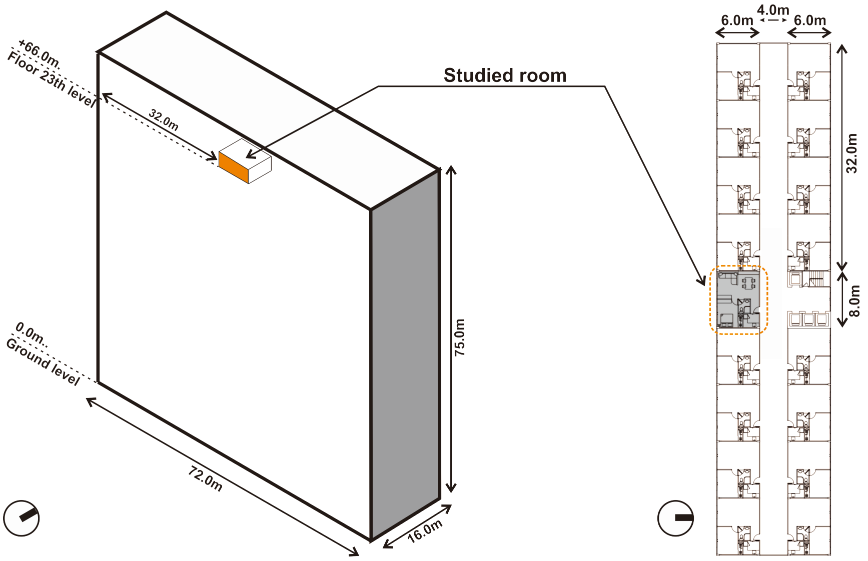

**Figure 5-1** Hypothetical building for the study: (left) geometry of the building; and (right) typical floor layout and orientation of the building (the studied room was presented in grey).

In order to test the study's hypothesis the south-facing apartment unit on the 23$^{rd}$ floor of the hypothetical building was chosen as the '*studied room*' (see Figure 5-1right). This is because it is located in the central part of the building layout and on the two floors below the building's roof, so that its thermal condition is merely affected by the radiated heat gain either from the building's roof or its east and west facades.

Figure 5-2 illustrates the geometry and the layout of the studied room, which contains one bedroom (14m$^2$), a bathroom (4m$^2$), a kitchen (5m$^2$), a doorway (2m$^2$) and a living and dining room (24m$^2$). The room's living and dining room (in grey) is further established as the main considered area for testing the study's hypothesis. This is because it is the main activity area for the occupants during the target time of the day when electricity demand in Thailand reaches its peak i.e. between 10:00AM and 8:00PM. During this period, however, the prevailing wind speed typically reaches its maximum speed, which is believed to give a good advantage for a wind-dominated strategy including the ventilation shaft.

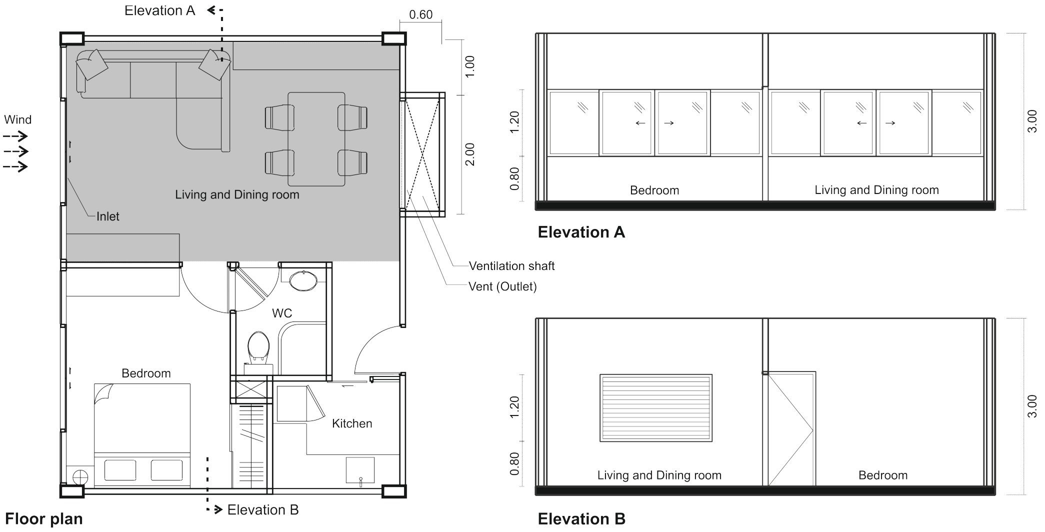

**Figure 5-2** Layout (left) and elevations (above and below right) of the studied room (with the main occupied area presented in grey).

In this study the living and dining room of the studied unit without the proposed ventilation shaft is called the '*reference room*', while that with the shaft attached at its rear wall is called the '*test room*' (Figure 5-3a and 5-3b, respectively). Both of these rooms are identical and they are singled-sided ventilated rooms as there is only one opening in the room on the external façade to connect the room's thermal conditions with its environment called '*inlet opening'*. However, it is only the test room that is attached to a vertical shaft through a set of small grilles called the '*outlet opening*'. Figure 5-3 also illustrates both rooms' main occupied level mainly consider in this study i.e. 1m above the room's floor. The geometry of the rooms and their elements are also summarized in Table 5-1. However, it should be noted that these geometries will be altered to allow the effects of the strategy's different designs to be investigated, which will be explained later.

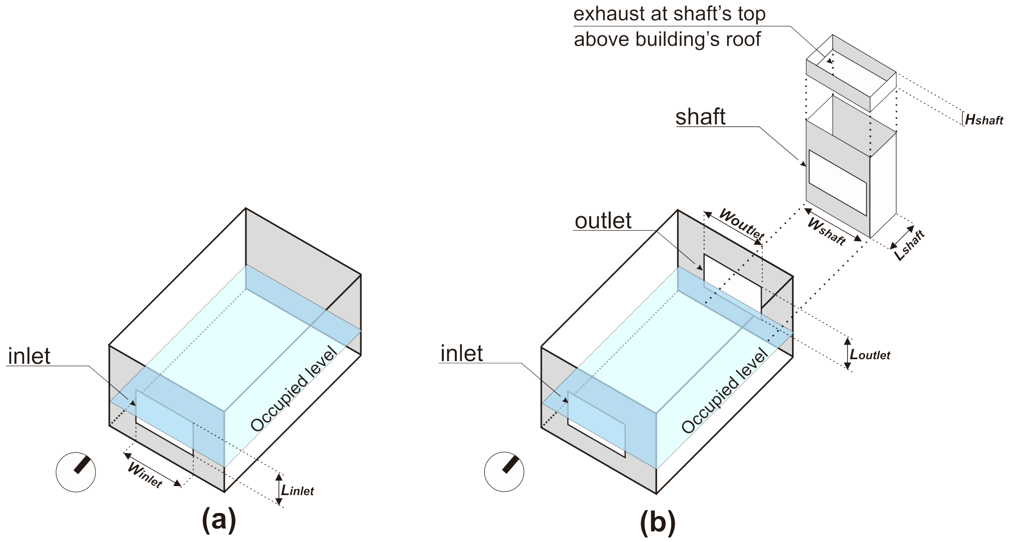

**Figure 5-3** The reference and the test room for the study (with the main occupied area in blue): (a) the reference room without the shaft; and (b) the test room with the ventilation shaft.

**Table 5-1** Geometries and main elements of the reference and the test room.

| Elements | Geometry |
|---|---|
| Reference and Test room (*WxLxH*) | 4x6x3 $m^3$ |
| Inlet opening (*WxL*) | 2x1.2$m^2$ with at 0.8m above the room's floor |
| Outlet openings (*WxL*) | 2x1.2$m^2$ with at 0.8m above the room's floor |
| Shaft's geometry (*WxL*) | 2x0.6$m^2$ with the height of 1.0m above the building's roof ($H_{shaft}$) |

In the next section the main criterion for the parametric study are explained.

## 5.3 Criteria for the study

Aiming at reducing the electricity consumption due to cooling systems in an apartment unit, the proposed ventilation shaft strategy is hypothesized to improve the occupants' thermal comfort by elevating the room's air movement and thus the physiological cooling effect. Then the reductions in electricity consumption will be achieved as the a/c systems are assumed, not to be operated when the occupants feel thermally comfortable. In this study the concept of comfort hour percentages will be adopted as the main criterion to assess the study's hypothesis. Any increase in these percentages when the ventilation shaft is employed would indicate its potential to increase the occupants' thermal comfort and decrease the electricity consumption due to the cooling systems. However, there are other criteria that are required for achieving the study's main objectives established in Chapter One. These include:

i) **Average indoor air velocity (*$V_{in.av}$*)**: The average air velocity within the room's main occupied level predicted by the validated DesignBuilder's CFD will be used as the study's first criterion for investigating the effects of various parameters on the strategy's performance and for optimizing the strategy's design, which are the objectives of the study. The higher the $V_{in.av}$ would indicate the greater the strategy's performance.

The percentage of the room's average air velocity ($V_{in.av}$) to the reference external wind speed ($V_{out}$) for each investigation will be also given in Appendix C. This is in order to present how great the effect of each variable is on the strategy's performance, and to compare to the findings from previous the literatures.

ii) **Room's operative temperature ($T_{op}$) and compensated temperature ($T_{comp}$)**: the room's operative temperature that will be estimated based on Bangkok weather data using EnergyPlus function will be another significant criterion required for assessing the occupants' thermal comfort as the room's $T_{op}$ can be calculated for the '*compensated temperature'* ($T_{comp.}$) or the room's operative temperature that is offset by the room's air velocity ($V_{in.av}$) and compared to the comfort temperature range. As a result the percentages of thermal comfort time that can be possibly obtained in the room can be achieved.

In order to estimate the compensated temperature ($T_{comp.}$) due to the elevated air movement, there are a number of guidelines and correlations proposed by many researchers (see Chapter Two). However, the physiological cooling comfort model developed by Szokolay (Szokolay, 2000, Szokolay, 2008) will be adopted for this study. This is because it can provide an average result of the cooling effect produced by elevated air velocities that are proposed by extensive studies (see Figure 2-31 in Chapter Two). Below is the Szokolay's model of physiological cooling effect of elevated air velocity (Eq. 5-1):

$$\boldsymbol{dT = 6Ve - (1.6Ve)} \qquad \textbf{Eq. 5-1}$$

where $dT$ is the cooling effect due to the elevated air velocity and $Ve$ is an effective velocity, which is equal to $V - 0.2ms^{-1}$. However, it should also be noted that this expression is valid up to $2ms^{-1}$**.**

In terms of thermal comfort, an adaptive thermal comfort model is found to preferable to conventional models for investigating thermal comfort in naturally ventilated buildings particularly for residential buildings in hot-humid climates. For this study the ASHRAE's adaptive thermal comfort model will be therefore adopted for calculating Bangkok's monthly comfort temperature range (Eq. 5-2):

$$\boldsymbol{Toc = 18.9 + 0.255Tout} \qquad \textbf{Eq. 5-2}$$

where $Toc$ is indoor operative temperature (˚C) and $Tout$ is outdoor air temperature (˚C). The upper and the lower limit of comfort temperature are $Toc + 2.5$˚C and $Toc - 2.2$˚C, respectively (ASHRAE, 2013).

Figure 5-4 illustrates Bangkok's monthly comfort temperature range according to ASHRAE's adaptive thermal comfort model (Eq.5-2) and Bangkok's monthly average mean dry-bulb temperatures obtained from the Thai Meteorological Department between1999 and 2008. Also, the upper limit of thermal comfort that is extended by the physiological cooling effect by the increase in air velocity 0.5ms$^{-1}$ according to Szokolay's physiological cooling effect model (Eq. 5-1) is illustrated. It can be seen that there are some months in Bangkok i.e. between March and August, when the average mean dry-bulb temperatures are beyond the upper limit of the comfort temperature range ($T_{com.upper}$). For this period, the increase in room's air movement can be helpful for creating physiological cooling effect and improving human thermal comfort. The chart also demonstrates that, with the increase in air movement to at least 0.5ms$^{-1}$, Bangkok's monthly average mean dry-bulb temperatures are almost completely within the new comfort range ($T_{comp}$), except for April.

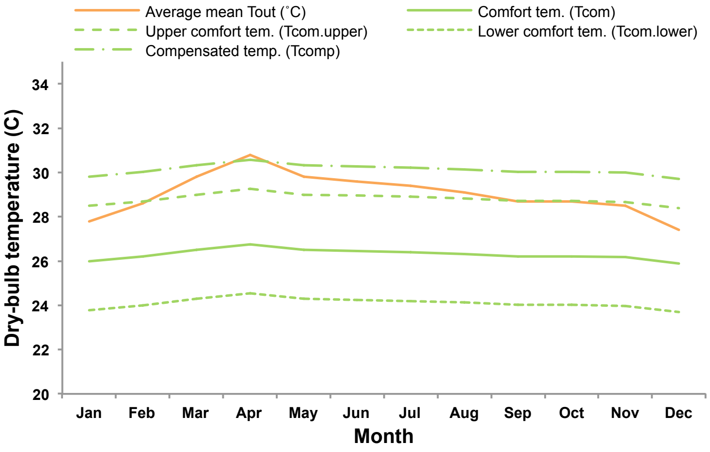

**Figure 5-4** Bangkok's monthly comfort temperature range based on ASHRAE's adaptive thermal comfort model (55-2004) and the extended upper limit based on the air velocity of 0.5ms$^{-1}$ according to Szokolay's physiological cooling effect model.

In summary, the percentage of thermal comfort hour will be employed as the main concept for testing the hypothesis in this study. To attain this, a room's operative temperature and average air velocity will be calculated into the room's compensated temperature based on Szokolay's model of physiological cooling effect due to the elevated air movement and compared to Bangkok's thermal comfort range estimated according to ASHRAE's adaptive thermal comfort. Both parameters i.e. a room's operative temperature and average air velocity are also significant for assessing the effects of different variables on the strategy's effectiveness. In the next section the CFD simulation settings and the study procedure for testing the study's hypothesis and achieving the study's objectives are explained in detail.

## 5.4 CFD simulation settings

In order to assess the study's hypothesis the formulated building will be modeled in the validated DesignBuilder v.2.3.5.034 software. Both of the reference and the test room with variations in design will be simulated under different climatic conditions considered by employing the software's internal 3-dimensional CFD function. As a result the required criterion previously established i.e. room's operative temperature and air velocity could be obtained. In this section the settings and some significant assumptions made for the CFD simulations in this study are described.

### *5.4.1 Boundary conditions and assumptions for the simulations*

The accuracy of the thermal conditions predicted by a CFD modeling software is highly dependent on the accuracy of the input, and the applicability of the model settings. For this study the simulation settings and assumptions made are kept identical throughout different cases to ensure that the results attained are influenced only by the considered variable(s). It should be also noted that these settings and assumptions were previously found to provide an acceptable accuracy in thermal conditions prediction without excessive time consuming (see Chapter Four).

Firstly, the model's computational domain for DesignBuilder's internal 3-dimensional CFD is limited as the air volume of the considered building i.e. the studied building for this study. Then the boundary conditions for each case will be calculated based on the pre-defined weather data and the building's construction materials by EnergyPlus which is built within the DesignBuilder's environment. The construction materials adopted for the studied building are defined according to the typical high-rise apartment buildings in Bangkok (the materials including their heat transmission properties are listed in Table 5-2). These materials will be kept identical as the fixed parameters for all simulations, while the weather data for each simulation case will be varied according to each study stage's objective. By manually altering the software's default hourly weather data for Bangkok for a particular day, such as March 21st in this study, the studied room's thermal conditions under the particular climatic conditions can be examined.

**Table 5-2** The studied building's materials and properties.

| Elements | Building Materials and their properties |
|---|---|
| External wall materials | Reinforced concrete (100mm thick) with cement plaster (12.5mm) on the external surface and plasterboard (9mm) with air gap (10mm) on the internal surface (U-Value of 2.5Wm$^{-2}$K). |
| Internal wall materials | Brick wall (105mm) with cement plaster (12.5mm) on either side (U-Value of 1.7Wm$^{-2}$K). |
| Floor materials | Reinforced concrete covered with ceramic tiles. |
| Building flat roof | Reinforced concrete (150mm) with fiberglass (20mm), air gap (200mm) and plasterboard (9mm)<br>(U-Value of 0.18Wm$^{-2}$K). |
| Ceiling materials | Gypsum board (9mm thick) with no insulation materials. |
| External window<br>(Inlet opening in this study) | Double clear glass (2x6mm) with air gap (13mm)<br>(U-Value of 1.8Wm$^{-2}$K). |
| Vent (Outlet openings in this study) | Small, light grilles with Discharge coefficient of 0.5. |

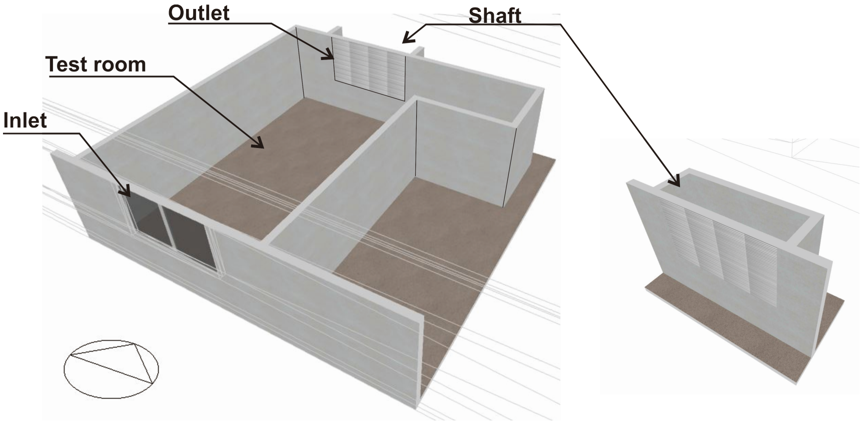

**Figure 5-5** The simulated model of the test room and the ventilation shaft.

Moreover, for the boundary conditions, there are some settings and significant assumptions that are made for all the simulations. The steady-state conditions are assumed in this study to achieve an acceptably accurate output without excessive computing time. The full treatment of wind effects is set in the simulations, while the CFD's isothermal function is '*off*' as to keep the energy equation for all the simulations. The surface heat transfer coefficients are also to be calculated based on wall functions rather than defined by the author. These assumptions may lead to more time-consuming, yet more accurate, predictions according to the study conditions. The automatically calculated false time step is employed as the relaxation method in order to slow the change in independent variables for a more stable and converged solution. The RANS's standard $k-\varepsilon$ turbulence model, which is suggested applicable for wind-induced natural ventilation study, is adopted as well as the power-law discretization scheme. Also, the CFD calculation results are only taken when the simulation solutions are fully converged or when the calculations reach beyond 2000 iterations when, for all simulation cases in this study, the solutions become acceptable stable.

For the wind pressure coefficient ($Cp$), the studied building's $Cp$ value will be predicted by the validated web-based application for estimating the $Cp$ values on the specific points called *CpGenerator* (see Chapter Four). This is because DesignBuilder's default $Cp$ values are restricted to a building that is not more than three stories high (DesignBuilder, 2006a). The $Cp$ values at the center level of the studied rooms' main window from floor 6 and floor 25 of the hypothetical building are predicted according to the building's geometry and its exposure to the surroundings. These $Cp$ values for different wind directions are summarized in Table A-5 in Appendix A and will be adopted for all the simulations in this study.

### 5.4.2 Computational grid system

In this study the non-uniform rectilinear Cartesian grid system was adopted for all simulation cases. This is because it is suggested as the suitable system for a case with normal geometry room. The grid dependency test is also performed and reported in this section in order to establish the most appropriate grid region for the study that can provide a good convergence and accurate results without excessive simulation time consuming.

For the grid dependency test, the test room on floor 23rd is simulated for the specified building materials (Table 5-2) and particular climatic conditions (in Table 5-3) using different grid regions. Four grid regions with different grid space between 0.05m and 0.5m that are suggested for a normal room size between 5m and 20m (Nielsen, 2007) are adopted in the test (see Table 5-4 and Figure 5-6 for the four considered grid regions).

**Table 5-3** Climatic conditions employed for grid dependency testing.

| **Weather data** | **Details** |
|---|---|
| Dry-bulb temperature ($T_{out}$) | 33°C (annually average maximum dry-bulb temperature during the target time i.e. 10AM to 8PM). |
| Relative Humidity (RH) | 72% (annually average mean RH). |
| Wind speed ($V_{out}$) | 4.0ms$^{-1}$ (annually average maximum hourly wind speed). |
| Wind direction | 180° (annually predominant wind direction) i.e. the wind incident angle ($\theta$) to the room's main window is 0°. 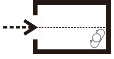 |

**Table 5-4** Different computational grid spaces for grid dependency test.

| Cases | Coarse grid | Normal grid | Fine grid | Very fine grid |
|---|---|---|---|---|
| Grid space and merge tolerance (m) | 0.5 and 0.05 | 0.3 and 0.03 | 0.1 and 0.03 | 0.05 and 0.025 |
| Numbers of grids in x-,y- and z-axis | 17x17x24 | 26x26x38 | 68x61x103 | 130x116x199 |
| Maximum aspect ratio | 18.1 | 16.5 | 3.3 | 2.1 |
| Required memory (MB) | 0.9 | 3.3 | 55.1 | 386.8 |

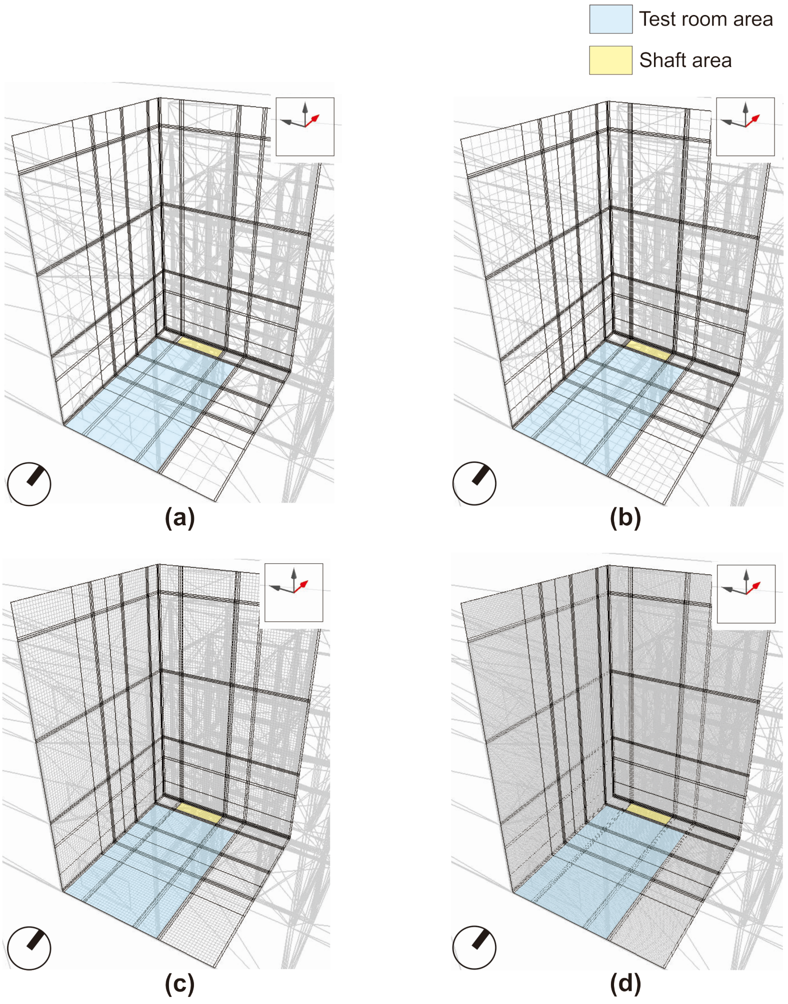

**Figure 5-6** Test room with different computational grid systems: (a) coarse grid; (b) normal grid; (c) fine grid; and (d) very fine grid.

After the test room with four different grid regions is simulated, the resultant air velocity and airflow distributions within the room's main occupied area are then compared and analyzed. It should be noted that the case with a very fine grid region is believed in this study to provide the most accurate results and will be used as the reference case. However, it is very time-consuming. The grid region, with less simulation time that can provide the results most adjacent to the reference case will be, therefore, established as the grid region for all the simulations in this study.

In Table 5-5 the results for air velocity at the occupied level i.e. approximately 1.0m above the floor that are obtained from different grid regions are shown. These involve the minimum, average and maximum air velocities, together with the average air velocities at the inlet and outlet openings. The table also gives the relative errors (%), which are the differences between the velocity results to that from the very fine grid region case i.e. the reference case. It can be seen that, among the three grid regions, the fine grid region case can provide the results that are most adjacent to the reference case for all considerations. The relative errors between the results of these two cases are found only within +/-5%. These results also support the grid region recommended by Nielsen (2007) discussed before (see Chapter Four).

**Table 5-5** Comparison of the results air velocity obtained from different grid regions with relative errors (R.E.) to the very fine cases.

| Considerations | Coarse | Normal | Fine | Very fine |
|---|---|---|---|---|
| Minimum air velocity ($ms^{-1}$) with R.E. (%) | 0.02 | 0.02 | 0.01 | 0.00 |
| Average air velocity ($ms^{-1}$) | 0.23 (-9.5%) | 0.20 (4.8%) | 0.20 (4.8%) | 0.21 |
| Maximum air velocity ($ms^{-1}$) | 0.58 (4.9%) | 0.59 (3.3%) | 0.60 (1.6%) | 0.61 |
| Air velocity at the inlet opening ($ms^{-1}$) | 0.36 (12.2%) | 0.36 (12.2%) | 0.39 (4.9%) | 0.41 |
| Air velocity at the outlet opening (vent) ($ms^{-1}$) | 0.35 (22.2%) | 0.41 (8.9%) | 0.45 (0%) | 0.45 |

Figure 5-7 presents the comparison of the air velocity results at the occupied level across the test room from the inlet to the outlet openings that are obtained from the four different grid regions. This figure indicates how well the different grid regions can provide an accurate prediction on airflow distribution across the specific space compared to the reference case i.e. the very fine grid region. It is obvious that all four cases provide a very similar trend of the airflow distribution across the room. The maximum velocities occur at the inlet opening before they start to drop continuously until reaching their minimum at a distance of approximately 4m from the inlet and begin to rise again in front of the outlet opening. It can be also seen that the find grid region case can provide the most adjacent results of airflow distribution to the reference case. As a consequence the fine grid region with a grid space of 0.1m and grid merge tolerance of 0.03m will be adopted for all the simulations in the main study.

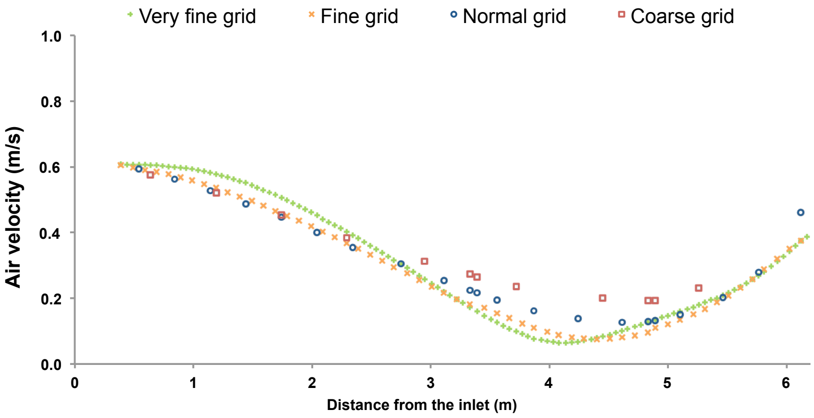

**Figure 5-7** Comparison of the results air velocity at occupied level across the test room obtained from different grid regions.

In summary, the CFD simulation settings and significant assumptions relating to the simulations for this study were established in this section. These include the building materials for calculating the model's boundary conditions, the *Cp* values for the studied building and the suitable grid regions. In Table 5-6 these important settings and assumptions used as the fixed parameters for all the simulations in the main study are summarized.

**Table 5-6** Lists of CFD simulation settings and assumptions for the study.

| **Settings and assumptions** | **Details** |
|---|---|
| Turbulence model and related assumptions for CFD simulations | - RANS's standard $k-\varepsilon$ turbulence model and Power-law discretization scheme.<br>- Steady-state conditions assumed.<br>- Wind factor of 1 i.e. full treatment of wind effects<br>- Isothermal Not assumed.<br>- Surface heat transfer coefficients calculated using wall functions. |
| *Cp* Values | Calculated by *CpGenerator* (see Appendix A). |
| Grid region | Fine grid space i.e.0.1m grid-space with 0.03 grid merge tolerance. |
| Converged results | Iteration beyond 2000 when all the solutions become stable, unless converged results obtained prior to 2000 iterations. |
| **Other assumptions** | **Details** |
| Number of the room attached to the shaft | - Only one test room is attached to the ventilation shaft assumed in the study. |
| Openings and internal heat gain | - All openings are set as fully open at all time, while all the doors are closed.<br>- All equipment in the test room set as '*OFF* ' and no furniture assumed to avoid their disturbances on the simulation results. |

## 5.5 Study procedure

In this section the procedure for achieving the study's objectives and for assessing the study's hypothesis are described in detail. Due to the complexity of the study objectives, the study is divided into five main stages, each of which has particular aim. These involve: i) preliminary test; ii) the effects of climatic conditions; iii) the strategy's optimal design; iv) implementing the ventilation shaft strategy; and v) the strategy's performance to extend thermal comfort hours.

### *5.5.1 Stage 1: Preliminary test*

In the first stage the preliminary test was conducted to test the ventilation shaft strategy's potential to increase the single-sided room's air velocity and to improve the occupants' thermal comfort. To achieve this the studied room without and with the ventilation shaft strategy (Figure 5-8) were simulated using DesignBuilder's internal CFD simulation based on the settings and assumptions explained in the previous section. The room on the 23rd floor of the hypothetical building formulated was adopted in this study, and the fixed and independent variables used in this stage are given in Table 5-6. For the input weather data, Bangkok's weather data obtained from the Thai Meteorological Department were adopted. Bangkok's average maximum dry-bulb temperature ($T_{out}$) found between the target period of a day between 10AM and 8PM i.e. 33°C was adopted in this stage to represent the worse conditions for the occupants to achieve thermal comfort, and Bangkok's average maximum wind speed ($V_{out}$) during this period i.e. 4ms$^{-1}$ were used to give the strategy its maximum potential to increase the considered room's average air velocity. Also, the annually average mean relative humidity ($RH$) of 72% as well as Bangkok's predominant wind direction ($\theta$) were employed for the simulations throughout this stage of the study (see also Table 5-7).

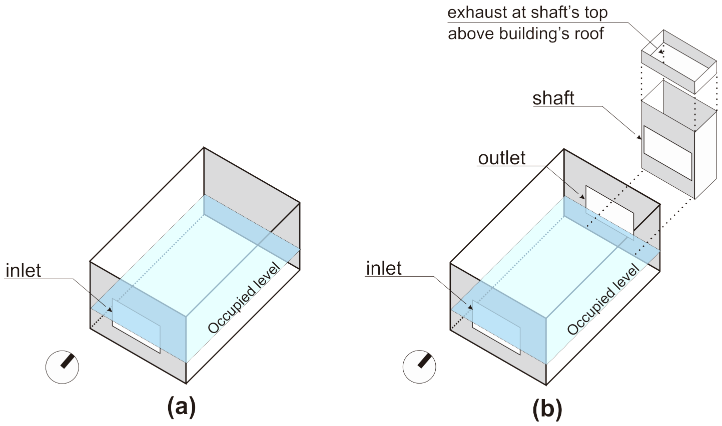

**Figure 5-8** Reference room and test room with the occupied area (in blue) for preliminary test: (a) reference room; and (b) test room.

**Table 5-7** Fixed and independent variables for the preliminary test.

| **Fixed Parameters** | **Details** |
|---|---|
| Weather data | Bangkok average maximum data of $T_{out}$ between the target time at 33°C; annually average *RH* of 72% and wind incident angle of 0°; and annually average maximum wind speed at 4.0 $ms^{-1}$. |
| Geometry and materials of the rooms and ventilation shaft | As in Table 5-1 and Table 5-2. |
| CFD Simulation settings and assumptions | As in Table 5-6. |
| **Independent variables** | **Details** |
| Rooms | 2 types i.e. the reference room (the room without the shaft); and the test room (the room with the ventilation shaft) (see Figure 5-8). |

After the simulations with settings explained above were completed, the resultant air velocities in the reference and test room under the same specific weather data could be obtained. The average air velocity ($V_{in.av}$) within the main area at the occupied level of these rooms can then be compared and analyzed. Any increase in the test room's $V_{in.av}$ compared to the reference room's $V_{in.av}$ would indicate the potential of the ventilation shaft to increase air flow across a single-sided apartment unit under Bangkok's typical climatic condition. Then the rooms' operative temperature ($T_{op}$) under the particular climate were predicted by DesignBuilder's EnergyPlus function. These $T_{op}$ values will be offset by the physiological cooling effect due to the increased air velocity (dT) i.e. the room's $V_{in.av}$ regarding to Szokolay's model and give the rooms' compensated operative temperatures ($T_{comp}$). Later the room's $T_{comp}$ will be compared to Bangkok's comfort temperature range during March, a summer month in Thailand. Finally, the numbers of comfort hour per day for each room, which is the study's main assessment criterion, will be considered. These results will provide an idea of how the proposed strategy performs to achieve the study's main aim i.e. to increase the thermal comfort of the occupants in a single-sided apartment unit and thus reducing the building's high electricity consumption due to its cooling systems.

### *5.5.2 Stage 2: The effects of climatic conditions*

In this stage a parametric study was conducted to investigate the influences of different climatic elements on the ventilation shaft strategy's effectiveness to induce the room's air velocity. Four major climatic elements that have either an effect on human thermal comfort or the influence on passive ventilation strategies found in many research were studied. These elements involve: i) dry-bulb air temperatures ($T_{out}$); ii) relative humidity (*RH*); iii) external wind speeds ($V_{out}$) and iv) wind direction ($\theta$). To achieve this the test room (Figure 5-8b) was simulated under the variations of climatic conditions. By modifying each of the climatic elements in the input weather data while keeping all other parameters fixed constant, the change in the room's thermal conditions indicated the influence of each element on the strategy's performance.

The fixed and independent variable for this stage are summarized in Table 5-8. In total there are 20 simulation cases to be performed. Also it should be noted that, for each climatic element, only the range of data commonly found in Bangkok would be investigated in this study. These include:

i) Four dry-bulb temperatures ($T_{out}$): 25°C, 29°C, 31°C and 33°C, which are Bangkok's annually average minimum, annually average mean, annually average maximum dry-bulb temperature, and the average maximum dry-bulb temperature during the target time of a day i.e. 10Am and 8PM, respectively (see also the summary of Bangkok's weather data in Appendix A);

ii) Three relative humidity (RH): 55%, 72%, and 89%, which are Bangkok's average minimum, average mean and average maximum *RH*, respectively;

iii) Seven wind speeds ($V_{out}$) between 0ms$^{-1}$ (no wind) and 4ms$^{-1}$, which are Bangkok's annually average minimum and average maximum wind speed, respectively; and

iv) Six wind directions in terms of the wind incident angles to the room's inlet opening ($\theta$) between 0° and 180° (see Figure 5-9).

**Table 5-8** Fixed and independent variables for study stage two (The effect of climatic conditions).

| **Fixed Parameters** | **Details** |
|---|---|
| Room | Test room |
| Geometry and materials of the rooms and ventilation shaft | As in Table 5-1 and Table 5-2. |
| CFD Simulation settings and assumptions | As in Table 5-6. |
| **Independent variables** | **Details** |
| Dry-bulb temperature ($T_{out}$) | 4 cases i.e. 25°C, 29°C, 31°C, and 33°C. |
| Relative humidity (*RH*) | 3 cases i.e. 55%, 72%, and 89%. |
| External wind speed ($V_{out}$) | 7 cases i.e. 0ms$^{-1}$, 1.0 ms$^{-1}$, 1.5 ms$^{-1}$, 2.0 ms$^{-1}$, 2.5 ms$^{-1}$, 3.0 ms$^{-1}$, and 4.0 ms$^{-1}$. |
| Wind direction<br>(Wind incident angle to the room's main window) | 6 cases i.e. 0°, 30°, 45°, 60°, 90°, and 180° (see Figure 5-9). |

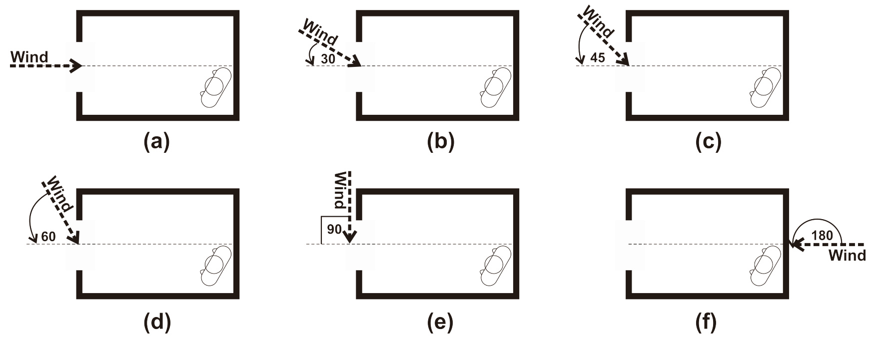

**Figure 5-9** Wind incident angles for the study stage two (The effect of the climatic conditions): (a) 0˚; (b) 30˚; (c) 45˚; (d) 60˚; (e) 90˚; and (f) 180˚.

After the test room under the different climatic conditions was simulated, the room's air velocity ($V_{in}$) and operative temperature ($T_{op}$) for each case were obtained. First, the average air velocity within the occupied area at the considered level i.e. 1m above the floor ($V_{in.av}$) in the room under the alterations in each climatic element was compared with each other. Any changes in the result $V_{in.av}$ will indicate the influence of the particular climatic element on the strategy's effectiveness to induce the room's air velocity and thus the occupants' thermal comfort. Also, the simulated air distribution at the occupied level from different cases were obtained and analyzed. These results indicated the effect of each climatic element on the airflow behavior inside the room. At the end of this study stage the most significant climatic element(s) on the strategy's effectiveness to induce a single-sided apartment unit and the occupants' thermal comfort, which is one of the study's objectives established in Chapter One, would, therefore, be obtained.

### *5.5.3 Stage 3: The strategy's optimal design*

For this study stage the test room with the variations in sizes and positions of its main elements were investigated in order to obtain the strategy's optimal design for producing the occupants' thermal comfort. The main elements are those thought to have an effect on the strategy's performance based on findings from in many research (see in Chapter Two) include the geometrical size and position of i) the ventilation shaft; ii) the room's main window (the inlet) and iii) the grilles that connect the room to the ventilation shaft (the outlet).

The fixed variables employed throughout the simulations in this study stage are summarized in Table 5-9. However, there are some differences in the fixed and independent variables for each set of the parametric study, which focuses on different elements.

**Table 5-9** Fixed variables for study stage three (the optimal design of ventilation shaft strategy).

| **Fixed Parameters** | **Details** |
|---|---|
| Room type | Test room |
| Building materials | As in Table 5-2. |
| Weather data and building materials | As in Table 5-3. |
| CFD Simulation settings and assumptions | As in Table 5-6. |

In total there are forty-two simulation cases to be performed in this stage. These involve:

i) Thirteen shaft's sizes involving: Four shaft's height ($H_{shaft}$) above the building roof between 0m (at the building roof level) and 4m (see Figure 5-10); and Nine combinations of shaft's length and width ($L_{shaft}$ and $W_{shaft}$) (see Figure 5-11 and 5-12). The considered shaft's width ($W_{shaft}$) is between 0.3m and 1.2m and the shaft's length ($L_{shaft}$) is between 2.0m and 4.0m, which are the possible sizes for the real construction situation. The summary of the fixed and independent parameters in this stage is summarized in Table 5-10.

**Table 5-10** Fixed and independent variables for investigating the effect of vertical shaft's sizes.

| **Fixed variables** | **Details** |
|---|---|
| Size of the test room (*WxLxH*) | 4x6x3 m$^{3}$ |
| Inlet and outlet opening (*WxL*) | 2x1.2m$^{2}$ with at 0.8m above the room's floor |
| **Independent variables** | **Details** |
| Shaft's height above the roof level ($H_{shaft}$) | 4 cases i.e. 0m (at the roof level), 1m, 2m and 4m. For these cases, shaft's geometry (*WxL*) is kept as 0.6x2m$^{2.}$ (see Figure 5-10). |
| Shaft's length and width ($L_{shaft}$ and $W_{shaft}$) as *WxL* | 9 cases i.e. 0.3x2.0m$^{2}$, 0.6x2.0m$^{2}$, 1.2x2.0m$^{2}$, 0.3x3.0m$^{2}$, 0.6x3.0m$^{2}$, 1.2x3.0m$^{2}$, 0.3x4.0m$^{2}$, 0.6x4.0m$^{2}$ and1.2x4.0m$^{2}$. For these cases, the shaft's height is kept as 1.0m above the building roof (see Figure 5-11 and 5-12). |

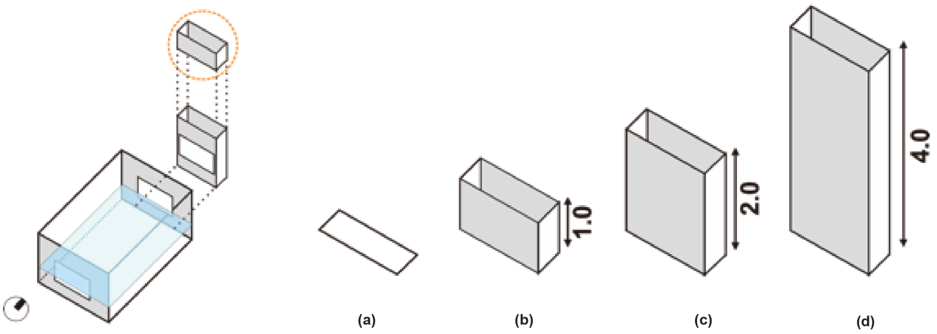

**Figure 5-10** Different shaft's heights ($H_{shaft}$) for study stage three: (a) shaft's exhaust at the building roof level; (b) $H_{shaft}$ of 1m; (c); $H_{shaft}$ of 2m; and (d) $H_{shaft}$ of 4m above the building roof.

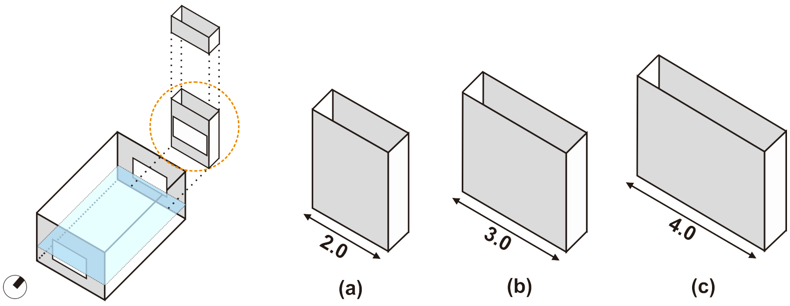

**Figure 5-11** Different shaft's lengths ($L_{shaft}$) for study stage three: (a) $L_{shaft}$ of 2m; (b); $L_{shaft}$ of 3m; and (c) $L_{shaft}$ of 4m.

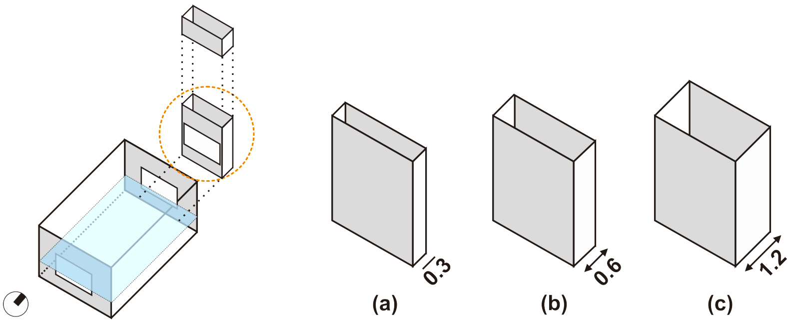

**Figure 5-12** Different shaft's widths ($W_{shaft}$) for study stage three: (a) $W_{shaft}$ of 0.3m; (b) $W_{shaft}$ of 0.6m; and (c) $W_{shaft}$ of 1.2m.

ii) Twenty combinations of inlet and outlet's sizes involving: Sixteen cases of inlet and outlet widths ($W_{inlet}$ and $W_{outlet}$) between 1.0m and 4.0m (Figure 5-13); and Four inlet's length ($L_{inlet}$) between 0.6m and 1.5m (Figure 5-14). The summary of the fixed and independent parameters in this stage is summarized in Table 5-11. It should be noted that the shaft's size of 0.6x4 m$^2$ (*WxL*) with $H_{shaft}$ of 1.0m above the roof would be adopted throughout this stage as it can cover all the considered outlet's widths. Also the inlet and outlet opening's length ($L_{inlet}$ *and* $L_{outlet}$) will be kept constant at 1.2m in all simulations when the Inlet and outlet opening's width is investigated; and the openings' width ($W_{inlet}$ *and* $W_{outlet}$) will be kept constant at 3m when the opening's length is investigated.

**Table 5-11** Fixed and independent variables for investigating the effect of inlet and outlet's sizes.

| **Fixed variables** | **Details** |
|---|---|
| Size of the test room (*WxLxH*) | $4 \times 6 \times 3 m^3$ |
| Shaft's size (*WxL)* | $0.6 \times 4 m^2$ with $H_{shaft}$ of 1.0m above the roof as it can cover all the considered outlet's widths. |
| **Independent variables** | **Details** |
| Inlet and outlet opening's width ($W_{inlet}$ *and* $W_{outlet}$) | 16 cases i.e. 1m to 1m, 1m to 2m, 1m to 3m, 1m to 4m, 2m to 1m, 2m to 2m, 2m to 3m, 2m to 4m, 3m to 1m, 3m to 2m, 3m to 3m, 3m to 4m, 4m to 1m, 4m to 2m, 4m to 3m, and 4m to 4m. For these cases, the inlet and outlet's length ($L_{inlet}$ *and* $L_{outlet}$) are kept identical as 1.2m, and both openings are at 0.8m above the room's floor (see Figure 5-13). |
| Inlet's length ($L_{inlet}$) | 4 cases i.e. 0.6m, 0.9m, 1.2m and 1.5m. For these cases, the $W_{inlet}$ *and* $W_{outlet}$ is fixed as 3m as well as the outlet's length is fixed as 1.2m (see Figure 5-14). |

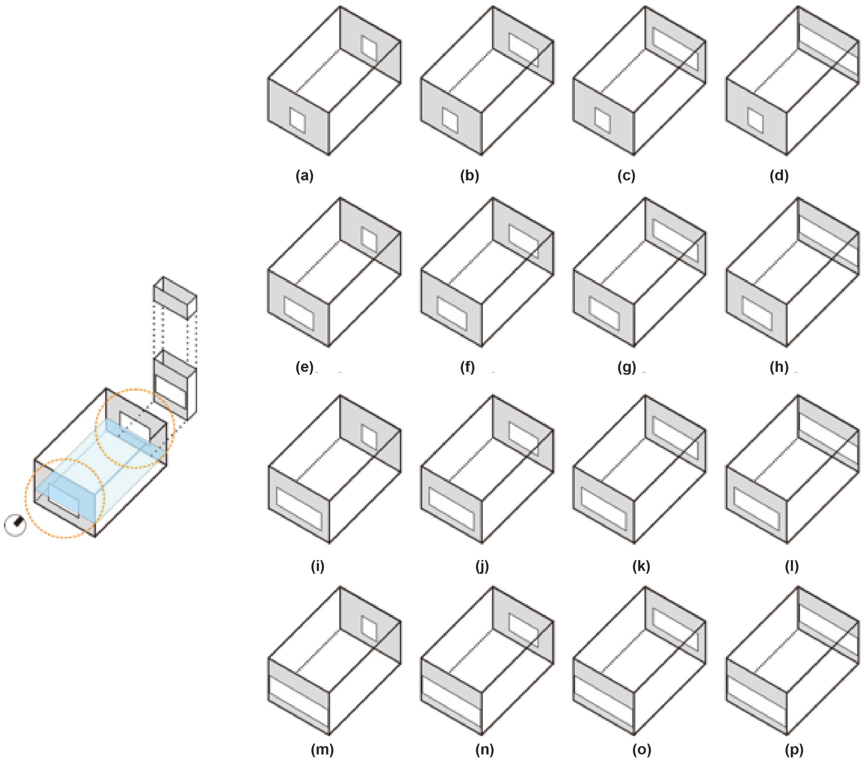

**Figure 5-13** Different combinations of inlet and outlet's widths ($W_{inlet}$ and $W_{outlet}$) for study stage three: (a) $W_{inlet}$ and $W_{outlet}$ of 1m and 1m; (b) 1m and 2m; (c) 1m and 3m; (d) 1m and 4m; (e) 2m and 1m; (f) 2m and 2m; (g) 2m and 3m; (h) 2m and 4m; (i) 3m and 1m; (j) 3m and 2m; (k) 3m and 3m; (l) 3m and 4m; (m) 4m and 1m; (n) 4m and 2m; (o) 4m and 3m; and (p) 4m and 4m.

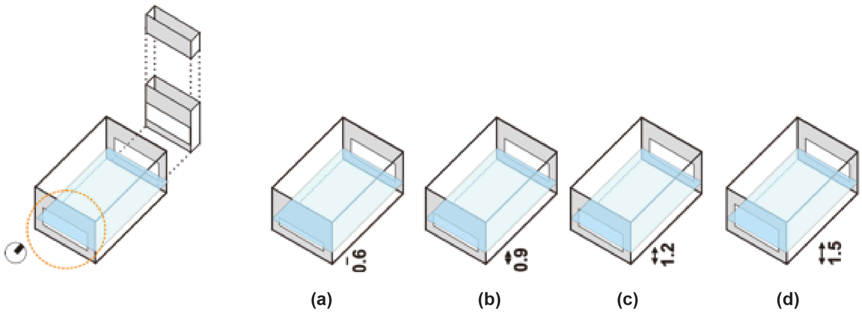

**Figure 5-14** Different inlet's lengths ($L_{inlet}$) for study stage three: (a) $L_{inlet}$ of 0.6m; (b) $L_{inlet}$ of 0.9m; (c) $L_{inlet}$ of 1.2m; and (d) $L_{inlet}$ of 1.5m.

iii) Nine combinations of inlet and outlet's positions ($H_{inlet}$ and $H_{outlet}$). The considered openings' vertical positions include: low position (the center of the openings are at 0.5m above the room's floor); middle position ($H_{inlet}$ and $H_{outlet}$ are 1.1m) and high position ($H_{inlet}$ and $H_{outlet}$ are 1.4m above the room's floor) (see Figure 5-15). The summary of the fixed and independent parameters in this stage is summarized in Table 5-12.

**Table 5-12** Fixed and independent variables for investigating the effect of inlet and outlet's positions.

| **Fixed variables** | **Details** |
|---|---|
| Size of the test room (*WxLxH*) | 4x6x3m$^3$ |
| Shaft's size (*WxL)* | 0.6x4m$^2$ with $H_{shaft}$ of 1.0m above the roof as it can cover all the considered outlet's widths. |
| Inlet and outlet opening's size (*WxL)* | 3x0.6m$^2$ |
| **Independent variables** | **Details** |
| Inlet and outlet opening's positions ($H_{inlet}$ *and* $H_{outlet}$) | 9 cases i.e. low to low, low to middle, low to high, middle to low, middle to middle, middle to high, high to low, high to middle and high to high (see Figure 5-16). |

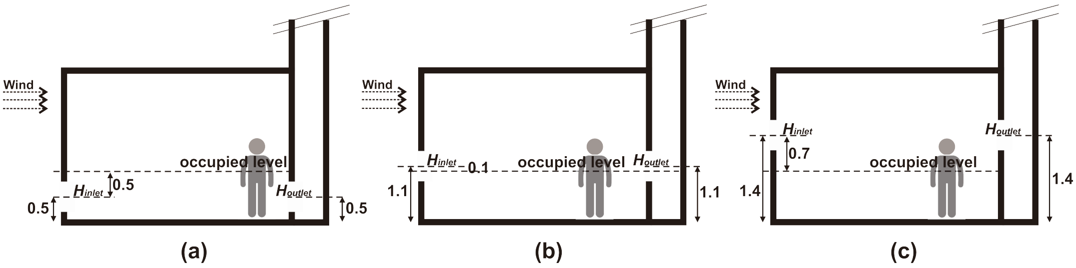

**Figure 5-15** Different inlet and outlet's positions ($H_{inlet}$ and $H_{outlet}$) regarding to the occupied level ($H_{occ}$): (a) the low position i.e. $H_{inlet}$ at 0.5m below $H_{occ}$; (b) the middle position i.e. $H_{inlet}$ at 0.1m above $H_{occ}$; (c) the high position i.e. $H_{inlet}$ at 0.7m above $H_{occ}$.

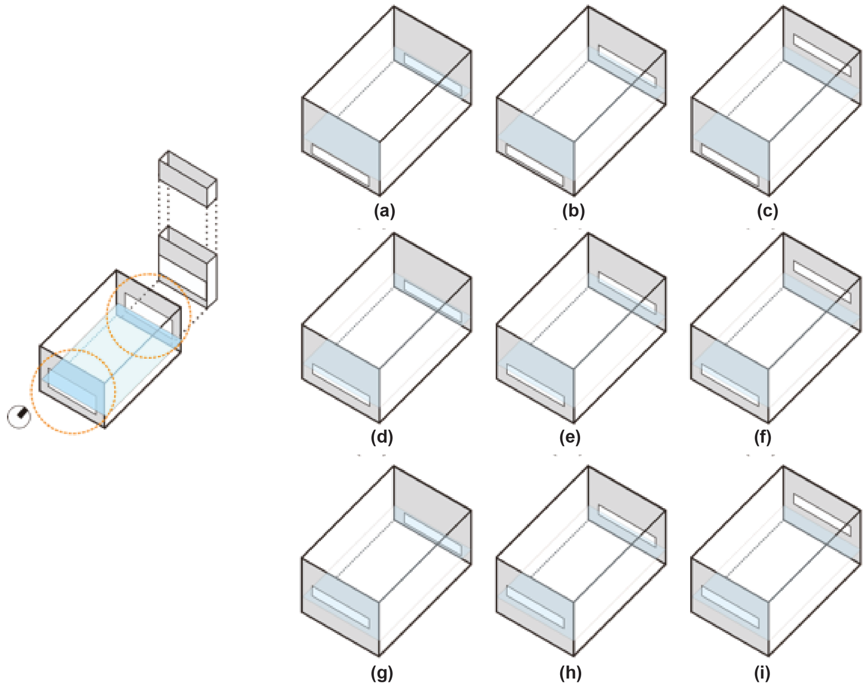

**Figure 5-16** Different combinations of inlet and outlet's positions for study stage three: (a) low inlet and outlet; (b) low inlet and middle outlet; (c) low inlet and high outlet; (d) middle inlet and low outlet; (e) middle inlet and outlet; (f) middle inlet and high outlet; (g) high inlet and low outlet; (h) high inlet and middle outlet; and (i) high inlet and outlet.

From these simulations the average air velocity ($V_{in.av}$) and the operative temperature ($T_{op}$) of the test room with variations in designs were obtained. First, the average air velocities within the occupied area in the test room from each investigation set were compared. Any changes in the result $V_{in.av}$ indicate the effect of the specific element on the strategy's performance to induce the room's air velocity. Then the results of airflow distribution from each set will be examined in order to attain the best airflow pattern within the main occupied area. The room's operative temperature ($T_{op}$) in each set will also be compared. Together with the room's $V_{in.av}$, the effect of each element on the occupants' thermal comfort can be analyzed. Finally the strategy's optimal design, which is one of the study's objectives, can be obtained.

### *5.5.4 Stage 4: Implementing the ventilation shaft strategy*

In this stage the ventilation shaft strategy with its optimum design found previously in the last stage will be implemented into the hypothetical building. This is in order to assess its performance to increase the room's air movement in the actual situation when the shaft is attached to more than one apartment unit. To achieve this the test rooms from floor 6th to floor 25th were attached to one vertical shaft (Figure 5-17). These rooms were then simulated under different wind conditions commonly found in Bangkok. At the same time the reference rooms on the same floor levels was also simulated under the same wind conditions as their results of air velocity will be compared to that from the test rooms.

The fixed and independent variables for this study stage are summarized in Table 5-13. In total there are twelve simulated cases to be performed in this stage. These involve: i) two room types i.e. reference and test rooms; ii) three external wind speeds i.e. $0ms^{-1}$, $1ms^{-1}$ and $4ms^{-1}$, which are Bangkok's average minimum, average mean and average maximum wind speeds, respectively; and iii) two wind directions in terms of wind incident angles to the room's main opening i.e. θ of 0° and 180°.

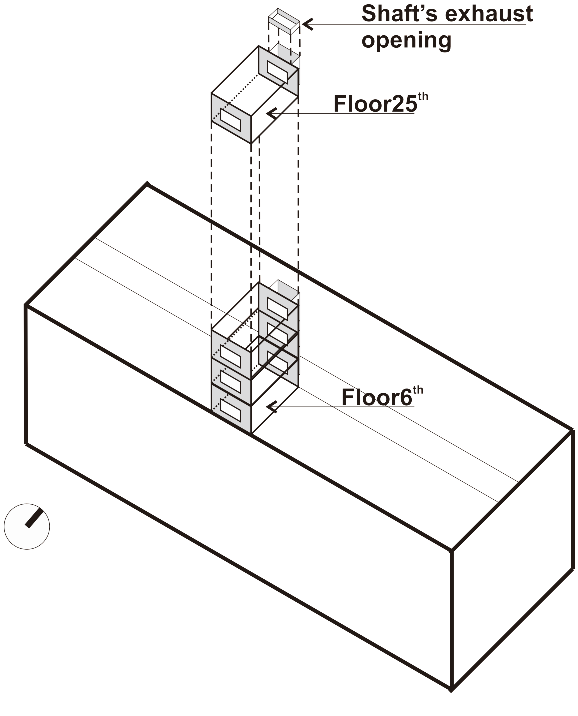

**Figure 5-17** Ventilation shaft implemented to the test rooms between floor 6th and floor 25th.

**Table 5-13** Fixed and independent variables for study stage four (implementing the ventilation shaft strategy).

| **Fixed Parameters** | **Details** |
|---|---|
| Geometry of the rooms and building materials | As in Table 5-1 and Table 5-2. |
| CFD Simulation settings and assumptions | As in Table 5-6. However, it is assumed that the shaft is attached to the rooms from floor 6th and floor 25th and there is only one room per floor that is connected to the shaft. |
| Weather data | As in Table 5-3. |
| Size of the strategy's elements | Shaft: $H_{shaft}$ of 1m above the roof, $W_{shaft}$ of 0.6m, $L_{shaft}$ of 3m<br>Inlet and outlet: $W_{inlet}$ and $W_{outlet}$ of 3.0m, $L_{inlet}$ and $L_{outlet}$ of 1.2m, and $H_{inlet}$ and $H_{outlet}$ at 0.1m above the occupied level ($H_{occ}$). |
| **Independent variables** | **Details** |
| Rooms | 2 types i.e. reference and test rooms from floor 6th to floor 25th. |
| External wind speeds | 3 speeds i.e. $0ms^{-1}$ (no wind), 1 $ms^{-1}$ and $4ms^{-1.}$ |
| External wind directions | 2 wind incident angles i.e. 0° and 180°. |

From the simulations the average air velocity ($V_{in.av}$) within the occupied area of the test rooms when the proposed strategy is operated under the real situation i.e. when the shaft is attached to the test rooms from floor 6th to 25th under Bangkok's typical climatic conditions, were obtained. These results were compared to those from the reference rooms located on the same floor levels. Any increase in the room's $V_{in.av}$ when the ventilation shaft strategy was employed, i.e. the test rooms compared to the reference rooms under the same climatic conditions, would indicate the strategy's effectiveness to improve the thermal comfort of the occupants in a single-sided apartment unit. Finally, the performance of the proposed strategy when it is employed for the studied building can be discovered.

### 5.5.5 Stage 5: The strategy's performance to extend thermal comfort hours

In this final stage the study's hypothesis i.e. the proposed ventilation shaft can increase air movement and improve thermal comfort condition in a single-sided apartment unit in Bangkok was tested. The effectiveness of the proposed ventilation shaft strategy to improve the occupants' thermal comfort was assessed based on the concept of percentage thermal comfort hour. In order to achieve this aim, the reference and the test rooms' compensated temperatures ($T_{comp}$) due to the room's average air velocity ($V_{in.av}$) based on Bangkok's prevailing wind conditions (Table 5-3) obtained from the previous stage are compared to Bangkok's monthly comfort temperature ranges during three different seasons. This would provide the percentages of thermal comfort hour that could be achieved in these two room types. Any increase in this percentage when the strategy was employed would indicate the effectiveness of the strategy to improve thermal comfort and extend the comfort hour, which is the study’s hypothesis. Furthermore, the electricity saving that could possibly be achieved for the whole building when employing the ventilation shaft could also be estimated.

## 5.6 Conclusion

This chapter presented the research design for testing the hypothesis and achieving the complex objectives of this study. First the hypothetical building that is specially formulated for this study was introduced. It was designed according to the typical characteristics of high-rise apartment recently built in Bangkok. The ‘*studied room’*, which is a south-facing, one-bedroom apartment unit on floor 23rd was established. The ‘*reference room*’ and the ‘*test room’*, which is the studied room’s living and dining room without and with the ventilation shaft were also described as the main considered rooms for the simulations. Next, the concept of percentage of thermal comfort hours, which was adopted as the main criterion for testing the study’s hypothesis, was presented. This parameter will be used for assessing the proposed ventilation shaft’s effectiveness to extend the occupants’ thermal comfort time during the target period of a day i.e. 10AM to 8PM. Two other significant parameters that are needed for achieving the study’s objectives have been also established. These include the room’s operative temperature and air velocity. Then, the CFD settings and some significant assumptions that will be adopted for all the simulations in this study were explained and summarized.

In the last section of the chapter the study procedure was presented in detail. In order to test the hypothesis and to achieve the study’s objectives, the study was divided into five main stages involving: i) ‘*Preliminary test*’ as to test the strategy’s potential to increase a single-sided ventilated room’s air movement and thermal comfort conditions; ii) ‘*The effects of climatic conditions’* as to determine the most influencing climatic element(s) on the strategy’s performance; iii) ‘*The strategy’s optimal design’* as to attain the strategy’s best design for increase the occupants’ thermal comfort; iv) ‘*Implementing the ventilation shaft strategy’* as to reveal the strategy’s effectiveness to increase room’s air movement when it is implemented into the building; and v) ‘*The strategy’s performance to extend thermal comfort hours’* as to test the strategy’s effectiveness to extend thermal comfort hour. The aim and the process as well as the fixed and independent variables for each stage were explained in detail.

In the next chapter the results of these study stages will be presented accordingly, while the discussion of these results will be given in Chapter Seven.

# Chapter Six

## Results

### 6.1 Introduction

This chapter presents the key results of the parametric study conducting to examine the study's hypothesis established i.e. the proposed ventilation shaft strategy is able to increase the air movement in an apartment unit with single-sided ventilation and thus improving the residences' thermal comfort. To achieve this, the concept of thermal comfort hour percentages was established previously as the main criteria, while the simulated results of room's operative temperature and air velocity obtained from the DesignBuilder modeling software were adopted as the significant parameters for investigating the strategy's effectiveness for improving the residences' thermal comfort.

Below are the results of the study stages according to the procedure established in the previous chapter involving: i) Preliminary study; ii) The effect of the climatic conditions; iii) The strategy's optimal design; iv) Implementing the ventilation shaft strategy; and v) The strategy's performance to extend thermal comfort hours.

### 6.2 Stage 1: Preliminary study

In the first stage of the study the potential of the ventilation shaft strategy to increase the air velocity in a single-sided ventilated room, which produces the occupants' physiological cooling effect and thus improves the occupants' thermal comfort was examined. The studied room that is without and with the ventilation shaft, called '*the reference*' and '*the test room*', respectively were simulated using DesignBuilder's internal CFD under the particular conditions (see Figure 5-8 and Table 5-7 in Chapter Five).

The error bar chart below (Figure 6-1) presents the means of simulated air velocity ($V_{in}$) within the room's main occupied area at the occupied level i.e. about 1m above the floor, that were obtained from the reference and the test room. For both rooms the minimum velocities ($V_{in.min}$) were found to be very low i.e. 0ms$^{-1}$ for the reference room and 0.03ms$^{-1}$ for the test room. The average air velocity in the reference room ($N$=1829) was found to be much lower ($M$=0.05ms$^{-1}$, $SD$=0.02) compared to that in the test room ($N$=1829, $M$=1.47ms$^{-1}$, $SD$=0.734). The maximum velocity ($V_{in.max}$) in the reference room i.e. 0.18ms$^{-1}$ was also found to be much lower than that in the test room i.e. 2.59ms$^{-1}$ (see detailed results in Table C-1 in Appendix C).

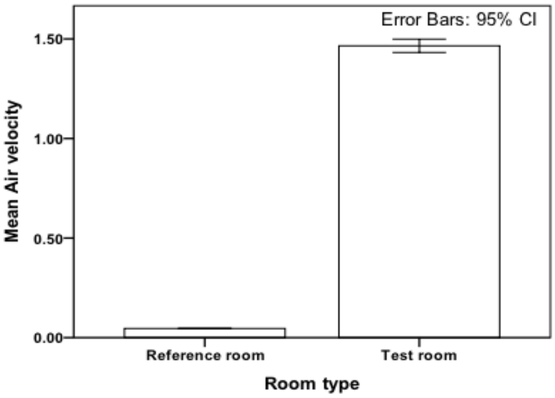

**Figure 6-1** The result of simulated air velocities ($V_{in}$) in the occupied area of the reference (left) and the test (right) room under the defined climatic conditions.

In Figure 6-2 the resultant air velocity distributions at the occupied level of the reference (a) and the test room (b) are shown. For the former case, the incoming air entered into the room through the upper part of the opening with a very low velocity. The air was then found to flow into the room before it was exhausted through the lower part of the same opening (see also Figure 6-3). This result occurs as a result of the combined wind and stack forces when the external wind force is dominant i.e. external wind speed for this case was 4ms$^{-1}$. This similar result was also found in the literature explained in Chapter Two (Allocca et al., 2003). Figure 6-2a also shows that the air velocity was found to be constantly low i.e. close to 0 ms$^{-1}$ throughout the reference room.

Conversely, the external air entered into the test room with a relatively higher velocity i.e. beyond 2.5ms$^{-1}$, regarding to the same climatic conditions, before it moved throughout the room and was exhausted through the vent at the rear wall called the outlet opening (Figure 6-2b and Figure 6-3b). The air between the inlet and outlet opening in this case was found to have an obviously greater velocity compared that close to the sidewalls and the maximum air velocity occurred at the inlet opening before the air velocity slightly declined with a distance from the inlet and rose again in front of the outlet. What is interesting is that the studied room with only one window became a cross-ventilated room when the ventilation shaft strategy was employed.

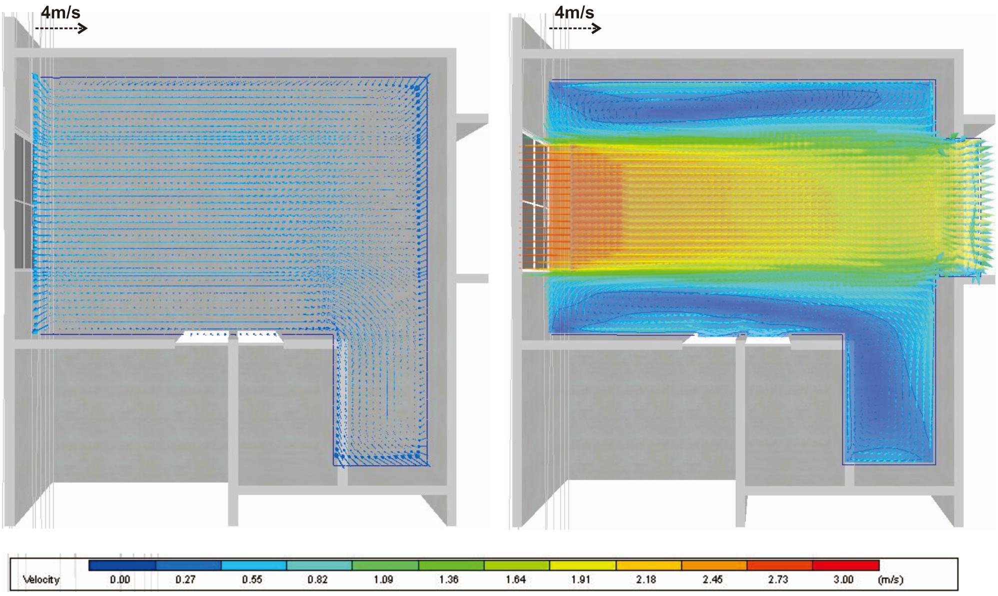

**(a)** **(b)**

**Figure 6-2** Velocity vector plot at the occupied level of the studied room: (a) the reference room; and (b) the test room.

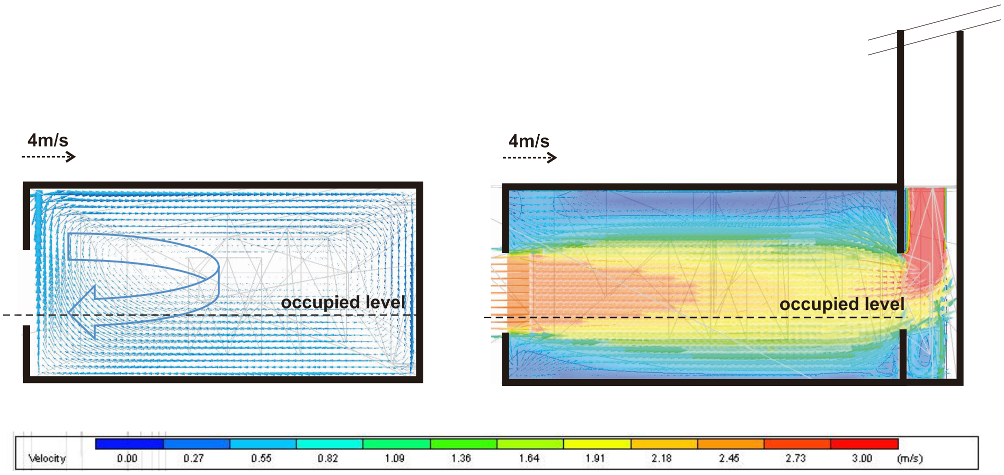

**(a)** **(b)**

**Figure 6-3** Velocity vector plot across the room between the inlet and outlet opening in the studied room: (a) reference room; and (b) test room.

Figure 6-4 compares the operative temperature ($T_{op}$) and the compensated operative temperature ($T_{comp}$) due to the room's air movement in the reference and the test room to Bangkok's monthly comfort temperature range according to ASHRAE's adaptive comfort model (Eq.5-2 in Chapter five). The graphs show the temperatures that were obtained during the target time of a day i.e. 10AM to 8PM of March 21st. The $T_{comp}$ of both rooms were calculated based on their average air velocity ($V_{av}$) according to Szokolay's physiological cooling effect model (Eq.5-1 in Chapter five). However, it must be noted that the air velocity in the reference room was very low i.e. less than 0.2ms$^{-1}$ and insufficient for producing any physiological cooling effect even under Bangkok's average maximum wind speed i.e. 4ms$^{-1}$. The reference room's $T_{comp}$ in the chart were therefore similar to its $T_{op}$ (Figure 6-4a). On the contrary the higher average air velocity in the test room was calculated into the cooling effect ($dT$) for compensating the room's high $T_{op}$ (detailed information can be found in Table C-2 and C-3 in Appendix C).

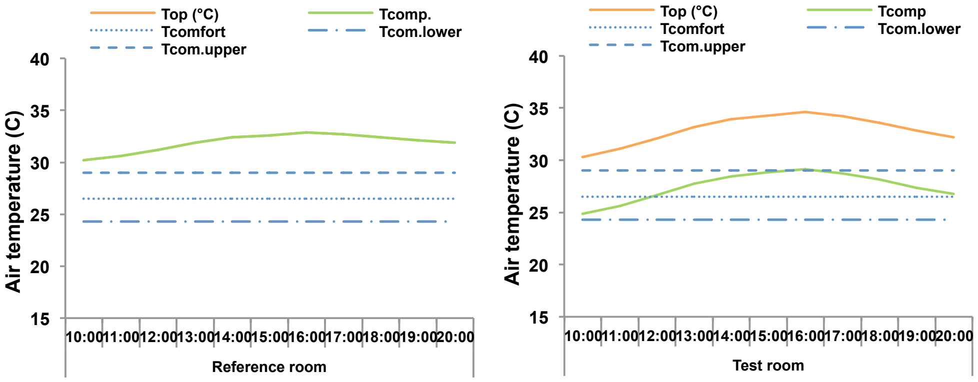

**Figure 6-4** Operative temperature ($T_{op}$) and compensated temperatures ($T_{comp}$) due to the room's air movement during 10AM to 8PM comparing to comfort temperature range in March: (left) the reference room; and (right) the test room.

According to the graphs it is apparent that the hourly operative temperatures ($T_{op}$) of both rooms lie outside the monthly comfort temperature range all the time. However, the test room's compensated temperatures ($T_{comp}$) were found within the comfort temperature range almost all the time. These results indicate the proposed ventilation shaft strategy's potential to induce the room's air velocity and improve the occupants' thermal comfort during the target time of the chosen day.

## 6.3 Stage 2: The effect of climatic conditions

After the proposed strategy was previously found to have a high potential to induce the room's air movement and extend the occupants' thermal comfort period, the influence of four main climatic elements on the strategy's effectiveness to induce room's air movement was investigated. These elements involve outdoor dry-bulb temperature ($T_{out}$), relative humidity ($RH$), external wind speed ($V_{out}$), and wind direction in term of wind incident angle to the room's main window ($\theta$) i.e. the inlet opening (see Table 5-8 for the summary of the fixed and independent variables for this study stage, and Figure 5-9 for the considered wind incident angles).

The error bar charts in Figure 6-5 present the results of average air velocity within the test room's occupied area at the main occupied level that were influenced by the considered climatic elements. In chart (a) of Figure 6.5 the relationship between the outdoor dry-bulb temperatures ($T_{out}$) and the room's average indoor air velocity ($V_{in}$) is illustrated. It is clearly shown that $T_{out}$ had almost no effect on the test room's $V_{in}$ as the results velocity within the room's occupied area were found constant i.e. $M$=1.46-1.49ms$^{-1}$, $SD$=0.73-0.74 across the different dry-bulb temperatures ($T_{out}$) ($N_{total}$=7316) (see Table C-4 in Appendix C for data summary). According to these findings, it could be concluded that the dry-bulb temperature ($T_{out}$) had no significant effect on the strategy's effectiveness to induce indoor air movement.

Similar result was also found for the relative humidity (*RH*) (chart (b) in Figure 6-5) as the test room's air velocities were found to remain constant i.e. M= 1.44-1.48ms$^{-1}$, $SD$= 0.72-0.74 across the different *RH* ($N_{total}$=5428). This result demonstrates that the *RH* also had no significant influences on the test room's air movement and so the strategy's performance to induce room's air velocity (see Table C-5 in Appendix C for data summary).

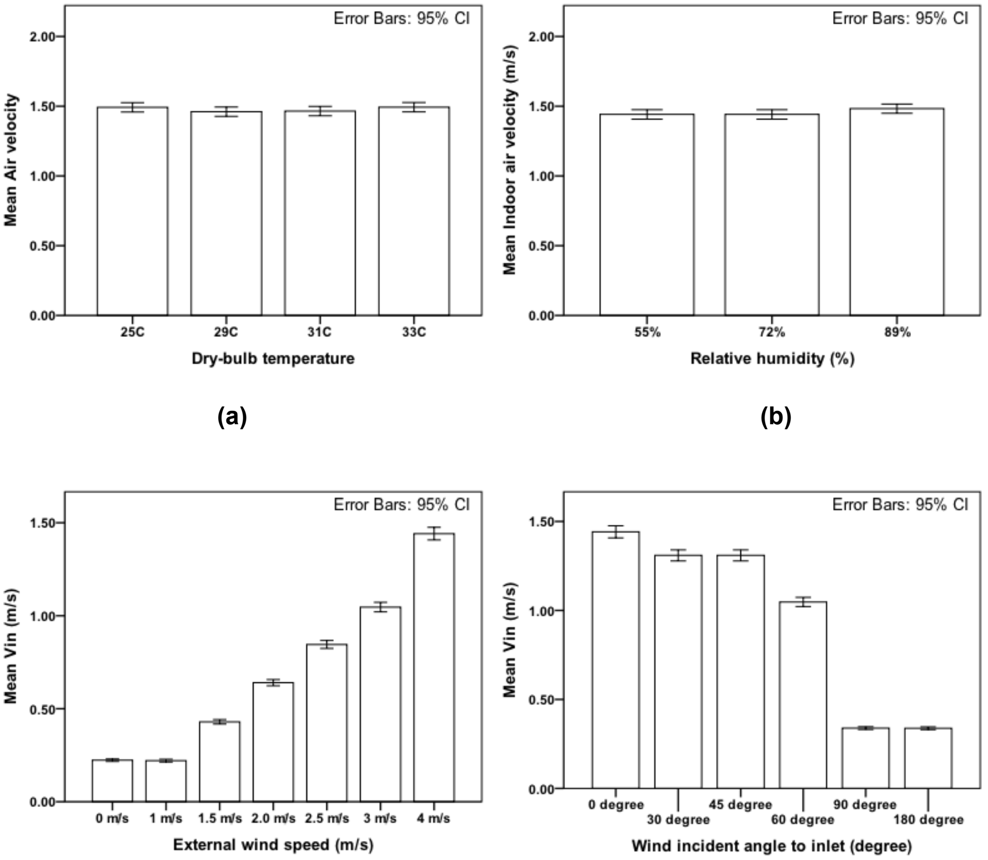

**(a)** **(b)**

**(c)** **(d)**

**Figure 6-5** The correlation between the test room's air velocity ($V_{in}$) and four climatic elements: (a) dry-bulb temperature ($T_{out}$); (b) relative humidity (*RH*); (c) external wind speeds ($V_{out}$); and (d) wind incident angle to the inlet opening ($\theta$).

Conversely, a strong positive correlation was found between the external wind speed ($V_{out}$) and the room's air velocity, as shown in Figure 6-5c. The air velocities were revealed to increase steadily with the rise of $V_{out}$ i.e. the mean velocity induced from M= 0.22ms$^{-1}$, *SD*=0.15 to M=1.44ms$^{-1}$,*SD*= 0.74 when the $V_{out}$ rose from 0ms$^{-1}$ (no wind) to 4ms$^{-1}$ (see Table C-6 in Appendix C). In Figure 6-5d a strong negative relationship between the wind incident angle and the room's air velocity was also found. There was a gradual decline in $V_{in}$ with the increase of wind incident angle ($\theta$). The maximum $V_{in}$ i.e. *M*=1.44ms$^{-1}$, *SD*=0.74 was found when the $\theta$ was perpendicular to the room's main window ($\theta$ of 0°). Then the room's velocity started to drop as $\theta$ moved to 30°, 45° and 60° and reached its minimum i.e. *M*=0.34ms$^{-1}$, *SD*=0.17 when $\theta$ was at 90° and 180° (see Table C-7 in Appendix C).

According to these results the external wind condition involving wind speed and wind direction were found to be the most influential climatic parameters, while the dry-bulb temperature and the relative humidity had no significant effect on the ventilation shaft strategy's effectiveness to induce the test room's air velocity.

Figure 6-6 and 6-7 present the simulated air distributions at the occupied level of the test room under different external wind speeds ($V_{out}$) and wind incident angles ($\theta$), respectively. For all different $V_{out}$, it can be seen that the external air entered into the test room from the inlet opening. The air then flew through the room's main occupied area, particularly the area along the center axis of the room between the inlet and outlet opening. The maximum air velocity in every case was found at the inlet opening before the velocity gradually dropped with a distance from the inlet and slightly increased again in front of the outlet opening at the rear wall. These velocity vector plots in Figure 6-6 also support the strong positive relation between the external wind speed and the room's air velocity previously found.

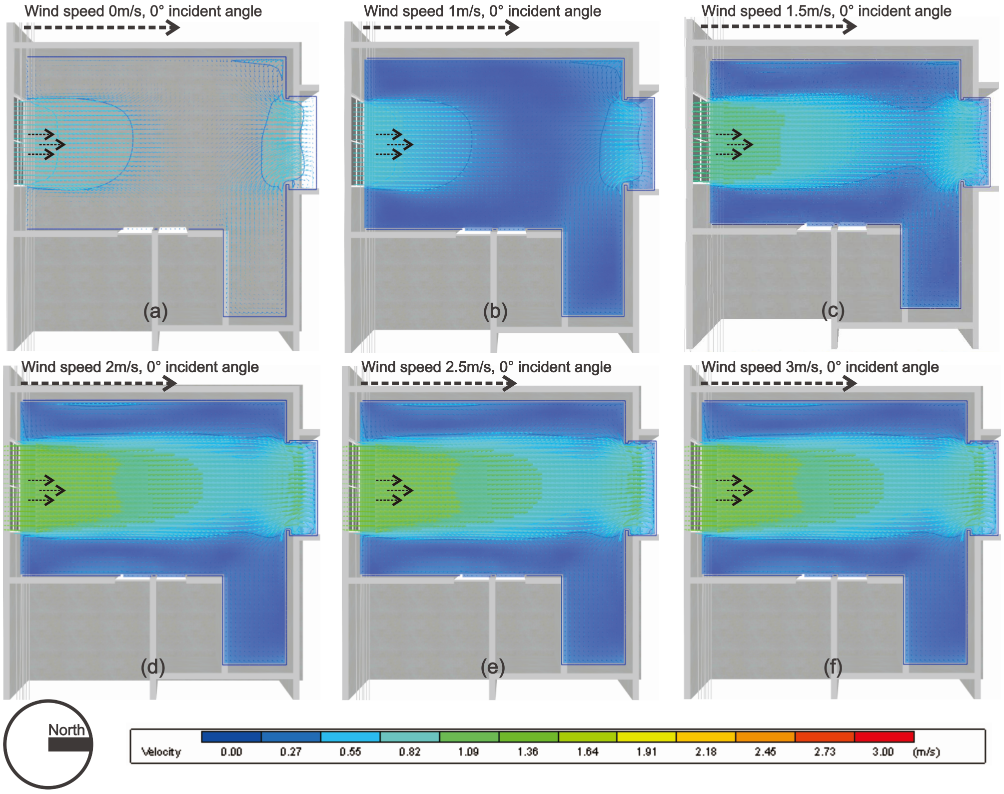

**Figure 6-6** Velocity vector plot at the occupied level of the test room under different external wind speeds ($V_{out}$):(a) $V_{out}$ at 0ms$^{-1}$;(b) 1ms$^{-1}$;(c) 1.5ms$^{-1}$;(d) 2ms$^{-1}$;(e) 2.5ms$^{-1}$; and (f) 3ms$^{-1}$.

Similar airflow patterns i.e. air flowing from the inlet to the outlet openings were also found for most of the wind directions (Figure 6-7a to 6-7d), and the very weak airflow found when $\theta$ was at 90° also confirmed the simulated air velocity reported previously (Figure 6-7e). On the other hand the reverse flow direction occurred when the $\theta$ was at 180° (Figure 6-7f). For this particular case the external air entered into the studied building through the shaft's exhaust beyond the building roof and travelled downward before it penetrated into the test room via the outlet opening and exhausted through the room's main window i.e. the inlet opening.

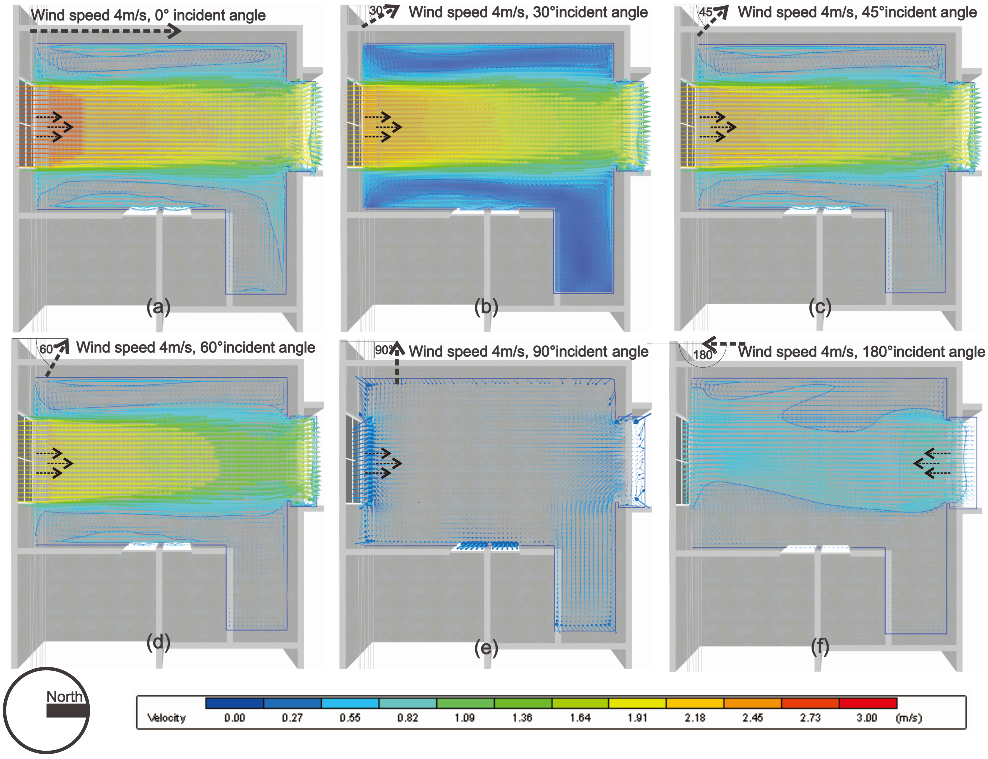

**Figure 6-7** Velocity vector plot at the occupied level of the test room under different wind incident angles to the inlet opening (*θ*)*:* (a) *θ* at 0°; (b) *θ* at 30°; (c) *θ* at 45°; (d) *θ* at 60°; (e) *θ* at 90°; (f) and *θ* at 180°.

Besides the air velocity and airflow distribution, the predicted operative temperatures ($T_{op}$) of the room under different climatic conditions were also investigated in this stage. Figure 6-8 displays the simulated operative temperature ($T_{op}$) against the average air velocity ($V_{in.av}$) found in the test rooms. It can be seen that the room's average operative temperature ($T_{op.av}$) unsurprisingly followed the external dry-bulb temperature ($T_{out}$) closely in chart (a), while both of the room's $T_{op.av}$ and $V_{in.av}$ remained unaffected for different relative humidity (*RH*) (Figure 6-8b). Differently, it was interestingly found that the room's $T_{op}$ had a connection with the room's $V_{in.av}$ (Figure 6-8c and 6-8d). The room's $T_{op}$ was found to slightly increase from 30.4°C to 30.7°C when the $V_{in.av}$ increased, and it was found to drop from 30.7°C to 30°C when the $V_{in.av}$ dropped as can be seen in the chart (c) and (d), respectively. Although this positive correlation between $T_{op}$ and $V_{in.av}$ may not be a direct relationship as the variation in $T_{op}$ was mainly due to the change in the incoming air volume with relatively greater temperature, this correlation should be considered as a significant issue when introducing the external air into a building particularly for tropical countries.

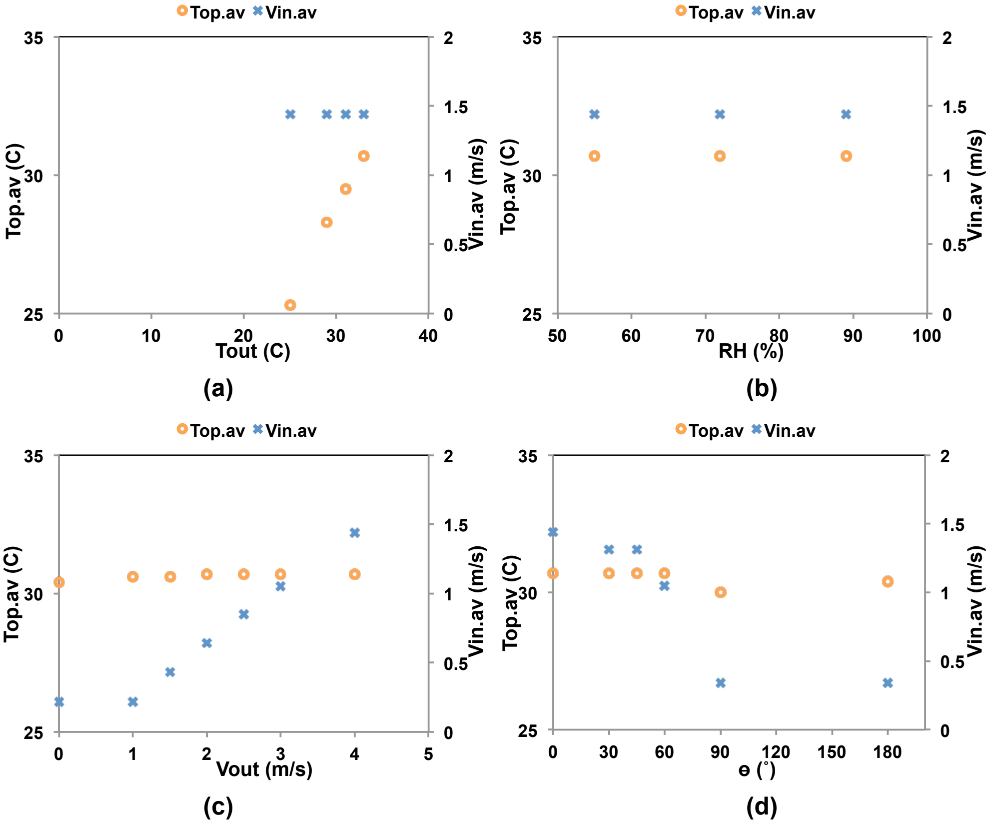

**Figure 6-8** Average operative temperature ($T_{op.av}$) and average air velocity ($V_{in.av}$) at the occupied level of the test room under the variations in four climatic elements: (a) $T_{out}$; (b) $RH$; (c) $V_{out}$; and (d) $\theta$.

In this stage, four climatic elements that may have an influence on the ventilation shaft's effectiveness to induce the room's air movement and thus the occupants' thermal comfort were investigated. The external wind conditions i.e. wind speeds and directions regarding to the room's window were found as the most influential factors on the strategy's success. On the other hand the external dry-bulb temperature and the relative humidity were found to have no significant effect. However, an increase in the room's air velocity by introducing external air at a comparatively high temperature into the room may induce the room's operative temperature. This issue will be considered again in study stage five i.e. the strategy's performance to extend thermal comfort hours.

## 6.4 Stage 3: The strategy's optimal design

In the previous stage the most significant climatic parameters that have effects on the ventilation shaft strategy's performance were revealed. In this stage the strategy's geometry and design were optimized. These include the size and the position of the vertical shaft, the inlet and outlet's opening.

### 6.4.1 Shaft size

First the effects of the vertical shaft's size on the room's air movement were examined. These included the shaft's height above the building roof ($H_{shaft}$), its length ($L_{shaft}$), and its width ($W_{shaft}$) (see Figure 5-10, 5-11 and 5-12, respectively for the considered shaft's sizes). To achieve this the test room with variations in shaft's size was simulated under the constant settings (see Table 5-9 for the summary of the fixed variables adopted for stage three and Table 5-10 for the variables list for investigating the effect of shaft's size).

Figure 6-9 presents the result average air velocities that were obtained from the test room's occupied area when different shaft's sizes were employed. In the error bar chart, the constant $V_{in}$ at $M$=1.44ms$^{-1}$, $SD$=0.74 across the varied $H_{shaft}$ between 1m and 4m indicates a very weak correlation between these two variables. Differently the relatively weaker air velocity in the room i.e. $M$=1.33ms$^{-1}$, $SD$=0.69 was found when the shaft's exhaust was at the building roof level ($H_{shaft}$ of 0m). It is therefore suggested to have the shaft's exhaust at any height beyond the building roof level to attain a good result comparing to that with the exhaust at the roof level (see also Table C-9 for detailed results).

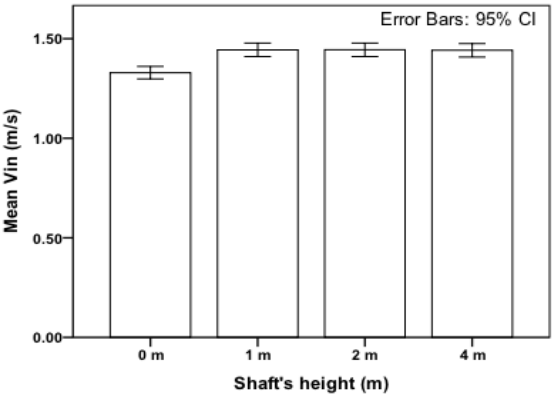

**Figure 6-9** Average air velocities ($V_{in}$) in the test room with different shaft's heights ($H_{shaft}$).

Conversely, positive correlations were found between the shaft's length and width ($L_{shaft}$ and $W_{shaft}$), and the room's air velocity ($V_{in}$). As can be seen in Figure 6-10, the room's $V_{in.av}$ increased with the shaft's size. This is particularly true for the shaft's width ($W_{shaft}$) as the room's average air velocity ($V_{in.av}$) was found to progressively rise when the $L_{shaft}$ was constant and the $W_{shaft}$ increased from 0.3m to 0.6m and 1.2m. For instance, in the case of $L_{shaft}$ = 4m, the average air velocity was found to increase from $M$=1.71ms$^{-1}$, $SD$=0.89 to

*M*=2.26ms$^{-1}$, *SD*=1.16 when the $W_{shaft}$ increased from 0.3m to 1.2m, respectively (detailed results can be found in Table C-10 in Appendix C).

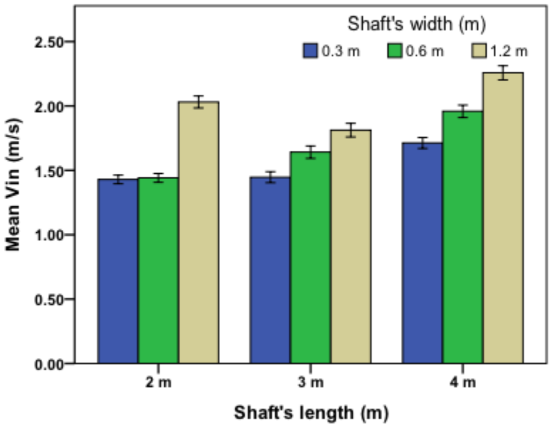

**Figure 6-10** Average air velocities ($V_{in}$) in the test room with different shaft's lengths and widths ($L_{shaft}$ and $W_{shaft}$).

According to these findings the vertical shaft is suggested to be as wide as possible to ensure the room's high air velocity. This finding is also supported by the results of airflow patterns obtained from the occupied level of the test room under different shaft's widths (Figure 6-11). Although a similar airflow pattern was found across different $W_{shaft}$ i.e. external air entered into the room from the inlet opening with its maximum velocity and flew through the room's main occupied area before leaving the room through the outlet opening, the air with high velocity was found to reach to the greater area of the room when the shaft's width increased (comparing Figure 6-11a to Figure 6-11c).

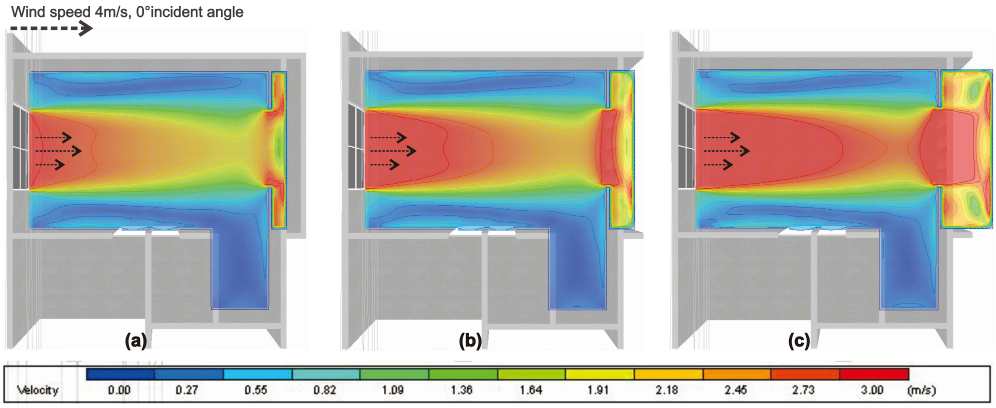

**Figure 6-11** Air velocity contour at the occupied level of the test room obtained from different shaft's widths ($W_{shaft}$) with constant shaft's length ($L_{shaft}$) of 4m: (a) $W_{shaft}$ of 0.3m; (b) $W_{shaft}$ of 0.6m; and (c) $W_{shaft}$ of 1.2m.

However, the $W_{shaft}$ over 1.2m is unlikely to happen in a real situation, as it would take a large proportion of a building's usable space. For the next stage a practical shaft width at 0.6m and shaft length of 4m that is able to cover all considered outlet opening's widths was, therefore, adopted as a fixed variable.

### 6.4.2 Inlet and outlet opening's size

After the vertical shaft's optimal size was found, the influence of the inlet and outlet opening's size on the strategy's performance was then investigated. To begin with, the effects of both openings' width ($W_{inlet}$ and $W_{outlet}$) on the room's air movement were studied. The test room with various combinations of $W_{inlet}$ and $W_{outlet}$ between 1m and 4m was simulated under the fixed settings and climatic conditions summarized in Table 5-9, while both the inlet's and outlet's length ($L_{inlet}$ and $L_{outlet}$) were kept constant at 1.2m (see Figure 5-13 for the considered cases and Table 5-11 for the summary of fixed and independent variables for this stage).

The error bar chart in Figure 6-12 display the average air velocity ($V_{in.av}$) within the occupied area of the test room that employed considered inlet and outlet opening's widths. The chart reveals a very weak relation between the $V_{in}$ and $W_{outlet}$ i.e. there was a barely change in $V_{in.av}$ when the $W_{outlet}$ was altered (detailed results can be found in Table C-11 in Appendix C). Differently the results $V_{in}$ were found comparatively more sensitive to the $W_{inlet}$. As can be seen that the room's average air velocity grew with the inlet's width. This is particularly when the $W_{inlet}$ increased from 1m to 2m as the $V_{in.av}$ was found to increase from $M$=1.35ms$^{-1}$, $SD$=1.12 to $M$=2.00ms$^{-1}$, $SD$=0.94 when the $W_{outlet}$ was fixed as 3m. However, the $V_{in.av}$ was found to drop slightly when the $W_{inlet}$ went beyond 3m (see Table C-11 in Appendix C). According to these findings the inlet opening's width of at least 2m or about 50% of the wall's width is suggested for ensuring a greater air velocity in the test room.

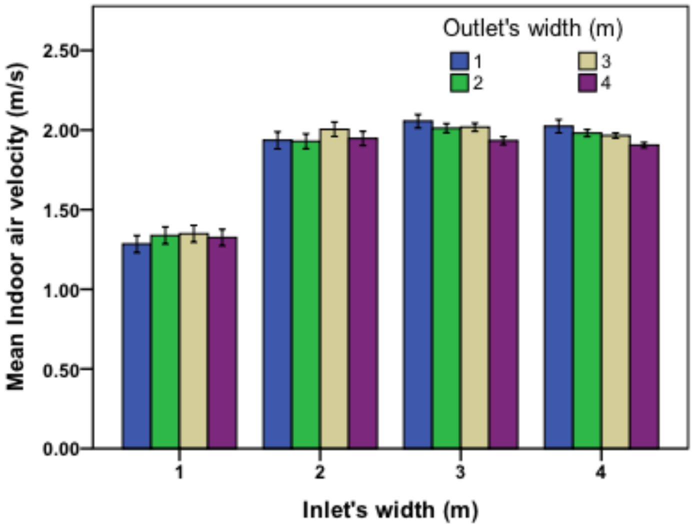

**Figure 6-12** The result air velocities ($V_{in}$) in the test room with different inlet and outlet's widths.

The comparison of the average air velocity ($V_{in.av}$) in the test room with various combinations of inlet and outlet opening's widths in Figure 6-13 also supports the recommendation made above. An obviously lower $V_{in.av}$ was found across different $W_{outlet}$ when the $W_{inlet}$ was at 1m. The inlet opening with any widths greater than 1m was therefore preferred as they could produce greater $V_{in.av}$. However, it can be seen that there was a slight increase in the room's average operative temperature ($T_{op.av}$) when the average air velocity ($V_{in.av}$) increased (see also Table C-14 for the results $T_{op.av}$). These findings support the correlation between the room's operative temperature and the air velocity found in the previous stage. It is therefore important to consider both the room's $T_{op.av}$ and $V_{in.av}$ when investigating the strategy's performance to increase the occupants' thermal comfort in the final study stage.

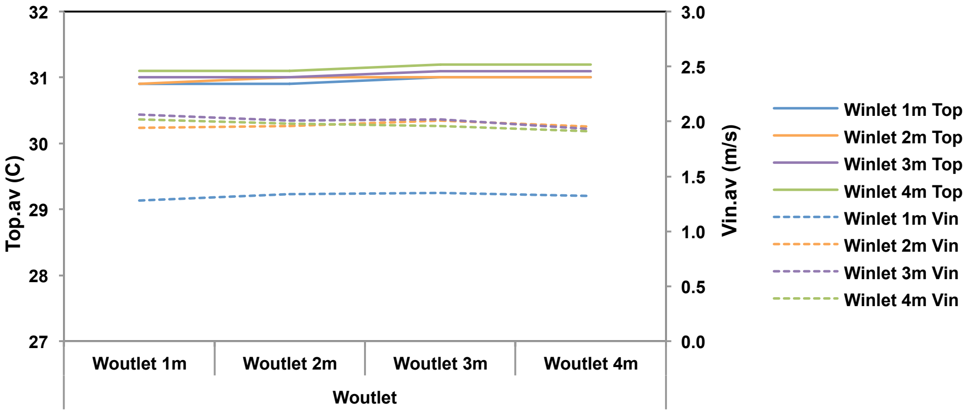

**Figure 6-13** Results of average operative temperature ($T_{op.av}$) (lines) and average air velocity ($V_{in.av}$) (dashed lines) in the test room with different inlet and outlet's widths ($W_{inlet}$ and $W_{outlet}$).

Figure 6-14 shows the airflow distributions at the occupied level of the test room with various combinations of inlet and outlet opening widths ($W_{inlet}$ and $W_{outlet}$). It can be seen that the maximum $V_{in}$ was found at the inlet in almost all cases, particularly when the $W_{Inlet}$ was small (comparing Figure 6-14d and Figure 6-14p, for instance). For such cases the incoming air entered into the test room with a jet-like characteristic. On the contrary the maximum air velocity was not only found at the inlet but also in front of the vent or the outlet opening when the $W_{outlet}$ were small i.e. 1m and 2m, especially when the $W_{outlet}$ was smaller than the $W_{inlet}$ i.e. in case (a), (e), (f), (i), (j), (k), (m), (n) and (o). In conclusion, the high airflow fluctuations, which may create the disturbance for the occupants, could be found in the room with either very small inlet or small outlet widths. Conversely a smoother airflow pattern was found when both the $W_{inlet}$ and the $W_{outlet}$ were expanded, especially the $W_{outlet}$, as in the cases of $W_{outlet}$ between 3m to 4m (comparing Figure 6-14l and 6-14p to 6-14i and 6-14m). The inlet and outlet openings' widths of 3m and 4m i.e. 75% and 100% of the wall's width, respectively are therefore suggested in order to induce the room's air velocity while reduce the high airflow fluctuation.

For the next stage the width of both inlet and outlet opening will be fixed at 3m as this opening size is expected to produce the required indoor air velocity in most area of the test room, while keeping the room's operative temperature at an acceptable range to lessen the chance of incoming radiation through the large room's main window (see data summary of $T_{op.av}$ and $V_{in.av.}$ in Table C-14).

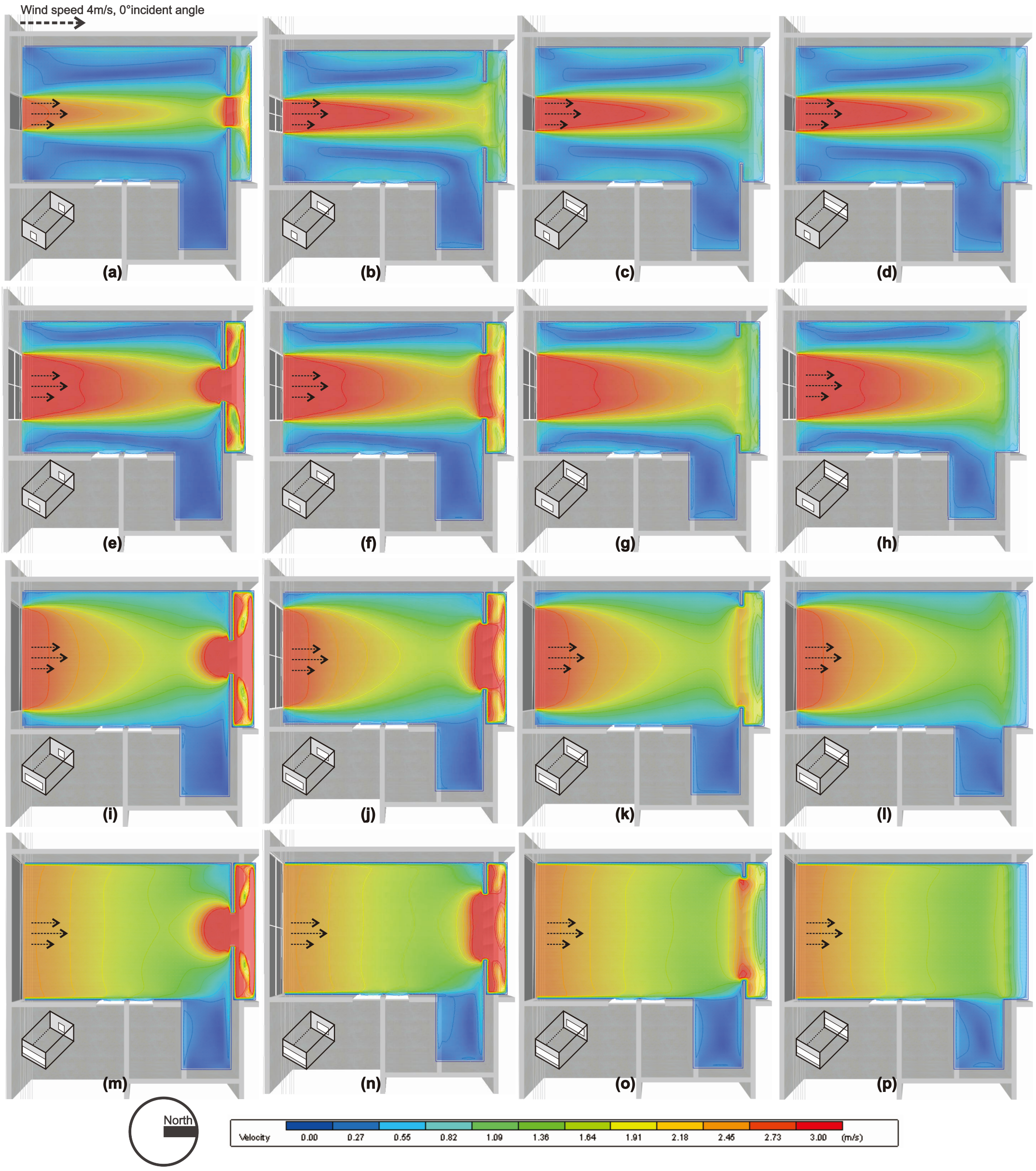

**Figure 6-14** Air velocity contour at the occupied level of the test room under different combinations of inlet and outlet's width: (a) $W_{inlet}$ and $W_{outlet}$ of 1m and 1m; (b) 1m and 2m; (c) 1m and 3m; (d) 1m and 4m; (e) 2m and 1m; (f) 2m and 2m; (g) 2m and 3m; (h) 2m and 4m; (i) 3m and 1m; (j) 3m and 2m; (k) 3m and 3m; (l) 3m and 4m; (m) 4m and 1m; (n) 4m and 2m; (o) 4m and 3m; and (p) 4m and 4m.

After the influence of the inlet and outlet openings widths on the strategy's effectiveness was revealed, the effect of the opening's length was then investigated. According to the previous investigation, it was discovered that the size of the inlet opening had comparatively more influence on the room's air velocity to that of the outlet opening. Only the effect of the inlet's length ($L_{inlet}$) was therefore studied in this stage. To achieve this the test room with four different $L_{inlet}$ between 0.6m and 1.5m was simulated, while the $W_{inlet}$ and the $W_{outlet}$ were fixed at 3m and the $L_{outlet}$ was held constant at 1.2m (see Figure 5-14 for the considered cases and Table 5-11 for the fixed and independent variables). In Figure 6-15, the bar chart of average air velocities obtained at the occupied level of the test rooms with considered inlet's lengths are shown. According to the chart a strong negative correlation between the room's air velocity and the inlet's length is demonstrated. The highest $V_{in.av}$ i.e. $M$= 2.35ms$^{-1}$, SD=0.72 was found when the $L_{inlet}$ was 0.6m. Then the $V_{in}$ started to drop with the increase of $L_{inlet}$ until the $L_{inlet}$ reached 1.5m when the weakest $V_{in.av}$ was found as $M$= 1.80ms$^{-1}$, SD=0.45 (see also Table C-12 in Appendix C).

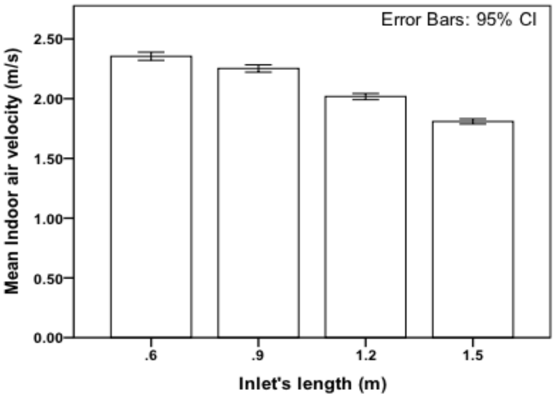

**Figure 6-15** The result air velocities ($V_{in}$) in the test room with different inlet's lengths ($L_{inlet}$).

This relationship between the indoor air velocity and the inlet's length was also found when looking at the room's airflow distribution in Figure 6-16. For all cases the external air with its maximum velocity similarly entered into the test room and then flew through the room before leaving at the outlet opening. However, the comparatively weaker air velocity at the room's main occupied level (shown by dashed lines) was found when the inlet's length increased (comparing Figure 6-16a and Figure 6-16d). To ensure a good result of air velocity and the occupants' thermal comfort, it is therefore suggested to have the inlet opening with a small length that can cover the room's main occupied level.

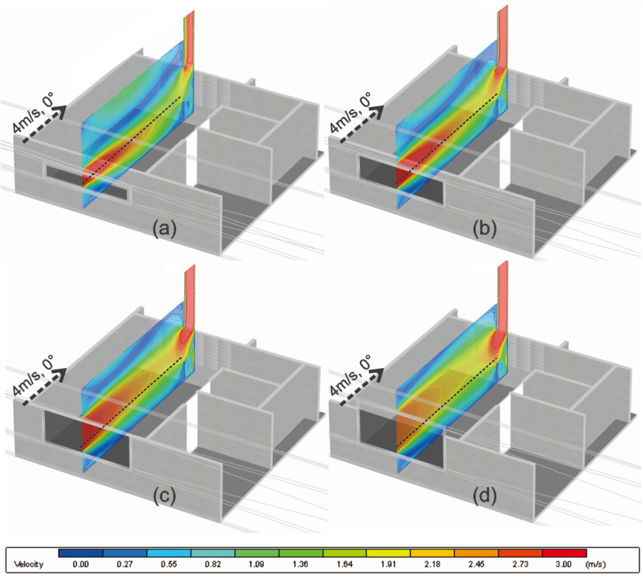

**Figure 6-16** Air velocity contour along the center of the test room with different inlet's lengths ($L_{inlet}$): (a) $L_{inlet}$ of 0.6m; (b) $L_{inlet}$ of 0.9m; (c) $L_{inlet}$ of 1.2m; and (d) $L_{inlet}$ of 1.5m with the room's main occupied level (dashed line).

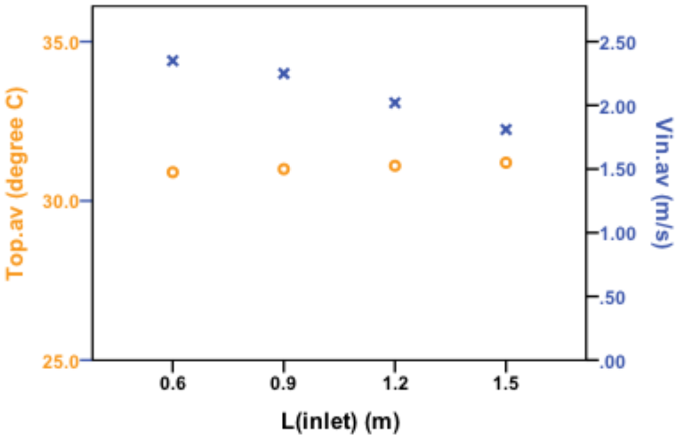

**Figure 6-17** Average operative temperature ($T_{op.av}$) and average air velocity ($V_{in.av}$) at the occupied level obtained from the test room with different inlet's lengths ($L_{inlet}$).

Moreover, the small inlet's length was also favourable in terms of the room's operative temperature ($T_{op}$). In Figure 6-17 the results of the room's average air velocities ($V_{in.av}$) in the room with different inlet's lengths ($L_{inlet}$) were plotted against its average operative temperature ($T_{op.av}$). It was found that the $V_{in.av}$ dropped from 2.35ms$^{-1}$ to 1.81ms$^{-1}$, while the $T_{op.av}$ increased from 30.9°C to 31.2°C, when the inlet's lengths increased from 0.6m to 1.5m (see Table C-14 for data summary). This is because less solar radiation could enter into the room when the inlet was smaller in size. The inlet and outlet opening's length of 0.6m would therefore be adopted as the optimal design for the rest of the study stages.

### 6.4.3 Inlet and outlet opening's position

After the optimal size of the inlet and outlet opening were identified, the influence of the vertical positions of the inlet and outlet opening on the strategy's performance to increase air movement in the room's main activity area was examined. The test room with variations in the inlet and outlet openings' vertical positions ($H_{inlet}$ and $H_{outlet}$) regarding their distances to the room's main occupied level ($H_{occ}$) was simulated under the constant settings and climate listed in Table 5-9. There were three considered positions including: i) low position ($H_{inlet} - H_{occ}$=-0.5m as $H_{inlet}$ was at 0.5m and $H_{occ}$ at 1m above the floor); ii) middle position ($H_{inlet}$-$H_{occ}$=0.1m); and iii) high position ($H_{inlet}$-$H_{occ}$=0.7m) (see Figure 5-15 and 5-16 for the considered positions and Table 5-12 for the summary of fixed and independent variables).

The error bar chart in Figure 6-18 illustrates the relationship between the room's average air velocity at the occupied level and the considered openings' positions. As shown in the chart, there was a significant relationship between the room's air velocity ($V_{in}$) and the inlet opening's vertical position ($H_{inlet}$). The resultant $V_{in}$ apparently changed when the inlet's position was altered (see Table C-13 in Appendix C). The highest $V_{in}$ was found when both inlet and outlet openings were at the middle position i.e. *M*=2.42ms$^{-1}$, *SD*=0.68, while the velocity fell when both inlet and outlet openings were both at either low or high position (*M*=1.36ms$^{-1}$, *SD*=0.37 and *M*=0.34ms$^{-1}$, *SD*=0.16, respectively). On the other hand, the vertical position of the outlet opening ($H_{outlet}$) was found to have much weaker influence on the room's air velocity as the results $V_{in.av}$ were found almost stable as *M*=2.33ms$^{-1}$, 2.42ms$^{-1}$ and 2.25ms$^{-1}$ across the different $H_{outlet}$ of low, middle and high position, respectively while the $H_{inlet}$ was kept constant at middle position.

According to these results it is suggested to have the openings, especially the inlet, at the room main activity level to ensure the maximum average air velocity and thus the occupants' thermal comfort. In this study as the occupied level was established as about 1m above the floor, the inlet opening at the middle position was therefore favourable.

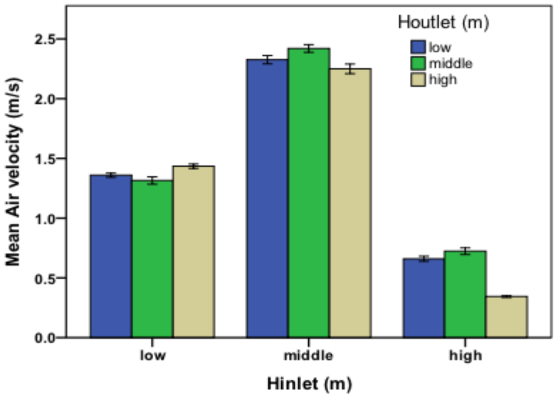

**Figure 6-18** The relationship between indoor air velocity ($V_{in}$) and the vertical position of inlet and outlet opening ($H_{inlet}$ and $H_{outlet}$) regarding to their distances to the occupied level ($H_{occ}$).

In Figure 6-19 the resultant air distributions at the vertical axis between the inlet and outlet opening across the test room with different inlet and outlet opening's positions are displayed. The dashed lines were used for indicating the main occupied level i.e. 1m above the floor. For all cases the incoming air penetrated into the room with its maximum velocity and flew through the occupied area before leaving the room through the outlet opening. The main airflow path in each case was therefore found between the inlet and the outlet opening. It was also found that the best airflow with maximum velocity at the considered level (dashed line) occurred when both the inlet and outlet openings were at the middle position (Figure 6-19e), which supports the previous findings.

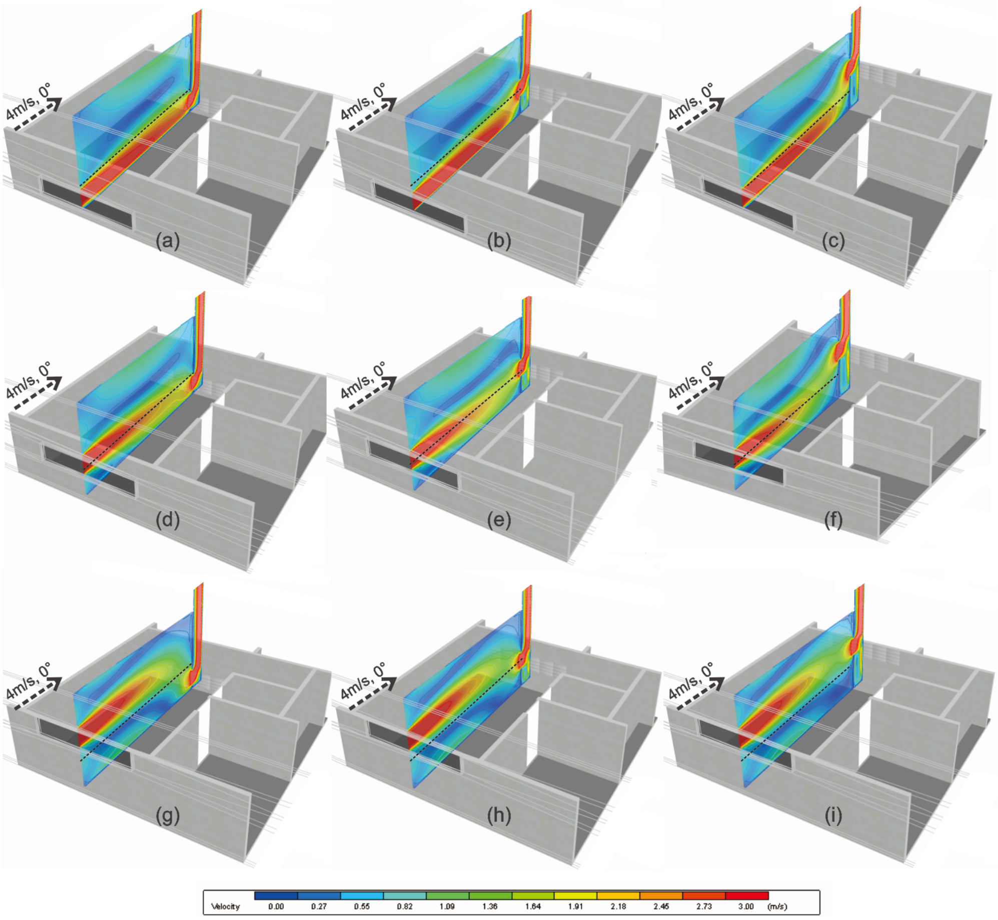

**Figure 6-19** Air velocity contour along the center of the room between the inlet and outlet opening obtained from the test room with different inlet and outlet's vertical positions ($H_{inlet}$ and $H_{outlet}$) according to the occupied level ($H_{occ}$): (a) low to low; (b) low to middle; (c) low to high; (d) middle to low; (e) middle to middle; (f) middle to high; (g) high to low; (h) high to middle; and (i) high to high.

In terms of the room's operative temperature ($T_{op}$) the openings' different vertical locations were found to have no significant effect, as shown in Figure 6-20. Although the room's $V_{in.av}$ was found to vary, the room's $T_{op.av}$ were found constant at 30.9°C across different inlet and outlet's positions (see also Table C-14). This may be because there was the same amount of incoming air with high temperature entering into the test room under the particular climatic conditions regardless of the room's openings position.

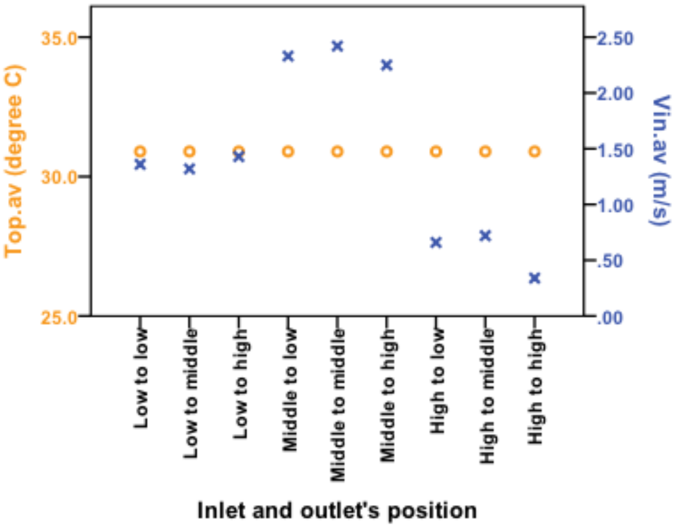

**Figure 6-20** Room's average operative temperature ($T_{op.av}$) and average air velocity ($V_{in.av}$) at the occupied level obtained from different combinations of inlet and outlet's heights ($H_{inlet}$ and $H_{outlet}$).

In conclusion, the differences in inlet and outlet vertical positions were found to have no crucial effect on the room's operative temperature but a great effect on the air velocity at the room's occupied level. The room's inlet and outlet openings should be therefore positioned at its main activity level for ensuring a good thermal comfort for the occupants.

## 6.5 Stage 4: Implementing the ventilation shaft strategy

According to the previous stage, the optimal design of the ventilation shaft strategy to produce the best results of the room's air velocity and operative temperature was discovered. These include the vertical shaft size of 4x0.6m2 ($L_{shaft}$ x $W_{shaft}$) with $H_{shaft}$ of 1m above the building roof; and the inlet and outlet size of 0.6x3m2 (*LxW*) at 0.8m above the floor. However, in such cases, the ventilation shaft was attached only to one test room on floor 23rd.

In this stage the strategy's performance when it was implemented to a more practical situation was investigated. To achieve this, the studied building with the ventilation shaft attaching to one test room per floor from floor 6th to floor 25th (see Figure 5-17) was simulated under three external wind speeds as listed in Table 5-13. The three considered wind speeds ($V_{out}$) include: 0ms$^{-1}$ ('*no wind'* situation); 1ms$^{-1}$ (Bangkok's annually average wind speed); and 4ms$^{-1}$ (Bangkok's annually average maximum wind speed). Then the resultant air velocities obtained from the test rooms and the reference rooms on the same floors were compared. Any increase in air velocity in the room when the strategy was employed would indicate the strategy's effectiveness in inducing room's air velocity and therefore the occupants' thermal comfort.

Figure 6-21 displays the average air velocities ($V_{in.av}$) within the occupied area of the reference and the test rooms on different levels that were obtained under different external wind speeds ($V_{out}$) (detailed results can be found in Table C-15 in Appendix C). It should be noted that the positive values of $V_{in.av}$ in the chart indicate the air flowing from the inlet to the outlet opening, while the negative values indicate the reverse flow. It is apparent that the $V_{in.av}$ in the reference rooms were constantly low across different floor levels i.e. approximately 0.05ms$^{-1}$ even under the $V_{out}$ of 4ms$^{-1}$, which is Bangkok's annual average maximum wind speed. This $V_{in.av}$ was only approximately 1% of the $V_{out}$. Conversely, the results air velocity in the test rooms were found to increase with the rise in $V_{out}$ as the overall $V_{in.av}$ were found as 0.36ms$^{-1}$, 0.38ms$^{-1}$ and 0.66ms$^{-1}$ under the $V_{out}$ of 0ms$^{-1}$, 1ms$^{-1}$ and 4ms$^{-1}$, respectively (see Table C-15 in Appendix C). The resultant $V_{in.av}$ from the test rooms were therefore apparently greater than that in the reference rooms for almost all levels as the $V_{in.av}$ was found as between 0.05ms$^{-1}$ and 1.07ms$^{-1}$, which was approximately 2% and up to 58% of the $V_{out,}$ depending on the room's different level and different wind conditions.

According to these findings, even the $V_{in.av}$ in the test room without the support of external wind speed i.e. $V_{out}$ of 0ms$^{-1}$ was greater than that in the reference rooms, and they were still high enough to produce a physiological cooling effect for offsetting the room's high operative temperature. Employing the proposed ventilation shaft strategy was therefore an effective way to increase the air movement and thermal comfort condition in the room with one-side opening.

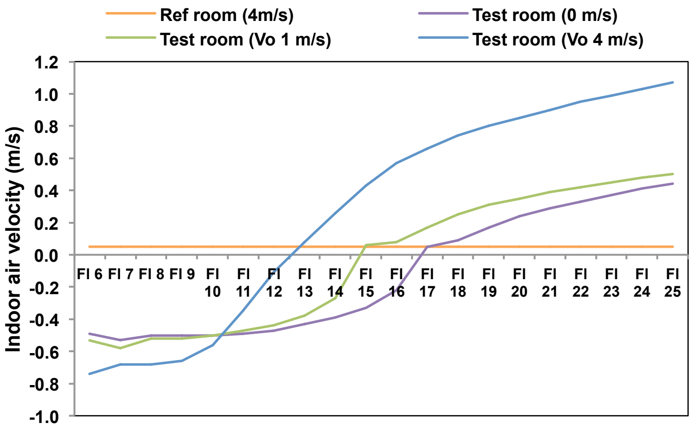

**Figure 6-21** Average air velocity ($V_{in.av}$) in the occupied area of the test rooms under various external wind speeds ($V_{out}$) when the ventilation shaft is attached to the rooms from floor 6th to floor 25th comparing to that of the reference rooms.

Figure 6-21 also displays that the $V_{in.av}$ in the test rooms varied across the different floor levels, contrasting to the constant velocities across different floors in the reference room cases. The test room's minimum average velocities were found in the rooms located on the middle floors that attached to the vertical shaft i.e. between floor 13rd and 17th, whereas the relatively higher velocities were found when the room levels moved either downward or upward. For instance, the minimum $V_{in.av}$ i.e. $0.05ms^{-1}$ was found on floor 17th in case of $V_{out}$ of $0ms^{-1}$ while the average velocity continually rose to $0.49ms^{-1}$ and $0.44ms^{-1}$ on floor 6th and floor 25th, respectively.

Also, different airflow pattern results were found across the test rooms on different floor levels (Figure 6-22). For every external wind speed the air was found to flow from the outlet to the inlet opening in the rooms on the lower floors. This was the case, for instance, between floor 6th to floor 14th under the $V_{out}$ of $1ms^{-1}$. In such cases the air flew from the vertical shaft and entered into the rooms through the vent before it was exhausted at the rooms' main window. The air exhausted from the rooms in the upper floors may be therefore mixed with incoming fresh air from the ambient through the shaft exhaust and enter into the rooms on the lower levels (see also Figure 2-23).

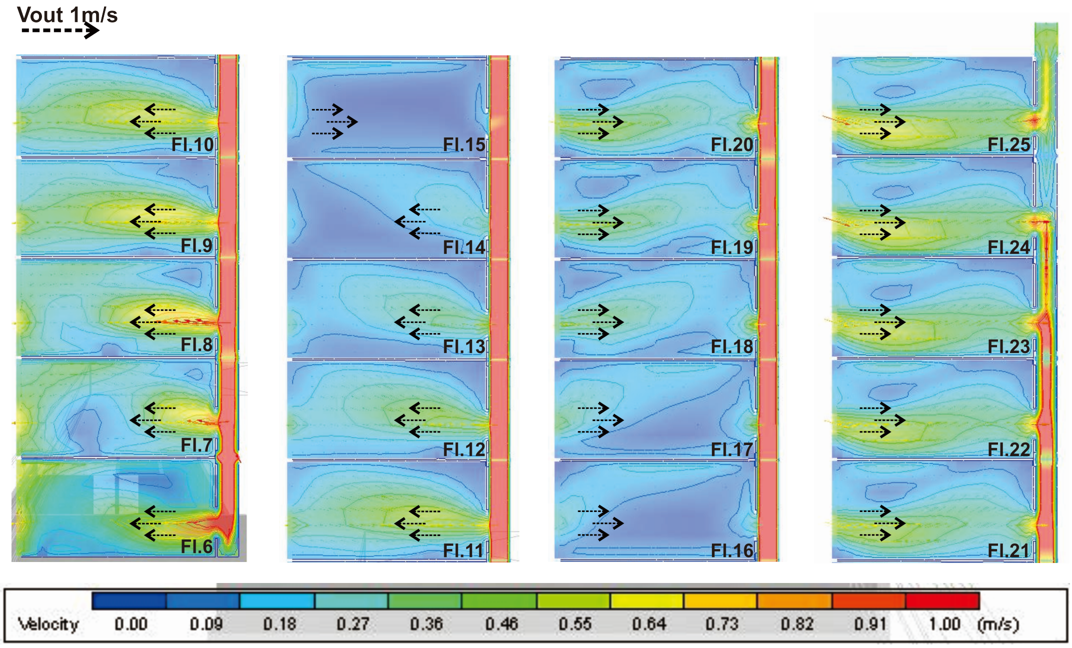

**Figure 6-22** Air velocity contour along the center of the test rooms between floor 6th and floor 25th under $V_{out}$ of $1ms^{-1}$ and $\theta$ of 0°:

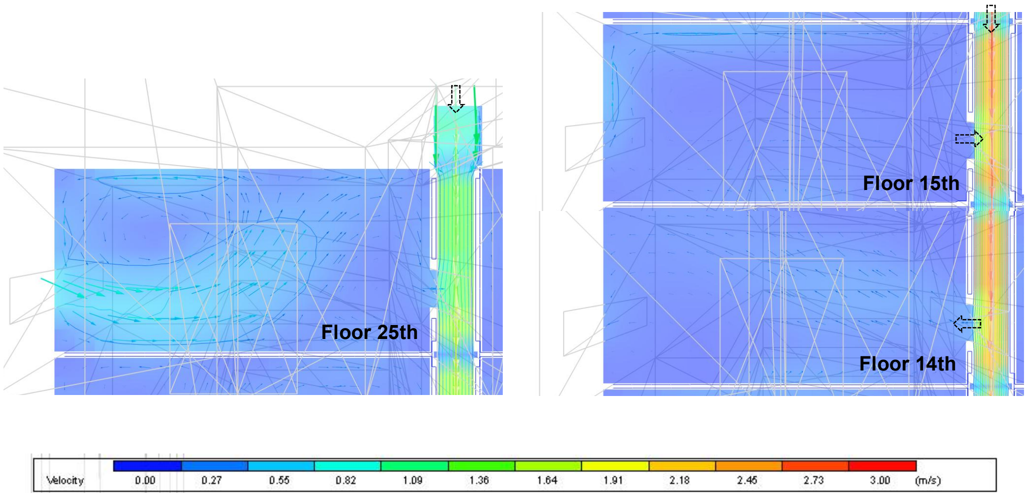

**(a)** **(b)**

**Figure 6-23** Detailed airflow along the center of the test rooms when the vertical shaft connected to multiple floors: (a) incoming air through the exhaust of the vertical shaft; and (b) airflow within the shaft between floor 15 and floor 14 where the air from the vertical shaft starts to flow into, rather than out of the unit.

According to these findings the proposed ventilation shaft was found to be an effective strategy to induce the air movement in a single-sided residential unit. Although the $V_{in.av}$ in the test rooms were comparatively weaker when the shaft was employed to a number of test rooms on different floors i.e. from floor 6th to floor 25th comparing to the result velocities in the previous stages, the ventilation shaft was still able to provide an sufficient air velocity for producing physiological cooling effect i.e. at least $0.2\text{ms}^{-1}$ for most rooms. Also, it was able to induce the rooms' air velocity even under the '*no wind*' condition i.e $V_{out}$ at $0\text{ms}^{-1}$.

In the next stage the effectiveness of the ventilation shaft strategy to improve the occupants' thermal comfort and thus reducing the building's energy consumption due to the cooling system under Bangkok's typical climatic conditions examined was reported.

## 6.6 Stage 5: The strategy's performance to extend thermal comfort hours

In this final stage the performance of the proposed ventilation shaft strategy to improve the occupants' thermal comfort was assessed, and the possible saving of the building's energy consumption was estimated. This would provide a picture of how effective the strategy might be to help reducing the high electricity demand due to mechanical cooling systems in single-sided apartment units, which is the main aim of this study. To accomplish this, the concept of thermal comfort hour percentages was adopted. Any increase in these percentages in a test room comparing to that in a reference room under the same situation would indicate the strategy's performance on improving the occupants' thermal comfort and reducing the building's energy consumption.

To start with, two test rooms involving a south-facing room on floor 21st and a north-facing room on floor 23rd, of which their average air velocity ($V_{in.av}$) were close to the overall $V_{in.av}$ of the south-facing and north-facing units, respectively found in the previous stage were chosen as the representative rooms for this stage (see previous study stage and data in Table C-15 in Appendix C). Regarding to Szokolay's physiological cooling model, the rooms' $V_{in.av}$ under Bangkok's typical wind condition i.e. $V_{out}$ of $1ms^{-1}$ and $\theta$ of 0° found in the previous stage was calculated into the physiological cooling effect ($dT$) for compensating the rooms' hourly operative temperatures ($T_{op}$) predicted by EnergyPlus (see Table C-16 in Appendix C). Then these two test rooms' compensated temperatures ($T_{comp}$) were compared to Bangkok's comfort temperature ranges for different seasons according to ASHRAE's adaptive comfort model. This gave the percentages of the thermal comfort time during the day for each season when the strategy was employed. By comparing these percentages to those found in the reference rooms locating on the same floors under the identical climate, the extension of comfort hours and also the possible energy saving when the strategy was employed could be achieved.

Figure 6-24 shows the comparison of the compensated temperatures ($T_{comp}$) of the south-facing test and reference room on 21st floor to Bangkok's comfort temperature range in different seasons (the calculation results can be found in Table C-17 in Appendix C). However, it should be noted that the $T_{comp}$ and $T_{op}$ of the reference room were identical as the air movement in such room was found too low to produce any cooling effect.

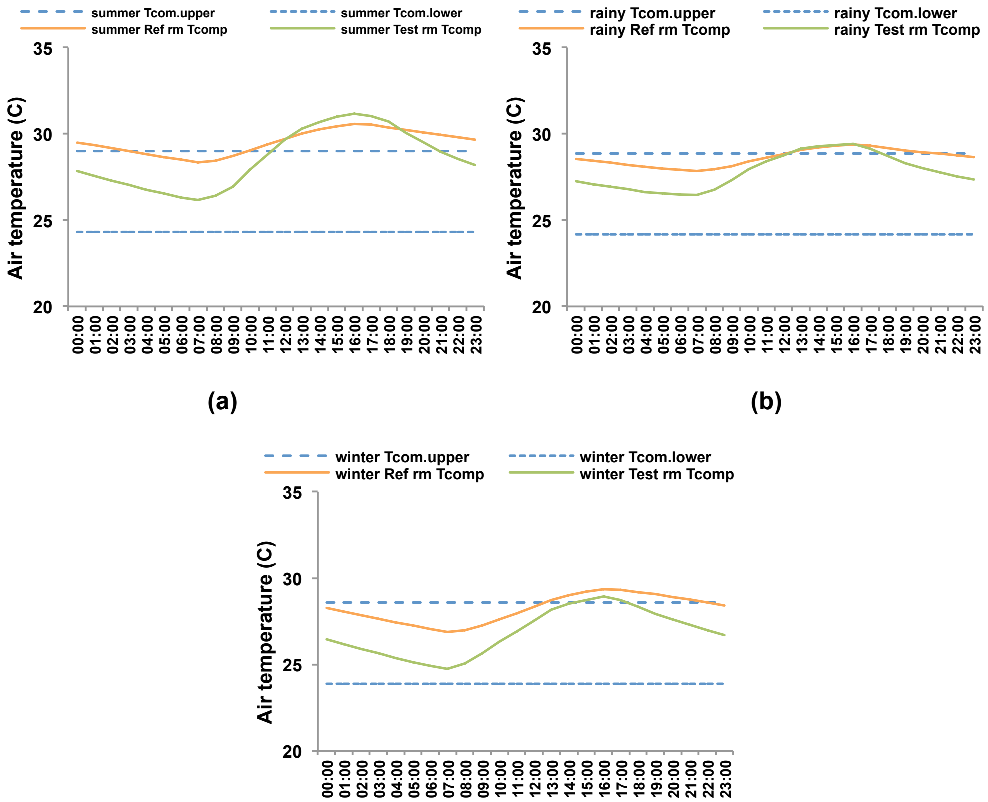

(a) (b)

(c)

**Figure 6-24** Compensated temperatures ($T_{comp}$) in the south-facing reference and test room on floor 21st under Bangkok's typical climatic conditions comparing to Bangkok's comfort temperature range: (a) during summer; (b) during rainy; and (c) during winter.

From the charts in Figure 6-24, the test room's $T_{comp}$ were apparently lower than those of the reference room for almost all the time, particularly during the early morning and late night i.e. between 8PM and 10AM. Moreover, it was interesting that the test room's operative temperatures ($T_{op}$) were found to be even lower than those of the reference room during this period (see Table C-17 in Appendix C). This was due to the high volume of the external air with relatively lower temperature compared to the indoor air entering into the test room. Moreover, an increased air movement in the test room also produced a further cooling effect for compensating the room's temperatures. Differently, during the target period of a day i.e. between 10AM to 8PM, the test room's $T_{comp}$ were found to be relatively closer to that of the reference room. This was particularly the case between 12AM and 6PM during summer months when the test room's $T_{comp}$ were greater than that of the reference room (Figure 6-24a). This was because the large volume of the external air with high temperature penetrated into the test room during this period. This high temperature incoming air was found to increase the room's operative temperature by up to 1.7°C, while the increased air velocity could produce the cooling effect for compensating the room's temperature only for 1.1°C (see also Table C-17 in Appendix C).

However, the $T_{comp}$ in the test room were still found to lie mostly within the comfort temperature ranges. As can be seen in Figure 6-25, the comparison of the south-facing test and reference room during different seasons is demonstrated. In chart (a) the reference room's comfort hour was discovered as 29%, 67% and 63% per day; while that of the test room was found as 63%, 79% and 88% during summer, rainy and winter months, respectively (see Table C-18 in Appendix C). These results indicate the increase in comfort hour percentages per day by 13%-33%. The comfort hour percentages during the target time of the day when the peak electricity demand of Bangkok commonly occurs was also found as 18%-73% when the proposed ventilation shaft was employed (see Table C-19 in Appendix C).

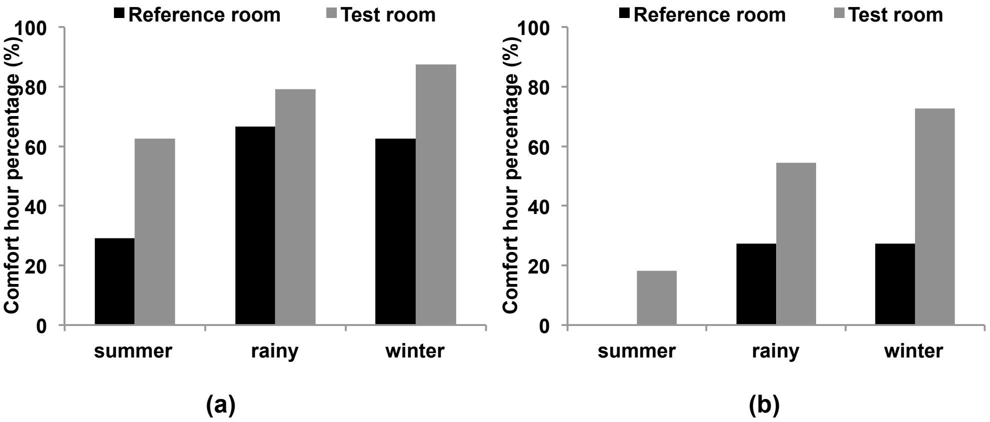

**Figure 6-25** Percentage of thermal comfort hours per day of the south-facing reference and test room on floor 21st: (a) all day period; and (b) target time period i.e. 10AM to 8PM.

Similar findings were also found for the north-facing units case. The compensated temperatures ($T_{comp}$) in the test room on floor 23, calculated based on the room's $V_{in.av}$ of 0.35ms$^{-1}$ and the $dT$ of 0.9K, were found to lie mostly within the comfort temperature range and lower than that in the reference room at all time (see Figure 6-26 and also Table C-20 in Appendix C). This was especially true during the morning and late night i.e. between 8PM and 10AM.

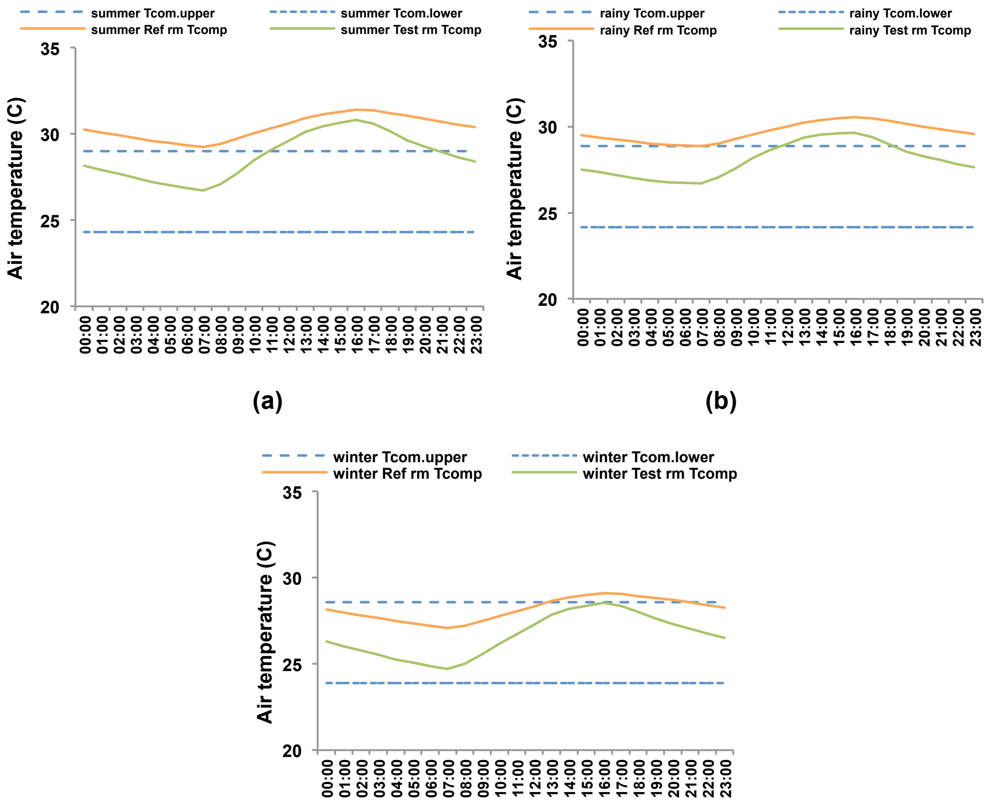

(a)

(b)

(c)

**Figure 6-26** Compensated temperatures ($T_{comp}$) in the north-facing reference and test room on floor 23rd under Bangkok's typical climatic conditions comparing to Bangkok's comfort temperature range: (a) during summer; (b) during rainy; and (c) during winter.

The comfort hours in the room were found extend when the ventilation shaft was employed. As can be seen in Figure 6-27a, the comfort hours per day increased from 0%, 8% and 71% to 58%, 71% and 100% during summer, rainy and winter months, respectively (see Table C-21 in Appendix C). This was especially true during winter months when 100% comfort was reached in the test room. According to this finding, employing the ventilation shaft was therefore able to extend the occupants' comfort time per day for up to 29% to 79% in different seasons. In Figure 6-27b the increase in comfort hours during the target period of the day were also apparent as it was extended by 9%, 36% and 64% during summer, rainy and winter months, respectively (see Table C-22 in Appendix C). According to these results the ventilation shaft strategy was obviously found to be an effective passive design strategy to increase a single-sided residential unit's average air velocity and to extend its occupants' thermal comfort time.

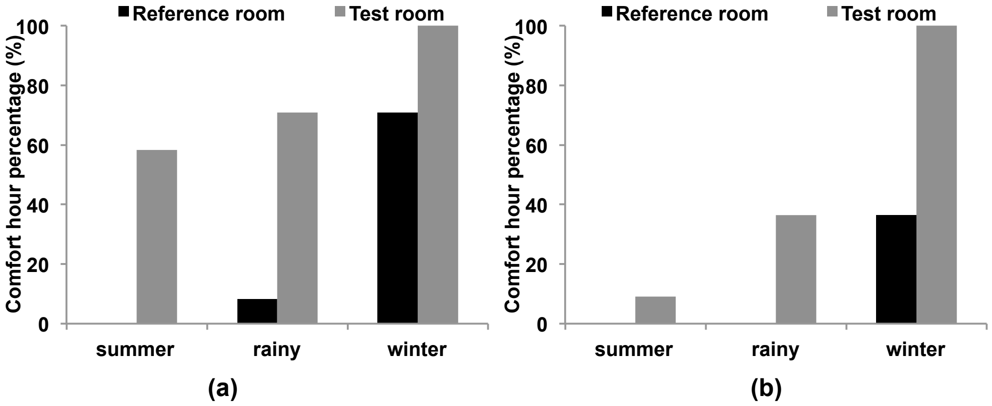

**Figure 6-27** Percentage of thermal comfort hours per day of the north-facing reference and test room on floor23$^{rd}$: (a) all day period; and (b) target time period.

After the extension of thermal comfort hour percentage in a single-sided unit was attained, the energy saving for the whole studied building that could be achieved was estimated by looking at the comfort hours extended in the representative units and the assumption made before i.e. the a/c systems were turned off when the occupants feel thermally comfortable. For a typical 5kW split type, wall-mounted air conditioners typically used in such apartments in Bangkok the possible electricity saving per annum for a south-facing and a north-facing unit was found as 10.2MW and 21.6MW, respectively (see Table C-23 in Appendix C). Then, this possible energy saving per apartment was multiplied by the number of apartments in the studied building i.e. 180 units on the south and 160 units on the north, and gave the whole building's estimated electricity saving per annum as up to approximately 5291MW. Among these, the electricity saving of approximately 22.3MW per annum was found during the target time (see Table C-25 in Appendix C). These numbers significantly demonstrate that the proposed ventilation shaft effectively increase the occupants' thermal comfort time and reduce the energy consumption in high-rise residential buildings in Thailand.

Also the electricity saving possibly achieved in case of the whole units employing electric ceiling fans, rather than a/c was estimated based on typical electric ceiling fans employed in Thailand for such a unit size (65Wh). By using the same estimation process as above, the maximum electricity saving for a south- and a north-facing unit was found as 132.5 kW and 280.8 kW per annum, respectively (Table C-24 in Appendix C) and overall electricity saving for the whole studied building could be up to 29MW per annum (Table C-26 in Appendix C).

In conclusion, the main results for the study have been reported in this chapter. For the first stage the potential of the proposed strategy was investigated and it was found to effectively increase the representative room's air velocity and to extend the occupants' thermal comfort hour under the particular climate. Then the effects of various climatic elements on the strategy's performance were studied in the second stage. External wind speed and direction (relative to the room's main window) were revealed to be the most influential elements, while the relative humidity and external dry-bulb temperature had no significant effect on the strategy's performance. It was also found that the increased air velocity has a strong relationship to the room's operative temperature. This was because of the increase in hot external air entering into the room. On the third stage the parametric study was conducted for investigating the influence of different sizes and designs of the strategy's main elements on its performance, and the strategy's optimal design was revealed. The ventilation shaft with its optimal design was then attached to the test rooms from floor 6th to floor 25th in stage four to assess the strategy's performance under a more practical situation. The results showed that the preferred air velocity for producing physiological cooling effect was still attained even when the vertical shaft was attached to numbers of room. This indicates the strategy's high potential for increasing room's air movement. For the final stage, the percentages of thermal comfort hour in the test room and the reference room were calculated according to the rooms' operative temperatures compensated by their average air velocity. The ventilation shaft strategy was found to extend the occupants' comfort hours for up to 33% per day for the south-facing unit and 64% per day for the north-facing unit, depending on seasons. Finally the studied building's possible electricity saving was found up to 5291 MW per annum when the ventilation shaft was employed. However, it should be noted that this estimation was calculated based on the simulated results of air velocity under the particular conditions and the assumption made for this study i.e. the a/c systems were only used when the room's thermal condition was outside Bangkok's monthly comfort temperature ranges.

In the next chapter the main results of the study will be discussed and compared to existing theories and studies.  Also, the conclusion and the implications of the study results will also be given.

# Chapter Seven

## Discussion and Conclusions

### 7.1 Introduction

In the previous chapter the results of the study were presented accordingly to the study procedure established in Chapter Five. In this chapter the results found previously are discussed and compared to the relevant theory and previous research in the field as to give the idea of how they are related to the current knowledge framework. The limitations of this study and suggestions for future work are also given before the main conclusion of this study is presented at the final part.

### 7.2 Discussion

In the previous chapter the proposed comfort ventilation strategy called '*ventilation shaft*' was found to successfully induce a higher air velocity and thus improve the thermal comfort conditions of a typical residential unit with one external window in Bangkok. By employing the proposed strategy the percentage of the occupants' comfort hours was found to increase by up to 33% and 64% per day, for the south-facing and north-facing unit respectively. As a result the energy consumption due to a/c systems could be significantly reduced by as much as 5291MW electricity saving per annum for a typical apartment building in Bangkok. According to these results the study's main hypothesis i.e. the ventilation shaft is able to effectively increase a single-sided ventilated room's average air velocity to achieve the required velocity and thus thermal comfort for the residences was assessed and accepted. Also, the main aim for the study i.e. to develop a ventilation strategy that is able to reduce high electricity demand in a residential unit in Bangkok due to cooling systems was successfully achieved.

In addition, the study's main objectives are also accomplished. The effects of different climatic elements on the strategy's performance were investigated and the most influential factors were found as the external wind conditions involving wind speeds and wind directions according to the room's main window. On the other hand, the relative humidity and external dry-bulb temperature were found to have no significant effect on the strategy's effectiveness on inducing the room's air velocity. The strategy's optimal design to produce the highest average air velocity and thus thermal comfort for the occupants during the target time of the day i.e. 10AM to 8PM was also revealed as the following: i) the vertical shaft should be as large as possible and its exhaust opening should be at least 1m above the building roof; and ii) the inlet and outlet openings size should be 3 x 0.6m$^2$ ($W \times L$) and placed at the occupied level.

Moreover there are some significant issues that are exposed in the study:

### *7.2.1 Suitable ventilation strategy for hot-humid regions*

Firstly, the investigations in the study demonstrate that wind-induced ventilation strategies are much more effective to induce indoor air velocity and thus improve the occupants' thermal comfort in tropical regions compared to stack-induced strategies, which agrees with the findings suggested in other studies (Givoni, 1976, Awbi, 2003, Ghiaus and Allard, 2005).

Based on the principal of physiological cooling effect due to elevated air movement reviewed in Chapter Two, an increase in air velocity directly improve the occupants' thermal comfort in hot-humid climates by i) increasing convective heat transfer and thus improving thermal sensation (Fountain and Arens, 1993); and ii) increasing the efficiency of sweat evaporation from the skin, thus minimizing discomfort due to skin wetness under high humidity situations (Givoni, 1981, Allard, 1998, Szokolay, 2008, Givoni, 1994, Givoni, 1998). However, wind-dominated ventilation is required to achieve such a cooling effect i.e. at least 0.2ms$^{-1}$ (Szokolay, 2000, Szokolay, 2008) to 0.29ms$^{-1}$ (Bansal et al., 1994a). Based on high wind pressure difference between the inlet and outlet openings, wind-dominated ventilation strategies such as cross ventilation (Givoni, 1976, Awbi, 2003, Ghiaus and Allard, 2005), wing-walls (Givoni, 1994) (Givoni, 1976, Givoni, 1991, Givoni, 1998) as well as the proposed ventilation shaft are much more powerful in creating room airflows with high average velocity for up to 35%-65% of the external wind speed. This is significant in terms of natural ventilation, particularly when comparing to stack-dominated ventilation that is driven mainly by the temperature difference between the inlet and outlet openings and can produce an airflow with very small velocity i.e. less than 0.05ms$^{-1}$ to 0.2ms$^{-1}$ due to its relatively small inertia (Khedari et al., 2000a).

This favorable wind-dominated ventilation is also confirmed in this study as the test room's average air velocity was found to be as high as 17%-38% of the reference wind speed, while that of the reference room velocity was found very small i.e. 0.05ms$^{-1}$ even under the reference wind speed was at 4ms$^{-1}$ (see the results of study stage four in Appendix C). However, it should be noted that although the characteristic of the proposed ventilation shaft i.e. a vertical shaft with an exhaust at its top is similar to a traditional wind-tower, they are operated with a slightly different principle. While the former is mainly stack-dominated as the air is driven mainly by the temperature difference between the shaft and the activity area below, the latter is wind-dominated strategy as the air is mainly driven by the pressure difference between the openings locating on the windward and leeward sides.

On the other hand, comfort ventilation may produce thermal discomfort conditions in hot-humid regions, particularly during daytime as it is suggested to be applicable in the regions with the outdoor maximum temperature less than 28°C to 32°C and diurnal temperature range less than 10°C, depending on comfort expectation of the occupants (Givoni, 1994, Givoni, 1998). This is because there could be a greater volume of incoming air with high temperature entering the indoor space so that the room's air temperature as well as its internal surfaces may be warmed, particularly a south-facing room without proper shading as high solar radiation could directly penetrate into it. In this study, similar results were found as the test room's temperature increased with the room's average air velocity (Figure 6-8c and Figure 6-8d) and reached its maximum between 3PM and 4PM, particularly for a south-facing room (comparing Figure 6-24 and Figure 6-26). For such cases careful shading is recommended to reduce the risk of excessive radiation heat gain accessing the room during daytime (Givoni, 1994, Givoni, 1998). Even so, the thermal conditions of the test room were still found to be favourable to the reference room with respect to the percentage of thermal comfort hours as the greater percentage was found in the test room for all three seasons (Figure 6-25 and Figure 6-27). According to these a wind-dominated, rather than stack-dominated strategies, are more effective and recommended for improving the occupants' thermal comfort in hot-humid countries, including Thailand, even during the daytime.

### *7.2.2 Natural ventilation behaviours*

Secondly, most of the natural ventilation behaviours found in this study are consistent with current theories and studies on natural ventilation. This involves the most influential climatic factors and the effect of building design on its performance. The most significant climatic elements that determine the natural ventilation performance include external wind speed and wind direction (with respect to the room's main window), particularly that for a wind-dominated case. As found in previous guidelines a room's average air velocity increases with reference wind speed (Givoni, 1998, Szokolay, 2008). This is confirmed by the results in study stage two when there was only one test room attached to the optimal sized vertical shaft i.e. the average air velocity in the test room increased from 0.22ms$^{-1}$ to 1.44ms$^{-1}$ when the external wind speed increased from 0ms$^{-1}$ and 1ms$^{-1}$ to 4ms$^{-1}$. Similarly, the maximum air velocity in the test room was found to increase from 0.50ms$^{-1}$ to 2.59ms$^{-1}$ when the external wind speed rose from 0ms$^{-1}$ to 4ms$^{-1}$.

In terms of wind direction, there is no exact wind incident angle suggested for achieving best results of room air velocity. However, the inlet and outlet openings are recommended to be located in the windward (high pressure zone) and leeward (high suction zone) side of the building (Givoni, 1998, Givoni, 1994, Szokolay, 2008, Olgyay, 1992, Allard, 1998, Aynsley, 2007). As a result the wind incident angle or the wind direction regarding to a room's main window i.e. inlet opening should be between 0° i.e. wind direction is perpendicular to the room's main window and 45° to ensure a good room ventilation as the inlet opening would be in a high pressure area while the outlet opening would be in the high suction area. Likewise, the highest room's average air velocity was found in this study when the wind incident angle was at 0° as the inlet opening was in the high pressure area, while the room's air velocity became weaker when the wind direction moved away from 0° and the worst cases were found when the wind incident angle was between 90° and 180° i.e. the average air velocity in the room was found as 1.44ms$^{-1}$ under the wind incident angle at 0° and 0.34ms$^{-1}$ under 90° and 180° based on the external wind speed of 4ms$^{-1}$ (see Table C-3 in Appendix C).

For a building design it is recommended from extensive studies that the size and placement of a room's openings, particularly the inlet opening, are the most crucial parameters to determine the room's natural ventilation (Givoni, 1998, Bansal et al., 1994a, Szokolay, 2008, Olgyay, 1992, Allard, 1998, Givoni, 1994, Aynsley, 2007). In terms of openings' size, there is a slight difference in recommendations as some suggested a smaller inlet to outlet openings, while others suggested equal sized inlet and outlet openings. For the former case, the smaller sized inlet opening was suggested to produce a venturi effect and thus maximize air velocity in the room (Szokolay, 2008, Olgyay, 1992). However, it was found here that this technique could provide an extremely high velocity but only for a small area in the room, specifically the area in front of the inlet opening as the external air enters into the room with a jet-like character, while the rest of the room area had a much weaker velocity (see Figure 6-14a, b, c and d). On the other hand the latter technique suggested i.e. the equal sized inlet and outlet openings (Allard, 1998) provided a more even airflow throughout the room with acceptable air velocity i.e. the average air velocity at the occupied area was found between 48%-51% of the reference wind speed when the inlet and outlet openings' width both reached 75% and 100% of the wall's width comparing to the average air velocity of less than 35% of the reference wind speed when the inlet opening's width was about 25% of the wall's width in this study (see Figure 6-12 and Table C-11 in Appendix C). Large and equal sized inlet and outlet openings to cover the room's main occupied area are therefore recommended for ensuring good air movement and the occupants' thermal comfort.

However, the smaller length of both inlet and outlet openings was preferable for providing airflow with high velocity at a particular level i.e. 1m above the floor in this study as an opening with shorter length would produce a more concentrated airflow pattern. As found in study stage three, the average air velocity at the occupied level reached its maximum i.e. 2.35ms$^{-1}$ when the inlet opening's length was at the shortest i.e. 0.6m, while the average air velocity became weaker when the inlet opening's length increased i.e. 1.81ms$^{-1}$ at 1.5m (see Figure 6-15, Figure 6-16 and Table C-12 in Appendix C). In addition, inlet opening's smaller length also give further advantage to the occupants in terms of thermal comfort as smaller solar radiation would enter into the room so that the lower room' s operative temperature can be expected (Figure 6-17).

In additional to its size, the vertical location of a room's openings, particularly the inlet, was found in this study as the crucial parameter for determining indoor airflow pattern as suggested in extensive studies (Givoni, 1998, Bansal et al., 1994a, Olgyay, 1992, Allard, 1998, Aynsley, 2007). According to the suggestions and also the results of this study, the inlet opening should be placed at the main occupied level to ensure a good cooling effect and thus the occupants' thermal comfort as the average air velocity was found as high as 61% of the reference wind speed when both the inlet and outlet openings were placed at the occupied level. On the other hand the weakest average air velocity i.e. 9% of the reference wind speed was found when both openings were at the high position closing to the ceiling (see Figure 6-18, Figure 6-19 and Table C-13 in Appendix C).

In conclusion, the passive ventilation design guidelines suggested for a building in hot-humid regions by many researchers are confirmed by the results found in this study. These involve: i) the location of room's main window regarding to the prevailing wind direction; ii) the shape and size of inlet and outlet openings; and iii) the vertical placement of the openings regarding to the main activity level.

### *7.2.3 CFD modeling software as a tool for evaluating natural ventilation strategies*

Finally, CFD modeling software is found in the study as a useful tool for investigating natural ventilation in a building. As natural ventilation behaviours are complex and variable due to many factors, it is challenging to investigate its performance. This is especially true when a study is focusing on a new natural ventilation strategy that has never been used in practice. To achieve this study's aim the Computational Fluid dynamics (CFD) code from DesignBuilder software v.2.3.5.034 (DesignBuilder, 2006b) was employed for predicting the thermal conditions especially for room's temperature, air velocity and airflow pattern in the chosen room under numbers of different situations.

Although there are a number of methods and tools for studying natural ventilation's performance, CFD model is advantageous as it offers rich detail of indoor airflow driven both by stack and wind effect with a smaller cost and time. In addition, it is an effective tool for a parametric study as it provides flexibility for different changes in design and condition. In this study the CFD code with RANS's standard *k- ε* turbulence model was found to provide an accurate prediction in indoor thermal condition, as the results from this study are consistent with natural ventilation behaviours found in previous studies that employed other methods, especially a full-scale experiment, which is accepted to provide the most realistic information on natural ventilation. This consistency can be found in the validation of DesignBuilder section in Chapter Four. The simulated results of the chosen room's average air temperature and air velocity were found to be very close to the measured data, both in cases of wind-dominated ventilation i.e. a room with cross ventilation in an existing two-storey house and stack-dominated ventilation i.e. the units in an existing apartment building. For both cases, the deviation between the measured and predicted data was mostly within +/-5%. The predicted airflow pattern in the test room i.e. wind-dominated ventilation under different opening vertical placements (see Figure 6-19) was also found to be consistent with the previous studies conducted by Evans (1980), cited in Bansal et al (1994) and Olgyay (1992) that employed small-scale methods.

These results indicate that CFD code can be a useful tool for investigating natural ventilation in a building, especially during the primary stage of design and development as it can provide an acceptable accuracy in prediction of indoor thermal condition with small cost and time. It is also favorable for a parametric study when there are numbers of changes and variables concerned. The results from this study also show that RANS's standard *k- ε* turbulence model can provide a reasonably accurate prediction in thermal parameters, particularly when only the overall performance of indoor natural ventilation is considered. For such cases LES turbulence model that is suggested as providing an extreme precision (Caciolo et al., 2012, Evola and Popov, 2006, Nielsen, 2007, Awbi, 2003), but much greater computer time, is not required.

## 7.3 Implications, limitations and suggestions for future work

On a broader perspective this thesis has provided a greater insight into the natural ventilation behavior in a normal sized room with a number of different changes in driven effect (stack-dominated and wind-dominated ventilation), climatic conditions and building design. It also introduced an alternative comfort ventilation strategy specifically designed to promote natural ventilation as well as to reduce the high dependency on a/c systems for a typical apartment building in tropical countries including Thailand. This would be a good start to broaden the perspective of the research in Thailand to comfort ventilation and physiological cooling effect due to the elevated air movement. In addition, this study would lead the designing of apartment building in Thailand to the next step with greater consideration on the occupants' thermal comfort and building energy efficiency. The results of this thesis also make a novel contribution to the knowledge of natural ventilation in buildings under tropical climates as follows:

i) Comfort ventilation is confirmed in this study as the most crucial parameter to improve human thermal comfort in tropical regions and only wind-dominated ventilation strategies can provide such required air velocity. Stack-dominated strategies can only small air velocities to improve indoor air conditions, which is insufficient for produce any physiological cooling effect or thermal comfort.

ii) The study has introduced a new and effective comfort ventilation strategy that is designed specifically for an apartment building.

iii) The opening design is confirmed in this study to have significant effects on the indoor airflow. The openings with large sized and positioned to cover the main occupied area at the occupied level are crucial for ensuring the occupants' most comfort in tropical countries.

However, there are some limitations in the study that should be mentioned.

i) Due to the limitation of measurement devices available, only one hand-held anemometer was used for measuring indoor air velocity in the two-storey house measurement (Chapter Two). This may cause a disturbance of the recorded air velocities as a person who held the anemometer might block or interrupt the incoming air. Also, the recorded air velocity at one location may be influenced by different external wind conditions to that at another location.

ii) It should be noted that the results in this study are based on the simulated data predicted by the CFD package in the DesignBuilder modeling software together with particular assumptions (see Chapter Four for the software's principles and Chapter Five for assumptions made for this study). It should be also noted that the characteristics of the unit's main window in the simulation process were treated as simple as possible i.e. a hole in the wall with no pane or screen to avoid their possible effects on the incoming air.

iii) It should be borne in mind that the energy savings due to employing the proposed ventilation shaft strategy were simply estimated by calculating the electricity consumption of a typical air conditioning system or electric ceiling fans employed in Thailand to give an indication of how much electricity may be saved (see Tables C-23 to C-26). A very detailed thermal analysis of electricity usage and potential savings would represent a significant task, given the very large number of variables involved, and was considered to be beyond the scope of this study.

iv) Finally, it should be noted that this study is only the first step of a ventilation shaft strategy study and the aim here is scoped only at initial assessment of its potential to induce air velocity in a typical apartment unit with one external opening. However, due to the limit of time, there are still other concerns those should be focused on in the future so that the strategy can be applied more practically in real situations. For example, i) the concern of high room air temperatures during daytime due to the incoming air with a high temperature and ii) the noise disturbance that may occur when a vertical shaft is employed for many residential units. For the former concern, a future study should be conducted to investigate different schedule of ventilation shaft operation during the day i.e. daytime, nighttime and all-day operation. The smaller room's air temperature may be achieved if the strategy was closed during noon and 4PM when the dry-bulb temperature reaches its maximum in Bangkok (see Chapter One). Also, building design with proper shading to protect the indoor environment from direct solar radiation may be beneficial for this concern. For the noise issue, different absorbing materials and detail designs of a vertical shaft should be studied in order to reduce the risk of noise transmission.

## 7.4 Conclusions

Thailand is a hot-humid country that experiences uniformly high air temperature and relative humidity, yet low wind speeds. For approximately 51% of the time in the year air temperatures are considered to lie mostly outside the thermal comfort range according to ASHRAE's adaptive comfort model (ASHRAE, 2013). During these periods, air conditioning (a/c) systems are widely used to provide thermal comfort. However, a/c systems are energy intensive. One key building that is responsible for Bangkok's high electricity consumption is high-rise residential buildings, which were recently introduced and which have become popular in Bangkok. Due to its characteristics, particularly that they are single-sided ventilated, such buildings are far from successful in adopting natural ventilation to provide indoor thermal comfort conditions. As a result, almost all of the residential units in such buildings are dependent on a/c systems to provide the occupants thermal comfort. To the author's knowledge, there is no research on passive ventilation strategies designed specifically for improving such buildings' thermal conditions and thus reducing their high energy intensive due to cooling systems, particularly in Thailand.

In this study a comfort ventilation strategy called '*ventilation shaft*' is proposed that is aiming at improving the thermal comfort of the occupants and reducing the a/c dependency in high-rise residential buildings in Bangkok. The strategy is based on the particular characteristics of typical apartment buildings in Bangkok and the principle of high wind pressure differences between the inlet and outlet openings. According to the results the ventilation shaft strategy is found to be an effective strategy to induce the air velocity and create cross ventilation in a residential unit with only one window even when there was an absent of wind i.e. external wind speed of $0ms^{-1}$. By employing the ventilation shaft strategy the occupants' comfort hours is increased by 33% to 64% per day, depending on the location of the residential unit and seasons (see Chapter Six). This indicates, for one building based on a typical electric ceiling fan and split type air conditioner, a significant energy saving of up to 68.8MW and 5,291MW per annum respectively. The proposed ventilation shaft is, therefore, a potentially simple but effective comfort ventilation strategy for enhancing natural ventilation and reducing the a/c systems dependency in typical high-rise apartment buildings in Bangkok and other tropical countries.

# Appendix A

## Bangkok weather data and Wind pressure coefficient (*Cp*)

**Table A- 1** Bangkok's average hourly weather data in different months obtained from MET between 1999 and 2008 (MET, 2010).

| Weather variables | Jan | Feb | Mar | Apr | May | Jun | Jul | Aug | Sep | Oct | Nov | Dec | Annually av. |
|---|---|---|---|---|---|---|---|---|---|---|---|---|---|
| Average minimum $T_{out}$ (˚C) | 23.9 | 24.6 | 25.4 | 26.5 | 26.0 | 26.1 | 26.1 | 25.6 | 25.4 | 25.2 | 24.8 | 22.9 | **25** |
| Average mean $T_{out}$ (˚C) | 27.8 | 28.6 | 29.8 | 30.8 | 29.8 | 29.6 | 29.4 | 29.1 | 28.7 | 28.7 | 28.5 | 27.4 | **29** |
| Average maximum $T_{out}$ (˚C) | 30.4 | 30.8 | 32.0 | 32.9 | 32.3 | 31.8 | 31.6 | 31.4 | 31.1 | 31.0 | 31.1 | 30.4 | **31** |
| Average maximum $T_{out}$ (˚C) during 10AM to 8:00PM | 33.0 | 33.1 | 34.4 | 35.1 | 34.3 | 33.5 | 33.4 | 33.3 | 33.1 | 33.0 | 33.2 | 32.7 | **33** |
| Average minimum RH (%) | 49 | 51 | 52 | 60 | 61 | 61 | 60 | 61 | 62 | 59 | 50 | 48 | **56** |
| Average mean RH (%) | 67 | 71 | 71 | 72 | 75 | 75 | 74 | 74 | 77 | 76 | 66 | 62 | **72** |
| Average maximum RH (%) | 85 | 87 | 87 | 88 | 94 | 93 | 92 | 93 | 94 | 94 | 87 | 79 | **89** |
| Average minimum $V_{out}$ (ms$^{-1}$) | 0 | 0 | 0 | 0 | 0 | 0 | 0 | 0 | 0 | 0 | 0 | 0 | **0** |
| Average mean $V_{out}$ (ms$^{-1}$) | 0.9 | 1.2 | 1.4 | 1.4 | 1.3 | 1.3 | 1.3 | 1.3 | 1.0 | 0.8 | 0.8 | 0.8 | **1** |
| Average maximum $V_{out}$ (ms$^{-1}$) | 3.4 | 3.4 | 3.7 | 4.1 | 4.3 | 3.9 | 3.9 | 4.1 | 3.5 | 3.3 | 3.1 | 3.0 | **4** |

**Table A- 2** Bangkok's monthly comfort temperatures according to ASHRAE's adaptive model (55-2004).

| Bangkok's comfort temperature | Jan | Feb | Mar | Apr | May | Jun | Jul | Aug | Sep | Oct | Nov | Dec |
|---|---|---|---|---|---|---|---|---|---|---|---|---|
| Average mean $T_{out}$ (˚C) | 27.8 | 28.6 | 29.8 | 30.8 | 29.8 | 29.6 | 29.4 | 29.1 | 28.7 | 28.7 | 28.5 | 27.4 |
| Comfort tem. ($T_{com}$) | 26.0 | 26.2 | 26.5 | 26.8 | 26.5 | 26.4 | 26.4 | 26.3 | 26.2 | 26.2 | 26.2 | 25.9 |
| Upper comfort tem. ($T_{com.upper}$) | 28.5 | 28.7 | 29.0 | 29.3 | 29.0 | 28.9 | 28.9 | 28.8 | 28.7 | 28.7 | 28.7 | 28.4 |
| Lower comfort tem. ($T_{com.lower}$) | 23.8 | 24.0 | 24.3 | 24.6 | 24.3 | 24.2 | 24.2 | 24.1 | 24.0 | 24.0 | 24.0 | 23.7 |
| Compensated temp. ($T_{comp}$) due to increased air movement of 0.5ms$^{-1}$ | 29.8 | 30.0 | 30.3 | 30.6 | 30.3 | 30.3 | 30.2 | 30.1 | 30.0 | 30.0 | 30.0 | 29.7 |

**Table A- 3** The software's default wind pressure coefficient ($Cp$) values for a building with no more than three stories (DesignBuilder, 2006a).

| **Wind incident angles to the building surface** | **$Cp$ value** |
|---|---|
| 0° (normal to surface) | 0.40 |
| 45° | 0.10 |
| 90° | -0.30 |
| 135° | -0.35 |
| 180° | -0.20 |
| 225° | -0.35 |
| 270° | -0.30 |
| 315° | 0.10 |

**Table A- 4** Wind pressure coefficient ($Cp$) values for the floor 13rd,16th and 23rd of an existing 26-storey building (Lumpini Place Pinkloa 2*) for the software's validation study predicted by *CpGenerator*.

| **Floor no.** | **Height above** | **Incident wind angle (degree) to the room opening** | | | | | | | |
|---|---|---|---|---|---|---|---|---|---|
| | **ground (m)** | **0°** | **45°** | **90°** | **135°** | **180°** | **225°** | **270°** | **315°** |
| 13 | 34.6 | 0.864 | 1.311 | 0.434 | -0.876 | -0.619 | -0.58 | -0.55 | -0.152 |

** Lumpini Place Pinkloa 2 residential building with 26-storey (72.8m height). The input information for CpGenerator includes: the building geometry (H:W:L) of 72:36:72; the building orientation of 330degree; its location as normal suburban area with the surrounding of one- to four-storey buildings at a distance of 0.5 x the building height (3.0).*

**Table A- 5** Wind pressure coefficient ($Cp$) values for the hypothetical building* (26-storey) predicted by *CpGenerator.*

| **Floor no.** | **Height above** | **Incident wind angle (degree) to the room opening** | | | | | | | | **Roof** |
|---|---|---|---|---|---|---|---|---|---|---|
| | **ground (m)** | **0°** | **45°** | **90°** | **135°** | **180°** | **225°** | **270°** | **315°** | |
| 25 | 73.4 | 1.226 | 0.647 | -0.611 | -0.531 | -0.634 | -0.606 | -0.762 | 0.802 | -1.709 |
| 24 | 70.4 | 1.253 | 0.664 | -0.621 | -0.540 | -0.642 | -0.620 | -0.782 | 0.835 | |
| 23 | 67.4 | 1.278 | 0.680 | -0.631 | -0.548 | -0.648 | -0.632 | -0.801 | 0.867 | |
| 22 | 64.4 | 1.300 | 0.694 | -0.639 | -0.555 | -0.654 | -0.644 | -0.818 | 0.897 | |
| 21 | 61.4 | 1.318 | 0.707 | -0.646 | -0.562 | -0.659 | -0.653 | -0.832 | 0.923 | |
| 20 | 58.4 | 1.333 | 0.716 | -0.651 | -0.566 | -0.663 | -0.661 | -0.844 | 0.946 | |
| 19 | 55.4 | 1.334 | 0.723 | -0.655 | -0.570 | -0.666 | -0.667 | -0.853 | 0.963 | |
| 18 | 52.4 | 1.350 | 0.727 | -0.657 | -0.572 | -0.668 | -0.670 | -0.858 | 0.973 | |
| 17 | 49.4 | 1.351 | 0.728 | -0.658 | -0.584 | -0.668 | -0.671 | -0.859 | 0.975 | |
| 16 | 46.4 | 1.348 | 0.726 | -0.657 | -0.571 | -0.667 | -0.669 | -0.856 | -0.970 | |
| 15 | 43.4 | 1.340 | 0.721 | -0.654 | -0.569 | -0.665 | -0.665 | -0.850 | 0.956 | |
| 14 | 40.4 | 1.328 | 0.713 | -0.649 | -0.565 | -0.662 | -0.658 | -0.840 | 0.937 | |
| 13 | 37.4 | 1.311 | 0.702 | -0.643 | -0.559 | -0.658 | -0.650 | -0.827 | 0.913 | |
| 12 | 34.4 | 1.291 | 0.689 | -0.636 | -0.553 | -0.652 | -0.639 | -0.811 | 0.885 | |
| 11 | 31.4 | 1.268 | 0.674 | -0.627 | -0.545 | -0.646 | -0.627 | -0.794 | 0.854 | |
| 10 | 28.4 | 1.242 | 0.658 | -0.617 | -0.536 | -0.639 | -0.614 | -0.774 | 0.822 | |
| 9 | 25.4 | 1.215 | 0.640 | -0.607 | -0.527 | -0.631 | -0.600 | -0.753 | 0.789 | |
| 8 | 22.4 | 1.186 | 0.622 | -0.595 | -0.517 | -0.622 | -0.585 | -0.732 | 0.756 | |
| 7 | 19.4 | 1.156 | 0.604 | -0.583 | -0.506 | -0.613 | -0.570 | -0.710 | 0.723 | |
| 6 | 16.4 | 1.125 | 0.585 | -0.571 | -0.495 | -0.603 | -0.554 | -0.688 | 0.692 | |

** The height for each floor is calculated according to each floor's middle level based on floor-to-floor height of 3m.*

# Appendix B

## Validating DesignBuilder's CFD

**Table B - 1** Measured and predicted indoor and outdoor air temperature from the living room of the two-storey house, Nakhon Pathom, Thailand.

| Time | Measured Temperature (˚C) | | Simulated Temperature (˚C) | |
|---|---|---|---|---|
| | Tin (mea) | Tout (Av.May) | Tin (sim) | Tout (sim) |
| 00:00 | 26.9 | 26.5 | 24.5 | 24.5 |
| 02:00 | 26.2 | 26.2 | 24.7 | 24.4 |
| 04:00 | 25.9 | 25.7 | 25.2 | 24.6 |
| 06:00 | 25.1 | 25.2 | 25.6 | 25.1 |
| 08:00 | 27.3 | 28.4 | 27.5 | 25.8 |
| 10:00 | 30.2 | 30.2 | 30.5 | 28.9 |
| 12:00 | 31.3 | 31.2 | 31.8 | 31.1 |
| 14:00 | 32.9 | 32.3 | 32.5 | 32.3 |
| 16:00 | 34.1 | 33.2 | 32.6 | 32.5 |
| 18:00 | 30.8 | 31.2 | 28.1 | 30.3 |
| 20:00 | 29.4 | 29.5 | 27.6 | 27.8 |
| 22:00 | 28.9 | 28.7 | 27.1 | 27.3 |
| **Average** | **29.1** | **29.0** | **28.1** | **27.9** |

**Table B - 2** Average measured and predicted indoor and outdoor air velocity from at nine measuring points across the living room of the two-storey house.

| Point | Average Measured Velocity (m/s) | Average Simulated Velocity (m/s) |
|---|---|---|
| 1 | 0.27 | 0.28 |
| 2 | 0.49 | 0.3 |
| 3 | 0.47 | 0.3 |
| 4 | 0.28 | 0.26 |
| 5 | 0.42 | 0.29 |
| 6 | 0.33 | 0.27 |
| 7 | 0.17 | 0.24 |
| 8 | 0.32 | 0.28 |
| 9 | 0.27 | 0.26 |
| **Average** | **0.34** | **0.28** |

**Table B - 3** Measured and predicted indoor and outdoor air temperature from the laundry room of the apartment room on the floor13$^{rd}$, Lumpini Place Pinkloa 2, Bangkok.

| Time | Measured Temperature (˚C) | | Simulated Temperature (˚C) | |
|---|---|---|---|---|
| | Tin (mea) | Tout (Av.May) | Tin (sim) | Tout (sim) |
| 00:00 | 32.1 | 28.4 | 32.0 | 29.9 |
| 01:00 | 31.5 | 28.3 | 31.5 | 29.1 |
| 02:00 | 31.3 | 28.1 | 31.2 | 28.4 |
| 03:00 | 30.7 | 27.8 | 30.9 | 28.2 |
| 04:00 | 30.7 | 27.6 | 30.7 | 28.0 |
| 05:00 | 30.5 | 27.4 | 30.6 | 27.8 |
| 06:00 | 30.6 | 27.2 | 30.6 | 27.9 |
| 07:00 | 32.0 | 27.8 | 30.7 | 28.1 |
| 08:00 | 33.3 | 29.0 | 31.4 | 28.2 |
| 09:00 | 34.0 | 30.4 | 32.2 | 29.3 |
| 10:00 | 35.0 | 31.4 | 33.0 | 30.4 |
| 11:00 | 35.9 | 32.1 | 33.9 | 31.5 |
| 12:00 | 36.2 | 32.5 | 34.8 | 32.8 |
| 13:00 | 35.0 | 32.6 | 35.4 | 34.0 |
| 14:00 | 35.2 | 32.7 | 36.1 | 35.3 |
| 15:00 | 34.7 | 32.7 | 36.7 | 36.4 |
| 16:00 | 34.2 | 32.5 | 37.4 | 37.4 |
| 17:00 | 33.8 | 31.7 | 37.0 | 38.5 |
| 18:00 | 33.5 | 30.6 | 36.2 | 36.9 |
| 19:00 | 32.7 | 29.6 | 35.3 | 35.4 |
| 20:00 | 32.4 | 29.2 | 34.5 | 33.8 |
| 21:00 | 32.3 | 28.9 | 33.6 | 32.3 |
| 22:00 | 32.3 | 28.8 | 32.7 | 30.7 |
| 23:00 | 32.1 | 28.6 | 32.3 | 29.2 |

**Table B - 4** Measured and predicted indoor and outdoor air velocity from the laundry room of the apartment room on the floor13rd, Lumpini Place Pinkloa 2, Bangkok.

| Time | Measured Velocity (m/s) | | Simulated Velocity (m/s) |
|---|---|---|---|
| | Vout (Av.May) | Vin (mea) | Vin (sim) |
| 00:00 | 0.9 | 0.1 | 0.13 |
| 01:00 | 0.7 | 0.08 | 0.14 |
| 02:00 | 0.5 | 0.08 | 0.14 |
| 03:00 | 0.5 | 0.08 | 0.13 |
| 04:00 | 0.5 | 0.09 | 0.13 |
| 05:00 | 0.4 | 0.09 | 0.13 |
| 06:00 | 0.4 | 0.07 | 0.13 |
| 07:00 | 0.7 | 0.07 | 0.12 |
| 08:00 | 1.2 | 0.08 | 0.13 |
| 09:00 | 1.3 | 0.07 | 0.13 |
| 10:00 | 1.6 | 0.11 | 0.13 |
| 11:00 | 1.9 | 0.13 | 0.13 |
| 12:00 | 2.2 | 0.2 | 0.13 |
| 13:00 | 2.1 | 0.1 | 0.12 |
| 14:00 | 2.2 | 0.3 | 0.12 |
| 15:00 | 2.1 | 0.2 | 0.11 |
| 16:00 | 2.1 | 0.12 | 0.02 |
| 17:00 | 1.8 | 0.1 | 0.04 |
| 18:00 | 1.8 | 0.25 | 0.02 |
| 19:00 | 1.5 | 0.19 | 0.11 |
| 20:00 | 1.2 | 0.1 | 0.13 |
| 21:00 | 1.1 | 0.1 | 0.11 |
| 22:00 | 1 | 0.1 | 0.15 |
| 23:00 | 0.8 | 0.1 | 0.15 |
| **Average** | **1.27** | **0.12** | **0.12** |

# Appendix C

## Result data

**Table C- 1** Simulated data of indoor air velocity obtained from reference and test room under external wind speed of 4ms$^{-1}$ and wind direction of 0° for study stage 1 (Preliminary study).

| Room type | N | Mean | Std. Deviation | Std. Error | 95% Confidence Interval for Mean Lower Bound | 95% Confidence Interval for Mean Upper Bound | Min. | Max. |
|---|---|---|---|---|---|---|---|---|
| **Reference room** | 1829 | .0458 | .01794 | .00037 | .0451 | .0465 | .00 | .18 |
| **Test room** | 1829 | 1.4655 | .73358 | .01715 | 1.4306 | 1.4986 | .03 | 2.59 |
| **Total** | 3658 | .6599 | .85307 | .01312 | .6338 | .6841 | .00 | 2.59 |

**Table C- 2** Results of the reference and the test room's indoor thermal condition under the considered climatic conditions.

| Room type | $T_{out}$ (°C) | $T_{op}$ (°C) | $V_{in.min}$ (ms$^{-1}$) | $V_{in.av}$ (ms$^{-1}$) | $V_{in.max}$ (ms$^{-1}$) |
|---|---|---|---|---|---|
| **Reference room** | 33 | 29.4 | 0.00 | 0.05 | 0.18 |
| **Test room** | | 30.7 | 0.00 | 1.44 | 2.59 |

**Table C- 3** The results of operative ($T_{op}$) and compensated temperatures ($T_{comp}$) in the reference ad the test room during 10AM and 8PM based on the dry-bulb temperature of Bangkok on the 21$^{st}$ March under the $V_{out}$ of 4ms$^{-1}$ and $\Theta$ of 0° compared to the monthly comfort temperature range (March).

| Room type | Time | *Tout* (°C) | $T_{op}$ (°C) | $V_{in.av}$ (ms$^{-1}$) | $dT$ | $T_{comp}$ (°C) | $T_{com.lower}$ (°C) | $T_{com.upper}$ (°C) |
|---|---|---|---|---|---|---|---|---|
| **Reference room** | 10:00 | 29.4 | 30.2 | 0.05 | 0 | 30.2 | 24.3 | 29 |
| | 11:00 | 30.8 | 30.6 | | | 30.6 | | |
| | 12:00 | 32 | 31.2 | | | 31.2 | | |
| | 13:00 | 34 | 31.9 | | | 31.9 | | |
| | 14:00 | 36 | 32.4 | | | 32.4 | | |
| | 15:00 | 36.3 | 32.6 | | | 32.6 | | |
| | 16:00 | 36.7 | 32.9 | | | 32.9 | | |
| | 17:00 | 37 | 32.7 | | | 32.7 | | |
| | 18:00 | 35.7 | 32.4 | | | 32.4 | | |
| | 19:00 | 34.4 | 32.1 | | | 32.1 | | |
| | 20:00 | 33.1 | 31.9 | | | 31.9 | | |
| **Test room** | 10:00 | 29.4 | 30.3 | 1.44 | 5.46 | 24.8 | | |
| | 11:00 | 30.8 | 31.1 | | | 25.6 | | |
| | 12:00 | 32 | 32.1 | | | 26.6 | | |
| | 13:00 | 34 | 33.2 | | | 27.7 | | |
| | 14:00 | 36 | 33.9 | | | 28.4 | | |
| | 15:00 | 36.3 | 34.3 | | | 28.8 | | |
| | 16:00 | 36.7 | 34.6 | | | 29.1 | | |
| | 17:00 | 37 | 34.2 | | | 28.7 | | |
| | 18:00 | 35.7 | 33.6 | | | 28.1 | | |
| | 19:00 | 34.4 | 32.8 | | | 27.3 | | |
| | 20:00 | 33.1 | 32.2 | | | 26.7 | | |

**Table C- 4** Simulated data of indoor air velocity obtained from test room under different external air temperature (Tout).

| Tout | N | Mean | Std. Deviation | Std. Error | 95% Confidence Interval for Mean | | Min. | Max. |
|---|---|---|---|---|---|---|---|---|
| | | | | | Lower Bound | Upper Bound | | |
| **25C** | 1829 | 1.4919 | .72991 | .01707 | 1.4584 | 1.5254 | .04 | 2.59 |
| **29C** | 1829 | 1.4608 | .73588 | .01721 | 1.4271 | 1.4946 | .03 | 2.59 |
| **31C** | 1829 | 1.4650 | .73359 | .01715 | 1.4313 | 1.4986 | .03 | 2.59 |
| **33C** | 1829 | 1.4927 | .72920 | .01705 | 1.4593 | 1.5262 | .04 | 2.59 |
| **Total** | 7316 | 1.4776 | .73215 | .00856 | 1.4608 | 1.4944 | .03 | 2.59 |

**Table C- 5** Simulated data of indoor air velocity obtained from test room under different relative humidity (RH).

| RH | N | Mean | Std. Deviation | Std. Error | 95% Confidence Interval for Mean | | Min. | Max. |
|---|---|---|---|---|---|---|---|---|
| | | | | | Lower Bound | Upper Bound | | |
| **55%** | 1829 | 1.4413 | .74093 | .01732 | 1.4073 | 1.4753 | .02 | 2.59 |
| **72%** | 1829 | 1.4413 | .74098 | .01733 | 1.4073 | 1.4753 | .02 | 2.59 |
| **89%** | 1829 | 1.4824 | .71729 | .01705 | 1.4490 | 1.5159 | .02 | 2.59 |
| **Total** | 5487 | 1.4547 | .73344 | .00996 | 1.4352 | 1.4742 | .02 | 2.59 |

**Table C- 6** Simulated data of indoor air velocity obtained from test room under different external wind speed (Vout).

| Vout | N | Mean | Std. Deviation | Std. Error | 95% Confidence Interval for Mean | | Min. | Max. |
|---|---|---|---|---|---|---|---|---|
| | | | | | Lower Bound | Upper Bound | | |
| **0 m/s** | 1829 | .2234 | .14584 | .00341 | .2167 | .2301 | .02 | .50 |
| **1 m/s** | 1829 | .2208 | .16306 | .00381 | .2133 | .2283 | .02 | .60 |
| **1.5 m/s** | 1829 | .4294 | .26303 | .00615 | .4173 | .4414 | .02 | .95 |
| **2.0 m/s** | 1829 | .6402 | .36930 | .00864 | .6233 | .6572 | .03 | 1.28 |
| **2.5 m/s** | 1829 | .8454 | .46876 | .01096 | .8239 | .8669 | .01 | 1.61 |
| **3 m/s** | 1829 | 1.0465 | .56194 | .01314 | 1.0207 | 1.0723 | .01 | 1.94 |
| **4 m/s** | 1829 | 1.4414 | .74092 | .01732 | 1.4074 | 1.4753 | .02 | 2.59 |
| **Total** | 12803 | .6924 | .60490 | .00535 | .6820 | .7029 | .01 | 2.59 |

**Table C- 7** Simulated data of indoor air velocity obtained from test room under different wind direction regarding to the inlet opening.

| $\theta$ | N | Mean | Std. Deviation | Std. Error | 95% Confidence Interval for Mean | | Min. | Max. |
|---|---|---|---|---|---|---|---|---|
| | | | | | Lower Bound | Upper Bound | | |
| **0 degree** | 1829 | 1.4414 | .74092 | .01732 | 1.4074 | 1.4753 | .02 | 2.59 |
| **30 degree** | 1829 | 1.3094 | .68007 | .01590 | 1.2782 | 1.3405 | .02 | 2.37 |
| **45 degree** | 1829 | 1.3094 | .68007 | .01590 | 1.2782 | 1.3405 | .02 | 2.37 |
| **60 degree** | 1829 | 1.0473 | .56228 | .01315 | 1.0215 | 1.0731 | .01 | 1.94 |
| **90 degree** | 1829 | .3388 | .16779 | .00392 | .3311 | .3465 | .02 | .80 |
| **180 degree** | 1829 | .3381 | .16807 | .00393 | .3304 | .3458 | .02 | .80 |
| **Total** | 10974 | .9640 | .71901 | .00686 | .9506 | .9775 | .01 | 2.59 |

**Table C- 8** Results of the test room's indoor thermal condition under different climatic elements.

| Variable | $T_{op}$ (°C) | $V_{in.min}$ (ms$^{-1}$) | $V_{in.av}$ (ms$^{-1}$) | $V_{in.max}$ (ms$^{-1}$) | *Percentgage of $V_{in.av}$ to $V_{out}$ (%)* |
|---|---|---|---|---|---|
| **Different $T_{out}$ (°C)** | | | | | |
| $T_{out}$ of 25° | 25.3 | 0.02 | 1.44 | 2.59 | 35 |
| $T_{out}$ of 29° | 28.3 | 0.02 | 1.44 | 2.59 | 35 |
| $T_{out}$ of 31° | 29.5 | 0.02 | 1.44 | 2.59 | 35 |
| $T_{out}$ of 33° | 30.7 | 0.02 | 1.44 | 2.59 | 35 |
| **Different *RH* (%)** | | | | | |
| *RH* of 55% | 30.7 | 0.02 | 1.44 | 2.59 | 35 |
| *RH* of 72% | 30.7 | 0.02 | 1.44 | 2.59 | 35 |
| *RH* of 89% | 30.7 | 0.02 | 1.44 | 2.59 | 35 |
| **Different $V_{out}$ (ms$^{-1}$)** | | | | | |
| $V_{out}$ of 0 ms$^{-1}$ | 30.4 | 0.02 | 0.22 | 0.5 | 5 |
| $V_{out}$ of 1.0 ms$^{-1}$ | 30.6 | 0.02 | 0.22 | 0.6 | 5 |
| $V_{out}$ of 1.5 ms$^{-1}$ | 30.6 | 0.02 | 0.43 | 0.95 | 10 |
| $V_{out}$ of 2.0 ms$^{-1}$ | 30.7 | 0.02 | 0.64 | 1.28 | 15 |
| $V_{out}$ of 2.5 ms$^{-1}$ | 30.7 | 0.02 | 0.85 | 1.61 | 23 |
| $V_{out}$ of 3.0 ms$^{-1}$ | 30.7 | 0.02 | 1.05 | 1.94 | 28 |
| $V_{out}$ of 4.0 ms$^{-1}$ | 30.7 | 0.02 | 1.44 | 2.59 | 35 |
| **Different $\theta$ (°)** | | | | | |
| $\Theta$ of 0° | 30.7 | 0.02 | 1.44 | 2.59 | 35 |
| $\Theta$ of 30° | 30.7 | 0.02 | 1.31 | 2.37 | 33 |
| $\Theta$ of 45° | 30.7 | 0.02 | 1.31 | 2.37 | 33 |
| $\Theta$ of 60° | 30.7 | 0.02 | 1.05 | 1.94 | 28 |
| $\Theta$ of 90° | 30 | 0.02 | 0.34 | 0.8 | 8 |
| $\Theta$ of 180° | 30.4 | 0.02 | 0.34 | 0.8 | 8 |

**Table C- 9** Simulated data of indoor air velocity obtained from test room under different shaft's heights above the building roof.

| Shaft's height (m) | N | Mean | Std. Deviation | Std. Error of Mean | Min. | Max. |
|---|---|---|---|---|---|---|
| **0 m** | 1829 | 1.3293 | .68969 | .01613 | .02 | 2.42 |
| **1 m** | 1829 | 1.4440 | .74044 | .01731 | .02 | 2.59 |
| **2 m** | 1829 | 1.4442 | .74056 | .01732 | .02 | 2.59 |
| **4 m** | 1829 | 1.4418 | .74158 | .01734 | .02 | 2.60 |
| **Total** | 7316 | 1.4148 | .72992 | .00853 | .02 | 2.60 |

**Table C- 10** Simulated data of indoor air velocity obtained from test room under different shaft's lengths and widths.

| Shaft's length (m) | Shaft's width (m) | N | Mean | Std. Deviation | Std. Error of Mean | Min. | Max. |
|---|---|---|---|---|---|---|---|
| **2 m** | **0.3 m** | 1829 | 1.4292 | .73919 | .01728 | .02 | 2.59 |
| | **0.6 m** | 1829 | 1.4414 | .74092 | .01732 | .02 | 2.59 |
| | **1.2 m** | 1829 | 2.0305 | 1.02258 | .02391 | .04 | 3.58 |
| | **Total** | 5487 | 1.6337 | .89005 | .01202 | .02 | 3.58 |
| **3 m** | **0.3 m** | 1829 | 1.4466 | 1.00258 | .02156 | .02 | 3.13 |
| | **0.6 m** | 1829 | 1.6415 | 1.14221 | .02445 | .02 | 3.54 |
| | **1.2 m** | 1829 | 1.8126 | 1.26250 | .02702 | .03 | 3.88 |
| | **Total** | 5487 | 1.6342 | 1.15070 | .01424 | .02 | 3.88 |
| **4 m** | **0.3 m** | 1829 | 1.7125 | .88952 | .02150 | .05 | 3.05 |
| | **0.6 m** | 1829 | 1.9585 | 1.01149 | .02445 | .07 | 3.45 |
| | **1.2 m** | 1829 | 2.2576 | 1.16098 | .02807 | .09 | 4.02 |
| | **Total** | 5487 | 1.9762 | 1.05041 | .01466 | .05 | 4.02 |
| **Total** | **0.3 m** | 5487 | 1.5208 | .89964 | .01191 | .02 | 3.13 |
| | **0.6 m** | 5487 | 1.6723 | 1.01022 | .01335 | .02 | 3.54 |
| | **1.2 m** | 5487 | 2.0153 | 1.17388 | .01552 | .03 | 4.02 |
| | **Total** | 16461 | 1.7364 | 1.05465 | .00805 | .02 | 4.02 |

**Table C- 11** Simulated data of indoor air velocity obtained from test room under different inlet and outlet's widths.

| Inlet's width (m) | Outlet's width (m) | N | Mean | Std. Deviation | Std. Error of Mean | Min. | Max. |
|---|---|---|---|---|---|---|---|
| **1** | **1** | 1829 | 1.2842 | 1.13036 | .02733 | .02 | 3.94 |
| | **2** | 1829 | 1.3381 | 1.12178 | .02712 | .04 | 3.77 |
| | **3** | 1829 | 1.3490 | 1.11585 | .02698 | .05 | 3.79 |
| | **4** | 1829 | 1.3248 | 1.10824 | .02634 | .03 | 3.79 |
| | **Total** | 7316 | 1.3240 | 1.11902 | .01347 | .02 | 3.94 |
| **2** | **1** | 1829 | 1.9354 | 1.12533 | .02721 | .05 | 7.43 |
| | **2** | 1829 | 1.9295 | .99531 | .02406 | .07 | 3.40 |
| | **3** | 1829 | 2.0050 | .94281 | .02279 | .07 | 3.44 |
| | **4** | 1829 | 1.9468 | .96488 | .02293 | .06 | 3.44 |
| | **Total** | 7316 | 1.9541 | 1.00942 | .01215 | .05 | 7.43 |
| **3** | **1** | 1829 | 2.0553 | .89135 | .02155 | .39 | 9.44 |
| | **2** | 1829 | 2.0117 | .60055 | .01452 | .51 | 4.53 |
| | **3** | 1829 | 2.0178 | .54624 | .01321 | .83 | 2.94 |
| | **4** | 1829 | 1.9330 | .54573 | .01297 | .88 | 2.87 |
| | **Total** | 7316 | 2.0038 | .66216 | .00797 | .39 | 9.44 |
| **4** | **1** | 1829 | 2.0242 | .88665 | .02144 | .52 | 10.68 |
| | **2** | 1829 | 1.9804 | .47798 | .01156 | .57 | 5.45 |
| | **3** | 1829 | 1.9648 | .34934 | .00845 | 1.45 | 3.29 |
| | **4** | 1829 | 1.9056 | .36556 | .00869 | 1.44 | 2.57 |
| | **Total** | 7316 | 1.9682 | .56363 | .00678 | .52 | 10.68 |
| **Total** | **1** | 7316 | 1.8248 | 1.06305 | .01285 | .02 | 10.68 |
| | **2** | 7316 | 1.8149 | .88650 | .01072 | .04 | 5.45 |
| | **3** | 7316 | 1.8342 | .84687 | .01024 | .05 | 3.79 |
| | **4** | 7316 | 1.7776 | .84613 | .01006 | .03 | 3.79 |
| | **Total** | 29264 | 1.8126 | .91467 | .00550 | .02 | 10.68 |

**Table C- 12** Simulated data of indoor air velocity obtained from test room under different inlet and outlet's lengths.

| Inlet's length (m) | N | Mean | Std. Deviation | Std. Error of Mean | Minimum | Maximum |
|---|---|---|---|---|---|---|
| **.6** | 1829 | 2.3548 | .72477 | .01752 | .78 | 3.52 |
| **.9** | 1829 | 2.2527 | .65315 | .01579 | .83 | 3.28 |
| **1.2** | 1829 | 2.0178 | .54624 | .01321 | .83 | 2.94 |
| **1.5** | 1829 | 1.8096 | .44530 | .01077 | .90 | 2.81 |
| **Total** | 7316 | 2.1087 | .63776 | .00771 | .78 | 3.52 |

**Table C- 13** Simulated data of indoor air velocity obtained from test room under different inlet and outlet's vertical positions regarding to main occupied level.

| **Hinlet (m)** | **Houtlet (m)** | **N** | **Mean** | **Std. Deviation** | **Std. Error of Mean** | **Minimum** | **Maximum** |
|---|---|---|---|---|---|---|---|
| **low** | **low** | 1829 | 1.359 | .3724 | .0090 | .3 | 1.8 |
| | **middle** | 1829 | 1.315 | .6511 | .0157 | .4 | 4.0 |
| | **high** | 1829 | 1.435 | .3942 | .0095 | .4 | 2.0 |
| | **Total** | 5487 | 1.370 | .4916 | .0069 | .3 | 4.0 |
| **middle** | **low** | 1829 | 2.326 | .7352 | .0178 | .7 | 3.5 |
| | **middle** | 1829 | 2.421 | .6791 | .0164 | 1.2 | 3.6 |
| | **high** | 1829 | 2.251 | .8535 | .0206 | .5 | 3.5 |
| | **Total** | 5487 | 2.332 | .7625 | .0106 | .5 | 3.6 |
| **high** | **low** | 1829 | .660 | .4505 | .0109 | .1 | 1.7 |
| | **middle** | 1829 | .724 | .5859 | .0142 | .1 | 3.6 |
| | **high** | 1829 | .344 | .1569 | .0038 | .1 | .9 |
| | **Total** | 5487 | .576 | .4667 | .0065 | .1 | 3.6 |
| **Total** | **low** | 5487 | 1.448 | .8723 | .0122 | .1 | 3.5 |
| | **middle** | 5487 | 1.486 | .9508 | .0133 | .1 | 4.0 |
| | **high** | 5487 | 1.343 | .9554 | .0133 | .1 | 3.5 |
| | **Total** | 16461 | 1.426 | .9289 | .0075 | .1 | 4.0 |

**Table C- 14** Results of the test room's indoor thermal condition under different ventilation shaft's designs.

| Variable | $T_{op}$ (°C) | $V_{in.min}$ (ms$^{-1}$) | $V_{in.av}$ (ms$^{-1}$) | $V_{in.max}$ (ms$^{-1}$) | Fixed variables |
|---|---|---|---|---|---|
| **Different $H_{shaft}$** | | | | | |
| $H_{shaft}$ of 0m | 30.6 | 0.02 | 1.33 | 2.42 | i) Shaft's size of 2x0.6m2<br>ii) Winlet and Woutlet of 2x1.2m2<br>iii) Linlet and Loutlet of 1.2m<br>iv) Inlet and outlet's position at 0.8m |
| $H_{shaft}$ of 1m | 30.7 | 0.02 | 1.44 | 2.59 | |
| $H_{shaft}$ of 2m | 30.7 | 0.02 | 1.44 | 2.59 | |
| $H_{shaft}$ of 4m | 30.7 | 0.02 | 1.44 | 2.59 | |
| **Different $L_{shaft\ and\ Wshaft}$** | | | | | |
| Lshaft x Wshaft=2x0.3m2 (0.6m2) | 30.7 | 0.02 | 1.43 | 2.6 | i) Shaft's height of 1m<br>ii) Winlet and Woutlet of 2x1.2m2<br>iii) Linlet and Loutlet of 1.2m<br>iv) Inlet and outlet's position at 0.8m |
| Lshaft x Wshaft=2x0.6m2 (1.2m2) | 30.7 | 0.02 | 1.44 | 2.6 | |
| Lshaft x Wshaft=2x1.2m2 (2.4m2) | 31.2 | 0.04 | 2.03 | 3.6 | |
| Lshaft x Wshaft=3x0.3m2 (0.9m2) | 30.9 | 0.02 | 1.45 | 3.1 | |
| Lshaft x Wshaft=3x0.6m2 (1.8m2) | 31.1 | 0.02 | 1.64 | 3.5 | |
| Lshaft x Wshaft=3x1.2m2 (3.6m2) | 31.5 | 0.03 | 1.81 | 3.9 | |
| Lshaft x Wshaft=4x0.3m2 (1.2m2) | 30.8 | 0.05 | 1.71 | 3.1 | |
| Lshaft x Wshaft=4x0.6m2 (2.4m2) | 31.0 | 0.07 | 1.96 | 3.5 | |
| Lshaft x Wshaft=4x1.2m2 (4.8m2) | 31.5 | 0.09 | 2.26 | 4.0 | |
| **Different *combinations of $W_{inlet}$ and $W_{outlet}$*** | | | | | |
| $W_{inlet}$ and $W_{outlet}$ = 1 and 1m | 30.9 | 0.02 | 1.13 | 3.94 | i) Shaft's height of 1m<br>ii) Lshaft x Wshaft=4x0.6m2<br>iii) Linlet and Loutlet of 1.2m<br>iv) Inlet and outlet's position at 0.8m |
| $W_{inlet}$ and $W_{outlet}$ = 1 and 2m | 30.9 | 0.04 | 1.12 | 3.77 | |
| $W_{inlet}$ and $W_{outlet}$ = 1 and 3m | 31 | 0.05 | 1.12 | 3.79 | |
| $W_{inlet}$ and $W_{outlet}$ = 1 and 4m | 31 | 0.03 | 1.10 | 3.79 | |
| $W_{inlet}$ and $W_{outlet}$ = 2 and 1m | 30.9 | 0.05 | 1.93 | 7.43 | |
| $W_{inlet}$ and $W_{outlet}$ = 2 and 2m | 31 | 0.07 | 1.92 | 3.40 | |
| $W_{inlet}$ and $W_{outlet}$ = 2 and 3m | 31 | 0.07 | 2.00 | 3.44 | |
| $W_{inlet}$ and $W_{outlet}$ = 2 and 4m | 31 | 0.06 | 1.95 | 3.44 | |
| $W_{inlet}$ and $W_{outlet}$ = 3 and 1m | 31 | 0.39 | 2.06 | 9.44 | |
| $W_{inlet}$ and $W_{outlet}$ = 3 and 2m | 31 | 0.51 | 2.01 | 4.53 | |
| $W_{inlet}$ and $W_{outlet}$ = 3 and 3m | 31.1 | 0.83 | 2.02 | 2.94 | |
| $W_{inlet}$ and $W_{outlet}$ = 3 and 4m | 31.1 | 0.88 | 1.93 | 2.87 | |
| $W_{inlet}$ and $W_{outlet}$ = 4 and 1m | 31.1 | 0.52 | 2.02 | 10.68 | |
| $W_{inlet}$ and $W_{outlet}$ = 4 and 2m | 31.1 | 0.57 | 1.98 | 5.45 | |
| $W_{inlet}$ and $W_{outlet}$ = 4 and 3m | 31.2 | 1.45 | 1.96 | 3.29 | |
| $W_{inlet}$ and $W_{outlet}$ = 4 and 4m | 31.2 | 1.44 | 1.91 | 2.57 | |
| **Different $L_{inlet}$** | | | | | |
| $L_{inlet}$ of 0.6m | 30.9 | 0.78 | 2.35 | 3.52 | i) Shaft's height of 1m<br>ii) Lshaft x Wshaft=4x0.6m2<br>iii) Winlet and Woutlet = 3 and 3m<br>iv) Inlet and outlet's position at 0.8m |
| $L_{inlet}$ of 0.9m | 31 | 0.83 | 2.25 | 3.28 | |
| $L_{inlet}$ of 1.2m | 31.1 | 0.83 | 2.02 | 2.94 | |
| $L_{inlet}$ of 1.5m | 31.2 | 0.9 | 1.81 | 2.81 | |

**Table C – 14** Results of the test room's indoor thermal condition under different ventilation shaft's designs (*continued*).

| Variable | $T_{op}$ (°C) | $V_{in.min}$ (ms$^{-1}$) | $V_{in.av}$ (ms$^{-1}$) | $V_{in.max}$ (ms$^{-1}$) | Fixed variables |
|---|---|---|---|---|---|
| **Different combinations of $H_{inlet}$ and $H_{outlet}$** | | | | | |
| low inlet and outlet | 30.9 | 0.09 | 1.36 | 0.88 | i) Shaft's height of 1m<br>ii) Lshaft x Wshaft=4x0.6m2<br>iii) Inlet and outlet size of 3x0.6m2 |
| low inlet and middle outlet | 30.9 | 0.36 | 1.31 | 3.99 | |
| low inlet and high outlet | 30.9 | 0.44 | 1.43 | 2.03 | |
| middle inlet and low outlet | 30.9 | 0.72 | 2.33 | 3.49 | |
| Middle inlet and outlet | 30.9 | 1.22 | 2.42 | 3.59 | |
| middle inlet and high outlet | 30.9 | 0.45 | 2.25 | 3.52 | |
| high inlet and low outlet | 30.9 | 0.12 | 0.66 | 1.74 | |
| high inlet and middle outlet | 30.9 | 0.11 | 0.72 | 3.58 | |
| high inlet and outlet | 30.9 | 0.09 | 0.34 | 0.88 | |

**Table C- 15** Average air velocity (ms$^{-1}$) in the occupied area of the reference and the test rooms on different floors under different external wind speed conditions.

| Floor number | Reference room | | | Test room | | | |
|---|---|---|---|---|---|---|---|
| | 1m/s | | 4m/s, $\theta$ of 0°* | 0m/s, $\theta$ of 0° | 1m/s | | 4m/s, $\theta$ of 0° |
| | $\theta$ of 0° | $\theta$ of 180° | | | $\theta$ of 0° | $\theta$ of 180° | |
| Fl6 | 0.08 | 0.04 | 0.05 | -0.49 | -0.53 | -0.46 | -0.74 |
| Fl7 | 0.08 | 0.04 | 0.05 | -0.53 | -0.58 | -0.50 | -0.68 |
| Fl8 | 0.08 | 0.04 | 0.05 | -0.50 | -0.52 | -0.48 | -0.68 |
| Fl9 | 0.08 | 0.04 | 0.05 | -0.50 | -0.52 | -0.48 | -0.66 |
| Fl10 | 0.08 | 0.04 | 0.05 | -0.50 | -0.50 | -0.48 | -0.56 |
| Fl11 | 0.08 | 0.04 | 0.05 | -0.49 | -0.47 | -0.47 | -0.35 |
| Fl12 | 0.08 | 0.04 | 0.05 | -0.47 | -0.44 | -0.46 | -0.11 |
| Fl13 | 0.08 | 0.04 | 0.05 | -0.43 | -0.38 | -0.43 | 0.08 |
| Fl14 | 0.08 | 0.04 | 0.05 | -0.39 | -0.27 | -0.39 | 0.26 |
| Fl15 | 0.08 | 0.04 | 0.05 | -0.33 | 0.06 | -0.34 | 0.43 |
| Fl16 | 0.08 | 0.04 | 0.05 | -0.22 | 0.08 | -0.24 | 0.57 |
| Fl17 | 0.08 | 0.04 | 0.05 | 0.05 | 0.17 | 0.05 | 0.66 |
| Fl18 | 0.08 | 0.04 | 0.05 | 0.09 | 0.25 | 0.08 | 0.74 |
| Fl19 | 0.08 | 0.04 | 0.05 | 0.17 | 0.31 | 0.16 | 0.8 |
| Fl20 | 0.08 | 0.04 | 0.05 | 0.24 | 0.35 | 0.22 | 0.85 |
| Fl21 | 0.08 | 0.04 | 0.05 | 0.29 | 0.39 | 0.28 | 0.9 |
| Fl22 | 0.08 | 0.04 | 0.05 | 0.33 | 0.42 | 0.32 | 0.95 |
| Fl23 | 0.08 | 0.04 | 0.05 | 0.37 | 0.45 | 0.36 | 0.99 |
| Fl24 | 0.08 | 0.04 | 0.05 | 0.41 | 0.48 | 0.4 | 1.03 |
| Fl25 | 0.08 | 0.04 | 0.05 | 0.44 | 0.5 | 0.44 | 1.07 |
| **Overall $V_{in.av}$ (ms$^{-1}$)** | **0.08** | **0.04** | **0.05** | **0.36** | **0.38** | **0.35** | **0.66** |
| **Percentage of Overall $V_{in.av}$ to $V_{out}$ (%)** | **8** | **4** | **1** | **-** | **38** | **35** | **17** |

** The negative value of air velocities illustrates the airflow direction from the outlet to the inlet opening.*

**Table C- 16** The physiological cooling effect (*dT*) produced by the air velocity ($V_{in}$) according to Szokolay's model (2000, 2008).

| $V_{in}$ (ms$^{-1}$) | 0.05 | 0.2 | 0.5 | 0.6 | 0.7 | 0.8 | 0.9 | 1.0 | 1.1 |
|---|---|---|---|---|---|---|---|---|---|
| ***dT*** **(K)** | - | - | 1.66 | 2.14 | 2.60 | 3.02 | 3.42 | 3.78 | 4.10 |

**Table C- 17** Percentage of thermal comfort hours during the target time of the day of the south-facing reference and test rooms on floor 21st under external wind speed of 1ms$^{-1}$ and wind incident angle of 0°.

| **Season** | **Time** | **Reference room** | | | | | | **Test room** | | | | |
|---|---|---|---|---|---|---|---|---|---|---|---|---|
| | | **Tout (°C)** | $T_{op}$ **(°C)** | ***Vin.av (m/s)*** | **dT (°C)** | $T_{comp}$ **(°C)** | **Percentage of comfort hours (%)** | $T_{op}$ **(°C)** | ***Vin.av (m/s)*** | **dT (°C)** | $T_{comp}$ **(°C)** | **Percentage of comfort hours (%)** |
| **Summer** | 00:00 | 27.8 | 29.5 | 0.05 | 0 | 29.5 | 29.2 | 28.9 | 0.39 | 1.1 | ***27.8*** | 62.5 |
| | 01:00 | 27.4 | 29.3 | | | 29.3 | | 28.7 | | | ***27.6*** | |
| | 02:00 | 27.0 | 29.2 | | | 29.2 | | 28.4 | | | ***27.3*** | |
| | 03:00 | 26.6 | 29.0 | | | ***29.0*** | | 28.1 | | | ***27.0*** | |
| | 04:00 | 26.2 | 28.8 | | | ***28.8*** | | 27.9 | | | ***26.8*** | |
| | 05:00 | 26.1 | 28.6 | | | ***28.6*** | | 27.6 | | | ***26.5*** | |
| | 06:00 | 25.9 | 28.5 | | | ***28.5*** | | 27.4 | | | ***26.3*** | |
| | 07:00 | 25.7 | 28.3 | | | ***28.3*** | | 27.3 | | | ***26.2*** | |
| | 08:00 | 27.2 | 28.5 | | | ***28.5*** | | 27.5 | | | ***26.4*** | |
| | 09:00 | 28.8 | 28.7 | | | ***28.7*** | | 28.0 | | | ***26.9*** | |
| | 10:00 | 30.4 | 29.0 | | | 29.0 | | 29.0 | | | ***27.9*** | |
| | 11:00 | 31.4 | 29.4 | | | 29.4 | | 29.9 | | | ***28.8*** | |
| | 12:00 | 32.3 | 29.7 | | | 29.7 | | 30.8 | | | 29.7 | |
| | 13:00 | 33.3 | 30.0 | | | 30.0 | | 31.4 | | | 30.3 | |
| | 14:00 | 33.4 | 30.2 | | | 30.2 | | 31.8 | | | 30.7 | |
| | 15:00 | 33.6 | 30.4 | | | 30.4 | | 32.1 | | | 31.0 | |
| | 16:00 | 33.8 | 30.6 | | | 30.6 | | 32.3 | | | 31.2 | |
| | 17:00 | 32.7 | 30.5 | | | 30.5 | | 32.1 | | | 31.0 | |
| | 18:00 | 31.6 | 30.4 | | | 30.4 | | 31.8 | | | 30.7 | |
| | 19:00 | 30.4 | 30.2 | | | 30.2 | | 31.2 | | | 30.1 | |
| | 20:00 | 29.8 | 30.1 | | | 30.1 | | 30.6 | | | 29.5 | |
| | 21:00 | 29.2 | 29.9 | | | 29.9 | | 30.1 | | | ***29.0*** | |
| | 22:00 | 28.5 | 29.8 | | | 29.8 | | 29.6 | | | ***28.5*** | |
| | 23:00 | 28.2 | 29.7 | | | 29.7 | | 29.3 | | | ***28.2*** | |

** The **bold and italic** results of compensate temperatures (Tcomp) indicate the temperatures within the comfort temperature range calculated for each season according to its average dry-bulb temperatures and the colored boxes indicate the target time of the day i.e. 10am to 8pm.*

**Table C- 17** Percentage of thermal comfort hours during the target time of the day of the south-facing reference and test rooms on floor 21st under external wind speed of 1ms$^{-1}$ and wind incident angle of 0° (*continued*).

| Season | Time | Reference room | | | | | | Test room | | | | |
|---|---|---|---|---|---|---|---|---|---|---|---|---|
| | | Tout (°C) | $T_{op}$ (°C) | *Vin.av (m/s)* | dT (°C) | $T_{comp}$ (°C) | Percentage of comfort hours (%) | $T_{op}$ (°C) | *Vin.av (m/s)* | dT (°C) | $T_{comp}$ (°C) | Percentage of comfort hours (%) |
| **Rainy** | 00:00 | 27.3 | 28.6 | 0.05 | 0 | ***28.6*** | 66.7 | 28.3 | 0.39 | 1.1 | ***27.2*** | 79.2 |
| | 01:00 | 27.1 | 28.4 | | | ***28.4*** | | 28.2 | | | ***27.1*** | |
| | 02:00 | 26.9 | 28.3 | | | ***28.3*** | | 28.0 | | | ***26.9*** | |
| | 03:00 | 26.6 | 28.2 | | | ***28.2*** | | 27.9 | | | ***26.8*** | |
| | 04:00 | 26.4 | 28.1 | | | ***28.1*** | | 27.7 | | | ***26.6*** | |
| | 05:00 | 26.4 | 28.0 | | | ***28.0*** | | 27.6 | | | ***26.5*** | |
| | 06:00 | 26.4 | 27.9 | | | ***27.9*** | | 27.6 | | | ***26.5*** | |
| | 07:00 | 26.5 | 27.8 | | | ***27.8*** | | 27.6 | | | ***26.5*** | |
| | 08:00 | 27.7 | 27.9 | | | ***27.9*** | | 27.9 | | | ***26.8*** | |
| | 09:00 | 28.9 | 28.1 | | | ***28.1*** | | 28.4 | | | ***27.3*** | |
| | 10:00 | 28.4 | 28.4 | | | ***28.4*** | | 29.0 | | | ***27.9*** | |
| | 11:00 | 28.6 | 28.6 | | | ***28.6*** | | 29.5 | | | ***28.4*** | |
| | 12:00 | 28.8 | 28.8 | | | ***28.8*** | | 29.9 | | | ***28.8*** | |
| | 13:00 | 29.1 | 29.1 | | | 29.1 | | 30.2 | | | 29.1 | |
| | 14:00 | 29.2 | 29.2 | | | 29.2 | | 30.4 | | | 29.3 | |
| | 15:00 | 29.3 | 29.3 | | | 29.3 | | 30.5 | | | 29.4 | |
| | 16:00 | 29.4 | 29.4 | | | 29.4 | | 30.5 | | | 29.4 | |
| | 17:00 | 29.3 | 29.3 | | | 29.3 | | 30.2 | | | 29.1 | |
| | 18:00 | 29.2 | 29.2 | | | 29.2 | | 29.8 | | | ***28.7*** | |
| | 19:00 | 29.0 | 29.0 | | | 29.0 | | 29.4 | | | ***28.3*** | |
| | 20:00 | 28.9 | 28.9 | | | 28.9 | | 29.1 | | | ***28.0*** | |
| | 21:00 | 28.2 | 28.8 | | | ***28.8*** | | 28.9 | | | ***27.8*** | |
| | 22:00 | 27.7 | 28.7 | | | ***28.7*** | | 28.6 | | | ***27.5*** | |
| | 23:00 | 27.5 | 28.6 | | | ***28.6*** | | 28.5 | | | ***27.4*** | |
| **Winter** | 00:00 | 25.7 | 28.3 | 0.05 | 0 | ***28.3*** | 62.5 | 27.6 | 0.39 | 1.1 | ***26.5*** | 87.5 |
| | 01:00 | 25.2 | 28.1 | | | ***28.1*** | | 27.3 | | | ***26.2*** | |
| | 02:00 | 24.8 | 27.9 | | | ***27.9*** | | 27.0 | | | ***25.9*** | |
| | 03:00 | 24.4 | 27.7 | | | ***27.7*** | | 26.7 | | | ***25.6*** | |
| | 04:00 | 24.1 | 27.4 | | | ***27.4*** | | 26.5 | | | ***25.4*** | |
| | 05:00 | 23.9 | 27.2 | | | ***27.2*** | | 26.2 | | | ***25.1*** | |
| | 06:00 | 23.7 | 27.1 | | | ***27.1*** | | 26.0 | | | ***24.9*** | |
| | 07:00 | 24.0 | 26.9 | | | ***26.9*** | | 25.8 | | | ***24.7*** | |
| | 08:00 | 25.3 | 27.0 | | | ***27.0*** | | 26.2 | | | ***25.1*** | |
| | 09:00 | 26.6 | 27.3 | | | ***27.3*** | | 26.8 | | | ***25.7*** | |
| | 10:00 | 27.6 | 27.6 | | | ***27.6*** | | 27.4 | | | ***26.3*** | |
| | 11:00 | 28.0 | 28.0 | | | ***28.0*** | | 28.0 | | | ***26.9*** | |
| | 12:00 | 28.3 | 28.3 | | | ***28.3*** | | 28.6 | | | ***27.5*** | |
| | 13:00 | 28.7 | 28.7 | | | 28.7 | | 29.3 | | | ***28.2*** | |
| | 14:00 | 29.0 | 29.0 | | | 29.0 | | 29.6 | | | ***28.5*** | |
| | 15:00 | 29.2 | 29.2 | | | 29.2 | | 29.8 | | | 28.7 | |
| | 16:00 | 29.4 | 29.4 | | | 29.4 | | 30.0 | | | 28.9 | |
| | 17:00 | 29.3 | 29.3 | | | 29.3 | | 29.8 | | | 28.7 | |
| | 18:00 | 29.2 | 29.2 | | | 29.2 | | 29.4 | | | ***28.3*** | |
| | 19:00 | 29.1 | 29.1 | | | 29.1 | | 29.0 | | | ***27.9*** | |
| | 20:00 | 28.9 | 28.9 | | | 28.9 | | 28.7 | | | ***27.6*** | |
| | 21:00 | 27.1 | 28.8 | | | 28.8 | | 28.4 | | | ***27.3*** | |
| | 22:00 | 26.6 | 28.6 | | | ***28.6*** | | 28.1 | | | ***27.0*** | |
| | 23:00 | 26.2 | 28.4 | | | ***28.4*** | | 27.8 | | | ***26.7*** | |

**Table C- 18** Percentage of comfort hour (%) in the south-facing reference and test rooms on floor 21st under external wind speed of 1ms$^{-1}$ and wind incident angle of 0° during different seasons.

| Seasons | Reference room | Test room |
|---|---|---|
| summer | 29.2 | 62.5 |
| rainy | 66.7 | 79.2 |
| winter | 62.5 | 87.5 |

**Table C- 19** Percentage of comfort hour (%) in the south-facing reference and test rooms on floor 21st under external wind speed of 1ms$^{-1}$ and wind incident angle of 0° during target time i.e. 10am to 8pm in different seasons.

| Seasons | Reference room | Test room |
|---|---|---|
| summer | 0 | 18.2 |
| rainy | 27.3 | 54.5 |
| winter | 27.3 | 72.7 |

**Table C- 20** Percentage of thermal comfort hours during the target time of the day of the north-facing reference and test rooms on floor 23rd under external wind speed of 1ms$^{-1}$, wind incident angle of 0°.

| Season | Time | Reference room | | | | | | Test room | | | | |
|---|---|---|---|---|---|---|---|---|---|---|---|---|
| | | Tout (°C) | $T_{op}$ (°C) | *Vin.av (m/s)* | dT (°C) | $T_{comp}$ (°C) | Percentage of comfort hours (%) | $T_{op}$ (°C) | *Vin.av (m/s)* | dT (°C) | $T_{comp}$ (°C) | Percentage of comfort hours (%) |
| **Summer** | 00:00 | 27.8 | 30.2 | 0.04 | 0 | 30.2 | 0 | 29.1 | 0.35 | 0.9 | **28.2** | 58.3 |
| | 01:00 | 27.4 | 30.1 | | | 30.1 | | 28.8 | | | **27.9** | |
| | 02:00 | 27.0 | 29.9 | | | 29.9 | | 28.6 | | | **27.7** | |
| | 03:00 | 26.6 | 29.8 | | | 29.8 | | 28.4 | | | **27.5** | |
| | 04:00 | 26.2 | 29.6 | | | 29.6 | | 28.1 | | | **27.2** | |
| | 05:00 | 26.1 | 29.5 | | | 29.5 | | 27.9 | | | **27.0** | |
| | 06:00 | 25.9 | 29.4 | | | 29.4 | | 27.8 | | | **26.9** | |
| | 07:00 | 25.7 | 29.2 | | | 29.2 | | 27.6 | | | **26.7** | |
| | 08:00 | 27.2 | 29.4 | | | 29.4 | | 28.0 | | | **27.1** | |
| | 09:00 | 28.8 | 29.7 | | | 29.7 | | 28.6 | | | **27.7** | |
| | 10:00 | 30.4 | 30.0 | | | 30.0 | | 29.4 | | | **28.5** | |
| | 11:00 | 31.4 | 30.3 | | | 30.3 | | 30.0 | | | 29.1 | |
| | 12:00 | 32.3 | 30.6 | | | 30.6 | | 30.5 | | | 29.6 | |
| | 13:00 | 33.3 | 30.9 | | | 30.9 | | 31.0 | | | 30.1 | |
| | 14:00 | 33.4 | 31.1 | | | 31.1 | | 31.3 | | | 30.4 | |
| | 15:00 | 33.6 | 31.3 | | | 31.3 | | 31.5 | | | 30.6 | |
| | 16:00 | 33.8 | 31.4 | | | 31.4 | | 31.7 | | | 30.8 | |
| | 17:00 | 32.7 | 31.4 | | | 31.4 | | 31.5 | | | 30.6 | |
| | 18:00 | 31.6 | 31.2 | | | 31.2 | | 31.0 | | | 30.1 | |
| | 19:00 | 30.4 | 31.0 | | | 31.0 | | 30.5 | | | 29.6 | |
| | 20:00 | 29.8 | 30.9 | | | 30.9 | | 30.2 | | | 29.3 | |
| | 21:00 | 29.2 | 30.7 | | | 30.7 | | 29.9 | | | **29.0** | |
| | 22:00 | 28.5 | 30.6 | | | 30.6 | | 29.5 | | | **28.6** | |
| | 23:00 | 28.2 | 30.4 | | | 30.4 | | 29.3 | | | **28.4** | |

**Table C- 20** Percentage of thermal comfort hours during the target time of the day of the north-facing reference and test rooms on floor 23$^{rd}$ under external wind speed of 1ms$^{-1}$ and wind incident angle of 0° (*continued*).

| Season | Time | Reference room | | | | | | Test room | | | | |
|---|---|---|---|---|---|---|---|---|---|---|---|---|
| | | Tout (°C) | $T_{op}$ (°C) | *Vin.av (m/s)* | dT (°C) | $T_{comp}$ (°C) | Percentage of comfort hours (%) | $T_{op}$ (°C) | *Vin.av (m/s)* | dT (°C) | $T_{comp}$ (°C) | Percentage of comfort hours (%) |
| **Rainy** | 00:00 | 27.3 | 29.5 | 0.04 | 0 | 29.5 | 8.3 | 28.4 | 0.35 | 0.9 | **27.5** | 70.8 |
| | 01:00 | 27.1 | 29.4 | | | 29.4 | | 28.2 | | | **27.3** | |
| | 02:00 | 26.9 | 29.3 | | | 29.3 | | 28.1 | | | **27.2** | |
| | 03:00 | 26.6 | 29.1 | | | 29.1 | | 27.9 | | | **27.0** | |
| | 04:00 | 26.4 | 29.0 | | | 29.0 | | 27.8 | | | **26.9** | |
| | 05:00 | 26.4 | 28.9 | | | 28.9 | | 27.7 | | | **26.8** | |
| | 06:00 | 26.4 | 28.9 | | | **28.9** | | 27.6 | | | **26.7** | |
| | 07:00 | 26.5 | 28.9 | | | **28.9** | | 27.6 | | | **26.7** | |
| | 08:00 | 27.7 | 29.0 | | | 29.0 | | 27.9 | | | **27.0** | |
| | 09:00 | 28.9 | 29.3 | | | 29.3 | | 28.5 | | | **27.6** | |
| | 10:00 | 28.4 | 29.5 | | | 29.5 | | 29.1 | | | **28.2** | |
| | 11:00 | 28.6 | 29.8 | | | 29.8 | | 29.5 | | | **28.6** | |
| | 12:00 | 28.8 | 30.0 | | | 30.0 | | 29.9 | | | 29.0 | |
| | 13:00 | 29.1 | 30.2 | | | 30.2 | | 30.3 | | | 29.4 | |
| | 14:00 | 29.2 | 30.4 | | | 30.4 | | 30.4 | | | 29.5 | |
| | 15:00 | 29.3 | 30.5 | | | 30.5 | | 30.5 | | | 29.6 | |
| | 16:00 | 29.4 | 30.5 | | | 30.5 | | 30.5 | | | 29.6 | |
| | 17:00 | 29.3 | 30.5 | | | 30.5 | | 30.3 | | | 29.4 | |
| | 18:00 | 29.2 | 30.3 | | | 30.3 | | 29.9 | | | 29.0 | |
| | 19:00 | 29.0 | 30.1 | | | 30.1 | | 29.5 | | | **28.6** | |
| | 20:00 | 28.9 | 30.0 | | | 30.0 | | 29.2 | | | **28.3** | |
| | 21:00 | 28.2 | 29.9 | | | 29.9 | | 28.9 | | | **28.0** | |
| | 22:00 | 27.7 | 29.7 | | | 29.7 | | 28.7 | | | **27.8** | |
| | 23:00 | 27.5 | 29.6 | | | 29.6 | | 28.5 | | | **27.6** | |

**Table C- 20** Percentage of thermal comfort hours during the target time of the day of the north-facing reference and test rooms on floor 23rd under external wind speed of 1ms$^{-1}$ and wind incident angle of 0° (*continued*).

| Season | Time | Reference room | | | | | | Test room | | | | |
|---|---|---|---|---|---|---|---|---|---|---|---|---|
| | | Tout (°C) | $T_{op}$ (°C) | *Vin.av (m/s)* | dT (°C) | $T_{comp}$ (°C) | Percentage of comfort hours (%) | $T_{op}$ (°C) | *Vin.av (m/s)* | dT (°C) | $T_{comp}$ (°C) | Percentage of comfort hours (%) |
| **Winter** | 00:00 | 25.7 | 28.2 | 0.04 | 0 | **28.2** | 70.8 | 27.2 | 0.35 | 0.9 | **26.3** | 100 |
| | 01:00 | 25.2 | 28.0 | | | **28.0** | | 26.9 | | | **26.0** | |
| | 02:00 | 24.8 | 27.8 | | | **27.8** | | 26.7 | | | **25.8** | |
| | 03:00 | 24.4 | 27.7 | | | **27.7** | | 26.4 | | | **25.5** | |
| | 04:00 | 24.1 | 27.5 | | | **27.5** | | 26.2 | | | **25.3** | |
| | 05:00 | 23.9 | 27.3 | | | **27.3** | | 26.0 | | | **25.1** | |
| | 06:00 | 23.7 | 27.2 | | | **27.2** | | 25.8 | | | **24.9** | |
| | 07:00 | 24.0 | 27.1 | | | **27.1** | | 25.6 | | | **24.7** | |
| | 08:00 | 25.3 | 27.2 | | | **27.2** | | 25.9 | | | **25.0** | |
| | 09:00 | 26.6 | 27.5 | | | **27.5** | | 26.5 | | | **25.6** | |
| | 10:00 | 27.6 | 27.8 | | | **27.8** | | 27.1 | | | **26.2** | |
| | 11:00 | 28.0 | 28.0 | | | **28.0** | | 27.6 | | | **26.7** | |
| | 12:00 | 28.3 | 28.3 | | | **28.3** | | 28.2 | | | **27.3** | |
| | 13:00 | 28.7 | 28.6 | | | **28.6** | | 28.7 | | | **27.8** | |
| | 14:00 | 29.0 | 28.8 | | | 28.8 | | 29.1 | | | **28.2** | |
| | 15:00 | 29.2 | 29.0 | | | 29.0 | | 29.3 | | | **28.4** | |
| | 16:00 | 29.4 | 29.1 | | | 29.1 | | 29.4 | | | **28.5** | |
| | 17:00 | 29.3 | 29.1 | | | 29.1 | | 29.3 | | | **28.4** | |
| | 18:00 | 29.2 | 28.9 | | | 28.9 | | 28.9 | | | **28.0** | |
| | 19:00 | 29.1 | 28.8 | | | 28.8 | | 28.5 | | | **27.6** | |
| | 20:00 | 28.9 | 28.7 | | | 28.7 | | 28.2 | | | **27.3** | |
| | 21:00 | 27.1 | 28.6 | | | **28.6** | | 27.9 | | | **27.0** | |
| | 22:00 | 26.6 | 28.4 | | | **28.4** | | 27.7 | | | **26.8** | |
| | 23:00 | 26.2 | 28.3 | | | **28.3** | | 27.4 | | | **26.5** | |

** The **bold and italic** results of compensate temperatures (Tcomp) indicate the temperatures within the comfort temperature range calculated for each season according to its average dry-bulb temperatures and the colored boxes indicate the target time of the day i.e. 10am to 8pm.*

**Table C- 21** Percentage of comfort hour (%) in the north-facing reference and test rooms on floor 23rd under external wind speed of 1ms$^{-1}$ and wind incident angle of 0° during different seasons.

| Seasons | Reference room | Test room |
|---|---|---|
| summer | 0 | 58.3 |
| rainy | 8.3 | 70.8 |
| winter | 70.8 | 100 |

**Table C- 22** Percentage of comfort hour (%) in the north-facing reference and test rooms on floor 23rd under external wind speed of $1\mathrm{ms}^{-1}$ and wind incident angle of 0° during target time i.e. 10am to 8pm in different seasons.

| Seasons | Reference room | Test room |
|---|---|---|
| summer | 0 | 9.1 |
| rainy | 0 | 36.4 |
| winter | 36.4 | 100 |

**Table C- 23** Energy saving per annum of the studied building by employing ventilation shaft strategy comparing to typical air conditioner (5kWh).

| Electricity saving compared to a/c | South facing room | | | North facing room | | |
|---|---|---|---|---|---|---|
| | Summer | Rainy | Winter | Summer | Rainy | Winter |
| Comfort hour per day of a reference room (%) | 29.2 | 66.7 | 62.5 | 0 | 8.3 | 70.8 |
| Comfort hour per day of a test room (%) | 62.5 | 79.2 | 87.5 | 58.3 | 70.8 | 100 |
| Extension of comfort hour per day (%) | 33.3 | 12.5 | 25 | 58.3 | 62.5 | 29.2 |
| Electricity saving per unit per day (W)* | 39960 | 15000 | 30000 | 69960 | 75000 | 35040 |
| Electricity saving per unit per season (MW) | 4.7952 | 1.8 | 3.6 | 8.3952 | 9 | 4.2048 |
| Electricity saving per unit per annum (MW) | | 10.1952 | | | 21.6 | |
| Electricity saving per annum (MW)** | | 1835.136 | | | 3456 | |
| **Overall energy saving per annum (MW)** | **5291.136** | | | | | |

** Calculating based on a typical 5kWh split type.*

*** There are 180 south-facing units and 160 north-facing units in the building.*

**Table C- 24** Energy saving per annum of the studied building by employing ventilation shaft strategy comparing to typical ceiling fan (65Wh).

| Electricity saving compared to electric fan | South facing room | | | North facing room | | |
|---|---|---|---|---|---|---|
| | Summer | Rainy | Winter | Summer | Rainy | Winter |
| Comfort hour per day of a reference room (%) | 29.2 | 66.7 | 62.5 | 0 | 8.3 | 70.8 |
| Comfort hour per day of a test room (%) | 62.5 | 79.2 | 87.5 | 58.3 | 70.8 | 100 |
| Extension of comfort hour per day (%) | 33.3 | 12.5 | 25 | 58.3 | 62.5 | 29.2 |
| Electricity saving per unit per day (W)* | 519.48 | 195 | 390 | 909.48 | 975 | 455.52 |
| Electricity saving per unit per season (W) | 62337.6 | 23400 | 46800 | 109137.6 | 117000 | 54662.4 |
| Electricity saving per unit per annum (W) | | 132537.6 | | | 280800 | |
| Electricity saving per annum (W)** | | 23856768 | | | 44928000 | |
| **Overall energy saving per annum (MW)** | **68.784768** | | | | | |

** Calculating based on a typical 65Wh electric ceiling fan (48inch).*

*** There are 180 south-facing units and 160 north-facing units in the building.*

**Table C- 25** Energy saving of the studied building during target time of a day by employing ventilation shaft strategy compared to typical a/c (5kWh).

| Electricity saving compared to a/c | South facing room | | | North facing room | | |
|---|---|---|---|---|---|---|
| | Summer | Rainy | Winter | Summer | Rainy | Winter |
| Comfort hour per day of a reference room (%) | 0 | 27.3 | 27.3 | 0 | 0 | 36.4 |
| Comfort hour per day of a test room (%) | 18.2 | 54.5 | 72.7 | 9.1 | 36.4 | 100 |
| Extension of comfort hour/day during target time (%) | 18.2 | 27.2 | 45.4 | 9.1 | 36.4 | 63.6 |
| Electricity saving per unit per day (W)* | 10010 | 14960 | 24970 | 5005 | 20020 | 34980 |
| Electricity saving per unit per season (MW) | 1.2012 | 1.7952 | 2.9964 | 0.6006 | 2.4024 | 4.1976 |
| Electricity saving per unit per annum (MW) | 5.9928 | | | 7.2006 | | |
| Electricity saving per annum (MW)** | 1078.704 | | | 1152.096 | | |
| **Overall energy saving per annum (MW)** | **2230.08** | | | | | |

** Calculating based on a typical 5kWh split type.*

*** There are 180 south-facing units and 160 north-facing units in the building.*

**Table C- 26** Energy saving of the studied building during target time of a day by employing ventilation shaft strategy compared to typical ceiling fan (65Wh).

| Electricity saving compared to electric fan | South facing room | | | North facing room | | |
|---|---|---|---|---|---|---|
| | Summer | Rainy | Winter | Summer | Rainy | Winter |
| Comfort hour per day of a reference room (%) | 0 | 27.3 | 27.3 | 0 | 0 | 36.4 |
| Comfort hour per day of a test room (%) | 18.2 | 54.5 | 72.7 | 9.1 | 36.4 | 100 |
| Extension of comfort hour/ day during target time (%) | 18.2 | 27.2 | 45.4 | 9.1 | 36.4 | 63.6 |
| Electricity saving per unit per day (W)* | 130.13 | 194.48 | 324.61 | 65.065 | 260.26 | 454.74 |
| Electricity saving per unit per season (W) | 15615.6 | 23337.6 | 38953.2 | 7807.8 | 31231.2 | 54568.8 |
| Electricity saving per unit per annum (W) | 77906.4 | | | 93607.8 | | |
| Electricity saving per annum (W)** | 14023152 | | | 14977248 | | |
| **Overall energy saving per annum (MW)** | **29.0004** | | | | | |

** Calculating based on a typical 65Wh electric ceiling fan (48inch).*

*** There are 180 south-facing units and 160 north-facing units in the building.*

# Appendix D

## Published Papers

The following papers have been published according to the results of this study:

1) PRAJONGSAN, P. & SHARPLES, S. 2012. Enhancing natural ventilation, thermal comfort and energy savings in high-rise residential buildings in Bangkok through the use of ventilation shafts. *Building and Environment,* 50**,** 104-113.

2) PRAJONGSAN, P. & SHARPLES, S. An alternative passive cooling strategy for high-rise residential buildings in hot-humid climates. PLEA2012 - 28th Conference, Opportunities, Limits & Needs Towards an environmentally responsible architecture, 7-9 November 2012 Lima, Peru.

# References

AFONSO, C. & OLIVEIRA, A. 2000. Solar chimneys: Simulation and experiment. *Energy and Buildings,* 32**,** 71-79.

AI, Z. T. & MAK, C. M. 2014. Determinination of single-sided ventilation rates in multistory buildings: Evaluation of methods. *Energy and Buildings,* 69**,** 292-300.

ALEMU, A. T., SAMAN, W. & BELUSKO, M. 2012. A model for integrating passive and low energy airflow compoenets into low rise buildings. *Energy and Buildings,* 49**,** 148-157.

ALLARD, F. (ed.) 1998. *Natural ventilation in buildings: a design handbook,* London: James&James (Science Publishers) Ltd,.

ALLOCCA, C., CHEN, Q. & GLICKSMAN, L. R. 2003. Design analysis of single-sided natural ventilation. *Energy and Buildings,* 35**,** 785-795.

ARENS, E., TURNER, S., ZHANG, H. & PALIAGA, G. 2009. Moving air for comfort. *ASHRAE Journal,* 51**,** 18-28.

ARUMI, F. & HOURMANESH, M. 1977. Energy performance of solar walls: A computer analysis. *Energy and Buildings,* 1**,** 167-174.

ASHRAE 2009. *ASHRAE handbook - fundamentals* American Society of Heating, Refrigerating and Air-Conditioning Engineers, Inc.

ASHRAE 2013. *ASHRAE handbook - fundamentals* American Society of Heating, Refrigerating and Air-Conditioning Engineers, Inc.

AULICIEMS, A. & SZOKOLAY, S. 2007. *Thermal comfort (2nd edition),* Brisbane, PLEA Notes.

AWBI, H. B. 1994. Design considerations for naturally ventilated buildings. *Renewable Energy,* 5**,** 1081-1090.

AWBI, H. B. 1998. Ventilation. *Renewable and Sustainable Energy Reviews,* 2**,** 157-188.

AWBI, H. B. 2003. *Ventilation of buildings (2nd edition),* London, Spon Press.

AWBI, H. B. (ed.) 2008. *Ventilation systems: design and performance,* London: Taylor&Francis.

AYNSLEY, R. 2007. *Natural ventilation in passive design* [Online]. The Environment Design Guider, Australia Institute of Architects. Available: http://www.environmentdesignguide.com.au/pages/content/tec--technology/tec-2-natural-ventilation-in-passive-design.php [Accessed June 2012].

BAHADORI, M. N. 1994. Viability of wind towers in achieving summer comfort in the hot arid regions of the middle east. *Renewable Energy,* 5**,** 879-892.

BAHADORI, M. N., M.MAZIDI & DEHGHANI, A. R. 2008. Experimental investigation of new designs of wind towers. *Renewable Energy,* 33**,** 2273-2281.

BALDINELLI, G. 2009. Double-skin facades for warm climate regions: Analysis of a solution with an integrated movable shading system. *Building and Environment,* 44**,** 1107-1118.

BANSAL, N. K., HAUSER, G. & MINKE, G. 1994a. *Passive building design: a handbook of natural climate control,* Amsterdam, Elseview Science.

BANSAL, N. K., MATHUR, J., MATHUR, S. & JAIN, M. 2005. Modeling of window-sized solar chimneys for ventilation. *Building and Environment,* 40**,** 1302-1308.

BANSAL, N. K., MATHUR, R. & BHANDARI, M. S. 1993. Solar chimney for enhanced stack ventilation. *Building and Environment,* 28**,** 373-377.

BANSAL, N. K., MATHUR, R. & BHANDARI, M. S. 1994b. A study of solar chimney assisted wind tower system for natural ventilation in buildings. *Building and Environment,* 29.

BAROZZO, G. S., M.S.E., I., E., N. & A.C.M., S. 1992. Physical and numerical modelling of a silar chimney-based ventilation system for buildings. *Building and Environment,* 27**,** 433-445.

BASSIOUNY, R. & KORAH, N. S. A. 2009. Effect of solar chimney inclination angle on space flow pattern and ventilation rate. *Energy and Buildings,* 41**,** 190-196.

BASTIDE, A., LAURET, P., GARDE, F. & BOYER, H. 2006. Building energy efficiency and thermal comfort in tropical climates: presentation of a numerical approach for predicting the percentage of well-ventilated living spaces in buildings using natural ventilation. *Energy and Buildings,* 38**,** 1093-1103.

BLOCKEN, B., HOOFF, T. V., AANEN, L. & BRONSEMA, B. 2011. Computational analysis of the performance of a venturi-shaped roof for natural ventilation: Venturi-effect versus wind-blocking effect. *Computers & Fluid,* 48**,** 202-213.

BOJIC, M. & KOSTIC, S. 2006. Application of COMIS software for ventilation study in a typical building in Serbia. *Building and Environment,* 41**,** 12-20.

BOUCHAHM, Y., BOURBIA, F. & BALHAMRI, A. 2011. Performance analysis and improvement of the use of wind tower in hot dry climate. *Renewable Energy,* 36**,** 898-906.

BRADLEY, D. E. & UTZINGER, D. M. 2007. Enhancement and use of combined simulation tools in the assessment of hybrid natural/ mechanical ventilation systems. *ASHRAE Transactions,* 113 part 2**,** 144-153.

BRAGER, G. S. & DE DEAR, R. J. 1998. Thermal adaptation in the built environment: a literature review. *Energy and Buildings,* 27**,** 83-96.

BRAGER, G. S. & DEAR, R. D. 2000. A standard for natural ventilation. *ASHRAE Journal,* 42**,** 21-28.

BRANAGE-THAICOON. 2010. Monitoring Real Estates in Bangkok (in Thai). *Siamrath*.

BYRNE, S. J., HUANG, Y. J., RITSCHARD, R. L. & FOLEY, D. M. The potential for wind induced ventilation to meet occupant comfort conditions. The second symposium on improving building systems in hot and humid climates, 1985 Texas. 166-174.

CACIOLO, M., CUI, S., STABAT, P. & MARCHIO, D. 2013. Development of a new correlation for single-sided natural ventilation adapted to leeward conditions. *Energy and Buildings,* 60**,** 372-382.

CACIOLO, M., STABAT, P. & MARCHIO, D. 2011. Full scale experimental study of single-sided ventilation: Analysis of stack and wind effects. *Energy and Buildings,* 43**,** 1765-1773.

CACIOLO, M., STABAT, P. & MARCHIO, D. 2012. Numerical simulation of single-sided ventilation using RANS and LES and comparison with full-scale experiments. *Building and Environment,* 50**,** 202-213.

CÂNDIDO, C., DE DEAR, R. J., LAMBERTS, R. & BITTENCOURT, L. 2010. Air movement acceptability limits and thermal comfort in Brazil's hot humid climate zone. *Building and Environment,* 45**,** 222-229.

CANDIDO, C., DEAR, R. D. & LAMBERTS, R. 2011. Combined thermal acceptability and air movement assessment in a hot humid climate. *Building and Environment,* 46**,** 379-385.

CHAN, A. L. S., CHOW, T. T., FONG, K. F. & LIN, Z. 2009. Investigation on energy performance of double-skin facade in Hong-Kong. *Energy and Buildings,* 41**,** 1135-1142.

CHAN, H.-Y., RIFFAT, S. B. & ZHU, J. 2010. Review of passive solar heating and cooling technologies. *Renewable and Sustainable Energy Reviews,* 14**,** 781-789.

CHEN, Q. 2009. Ventilation performance prediction for buildings: A method overview and recent applications. *Building and Environment,* 44**,** 848-858.

CHEN, Q., LEE, K., MAZUMDAR, S., POUSSOU, S. & WANG, L. 2010. Ventilation performance prediction for buildings: Model assessment. *Building and Environment,* 45**,** 295-303.

CHENVIDYAKARN, T. & WOODS, A. 2007. Stratification and oscillations produced by pre-cooling during transient natural ventilation. *Building and Environment,* 42**,** 99-112.

CHIRARATTANANON, S. & CHAIWIWATWORAKUL, P. Revised building energy code of Thailand: Potential energy and power demand savings. Conference on energy network of Thailand (2nd), 2006 Nakhon Rachasima, Thailand.

CHOU, S. K., CHUA, K. J. & HO, J. C. 2009. A study on the effects of double skin facades on the eneregy management in buildings. *Energy Conversion and Management,* 50**,** 2275-2281.

CHOW, T. T., FONG, K. F., GIVONI, B., LIN, Z. & CHAN, A. L. S. 2010. Thermal sensation of Hong Kong people with increased air speed, temperature and humidity in air-conditioned environment. *Building and Environment,* 45**,** 2177-2183.

CHUNGLOO, S. & LIMMEECHOKCHAI, B. 2007. Application of passive cooling systems in the hot and humid climate: The case study of solar chimney and wetted roof in Thailand. *Building and Environment,* 42**,** 3341-3351.

CHUNGLOO, S. & LIMMEECHOKCHAI, B. 2009. Utilization of cooling ceiling with solar chimney in Thailand: The experimental and numerical analysis. *Renewable Energy,* 34**,** 623-633.

CÓSTOLA, D., BLOCKEN, B. & HENSEN, J. L. M. 2009. Overview of pressure coefficient data in building energy simulation and airflow network programs. *Building and Environment,* 44**,** 2027-2036.

DAI, Y. J., SUMATHY, K., WANG, R. Z. & LI, Y. G. 2003. Enhancement of natural ventilation in a solar house with a solar chimney and a solid adsorption cooling cavity. *Solar Energy,* 74**,** 65-75.

DAVIDOVIC, D., PINON, J., BURNETT, E. F. P. & SREBRIC, J. 2012. Analytical procedures for estimating airflow rates in ventilated, screened wall systems (VSWS). *Building and Environment,* 47**,** 126-137.

DE DEAR, R. J. & BRAGER, G. S. 1998. Developing an adaptive model of thermal comfort and preference. *ASHRAE Transactions,* 104 Part 1.

DE DEAR, R. J. & BRAGER, G. S. 2001. The adaptive model of thermal comfort and energy conservation in the built environment. *International Journal of Biometeorol,* 45**,** 100-108.

DEBLOIS, J. C., BILEC, M. M. & SCHAEFER, L. A. 2013. Design and zonal building energy modeling of a roof integrated solar chimney. *Renewable Energy,* 52**,** 241-250.

DEDE 2010. Electric power in Thailand: Annual report. Bangkok: Alternative Energy and Efficiency Information Center, Department of Alternative Energy Development and Efficiency (DEDE), Ministry of Energy.

DEDE 2014. Energy in Thailand: Facts and Figures 2013. Department of Alternative Energy Development and Efficiency, Ministry of Energy.

DEHGHAN, A. A., ESFEH, M. K. & MANSHADI, M. D. 2013. Natural ventilation characteristics of one-sided wind catchers: experimental and analytical evaluation. *Energy and Buildings,* 61**,** 366-377.

DESIGNBUILDER 2006a. *DesignBuilder 1.2 User Manual*.

DESIGNBUILDER. 2006b. *DesignBuilder vesion 2.3.5.034* [Online]. Gloucestershire, UK. Available: http://www.designbuilder.co.uk/.

DJAMILA, H., CHU, C.-M. & KUMARESAN, S. 2013. Field study of thermal comfort in residential buildings in the equatorial hot-humid climate of Malaysia. *Building and Environment,* 62**,** 133-142.

DORER, V. & WEBER, A. 1999. Air, contaminant and heat transport models: intehration and application. *Energy and Buildings,* 30**,** 97-104.

DUTT, A. J., DEAR, R. J. D. & KRISHNAN, P. 1992. Full scale and model investigation of natural ventilation and thermal comfort in a building. *Journal of Wind Engineering and Industrial Aerodynamics,* 41-44**,** 2599-2609.

EFTEKHARI, M. M., MARJANOVIC, L. D. & PIMMOCK, D. J. 2003. Air flow distribution in and around a single-sided naturally ventilated room. *Building and Environment,* 38**,** 389-397.

EMMERICH, S. J., DOLS, W. S. & AXLEY, J. W. 2009. Natural ventilation review and plan for design and analysis tools. U.S.A: National institute of standards and technology.

ERNEST, D., BAUMAN, F. & ARENS, E. 1991. The prediction of indoor air motion for occupant cooling in naturally ventilated buildings. *ASHRAE Transactions,* 97**,** 539-552.

ETHERIDGE, D. & SANDBERG, M. 1996. *Building ventilation: theory and measurement,* Chichester, John Wiley & Sons.

EVOLA, G. & POPOV, V. 2006. Computational analysis of wind driven natural ventilation in buildings. *Energy and Buildings,* 38**,** 491-501.

FANGER, P. O. 1970. *Thermal comfort: analysis and applications in environmental engineering,* New York, McGraw-Hill.

FEUSTEL, H. E. & DIERIS, J. 1992. A survey of airflow models for multizone structures. *Energy and Buildings,* 18**,** 79-100.

FOUNTAIN, M. & ARENS, E. 1993. Air movement and thermal comfort: The new ASHRAE Standard 55 provides information on appropriate indoor air velocities for occupant comfort. *ASHRAE Journal,* 35**,** 26-30.

FOUNTAIN, M., BAUMAN, F., ARENS, E., MIURA, K. & DEAR, R. D. 1994. Locally controlled air movement preferred in warm isothermal environments. *ASHRAE Transactions,* 100**,** 937-952.

FREIRE, R. Z., ABADIE, M. O. & MENDES, N. 2013. On the improvement of natural ventilation models. *Energy and Buildings,* 62**,** 222-229.

GAN, G. 1998. A parametric study of Trombe walls for passive cooling of buildings. *Energy and Buildings,* 27**,** 37-43.

GAN, G. 2001. Thermal transmittance of multiple glazing: computational fluid dynamics prediction. *Applied Thermal Engineering,* 21**,** 1583-1592.

GAN, G. 2006. Simulation of buoyancy-induced flow in open cavities for natural ventilation. *Energy and Buildings,* 38**,** 410-420.

GAO, J., ZHOA, J. N., LI, X. D. & GAO, F. S. 2006. A zonal model for large enclosures with combined stratification cooling and natural ventilation: Part 1 - Model generation and its procedure. *Journal of Solar Energy Engineering,* 128**,** 367-375.

GHIAUS, C. & ALLARD, F. (eds.) 2005. *Natural ventilation in the urban environment: Assessment and design,* London: Earthscan.

GIVONI, B. 1976. *Man, climate and architecture (2nd edition),* London, Applied science publishers.

GIVONI, B. 1981. *Man, climate and architecture (2nd Edition),* London, Applied science publisher.

GIVONI, B. 1991. Performance and applicability of passive and low-energy cooling systems. *Energy and Buildings,* 17**,** 177-199.

GIVONI, B. 1992. Comfort, climate analysis amd building design guidelines. *Energy and Buildings,* 18**,** 11-23.

GIVONI, B. 1994. *Passive low energy cooling of buildings,* New York, John Wiley & Sons.

GIVONI, B. 1998. *Climate considerations in building and urban design,* New York, John Wiley & Sons,Inc.

GIVONI, B., KHEDARI, J., WONG, N. H. & NOGUCHI, M. 2006. Thermal sensation responses in hot, humid climates: effects of humidity. *Building Research & Information,* 34**,** 496-506.

GONG, N., THAM, K. W., MELIKOV, A. K., WYON, D. P., SEKHAR, S. C. & CHEONG, K. W. 2006. The acceptable air velocity range for local air movement in the tropics. *HVAC and R Research,* 12**,** 1065-1076.

GONZALEZ-TREVIZO, M. E., GONZALEZ-LICON, H. J., GOMEZ-AMADOR, A., POZO, C. E. D. & LOPEZ, C. J. E. Exhaust ventilation through a wind tower as response to high hermeticity in welfare housing. PLEA2013 - 29th Conference, Sustainable Architecture for a Renewable Future, 2013 Munich, Germany.

GOOD, J., FRISQUE, A. & PHILLIPS, D. The role of wind in natural ventilation simulations using airflow network models. Third National Conference of IBPSA-USA, July 30-August 1, 2008 2008 California.

GRATIA, E. & HERDE, A. D. 2004a. Natural ventilation in a double-skin facade. *Energy and Buildings,* 36**,** 137-146.

GRATIA, E. & HERDE, A. D. 2004b. Optimal operation of a south double-skin facade. *Energy and Buildings,* 36**,** 41-60.

GRATIA, E. & HERDE, A. D. 2007. Guidelines for improving natural daytime ventilation in an office building with a double-skin facade. *Solar Energy,* 81**,** 435-448.

HAASE, M. & AMATO, A. Sustainble facade design for zero energy buildings in the tropics. PLEA2006 - The 23rd Conference on Passive and Low Energy Architecture, 2006 Geneva, Switzerland. 6-8 September 2006.

HAASE, M. & AMATO, A. 2009. An investigation of the potential for natural ventilation and building orientation to achieve thermal comfort in warm and humid climates. *Solar Energy,* 83**,** 389-399.

HAASE, M., SILVA, F. M. D. & AMATO, A. 2009. Simulation of ventilated facades in hot and humid climates. *Energy and Buildings,* 41**,** 361-373.

HAGHIGHAT, F., LI, Y. & MEGRI, A. C. 2001. Development and validation of a zonal model - POMA. *Building and Environment,* 36**,** 1039-1047.

HAMDY, I. F. & FIRKRY, M. A. 1998. Passive solar ventilation. *Renewable Energy,* 14**,** 381-386.

HARRIS, D. J. & HELWIG, N. 2007. Solar chimney and building ventilation. *Applied Energy,* 84**,** 135-146.

HAW, L. C., SAADATIAN, O., SULAIMAN, M. Y., MAT, S. & SOPIAN, K. 2012. Empirical study of a wind-induced natural ventilation tower under hot and humid climatic conditions. *Energy and Buildings,* 52**,** 28-38.

HIRUNLABH, J., WACHIRAPUWADON, S., PRATINTHONG, N. & KHEDARI, J. 2001. New configurations of a roof solar collector maximizing natural ventilation. *Building and Environment,* 36**,** 383-391.

HITCHIN, E. R. & WILSON, C. B. 1967. A review of experimental techniques for the investigation of natural ventilation in buildings. *Building Sci.,* 2**,** 59-82.

HOOFF, T. V., BLOCKEN, B., AANEN, L. & BRONSEMA, B. 2011. A venturi-shaped roof wind-induced natural ventilation of buildings: Wind tunnel and CFD evaluation of different design configurations. *Building and Environment,* 46**,** 1797-1807.

HUGHES, B. R., CALUATIT, J. K. & GHANI, S. A. 2012. The development of commercial wind towers for natural ventilation: A review. *Applied Energy,* 92**,** 606-627.

HUNT, G. R. & KAYE, N. B. 2006. Pollutant flushing with natural displacement ventilation. *Building and Environment,* 41**,** 1190-1197.

HUSSAIN, S. & OOSTHIZEN, P. H. 2012. Validation of numerical modeling of conditions in an atrium space with a hybrid ventilation system *Building and Environment,* 52**,** 152-161.

HYDE, R. 2000. *Climate responsive design,* London, E&FN Spon.

IMANO, M., ZHENG, Y., AKAMINE, Y., AREEMIT, N., KAMATA, M. & SAKAMOTO, Y. 2008. Study on utility cross-ventilation in Guangzhou and Shenzhen, China. *Journal of Asian Architecture and Building Engineering,* 7**,** 131-138.

INDRAGANTI, M., OOKA, R., RIJAL, H. B. & BRAGER, G. S. 2014. Adaptive model of thermal comfort for offices in hot and humid climates of India. *Building and Environment,* 74**,** 39-53.

JAMALUDIN, A. A., HUSSEIN, H., ARIFFIN, A. R. M. & KEUMALA, N. 2014. A study on different natural ventilation approaches at a residential college building with the internal courtyard arrangement. *Energy and Buildings,* 72**,** 340-352.

JIANG, Y., ALEXANDER, D., JENKINS, H., ARTHUR, R. & CHEN, Q. 2003. Natural ventilation in buildings: measurement in a wind tunnel and numerical simulation with large-eddy simulation. *Journal of Wind Engineering,* 91**,** 331-353.

JIANG, Y. & CHEN, Q. 2003. Buoyancy-driven single-sided natural ventilation in buildings with large openings. *International Journal of Heat and Mass Transfer,* 46**,** 973-988.

JOHN D. ANDERSON, J. 1995. *Computational Fluid Dynamics: the basics with applications,* New York, McGraw-Hill.

KHAN, N., SU, Y. & RIFFAT, S. B. 2008. A review on wind driven ventilation techniques. *Energy and Buildings,* 40**,** 1586-1604.

KHANAL, R. & LEI, C. 2011. Solar chimney - A passive strategy for natural ventilation. *Energy and Buildings,* 43**,** 1811-1819.

KHEDARI, J., BOONSRI, B. & HIRUNLABH, J. 2000a. Ventilation impact of a solar chimney on indoor temperature fluctuation and air change in a school building. *Energy and Buildings,* 32**,** 89-93.

KHEDARI, J., HIRUNLABH, J. & BUNNAG, T. 1997. Experimental study of a roof solar collector towards the natural ventilation of new houses. *Energy and Buildings,* 26**,** 159-164.

KHEDARI, J., MANSIRISUB, W., CHAIMA, S., PRATINTHONG, N. & HIRUNLABH, J. 2000b. Field measurements of performance of roof solar collector. *Energy and Buildings,* 31**,** 171-178.

KHEDARI, J., YAMTRAIPAT, N., PRATINTONG, N. & HIRUNLABH, J. 2000c. Thailand ventilation comfort chart. *Energy and Buildings,* 32**,** 245-249.

KLEVIEN, T. 2003. *Natural ventilation in buildings: architectural concepts, consequences and possibilities.* PhD., Norwegian University of Science and Technology.

KOBAYASHI, T., CHIKAMOTO, T. & OSADA, K. 2013. Evaluation of ventilation performance of monitor roof in residential area based on simplified estimation and CFD analysis. *Building and Environment,* 63**,** 20-30.

KOINAKIS, C. J. 2005. The effect of the use of openings on interzonal air flows in buildings: an experimental and simulation approach. *Energy and Buildings,* 37**,** 813-823.

KUBOTA, T., CHYEE, D. T. H. & AHMAD, S. 2009. The effects of night ventilation technique on indoor thermal environment for residential buildings in hot-humid climate of Malaysia. *Energy and Buildings,* 41**,** 829-839.

KWONG, Q. J., ADAM, N. M. & SAHARI, B. B. 2014. Thermal comfort assessment and potential for energy efficiency enhancement in modern tropical buildings: A review. *Energy and Buildings***,** 547-557.

LARSEN, T. S. & HEISELBERG, P. 2008. Single-sided natural ventilation driven by wind pressure and temperature difference. *Energy and Buildings,* 40**,** 1031-1040.

LEE, K. H. & STRAND, R. K. 2009. Enhancement of natural ventilation in buildings using a thermal chimney. *Energy and Buildings,* 41**,** 615-621.

LEI, G. Naturally ventilated urban housing in Southern China: A research review on current Energy Efficient Residential Design Code. PLEA 2009 - 26th Conference on Passive and Low Energy Architecture, 2009 Quebec City, Canada.

LEITE, R. C. V. & FROTA, A. B. Evaluating thermal performance of residential buildings in different urban environments: Discussing a methodology to assess the impacts of densely built-up areas on indoor conditions. PLEA2013 - 29th Conference, Sustainable Architecture for a Renewable Future, 2013 Munich, Germany.

LI, L. & MAK, C. M. 2007. The assessment of the performance of a windcatcher system using computational fluid dynamics. *Building and Environment,* 42**,** 1135-1141.

LI, Y. & DELSANTE, A. 2001. Natural ventilation induced by combined wind and thermal forces. *Building and Environment,* 36**,** 59-71.

LI, Y., DELSANTE, A. & SYMONS, J. 2000. Prediction of natural ventilation in buildings with large openings. *Building and Environment,* 35**,** 191-206.

LI, Y., DUAN, S. & ZHANG, G. 2005. Multiple solutions in a building with four openings ventilated by combined forces. *Indoor and built environment,* 14**,** 347-358.

LIN, Y. J. P. & LIN, C. L. 2014. A study on flow stratification in a space using displacement ventilation. *International Journal of Heat and Mass Transfer,* 73**,** 67-75.

LIN, Y. J. P. & TSAI, T. H. 2013. The push-type displacement ventilation in two series-connected chambers. *Building and Environment,* 62**,** 89-101.

LIU, C.-H. Computational fluid dynamic analysis of the function f wing walls for natural ventilation in high-rise buildings. *In:* SIVYER, E., ed. The construction and building research conference of the Royal Institute of Chartered Surveyors (COBRA), 2006 London.

LIVERMORE, S. & WOODS, A. 2006. Natural ventilation of multiple storey buildings: The use of stacks for secondary ventilation. *Building and Environment,* 41**,** 1339-1351.

LIVERMORE, S. & WOODS, A. 2007. Natural ventilation of a building with heating at multiple levels. *Building and Environment,* 42**,** 1417-1430.

LO, L. J., BANKS, D. & NOVOSELAC, A. 2013. Combined wind tunnel and CFD analysis for indoor airflow prediction of wind-driven cross ventilation. *Building and Environment,* 60**,** 12-23.

LO, L. J. & NOVOSELAC, A. 2012. Cross ventilation with small openings: Measurements in a multi-zone test building. *Building and Environment,* 57**,** 377-386.

LO, L. J. & NOVOSELAC, A. 2013. Effect of indoor buoyancy flow on wind-driven cross ventilation *Build Simul,* 6**,** 69-79.

M.H., G., LUKMAN, N. & MOHAMED, M. F. 2014. Applying computational fluid dynamic to evaluate the performance of four-sided rectagular wind catcher with different height. *Research Journal of Applied Sciences: Engineering and Technology,* 7**,** 502-509.

MAK, C. M., NLU, J. L., LEE, C. T. & CHAN, K. F. 2007. A numerical simulation of wing walls using computational fluid dynamics. *Energy and Buildings,* 39**,** 995-1002.

MALLICK, F. H. 1996. Thermal comfort and building design in the tropical climates. *Energy and Buildings,* 23**,** 161-167.

MATHUR, J., BANSAL, N. K., MATHUR, S., JAIN, M. & ANUPMA 2006. Experimental investigations on solar chimney for room ventilation. *Solar Energy,* 80**,** 927-935.

MET 2010. Bangkok's weather data 1998-2009. Bangkok: Thailand Meteorological Department.

MIYAZAKI, T., AKISAWA, A. & NIKAI, I. 2011. The cooling performance of a building integrated evaporative cooling system driven by solar energy. *Energy and Buildings,* 43**,** 2211-2218.

NGUYEN, A.-T. & REITER, S. 2014. A climate analysis tool for passive heating and cooling strategies in hot humid climate based on Typical Meteorological Year data sets. *Energy and Buildings,* 68**,** 756-763.

NICOL, F. 2004. Adaptive thermal comfort standards in the hot-humid tropics. *Energy and Buildings,* 36**,** 628-637.

NICOL, F. & HUMPHREYS, M. 2002. Adaptive thermal comfort and sustainable thermal standards for buildings. *Energy and Buildings,* 34**,** 572.

NICOL, F., HUMPHREYS, M., SYKES, O. & ROAF, S. (eds.) 1995. *Standards for thermal comfort: indoor air temperature standards for the 21st century,* London: Chapman&Hall.

NIELSEN, P. V. (ed.) 2007. *Computational Fluid Dynamics in Ventilation Design,* Brussels: Rehva.

NUGROHO, A. M. 2009. Solar chimney geometry for stack ventilation in a warm humid climate. *International Journal of Ventilation,* 8**,** 161-173.

OESTERLE, E., LIEB, R. D., LUTZ, M. & HEUSLER, W. 2001. *Double-skin facades: Integrated planning,* Munich, Prestel.

OLESEN, B. W. 2004. International standards for the indoor environment. *Indoor Air,* 14**,** 18-26.

OLESEN, B. W. & PARSONS, K. C. 2002. Introduction to thermal comfort standards and to the proposed new version of EN ISO 7730. *Energy and Buildings,* 34**,** 537-548.

OLGYAY, V. 1992. *Design with climate: Bioclimatic approach to architectural regionalism,* New York, Van Nostrand Reinhold.

ONG, K. S. 2003. A mathematicl model of a solar chimney. *Renewable Energy,* 28**,** 1047-1060.

PAVLOU, K., VASILAKOPOULOU, K. & SANTAMOURIS, M. 2009. The impact of several construction elements on the thermal performance of solar chimneys. *International Journal of Ventilation,* 8**,** 277-285.

POIRAZIS, H. 2006. Double skin facades: A literature review. Lund: Lund University.

POSNER, J. D., BUCHANAN, C. R. & DUNN-RANKIN, D. 2003. Measurement and prediction of indoor air flow in a model room. *Energy and Buildings,* 35**,** 515-526.

PRAJONGSAN, P. & SHARPLES, S. An alternative passive cooling strategy for high-rise residential buildings in hot-humid climates. PLEA2012 - 28th Conference, Opportunities, Limits & Needs Towards an environmentally resposible architecture, 7-9 November 2012 2012a Lima, Peru.

PRAJONGSAN, P. & SHARPLES, S. 2012b. Enhacing natural ventilation, thermal comfort and energy savings in high-rise residential buildings in Bangkok through the use of ventilation shafts. *Building and Environment,* 50**,** 104-113.

PRIANTO, E., BONNEAUD, F., DEPECKER, P. & PENEAU, J. P. 2000. Tropical humid architecture in natural ventilation efficient point of view. *International Journal on Architectural Science,* 1**,** 80-95.

PRIANTO, E. & DEPECKER, P. 2002. Characteristic of airflow as the effect of balcony, opening design and internal division on indoor velocity: A case study of traditional dwelling in urban living quarter in tropical humid region. *Energy and Buildings,* 34**,** 401-409.

PRIANTO, E. & DEPECKER, P. 2003. Optimization of architectural design elements in tropical humid region with thermal comfort approach. *Energy and Buildings,* 35.

PRIYADARSINI, R., CHEONG, K. W. & WONG, N. H. 2004. Enhancement of natural ventilation in high-rise residential buildings using stack system. *Energy and Buildings,* 36**,** 61-71.

PUNYASOMPUN, S., HIRUNLABH, J., KHEDARI, J. & ZEGHMATI, B. 2009. Investigation on the application of solar chimney for multi-storey buildings. *Renewable Energy,* 34**,** 2545-2561.

PUTHIPIROT, P., SRISUWAN, M., MAHATTHAVEEWONG, P. & PRAJONGSAN, P. 2007. Energy efficiency house reserach project prepared for Energy Policy and Planning Office (EPPO), The Ministry of Eneregy, Thailand. Bangkok: Architecture School, Silpakorn University.

RUPP, R. F. & GHISI, E. 2014. What is the most adequate method to assess thermal comfort in hybrid commercial buildings located in hot-humid summer climate? *Renewable and Sustainable Energy Reviews,* 29**,** 449-462.

SADAFI, N., SALLEH, E., HAW, L. C. & JAAFAR, Z. 2011. Evaluating thermal effects of internal courtyard in a tropical terrace house by computational simulation. *43*.

SADINENI, S. B., MADALA, S. & BOEHM, R. F. 2011. Passive building energy savings: A review of building envelope components. *Renewable and Sustainable Energy Reviews,* 15**,** 3617-3631.

SANDBERG, M., LUNDSTROM, H., NILSSON, H. O. & STYMNE, H. 2008. Experimental methods in ventilation. *Advances in building energy research,* 2**,** 159-210.

SANTAMOURIS, M. & ASIMAKOPOULOS, D. N. (eds.) 1996. *Passive cooling for buildings,* London: James and James Science Publishers.

SCHULZE, T. & EICKER, U. 2013. Controlled natural ventilation for energy efficient buildings. *Energy and Buildings,* 56**,** 221-232.

SHEN, X., ZHANG, G. & BJERG, B. 2012. Comparison of different methods for estimating ventilation rates through wind driven ventilated buildings. *Energy and Buildings,* 54**,** 297-306.

SPAIN, S. The spacing of ceiling fans for human comfort in warm temperature conditions. Forth symposium on improving building systems in hot and humid climates, 1987 Houston, TX. 219-225.

STAVRAKAKIS, G. M., KOUKOU, M. K., VRACHOPOULOS, M. G. & MARKATOS, N. C. 2008. Natural cross-ventilation in buildings: Building-scale experiments, numerical simulation and thermal comfort evaluation. *Energy and Buildings,* 40**,** 1666-1681.

STAVRIDOU, A. & PRINOS, P. 2013. Natural ventilation of buildings due to buoyancy assisted by wind: Investigating cross ventilation with computational and laboratory simulation. *Building and Environment,* 66**,** 104-119.

STEPHEN, C. & TURNER, P. E. 2011. What's new in ASHRAE's Standard on comfort. *ASHRAE Journal***,** 42-48.

SZOKOLAY, S. Dilemmas of warm-humid climate house design: heavy vs. lightweight + cooling effect of air movement. PLEA2000, 2000 Cambridge, England. James + James (Science) Published Limited, 144-9.

SZOKOLAY, S. 2004. *Introduction to architectural science: the basic of sustainable design,* Oxford, Architectural Press.

SZOKOLAY, S. 2008. *Introduction to architectural science: the basis of sustainable design, 2nd ed.,* Oxford, Architectural Press.

TABLADA, A., CARMELIET, J., BAELMANS, M. & SAELENS, D. 2009. Exterior louvers as a passive cooling strategy in a residential building: Computational fluid dynamics and building energy simulation modeling. *PLEA2009.* Quebec, Canada.

TAN, A. Y. K. & WONG, N. H. 2012. Natural ventilation performance of classroom with solar chimney system. *Energy and Buildings,* 53**,** 19-27.

TANTASAVASDI, C., JAREEMIT, D., SUWANCHAISKUL, A. & NAKLADA, T. Natural ventilation: Evaluation and design of houses in Thailand. Conference on Energy Technology Network of Thailand (E-NETT), 2006 Bangkok.

TANTASAVASDI, C., SREBRIC, J. & CHEN, Q. 2001. Natural ventilation design for houses in Thailand. *Energy and Buildings,* 33**,** 815-824.

TECLE, A., BITSUAMLAK, G. T. & JIRU, T. E. 2013. Wind-driven natural ventilation in a low-rise building: A boundary layer wind tunnel study. *Building and Environment,* 59**,** 275-289.

TNO-BUILDINGRESEARCH. *TNO Webapplication - Cp Generator* [Online]. Delft, NL. Available: http://cpgen.bouw.tno.nl/cp/.

TNO-WEBAPPLICATIONS Cp Generator. Delft, NL.

TOE, D. H. C. & KUBOTA, T. 2013. Development of an adaptive thermal comfort equation for naturally ventilated buildings in hot-humid climates using ASHRAE RP-884 database. *Frontiers of Architectural Research,* 2**,** 278-291.

TOFTUM, J. 2004. Air movement - good or bad? *Indoor Air,* 14**,** 40-45.

VISAGAVEL, K. & SRINIVASAN, P. 2009. Analysis of single-sided ventilated and cross ventilated rooms by varying the width of the window opening using CFD. *Solar Energy,* 83**,** 2-5.

WAEWSAK, J., KHEDARI, J., SARACHITTI, T. & HIRUNLABH, J. 2002. Direction an velocity of surface wind in Bangkok. *Thammasat Int.J.Sc.Tech.,* 7**,** 56-63.

WANG, H. & CHEN, Q. 2012. A new empirical model for predicting single-sided, wind-driven natural ventilation in buildings. *Energy and Buildings,* 54**,** 386-394.

WEI, D., QIRONG, Y. & JINCUI, Z. 2011. A study of the ventilation performance of a series of connected solar chimneys integrated with building. *Renewable Energy,* 36**,** 265-271.

WONG, N. H. & HERYANTO, S. 2004. The stuyd of active stack effect to enhance natural ventilation using wind tunnel and computational fluid dynamics (CFD) simulations. *Energy and Buildings,* 36**,** 668-678.

WONG, P. C., PRASAD, D. & BEHNIA, M. 2008. A new type of double-skin facade configuration for the hot and humid climate. *Energy and Buildings,* 40**,** 1941-1945.

XU, L. & OJIMA, T. 2007. Field experiments on natural energy utilization in a residential house with a double skin facade system. *Building and Environment,* 42**,** 2014-2023.

YANG, A.-S., WEN, C.-Y., JUAN, Y.-H., SU, Y.-M. & WU, J.-H. 2014. Using the central ventilation shaft design within public buildings for natural aeratiion enhancement. *Applied Thermal Engineering,* 70**,** 219-230.

YANG, D., DU, T., PENG, S. & LI, B. 2013. A model for analysis of convection induced by stack effect in a shaft with warm airflow expelled from adjacent space. *Energy and Buildings,* 62**,** 107-115.

YANG, L., ZHANG, G., LI, Y. & CHEN, Y. 2005. Investigating potential of natural driving forces for ventilation in four major cities in China. *Building and Environment,* 40**,** 738-746.

YAU, Y. H. & CHEW, B. T. 2014. A review on predicted mean vote and adaptive thermal comfort models. *Building Serv.Eng.Res.Technol.,* 35**,** 23-35.

YIK, F. W. H. & LUN, Y. F. 2010. Energy saving by utilizing natural ventilation in public housing in Hong-Kong. *Indoor and built environment,* 19**,** 73-87.

ZALEWSKI, L., LASSUE, S., DUTHOIT, B. & BUTEZ, M. 2002. Study of solar walls - validating a simulation model. *Building and Environment,* 37**,** 109-121.

ZHAI, X. Q., SONG, Z. P. & WANG, R. Z. 2011. A review for the applications of solar chimneys in buildings. *Renewable and Sustainable Energy Reviews,* 15**,** 3757-3767.